ISTANBUL TECHNICAL UNIVERSITY ★ GRADUATE SCHOOL OF SCIENCE ENGINEERING AND TECHNOLOGY

EXPERIMENTAL AND NUMERICAL APPROACH FOR PAH ACCUMULATION AND DEPURATION KINETICS; A FOOD CHAIN STUDY WITH MARINE ALGAE AND MUSSELS

Ph.D. THESIS

Sevil Deniz YAKAN DÜNDAR

Department of Shipbuilding and Ocean Engineering

Naval Architecture and Marine Engineering Programme

JUNE 2013

ISTANBUL TECHNICAL UNIVERSITY ★ GRADUATE SCHOOL OF SCIENCE ENGINEERING AND TECHNOLOGY

EXPERIMENTAL AND NUMERICAL APPROACH FOR PAH ACCUMULATION AND DEPURATION KINETICS; A FOOD CHAIN STUDY WITH MARINE ALGAE AND MUSSELS

Ph.D. THESIS

Sevil Deniz YAKAN DÜNDAR
(508072103)

Department of Shipbuilding and Ocean Engineering

Naval Architecture and Marine Engineering Programme

Thesis Advisor: Prof. Dr. Oya OKAY

JUNE 2013

İSTANBUL TEKNİK ÜNİVERSİTESİ ★ FEN BİLİMLERİ ENSTİTÜSÜ

PAH BİRİKİM VE ARINIM KİNETİKLERİNE DENEYSEL VE SAYISAL YAKLAŞIM; DENİZ ALGİ VE MİDYESİ İLE BESİN ZİNCİRİ ÇALIŞMASI

DOKTORA TEZİ

Sevil Deniz YAKAN DÜNDAR
(508072103)

Gemi ve Deniz Teknolojisi Mühendisliği Anabilim Dalı

Gemi ve Deniz Teknolojisi Mühendisliği Programı

Tez Danışmanı: Prof. Dr. Oya OKAY

HAZİRAN 2013

Sevil Deniz Yakan Dündar, a **Ph.D.** student of ITU **Graduate School of Science Engineering and Technology** student ID 508072103, successfully defended the **dissertation** entitled "**EXPERIMENTAL AND NUMERICAL APPROACH FOR PAH ACCUMULATION AND DEPURATION KINETICS; A FOOD CHAIN STUDY WITH MARINE ALGAE AND MUSSELS**", which she prepared after fulfilling the requirements specified in the associated legislations, before the jury whose signatures are below.

Thesis Advisor :	**Prof. Dr. Oya OKAY** Istanbul Technical University	.....
Jury Members :	**Prof. Dr. Dr. Karl-Werner SCHRAMM** Munich Technical University	.....
	Prof. Dr. Enis MORKOÇ Marmara University	.....
	Assoc. Prof. Dr. Fatma YONSEL Istanbul Technical University	.....
	Assis. Prof. Dr. Şafak Nur ERTÜRK BOZKURTOĞLU Istanbul Technical University	.....

Date of Submission : 25 March 2013
Date of Defense : 4 June 2013

To my family,

FOREWORD

I would like to thank my supervisor Prof.Dr. Oya OKAY for her guidance and effort during my PhD. study. We have been shared a lot of nice and unforgettable moments after we have begun to work together. She always made me feel that she is not only an ordinary supervisor, but also like a friend who will always support me whenever I need. That means a lot for me during the long and stressful period of this study.

I would also thank my thesis committee jury members Assis.Prof.Dr. Şafak Nur ERTÜRK BOZKURTOĞLU and Prof.Dr.Dr. Karl-Werner SCHRAMM for their valuable comments during my study. They pointed out a lot of subjects that I missed out. This study will not be as it is now without their suggestions.

I also thank Prof.Dr.Dr. Karl-Werner SCHRAMM for introducing me to Dr. Jörg KLASMEIER in the University of Osnabrück. He warmly welcomed and helped me during my studies in Germany. He always listened and answered all my questions patiently. I also need to thank Dr. Andreas FOCKS who was also in the University of Osnabrück. I have learned a lot from him about writing the software code I used in this study. I can frankly say that he put the cornerstones of the model work. Both of them were very patient and collaborative.

I have to thank Prof.Dr. Oya OKAY and Prof.Dr.Dr. Karl-Werner SCHRAMM for letting me to use their laboratories in Istanbul Technical University and in Helmholtz Zentrum München, German Research Center for Environmental Health. I also need to inform that I had got a PhD. research scholarship from the Council of Higher Education of Turkey during my abroad stay in Germany.

I want to thank my laboratory colleagues in alphabetical order because I could not put them in an emotional order. I had several worthful moments with them. I am glad that I had the opportunity to work with Atilla YILMAZ, Burak KARACIK, Burcu DENİZLİ, Burcu ÖZTÜRK, Nazmi Can KOYUNBABA and Pınar ÖZDEMİR.

I want to thank, again in alphabetical order, my colleagues Bilge BAŞ, Çiğdem AKAN, Deniz BAYRAKTAR ERSAN, Emre PEŞMAN, Murat ÖZBULUT, Serdar KÖROĞLU and Şafak KARAKAŞ. This long period of study has been joyful with their friendship.

Finally, my deepest thanks are for my family. I realized that I have a huge and loving family when I tried to write each name. My feelings are much much deeper than the words I would have written here. I am very grateful to my parents, Pembegül and Ahmet YAKAN, my sister Seçil Öznur YAKAN and my husband Doruk DÜNDAR.

February 2013 Sevil Deniz YAKAN DÜNDAR

TABLE OF CONTENTS

Page

ABBREVIATIONS

ACN : Acetonitrile
ADME : Adsorption, distribution, metabolism, extraction
ATSDR : Agency for Toxic Substances and Disease Registry
BaA : Benzo(a)anthracene
BaA1 : 3 μg L^{-1} BaA in aquarium
BaA2 : 6 μg L^{-1} BaA in aquarium
BaA3 : 9 μg L^{-1} BaA in aquarium
BAF : Bioaccumulation factor
BCF : Bioconcentration factor
BMF : Biomagnification factor
BSAF : Biota sediment accumulation factor
C_m : Concentration in mussel
C_w : Concentration in seawater
CAS : Chemical abstracts service
CV : Solvent vehicle control
DCM : Dichloromethane
EQP : Equilibrium partitioning model
FR : Filtration rate
GC-MS : Gas chromatography-mass spectrophotometry
HPLC : High performance liquid chromatography
HRGC : High resolution gas chromatography
HRMS : High resolution mass spectrophotometry
HSDB : Hazardous Substances Data Bank
k_d : Depuration rate constant
K_{ow} : Octanol-water partition coefficient
k_u : Uptake rate constant
NRR : Neutral red retention
PAH : Polycyclic aromatic hydrocarbon
PBPK : Physiologically based pharmacokinetic model

PBTK : Physiologically based toxicokinetic modeling

PCB : Polychlorinatedbiphenyl

PHE : Phenanthrene

PHE1 : 250 µg L^{-1} PHE in aquarium

PHE2 : 500 µg L^{-1} PHE in aquarium

PHE3 : 750 µg L^{-1} PHE in aquarium

PK : Pharmacokinetic model

POP : Persistent organic pollutants

PT : Physiological toxicokinetic model

PTFE : Polytetrafluorethylene

QA/QC : Quality assurance/quality control

QSAR : Quantitative structure activity relationship

US EPA : United States environmental protection agency

VBA : Visual basic for applications

LIST OF TABLES

Page

LIST OF FIGURES

Page

EXPERIMENTAL AND NUMERICAL APPROACH FOR PAH ACCUMULATION AND DEPURATION KINETICS; A FOOD CHAIN STUDY WITH MARINE ALGAE AND MUSSELS

SUMMARY

In this study, a basic food chain of aquatic environment was formed with Mediterraneaen mussel species *Mytilus galloprovincialis* fed with marine diatom *Phaeodactylum tricornutum*. *P. tricornutum* was exposed to polyaromatic hydrocarbons (PAHs) during the uptake stage of the experiments. Two different kinds of PAHs were selected in order to represent two and three ring PAHs; phenanthrene (PHE) for two ring and benzo(a)anthracene for three ring PAH. Mussels were exposed to three different concentrations of selected PAHs under solubility limits through the routes of food (algae) and surrounding environment (seawater). Exposed concentrations were 3, 6 and 9 $\mu g\ L^{-1}$ for BaA and 250, 500 and 1000 $\mu g\ L^{-1}$ for PHE. Durations of the uptake stages were 15 days for BaA exposure and 11 days for PHE exposure. This period was followed by depuration stage as 14 days for BaA and 11 days for PHE exposures.

Two different scales of experiments were performed with the same exposure concentrations: large and small scale uptake and depuration experiments. Exposure concentrations remained same whereas the number of exposed mussels and the volume of seawater were reduced in the small scale experiments.

Mussels were sampled at each three or four days of the uptake and depuration periods of the large scale experiment. PAH concentrations in sampled mussel tissues were determined with GC-MS (gas chromatography-mass spectrophotometry). Kinetic rate constants of mussels were calculated with the first order differential equations during the uptake and depuration periods. These kinetic rate constants were used as input parameters of the developed model.

In addition, two biomarker methods were applied to the sampled mussels during the large scale experiment. These biomarkers were filtration rate and lysosomal membrane stability. Physiological and cellular effects of exposed PAH concentrations were observed with filtration rate and lysosomal membrane stability biomarkers, respectively.

In the small scale uptake and depuration experiment, filtration rates of mussels were observed during 24 hours and used as input parameters of the developed model.

Additional to the kinetic rate constants and filtration rate measurements, parameters such as mussel number, mussel weight, algae number, seawater volume and exposed PAH concentration were also used as input parameters of the developed model.

A mathematical model was developed by using the previously stated input parameters. Three differential equations were used to represent each compartment (seawater, algae and mussel compartments) of the model. The model was developed

to determine the concentration levels of exposed PAHs in the mussel tissues. The model code was written in Mathematica software, and the output graphs were represented in the same software workbook. After the execution of the model code, PAH concentration - exposure day graphs were generated as outputs of the model.

After the correctly execution of the model code, developed model was verified wih the experimental data. Although the model was developed as a closed system omitting evaporation and degradation of PAHs, experimental and model data had a good match with each other. Thus, new scenarios were generated using the same model code. These new sceanarios were generated by changing the input parameters of the model code. Input parameters of the new scenarios were different algae number, different types of marine algae, increased mussel number and increased duration of uptake and depuration periods. Input parameters were selected from field measurements and literature data for different algae number and different types of marine algae. All scenarios were successfully generated and the results indicated that the developed model can be evaluated as a prediction tool of PAH concentration levels in *Mytilus glloprovincialis* in the aquatic environment.

PAH BİRİKİM VE ARINIM KİNETİKLERİNE DENEYSEL VE SAYISAL YAKLAŞIM; DENİZ ALGİ VE MİDYESİ İLE BESİN ZİNCİRİ ÇALIŞMASI

ÖZET

Besin zincirinde PAH biyobirikimi ve transferinin modellenmesi çalışmasında, Akdeniz midye türü olan *Mytilus galloprovincialis* ve deniz mikroalglerinden *Phaeodactylum tricornutum* kullanılarak laboratuvar koşullarında, bir besin zinciri oluşturulmuştur. Laboratuvar deneyleri birikim ve arınım süreçleri olmak üzere iki aşamada gerçekleştirilmiştir. Birikim aşamasında, seçilen alg türü *P. tricornutum*, iki farklı halka sayısına sahip poliaromatik hidrokarbonlara (PAH) maruz bırakılmıştır. Laboratuvar deneylerinde kullanılmak üzere, iki halkalı PAH olarak fenantren (PHE) ve üç halkalı PAH olarak benzo(a)antrasen (BaA) seçilmiştir. Toksisite çalışmalarında biyo kullanılabilirlik açısından önemli olması nedeniyle deneylerde kullanılacak PAH konsantrasyonları, sudaki çözünürlük limitlerinin altında kalacak şekilde belirlenmiştir. BaA'in sudaki çözünürlük limiti 11 $\mu g\ L^{-1}$ civarında ve PHE'nin sudaki çözünürlüğünün 1200 $\mu g\ L^{-1}$ civarında olması nedeniyle, deneylerde kullanılmak üzere BaA için 3, 6 ve 9 $\mu g\ L^{-1}$ ve PHE için 250, 500 ve 1000 $\mu g\ L^{-1}$ konsantrasyonları çalışma konsantrasyonları olarak belirlenmiştir. Mikroalg ve midyeler, belirlenen konsantrasyonlara BaA için 15 ve PHE için 11 gün boyunca maruz bırakılmış, hemen ardından sırasıyla 14 ve 11 gün boyunca herhangi bir PAH'a maruz bırakılmadan temiz deniz suyu içinde arınmaya bırakılmışlardır.

Birikim ve arınma aşamalarından oluşan deney sistemi kısaca şöyle açıklanabilir: Deney düzeneğinde, maruz bırakılacak her bir PAH konsantrasyonu için farklı bir akvaryum oluşturulmuştur. Belirlenen PAH konsantrasyonlarına ek olarak deney sistemine, BaA ve PHE için ayrı birer kontrol akvaryumu eklenmiştir. Belirlenen konsantrasyonlardaki PAH'lar, besin kaynağı olarak kullanılan alg hücrelerine yeterince nüfus etmesi amacıyla 24 saat öncesinden alglerle birlikte karanlık bir ortamda tutulmuş, takip eden gün PAH'a maruz bırakılmş algler akvaryumlardaki midyelere besin kaynağı olarak verilmiştir. Maruz bırakılma süresince bu işlem, her bir akvaryum için günlük olarak tekrar edilmiştir. Arınım sürecinin deney düzeneği açısından tek farkı, besin kaynağı alglerin PAH'lara 24 saat öncesinden maruz bırakılmaması ve akvaryumlara her gün temiz deniz sularının eklenmesi olmuştur.

Yürütülen çalışmada, iki farklı ölçekte birikim ve arınım deneyleri gerekleştirilmiştir: büyük ve küçük ölçekli birikim ve arınım deneyleri. Bu deneylerdeki işlemler aynı sırayı takip etmekle birlike tek farkları midye sayısının ve deniz suyu hacminin 1/5 oranında azaltılmış olmasıdır. Azaltılan değişkenler dışında, maruz bırakılan PAH ve alg konsantrasyonlarında herhangi bir değişiklik yapılmamıştır.

Büyük ölçekli birikim ve arınım deneyleri esnasında, her üç ya da dört günde bir akvaryumlardan midye örnekleri alınarak midye dokularında biriken PAH konsantrasyonları, GC-MS (gaz komatografisi-kütle spektrofotometresi) ile analiz

edilmiştir. Bu analizler sonucunda, midyelerin birikim ve arınım dönemleri için kinetik hız sabitleri belirlenmiştir. Hız sabitlerinin belirlenmesinde, birinci derece diferansiyel denklemler kullanılmıştır. Daha sonra, belirlenen birikim ve arınım kinetik hız sabitleri, geliştirilen PAH biyobirikimi ve transferi model çalışmasında girdi verisi olarak kullanılmıştır.

Büyük ölçekli deney sisteminden alınan midye örneklerine aynı zamanda iki farklı biyogösterge deneyi de uygulanmıştır. Bu deneyler filtrasyon hızı ve lizozomal membran stabilitesidir. Midyelerin maruz bırakıldıkları PAH konsanstrasyonuna verdikleri fizyolojik tepkiler, filtrasyon hızı biyogösterge deneyi ve hücresel tepkiler lizozomal membran stabilite biyogösterge deneyi ile gözlemlenmiştir.

Küçük ölçekli deney sisteminde ise midyelerin filtrasyon hızları, içinde bulundukları akvaryumlardan her 24 saatte belirli aralıklarla alınan su örnekleri kulanılarak takip edilmiş ve hesaplanan filtrasyon hızı değerleri, geliştirilen model çalışmasında girdi verisi olarak kullanılmıştır.

Deniz ortamında yaşayan midyelerin, besin (algler) ve çevrelendikleri ortam (deniz suyu) aracılığıyla PAH'lara maruz bırakılması sonucunda dokularında biriken PAH konsantrasyonlarının belirlenmesi amacıyla matematiksel bir model oluşturulmuştur. Bu model, temel olarak laboratuvarda gerçekleştirilen birikim ve arınım deneylerine dayandırılmıştır. Kinetik hız sabitleri ve filtrasyon hızı gibi daha önce bahsedilmiş olan model girdi verilerine ek olarak akvaryumlardaki midye sayısı, midye ağırlığı, besin olarak kullanılan alg hücreleri sayısı, akvaryumlardaki deniz suyu hacmi ve her bir akvaryuma eklenen ve her biri deniz suyu çözünürlük limitlerinin altında kalmak üzere belirlenmiş PAH konsantrasyonları da modelin diğer girdi verilerini oluşturmaktadır.

Geliştirilen model, temel olarak her biri farklı bir bölmeyi temsil eden üç farklı diferansiyel denklemden oluşmaktadır. Bu bölmeler, maruz bırakılan organizma (midye), çevreleyen ortam (deniz suyu) ve organizmanın besin kaynağını (alg) temsil etmektedir. Her bir diferansiyel denklem, deney sistemi göz önünde tutularak ve her bir bölmenin birbirlerine kinetik hız sabitleri ve filtrasyon hızı ile bağlantılı olması düşünülerek formüle edilmiştir. Böylece, birbirleri ile etkileşimli; ancak dış etkenlere kapalı bir model oluşturulmuştur. Modelin, dış etkenlere kapalı çevrim sistemi düşünülerek oluşturulmasıyla, midyedeki PAH birikimi, arınımı ve transferi tahminleri için temel bir model çalışması gerçekleştirilmiştir. Böylece midyede birikebilecek en yüksek konsantrasyon oranları gözlemlenebilecektir. Buharlaşma ve bozunma gibi dış etkenler neticesinde oluşabilecek PAH konsantrasyonlarındaki olası azalmaların, denklemlere eklenecek çeşitli parametreler ile temsil edilmesi ve bunların daha sonraki model çalışmalarına ilave edilmesi düşünülmektedir.

Temel olarak, girdi verileri, diferansiyel denklem sistemi ve çıkış grafiklerinden oluşan model; bilim, mühendislik ve matematik konularında kullanılmakta olan hesaplama yazılımlarından *Mathematica* yazılım programında yazılmıştır. Diferansiyel denklem sistemi, seçilen yazılım programında var olan 4. derece Runge-Kutta sayısal entegrasyon yöntemi ile çözülmüş ve yine aynı programın eğri uydurumu özelliği ile grafik olarak elde edilebilmiştir. Bu özellikler aynı zamanda yazılım programı seçimi konusunda da etkili olmuştur.

Yazılan program kodu öncelikle başarılı bir şekilde çalıştırılmıştır ve maruz bırakılan konsantrasyonun günlere bağlı değişimleri görsel olarak elde edilmiştir. Ardından, teorik değerlere dayanarak elde edilmiş olan PAH konsantrasyonu-gün grafikleri,

deneysel verilerle karşılaştırılmıştır. Bu karşılaştırma işlemi, üç farklı konsantrasyon ve iki farklı PAH türü olmak üzere toplamda altı kez olmak üzere her bir akvaryum için ayrı ayrı yapılmıştır. Daha sonra, her bir PAH için elde edilen sonuçlar bir araya getirilerek tek bir grafik altında toplanmıştır. Tüm teorik hesaplamalar deneysel verilerle aynı grafik üzerinde karşılaştırılmış ve modelin, temelde PAH birikimi, arınımı ve transferini temsil edebilecek nitelikte olduğu görülmüştür. Bu nedenle, aynı model kodu kullanarak farklı senaryolar üzerinde çalışılmıştır.

Bu senaryolar sırayla şöyle özetlenebilir: Öncelikle besin kaynağı olarak kullanılan alglerin sayısındaki değişimin etkisi araştırılmıştır. Saha çalışmaları sırasında yapılan deniz suyundaki parçaçık sayımlarından görece yüksek olan sonuçlardan biri model girdisi olarak denenmiştir. Ölçülen deniz suyu parçacık miktarı, deneydeki alg sayısının yaklaşık üç katı olmasına rağmen sonuçlarda belirgin bir farklılık olmamıştır.

Bir diğer senaryo ise farklı türde deniz alglerinin midyelerin besin kaynağı olarak kullanılması üzerine gerçekleştirilmiştir. Literatür çalışmalarından altı farklı türde deniz algine ait biyokonsantrasyon değerleri hesaplanmış ve model girdisi olarak bu değerler kullanılmıştır. Deneylerde kullanılan alg sayısında hiçbir değişim yapmadan model kodu farklı alg türleri için çalıştırılmıştır. Tüm sonuçlar karşılaştırıldığında farklı biyokonsantrasyon faktörlerinin, sonuçları farklı şekillerde etkilediği gözlenmiştir. Bu gözlemler ile üç halkalı PAH'lardan olan BaA ve iki halkalı PAH'lardan olan PHE'in farklı birikim eğilimleri gösterdiği anlaşılmıştır. Alglerle yapılan model senaryoları sonucunda, alglerin biyokonsantrasyon değerlerinin artmasıyla BaA'in dokularda birikme oranının azaldığı, diğer yandan alglerin biyokonsantrasyon değeri arttıkça PHE'in dokularda birikme oranının arttığı sonucuna varılmıştır. Seçilen PAH'ların kimyasal özellikleri incelendiğinde, bu farklılığın sudaki biyolojik kullanılabilirlik farklılıklarından ve sudan uzaklaşma özelliklerinden meydana geldiği anlaşılmaktadır.

Algler dışında değiştirilebilecek başka bir parametre olan midye sayıları ile de çeşitli senaryolar gerçekleştirilmiştir. Aynı deney koşulları altında, sadece midye sayıları tüm deney boyunca hiç değişmeden (ara örneklemeler yapılmadan) olduğunun iki katına çıkarıldığında elde edilen PAH konsantrasyonlarında yaklaşık %30-35 oranında azalma göstermiştir.

Tüm bu senaryo değişkenlerine ek olarak, birikim ve arınım dönemlerinin süreleri de modelde değiştirilebilecek parametrelerdendir. Gün sayıları, deneylerdeki gün sayılarının iki ve dörder katına çıkarılmış ve model sonuçları elde edilmiştir. Sadece gün sayısı arttırılarak yapılan denemelerde, midyelerdeki BaA konsantrasyonu seviyesinin PHE konsantrasyonu seviyesine kıyasla 1/3 oranında daha yavaş bir hızla kararlı duruma ulaştığı gözlenmiştir.

Laboratuvar ortamında gerçekleştirilen deney sistemine dayanan matematiksel model, midyedeki PAH birikim, transfer ve arınımını göstermek açısından eksiksiz değildir. Tamamlanması gereken noktalardan en göze çarpanı uzun süreli maruz bırakma deneyleri için eklenmesi gereken midyelerin büyüme oranı parametresidir. Bunun dışında, PAH'ların buharlaşması ve bozunması gibi parametreler de modele eklenebilir. Bu gibi eksikler tamamlanmak üzere daha sonraki çalşmalara bırakılmıştır. Sonuç olarak, oluşturulan model çalışması, her seferinde yeniden deney yapma ihtiyacını azaltmış, elde edilen sonuçlar potansiyel senaryolar için midyelerde biriken PAH konsantrasyonu seviyelerinin ve ardından arınma süreci sonucu

ulaşılabilecek konsantrasyon seviyelerinin tahmini için bir öngörü aracı olarak kullanılabileceğini göstermiştir.

1. INTRODUCTION

1.1 Purpose of Thesis

The purpose of this study was to develop a computer based compartment model to understand the accumulation and transfer of polycyclic aromatic hydrocarbons (PAHs) in the food-chain. This computer model was considered as a tool for the PAH bioaccumulation and depuration predictions in the aquatic environment. A set of physiological parameters were used as inputs of the model. Thus, uptake and depuration experiments were performed in order to simulate a basic food-chain. This food-chain was formed of algae (*Phaeodactylum tricornutum*) and mussel (*Mytilus galloprovincialis*) species.

The scope of the model is to predict the PAH accumulation and depuration levels in the tissues of exposed organisms and to instruct further implementations of uptake and depuration experiments for PAHs under different conditions. This model is also a supportive tool for the interpretation of biomonitoring data under different exposure concentrations. Tissue concentration-time profiles of selected PAHs were predicted as the outcomes of the model based on physiological and metabolic parameters of selected mussel and algae species. Outputs of the model were verified with uptake and depuration experiment results using the uptake and depuration kinetic parameters, and close matches were obtained. Further predictions were performed considering different algal species, algae and mussel numbers, uptake and depuration periods and exposure PAH concentrations.

1.2 Literature Review

Mathematical models are used for a wide range of toxicological problems such as the level predictions of the bioaccumulative chemicals in aquatic organisms. There are several types of mathematical models used for these problems such as equilibrium partitioning model (EQP), mechanistic mass balance models, fugacity models, compartment based kinetic models, physiologically and bioenergetics based models.

Equilibrium partitioning model (EQP) is the simplest mathematical model for the prediction of accumulation levels. The model depends on the thermodynamic equilibrium of the exposed organism and exposure environment. Predictions of this model are independent from chemical properties, organism characteristics and environment conditions (Ryan, 2003).

Mechanistic mass balance models use mathematical descriptions of uptake and depuration phases of accumulation. These phases depend on organism characteristics and chemical properties, additional to EQP models. Early studies of bioaccumulation models were performed by Thomann (1989) and Gobas (1993). Rate constants were used for the development of these models. Fresh water food webs including sediment environment were set up in the models representing well the upper trophic level such as fish, but representing less accuracy of pollutant transfer for benthic invertebrates. Another mechanistic model study was developed by Morrison et.al. (1996) for benthic invertebrates. Pollutant uptake from water, sediment and plankton was considered in this model. Models developed by Morrison et al. (1996) and Gobas (1993) were combined for a new updated model of POP (Persistent Organic Pollutants) bioaccumulation in the food webs of Great Lakes ecosystem (Morrison et al, 1997; Morrison et al, 1999; Ryan, 2003).

Mechanistic models were mostly applied in freshwater ecosystems (e.g. Thomann, 1989; Gobas, 1993; Morrison et al, 1997). There have been few attempts of bioaccumulation modeling in marine ecosystems (e.g. Connolly, 1991; Linkov et al, 2002; Ryan, 2003). Ryan (2003) has been developed a food web bioaccumulation model to predict BSAF (biota sediment accumulation factor) for PCBs (Polychlorinated Biphenyls) (Log K_{ow} greater than 5.24) in benthic marine ecosystem. It has also been successfully applied for PAHs with log K_{ow} greater than 4.6 (Ryan, 2003).

Furthermore, Campfens and Mackay (1997) were developed a food web bioaccumulation model in Great Lakes ecosystem. This model is based on fugacity principle which uses the same mathematical approach with rate constant principle additional to EQP principle for the model evaluation. They have also used a food web matrix in their model to represent the non-linearity of aquatic food webs (Ryan, 2003).

Other models such as compartment based kinetic models, physiologically and bioenergetics based models are also usable for the determination of pollutant accumulation and distribution in aquatic organisms (Landrum et al, 1992)

Several toxicokinetic modeling studies were performed in order to predict the concentrations of organic chemicals especially in fish species. Advantages and disadvantages of both equilibrium and kinetic models were explained by comparing different model structures (Landrum et al, 1992). Mackay and Fraser (2000) were also compared empirical and mechanistic models in a review of bioaccumulation models (Stadnicka et al, 2012).

Toxicokinetic approaches like compartment and PBTK (physiologically based toxicokinetic modeling) models were also used to simulate the chemical concentrations in fish. A one-compartment model was developed by Arnot and Gobas (2004) to predict the bioaccumulation of organic chemicals in aquatic ecosystems. Additional to the predictions of bioaccumulation levels, acquiring site-specific toxicant concentrations, BCF (bioconcentration factor), BAF (bioaccumulation factor) and BSAF were amongst the objectives of the developed model. They also stated that the exchange of nonionic organic chemicals between the organisms and the surrounding environment can be represented using the same equation for different aquatic species. Another one compartment model was developed to represent the different accumulation levels between different species and organic chemicals (Hendriks et al, 2001). K_{ow} (octanol-water partition coefficient), lipid content, weight and trophic level of the species were the parameters used to predict the accumulation kinetics of selected chemicals. Besides one compartment models, multi compartment models were also used in toxicokinetic studies. Nichols et al. (1990; 1991; 1993) were developed and improved a physiologically based model for fish species using the relationship of the whole body lipid ratio with the volume of fat compartment. More physiological data were used for this model due to the number of compartments (Stadnicka et al, 2012).

Generally, fish species were used as target organisms of bioaccumulation modeling studies. BAF-QSAR (Quantitative Structure Activity Relationship) is a food web bioaccumulation model developed for fish species in upper, middle and lower trophic levels of aquatic food webs. It is based on the article of Arnot and Gobas (2003). The

code is written in Microsoft Excel workbook. Non-ionic organic chemicals can be classified with this model according to their bioaccumulative potential in the aquatic food web. FISH bioaccumulation model contains both bioconcentration and biomagnification processes. This model code is written in BASIC programming language and describes the uptake and depuration of organic chemicals by fish. MICHTOX is a coupled mass balance and bioaccumulation model developed by U.S. EPA for toxic chemicals in Lake Michigan (Rossmann, 2005). Accumulation of chemicals, especially PCBs in lake trout and bloater was predicted using MICHTOX model. Another bioaccumulation model, OMEGA, represents four trophic levels (phytoplankton, zooplankton, small and large fish) in marine and fresh water food chain. In OMEGA model, accumulation kinetics of the target organic chemicals are predicted with fugacity theory using both chemicals' and organisms' properties such as octanol–water partition ratio (K_{ow}) of the chemical, weight and lipid content of the organism additional to the trophic level.

Except the models mentioned above, there are also other computer models which can also be used for bioaccumulation studies besides their other properties like chemical fate modeling, toxicity and risk assessment. AQUATOX is a general ecological risk assessment model. Environmental fate and effects of pollutants can be represented with AQUATOX model. In this model, bioaccumulation process and its potential toxic effects are included. This model is used for streams, small rivers, ponds and reservoirs. BASS is another model used to predict the population and bioaccumulation dynamics of fish assemblages exposed to both hydrophobic organic pollutants and borderline metal complex with sulfhydryl groups like cadmium, copper, lead and mercury. Bioaccumulation algorithms of this model are based on diffusion kinetics. Also, the model is coupled to a process-based model for growth of individual fish. Biotic Ligand Model predicts the bioavailability, bioaccumulation and toxicity of metals. EcoFate is a time-dependent model used to predict the concentrations of organic chemicals in water, sediment, fish and fish eating birds. Predicted concentrations in lakes, rivers and marine inlets can be simulated with this model. E-MCM simulates the transfer of mercury in a linear food chain through dietary and direct uptakes. This model is executed both in steady state and dynamic modes. QEAFDCHN is a dynamic bioaccumulation model. This model assumes that the chemicals are uptake through the respiration and ingestion process and lost by

diffusion across the respiratory surfaces. These uptake and loss processes of toxic chemicals by forage and predatory fish are mechanistically simulated with this model. RAMAS Ecosystem models the bioaccumulation process in food chains. There are several options to select for the execution of this model such as specifying the nature and parametric description of uptake kinetics, survival and fecundity, density dependence, appropriate dose-response models. Additionally, 2^{nd} order Monte-Carlo analysis is used for the natural and temporal variability and measurement errors of the model. TRIM.FaTE is a multimedia compartment model developed to represent the fate and transfer of chemicals in both aquatic and terrestrial environments. Bioaccumulation of organic chemicals and metals can be modeled with this compartment based model. Equations and compartments can be edited and linked together due to its flexible interface.

All kinds of mentioned bioaccumulation models (equilibrium partitioning model, mechanistic mass balance models, fugacity models, compartment based kinetic models, physiologically and bioenergetics based models) are mainly aimed to predict the bioaccumulation levels of pollutants in aquatic ecosystems. This literature review revealed that the bioaccumulation modeling studies were mostly performed for fresh water food webs, especially for the upper trophic levels such as fish species. Bioaccumulation predictions are also focused on the levels of organic chemicals such as PCBs and metals in food webs. Beside these studies, there are also modeling studies including sediment environment and lower trophic levels such as planktons, zooplanktons and invertebrates.

In this study, PAH bioaccumulation and depuration in mussel tissues were investigated by using two model PAHs having different K_{ow} values and number of rings. The study also aimed to investigate the toxic effects of those PAHs along with their accumulation and depuration from the mussel tissues. Theoretical modeling part of the study was supported with the experimental study. Depuration periods followed immediately the uptake period in the performed experiments.The difference of this study comes from the combination of model and toxicity investigations, thus it is observed how the bioaccumulation affect the toxicity in mussels.

1.3 Hypothesis

Modeling of PAH bioaccumulation studies were generally performed with fish species due to their high mobility and ecological role in the food webs. Energy transfer between lower and upper trophic levels of the food chain makes fish species ecologically important (Beyer, 1996; Oost, 2003). Mussel species are also important elements of the food chain besides fish species. Even in some food cultures, they can directly reach to the upper level of the trophic level due to directly consumption by humans. Mussels accumulate and transfer PAHs to the higher levels of the food chain due to their low enzyme activity and low PAH metabolization. Thus, modeling studies with mussel species can highlight the concentration levels and transfer routes of PAHs in the food chain. If PAH concentration levels in mussels can be determined during or after the periods of PAH exposures, needed durations to depure the mussels can also be determined with modeling studies. Furthermore, if the routes of PAH transfer in the mussels can be determined with modeling studies, then the control mechanisms to prevent PAH bioaccumulation in mussels can be searched and applied.

1.4 Polycyclic aromatic hydrocarbons (PAHs)

Polycyclic aromatic hydrocarbons (PAHs) are environmental pollutants ubiquitously exist in aquatic ecosystems. Their mutagenic and carcinogenic properties make them a major environment concern (Baumard et al, 1999). Natural and anthropogenic processes are the sources of PAHs entering into the environment. Forest and grass fires, natural petroleum seeps, surface and stormwater runoff from land and atmospheric deposition and fallout of the combustion products can be counted as examples of natural processes. Fossil fuel production and distribution, tanker spills, oil platform releases, domestic and industrial effluents together with the high temperature combustion of organic matter like burning fossil fuels and industrial activities are the examples of anthropogenic activities. (Eisler, 1987; Fernandes et al, 1997; Baumard et al, 1998; Piccardo et al, 2001; Humhpries 2006).

PAHs can be classified as high and low molecular weight PAHs. Four to seven ring PAHs are accepted as high molecular weight PAHs. Main source of high molecular weight PAH contamination is anthropogenic activities such as high temperature

combustion of organic matter (Piccardo et al, 2001; Humhpries, 2006). They have mutagenic and carcinogenic properties (Eisler, 1987; Fernandes et al, 1997; Humhpries, 2006). After the entrance of high molecular weight PAHs into the aquatic environment, adsorption to particulate matters and solid surfaces or accumulation in the tissues of aquatic organisms is easy due to their low water solubility and hydrophobicity (Brooks, 1997).

Two and three ring PAHs are classified as low molecular PAHs (Poston, 2001). Petroleum products and natural processes are the main sources of low molecular weight PAHs (Eisler, 1987; Fernandes et al, 1997; Humhpries, 2006). Their water solubility is higher than the higher molecular weight PAHs (Poston, 2001). Due to the inverse relationship of molecular weight and water solubility, low molecular weight PAHs that adsorb to particles in the water column become more bioavailable to the aquatic organisms (Baumard et al, 1999). Once they enter into the organism, they can cause toxic effects by involving cellular processes due to their binding ability to lipophilic sites in cells (Neff, 1979; Humhpries, 2006).

After the release of PAHs into the aquatic environment, they follow different routes such as evaporation, oxidation, biodegradation, dispersion into the water column, mixing into the bottom sediment and accumulation into aquatic organisms. Ratio of dissolved form of PAHs is a third of all PAHs associated with particulate materials in aquatic environment (Brooks, 1997).

1.5 Accumulation of PAHs in Aquatic Organisms

Uptake and accumulation of PAHs into aquatic organisms can be via water, food and sediment (Brooks, 1997). All of these chemical exposure routes (such as dietary absorption, transport across the respiratory surface, dermal absorption, inhalation) of PAH accumulation into the organisms is called as bioaccumulation (Poston, 2001). Bioaccumulation is increase in the concentration of the exposed chemical in the organism tissues over time compared with the chemical concentration in the habitat of the organisms. It mainly involves uptake, storage and elimination (Zhou et al, 2008). Bioaccumulation occurs through any possible pathways, thus biomagnification (uptake of chemical through food chain) and bioconcentration (uptake of chemical through the surrounding environment such as water) can be

thought as subdivisions of bioaccumulation process (Nendza, 1998; Dearden, 2004).

PAH uptake through non-dietary routes (only water), which is specially named as bioconcentration, is higher compared with uptake through sediment and PAH uptake through food is higher compared with uptake through water in aquatic organisms (Poston, 2001; Brooks, 1997). It has been found that PAHs can be uptaken more efficiently from water compared with from sediment in a study performed by using three different invertebrate species (one worm and two clams). Additionally, accumulation of low molecular weight PAHs were found approximately three times higher than high molecular weight PAHs due to their higher water solubility and bioavailability (Roesijadi et al, 1978; Brooks, 1997).

1.6 Related Concepts

1.6.1 Biomagnification

A term to be mentioned related with bioaccumulation studies is biomagnification. It is the progressively accumulation of pollutants in higher trophic level organisms (Poston, 2001). Dietary assimilation efficiency of the pollutants and growth ratio of the organism are the main toxicokinetic parameters of biomagnification factor in the food chain (Dimitrov et al, 2005). Biomagnification of highly lipophilic pollutants like PAHs is rare or does not occur (van Brummelen, 1998; Poston, 2001). There is an inverse correlation of molecular weight and ring number of PAHs with gastro assimilation rates (Poston, 2001). Thus, PAHs with log K_{ow} values higher than 6 are more effective in biomagnification process (Dearden, 2004). Furthermore, metabolization of PAHs through enzymatic activities for high level aquatic organisms and depuration of PAHs exposed to clean water for low level aquatic organisms limit PAH biomagnification in the food chain (Brooks, 1997). However, in filter feeding aquatic organisms like bivalves, pollutants in water is absorbed and rapidly accumulated to high levels in tissues due to their low enzymatic activities (Brooks, 1997). This is observed with biomonitoring studies such as the Global Mussel Watch Programs in order to determine PAH accumulation levels in the tissues of filter feeding bivalves (Brooks, 1997).

1.6.2 Biomonitoring

Exposure to environmental pollutants may cause toxicity to organisms and it is possible to identify and determine these pollutant levels with biomonitoring (Clewell et al, 2008). Biomonitoring is a technique to assess the effect of pollutants by sampling and analyzing the organism tissues or surrounding fluids. It gives direct information about the potential effects and toxicities of pollutants (Zhou et al, 2008). Quantification of biomonitoring data provides evidence for the exposure of organisms to environmental pollutants. Systematic measurements by biomonitoring studies reveal baseline concentrations and trends over time. However, they do not give information about the routes of accumulation, pollutant persistence in the organisms and the risks of pollutants at the measured levels (Clewell et al, 2008).

The data obtained from biomonitoring is an indicator of internal exposure rather a direct measurement of environmental exposure. Because measured internal exposure is the result of all exposure routes (e.g. dietary and other environmental sources) and physiological mechanisms (e.g. clearance from body), biomonitoring data cannot be used to identify the contribution of these routes. Furthermore, obtained data in the biomonitoring studies give information only at the time of measurements. Thus, additional information is needed about the kinetics of the exposed pollutant related with the target organism (Clewell et al, 2008).

1.6.3 Biomarkers and bioindicator organisms

Pollutants entering into the organisms have markers of exposures. The level of pollutants accumulated in the organisms and their effects can be indicated with these markers. Those can be phyiological, cellular, biochemical and behavioural changes in the organism (Zhou et al, 2008). Bioindicator organisms are used in biomonitoring studies and their selection depends on their specificity, sensitivity, accessibility, and availability for measurement/analysis (Clewell et al, 2008). Furthermore, accumulation potential to high level of pollutants, immobility, abundance, extensive geographical distribution, long life time period, easy sampling, easy nurturing in the laboratory, live ability in aquatic environment, trophic level in the food chain and representativeness of dose-response relationship are the properties of a perfect bioindicator organism to be used (Zhou et al, 2008).

1.6.4 QSAR (Quantitative Structure Activity Relationship)

Quantitative Structure Activity Relationships (QSARs) are mathematical models used for the quantitatively predictions of the toxicity of chemicals (neutral, non-polar and non-ionised) based on their chemical structures (US EPA; Pavan, 2006).

QSARs are mostly used for the prediction of bioconcentration factors (BCFs). Although there is a quantity of QSAR models to predict bioaccumulation factors (BAFs), they are not appropriate to predict BAFs for a large number of chemicals. This is due to the effect of various site-specific environmental parameters besides their chemical characteristics (Arnot and Gobas, 2003).

Traditional bioassays are expensive, time consuming, unfeasible and impractical for a large number of chemicals additional to the ethical issues of animal testing. Thus, QSARs are alternative tools to traditional bioassays to predict the toxicity of untested chemicals (Pavan et al, 2006; Kumar et al, 2009). The correlation of the target chemical's hydrophobicity (Log K_{ow}) with their (Log BCF / BAF) values is described, BCF/BAF values are predicted and potential bioconcentration/ bioaccumulation can be directly assessed with QSAR models (Pavan et al, 2006).

Toxicity of chemicals can be determined with a simple linear function:

$$\text{Toxicity} = ax_1+bx_2+c \qquad \textbf{(1.1)}$$

where x_1 and x_2 are the chemical characteristics such as molecular weight and octanol-water partition coefficient and *a, b,* and *c* are constant parameters (US EPA).

This linear correlation of Log BCF and Log K_{ow} is subject to change for Log K_{ow} values of greater than approximately 6. Thus, nonlinear (parabolic and bilinear) models were proposed for QSAR models (Dimitrov et al, 2005). Lack of experimental values of Log K_{ow} and BCF for the upper limit of 10 results BCF values to be assessed only qualitative for Log K_{ow} values greater than 10 (Pavan et al, 2006).

Another correlated factor of BCF values in QSAR models is the water solubility of the target chemical (Chiou et al, 1977; Kenaga and Goring, 1980, Geyer et al, 1982; Davies and Dobbs, 1984; Isnard and Lambert, 1988; Jørgensen et al, 1998). The reason of using mostly Log K_{ow} in QSARs is due to the less accurate QSAR predictions of water solubility compared with the QSAR predictions of partition

coefficient Log K_{ow} (Dearden et al, 2002a, 2002b; Dearden, 2004).

A few QSAR studies of biomagnification were accomplished except bioconcentration and bioaccumulation predictions. In a study of aquatic food web performed with four trophic levels (plankton, benthic invertebrates, planktivorous fish, and piscivorous fish), all predictions were done using log K_{ow} and $(\log K_{ow})^2$ values (Voutsas et al. 2002; Dearden, 2004). It is also noted that QSAR results of biomagnification should be evaluated carefully due to the less number of related studies **(**Dearden, 2004).

1.7 Modeling Bioaccumulation Data

Bioaccumulation is a dynamic process occuring as the result of pollutant exposure, uptake, storage, excretion and degradation (Zhou et al, 2008). Bioaccumulation results from different routes of exposure. Trophic transfer is generally more effective compared with the dissolved uptake of pollutants in invertebrates (Wang, 2002; Zauke, 2008). Accumulated pollutant concentrations in organisms exposed to various concentrations can be estimated by using computational tools instead of performing experiments. In order to connect the pollutant exposures with accumulation measurements, evaluation of bioaccumulation data with a computational tool is needed (Zhou et al, 2008). Complex physiological processes can be described with mathematical models in the fields like toxicology, risk assessment and biomedical engineering (Marino, 2005). Modeling studies can be thought as complementary tools for the determination of the routes of exposure (Zauke, 2008). Accumulation patterns and concentrations in different aquatic organisms can be predicted with toxicokinetic models (Clason et al, 2004; Luoma and Rainbow, 2005; Zauke et al, 2008).

The relationship between external exposure, internal tissue dose and biological responses can be predicted using physiologically based pharmacokinetic models (PBPKs) (Clewell and Andersen 1985, 1989; Marino, 2005; D'Souza and Andersen, 1988; Leung, 1991; Clewell et al, 2008). Physiologically based pharmacokinetic (PBPK) or physiological toxicokinetic (PT) models are tools used to estimate risks of time-course tissue concentrations of chemicals under different circumstances in different species (Leung, 1991; Andersen, 2003; Bartels et al, 2012). In these models,

a combination of information related with physiology, chemistry and biochemistry are used. PBPK models are useful tools for the predictions of tissue concentrations in different species exposed to different levels and routes of pollutants (Marino 2005; Clewell et al, 2008). They are used for simultaneous predictions of concentration-effect and time-course patterns of pollutants in the exposed organisms or tissues (Bartels et al, 2012). Thus, responses of pollutants can be comprehended with respect to time and concentration. Organisms can be modeled as one homogenous compartment (pharmacokinetic (PK) model) (Gibaldi and Perrier, 1975) or a bunch of compartments each representing separate tissues with different physiological properties (physiologically based (PBPK) model) (Ramsey and Andersen, 1984; Bartels et al, 2012).

Idealized form of PBPK modeling is shown in Figure 1.1. Each compartment used in PBPK models is directly related with biochemical and physical chemical constants of the organism metabolism and tissue solubility (Bartels et al, 2012). ADME (adsorption, distribution, metabolism, extraction) processes can be described with PBPK models using physiological, biochemical, partitioning parameters and mass–balance relationships (Andersen, 1981; Bischoff, 1987). Compartments are used in PBPK models, each represents an organ or tissue of the target organism (Bischoff, 1987; Leung, 1991; Marino, 2005). Pathways of absorption, storage, metabolism and excretion with the chemical toxicity form the complexity of the model. Kinetic behavior of each pathway is represented with rate constants in the model. A set of mass balance differential equations combined with the rate constants was used to represent each compartment. Time course concentrations of the selected chemicals were estimated with the numerical integration of the differential equations. Model can be refined in the inconsistency of model predictions with the experiment observations (Andersen, 2003).

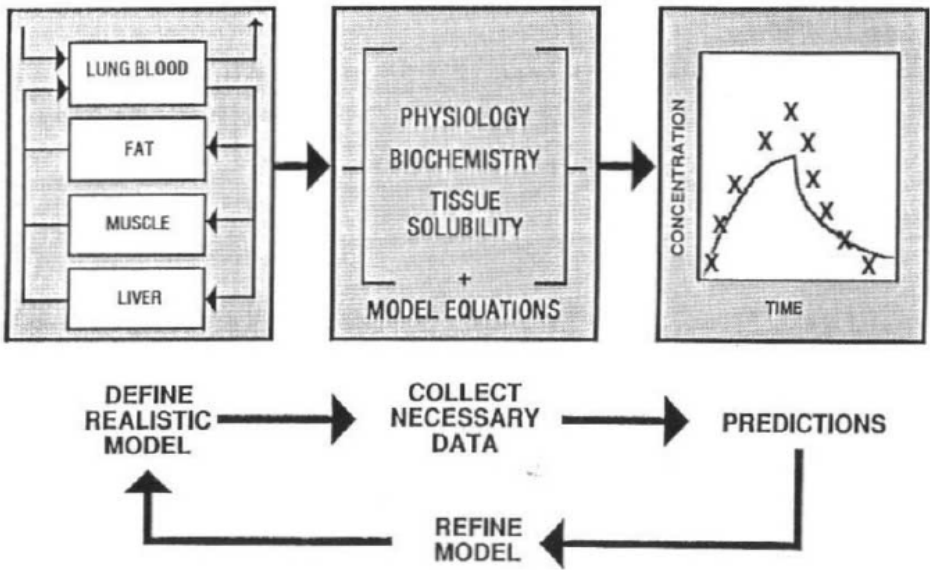

Figure 1.1 : Steps of PBPK modeling. Left panel shows the development of each compartment depending on the anatomy and physiology of test organisms. Middle panel consists the outputs of the model simulation. Right panel compares the model predictions with time course observations (Andersen, 2003).

Usage of PBPK models in risk assessment can be divided into three groups: Exploratory, interpretive and mechanistic evaluations. In exploratory evaluation, responses of different exposure concentrations are compared. In interpretive evaluation, exposure concentration is estimated in order to determine acceptable levels for the risk assessment. In mechanistic evaluation, dose response relationship is characterized and consistency of toxicity response with the specific assumptions is determined (Andersen, 2003). Although all of these three evaluations are tools used in toxicology studies and risk assessment practices, mechanistic evaluation is selected for the development of mathematical model of this study.

1.8 Computer Software for Modeling Study

Computer modeling is a tool for understanding the mechanisms of toxicokinetics. The principles of model coding are developing a relationship between model parameters and algorithms, sequence of algorithm for the model execution and integration techniques. Low number of parameters and simplicity are the elements of modeling assessments (Zauke, 2008). Microsoft Excel software can be used successfully for the initial PBPK model development due to its functions like Solver, Goal Seek, and Scenarios. However, the sufficiency of these functions for curve

fitting property is not clear. Parameter optimization, goodness-of-fit testing, and sensitivity analysis are additionally needed for PBPK modeling (Easterling et al, 2000). Numerical integration methods like 4^{th} order Runge-Kutta method can be used for the solution of differential equations developed to represent compartments in PBPK models. These numerical integration methods are not readily valid in the softwares like Microsoft Excel or VBA (Visual Basic for Applications). Instead, equations can be solved with this complex method that is already available in softwares like Mathematica. Thus, the code used in this study is written in Mathematica software.

2. MATERIALS AND METHODS

2.1 Biological Material

Mytilus galloprovincialis (Lamarck, 1819) (blue mussel or the Mediterranean mussel) is native to the Mediterranean coast and the Black and Adriatic Seas. It is dark blue or brown to almost black as seen in Figure 2.1. The two shells are equal and nearly quadrangular. The outside is black-violet colored; on one side the rim of the shell ends with a pointed and slightly bent umbo while the other side is rounded (Global Invasive Species Database). In its native range, it can be found from exposed rocky outer coasts to sandy bottoms (Ceccherelli and Rossi, 1984). Because it lives in the upper water layer, it is mainly exposed to the dissolved and particulate matter rather than sediment contamination. Thus, it can be thought as an indicator of water column rather than sediment contamination in non-turbid zones (Monteduro et al, 2007; Raoux and Garrigues, 1993; Baumard et al, 1999).

Figure 2.1 : Interior and outer pictures of *Mytilus galloprovincialis* (Url-1).

Phaeodactylum tricornutum belongs to the unicellular brown algal class Bacillariophyceae, or the diatoms. Different morphotypes of *P. tricornutum* are shown in Figure 2.2. Diatoms are found throughout marine and freshwater environments, and are one of the most important constituents of phytoplankton communities in aquatic environments; it is estimated that 20% to 25% of all organic carbon fixation on the planet is carried out by diatoms (Scala et al, 2002).

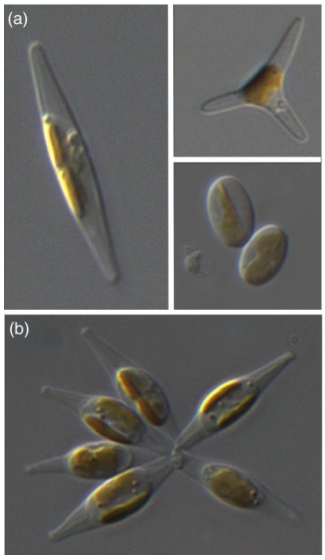

Figure 2.2 : Light micrographs of *P. tricornutum* as (a) fusiform, triradiate and oval types and (b) small clusters of cells. Images courtesy of Alessandra De Martino (Vardi et al, 2008).

Algae and bivalve mollusks can be counted as important bioindicators. Aquatic algae are key factors of aquatic environment. They are primary producers and if they are exposed to pollutants, the pollutants can bioaccumulate and biomagnify to high trophic level organisms in the food chain posing health risks. Additionally, mussels also bioaccumulate and biomagnify pollutants because they are filter feeding bivalves and their enzyme activities are low to metabolize the pollutants (Zhou et al, 2008).

2.2 Chemical Material

Benzo(a)anthracene (BaA) and phenanthrene (PHE) were selected as the model chemicals to be used in exposure experiments. BaA is one of the chemicals that take place in the U.S. EPA (Environmental Protection Agency) Priority Pollutants list (U.S. EPA). The criteria of the chemicals to be on the priority pollutants list are toxicity, persistence, and degradability of the pollutant, the potential presence and the importance of affected organisms in any waters, and the nature and extent of the effect of the toxic pollutant on such organisms. The CAS (Chemical Abstracts Service) registry number of BaA is 56-55-3 (Scorecard, The Pollution Information Site). Its molecular formula is C_{18}-H_{12} (Irwin et al, 1997). Its solubility in water is between 9 and 14 μg L^{-1} at 25°C, means that it is almost insoluble in water. But, it is

soluble in organic solvents like acetone and diethyl ether, very soluble in benzene and slightly soluble in acetic acid and hot ethanol (ATSDR, 1990; Irwin et al, 1997). It is a high-molecular-weight, four-ring PAH and probable human carcinogen (U.S. EPA, 1996; Irwin et al, 1997). Its molecular weight is 228.29 g mol^{-1}, melting point is 158°C, boiling point is 437.6°C at 760 mm Hg. Its octanol water coefficient (Log K_{ow}) which indicates the lipophilicity of BaA is 5.91 (ATSDR, 1990; Irwin et al, 1997). It is also a phototoxic PAH (Mekenyan et al, 1994; Arfsten et al, 1996; Newstead and Geisy, 1987; Irwin et al, 1997). It occurs as the result of pyrolytic processes such as burning of gasoline, garbage, or any animal or plant material, and occurs additionally in creosote. Then, it combines with dust particles in the air and is carried into water, soil and onto crops. 94% of environmental releases of BaA go to air and remaining 6% releases to water and land, approximately in equal amounts (ATSDR, 1990; Irwin et al, 1997). 1,2-benzanthracene (BaA) was purchased from Sigma Aldrich Inc. for the present study, and the purity of BaA was 99%.

Physical and chemical properties of selected PAHs are briefly shown in Table 2.1.

Table 2.1 : Physical and chemical properties of BaA and PHE (ATSDR, 1995).

Characteristics	**Benz(a)anthracene**	**Phenanthrene**
Chemical formula	$C_{18}H_{12}$	$C_{14}H_{10}$
CAS number	56-55-3	85-01-8
Molecular weight	228.9 [a]	178.2 [f]
Color	Yellow-blue fluorescence [b]	Colorless [f]
Physical condition	Solid	Solid [b]
Melting point	158-159°C [a]; 162°C [b]	100°C [b]
Boiling point	400°C [c]; 435°C (sublimes) [d]	340°C
Density	1.274 g cm^{-3} (20°C)	0.98 g cm^{-3} (4°C)
Solubility in water	0.010 mg L^{-1} [e]	1.20 mg L^{-1} (25°C) [e]
Solubility in organic solvents	Slightly soluble in acetic acid and hot ethanol; soluble in acetone and diethyl ether; very soluble in benzene [f]	Soluble glacial aceti acid, benzene, carbon disulphide, carbon tetrachloride, anhydrous diethyl ether, ethanol, toluene [f]
Partition coefficients		
Log K_{ow}	5.61 [g]	4.45 [g]
Log K_{oc}	5.3 [g]	4.15 [g]
Vapor pressure	2.2 x 10^{-8} mmHg (20°C) [h]	6.8 x 10^{-4} mmHg (25°C) [h]
Henry's law constant	1 x 10^{-6} atm m^3 mol^{-1} [i]	2.56 x 10^{-5} atm m^3 mol^{-1} [i]

[a] Eller, 1984; [b] Weast et.al., 1988; [c] Sax and Lewis, 1989; [d] Weast, 1987; [e] Yalkowsky et.al., 1993; [f] LARC, 1973; [g] Mabet et.al., 1982; [h] HSDB, 1994; [i] Nirmalakhandan and Speece, 1988
CAS (Chemical Abstract Service)
All information obtained from HSDB (Hazardous Substances Data Base) except where noted.

Phenanthrene (PHE) is also an important pollutant taking place in the US EPA Priority Pollutants list (US EPA). The CAS registry number of PHE is 85-01-8. Its molecular formula is C_{14}-H_{10} (Irwin et al, 1997). Its solubility in water is between 1.2 and 1.3 mg L^{-1} at 25°C, and it is also soluble in organic solvents like benzene, ethanol, ether, toluene, carbon tetrachloride and carbon disulfide (ATSDR, 1995; HSDB, 2001). It is a low-molecular-weight, three-ring PAH (Irwin et al, 1997). It is a photosensitive PAH. Its molecular weight is 178.24 g mol^{-1}, melting point is 98-100°C, and boiling point is 340°C. Its octanol water coefficient (Log K_{ow}) of PHE is 4.45 – 4.57 (ATSDR, 1995; HSDB, 2001). As a result of its abundance, PHE can be counted as a major component of total PAH compounds. It is a petrogenic PAH that highly available in refined oil products rather than crude oil (Irwin et al, 1997). It is also a man-made chemical used for making dyes, plastics, pesticides, explosives, drugs, bile acids, cholesterol and steroids (US EPA). In this study, PHE was purchased from Fluka Chemika and dissolved in an acetone solution. Purity of PHE was greater than 97% (HPLC grade).

The chemicals were dissolved in acetone (Merck) and stored in the fridge at 4°C in glass volumetric flasks prior to use in exposure experiments.

2.3 Design of Bioaccumulation and Depuration Experiments

Differences in body size and physiologic state of mussels with algal food concentrations affect the uptake rate and the accumulation potential of mussels (Gilek et al, 1996, Björk and Gilek, 1997). Accumulation kinetics is also affected by the environmental conditions and ambient contaminant levels (Richardson et al, 2005). In order to minimize these effects, collected mussels were selected between 45 – 60 mm and same concentration of algal food was added into each aquarium.

Bioaccumulation and depuration experiments were performed in two different scales: large and small. In each scale of experiments, two different sets were performed due to the selection of two different PAHs as model chemicals. In each set of experiments, four aquariums containing different concentrations of PAH under solubility limits in seawater were used including the solvent-vehicle-control (CV) aquarium. Acetone was used as vehicle solvent in CV aquarium. The daily routines of large and small scale experiments were same whereas some differences were

applied during the implementations of the experiments. Designs of the experiment sets are detailed below.

2.3.1 General design of large scale experiments with BaA and PHE

Approximately 230 mussels (*Mytilus galloprovincialis)* of similar shell length (51 ± 0.1 mm) were collected from a relatively uncontaminated site of the Marmara Sea for the experiments. Each mussel was gently cleaned of superficial debris and encrusting organisms, rinsed with clean filtered seawater (active carbon; GF6) and then acclimated in a temperature-controlled room at 21±1°C during 7 days before exposures. Filtered clean seawater was changed daily during this acclimation period. Mussels were fed daily during the acclimation, uptake and depuration periods with fresh unicellular algae (*Phaeodactylum tricornutum*) at a constant density of 20000 cells mL^{-1}. After the acclimation period, mussels were shared into four glass aquariums filled with 10 L of filtered seawater. The experiments were performed in the aquariums with a removable cardboard lid in a semi static test system with renewal of test solutions at every 24 h. Natural clean seawater (18 ppt) was used in the experiments. The seawater was filtered through active carbon and GF6 glass fiber filter paper (Schleicher and Schuell, Dassel, Germany) to remove organic contaminants and suspended particles. Stock solutions of BaA and PHE were prepared by dissolving in acetone and used to prepare daily exposure concentrations during the uptake period.

The alga species used in the experiments, *Phaeodactylum tricornutum*, is an easily cultured micro alga under laboratory conditions. The algae were cultured daily in 1 L volumetric glass flasks in filtered (0.45 µm, Millipore filter) seawater enriched with F/2 medium (Guillard and Ryther, 1962) at 21±1°C under a continuous light illumination of approximately 3800 lux. Algae numbers were counted by using a Beckman Z-2 Coulter counter with a 100 µm orifice.

After *P. tricornutum* cells have reached the early stationary phase (4-5 days), they were added into the filtered (active carbon; GFC filter) seawater at a cell density of 20000 cells mL^{-1}. The exposure concentrations were prepared by using double concentration of this specific algae density and also PAHs in 5 L of seawater and then left for mixing for PAH to be absorbed/adsorbed in/on the cells under dark conditions during 24 hours. Then, the mixture was diluted with another 5 L of

filtered seawater by adding into the aquariums in order to obtain a final volume of 10 L. This procedure was repeated daily for each set of experiments.

Additionally, physical parameters such as pH, temperature and salinity were measured daily twice a day during the all experiment period; before and after the seawater exchange. In order to reduce the possibility of PAH sorption, glassware were used during the whole experiment periods.

Details of large scale experiments with BaA

Three different BaA concentrations (3, 6 and 9 μg L^{-1} nominal values of BaA concentration) below its water solubility were used for the large scale exposure experiment set 1. The exposure experiment lasted 29 days. The first 15 days of the experiment was the uptake period. Later, mussels were transferred into filtered clean seawater for depuration of BaA in mussel tissues. The concentration of the vehicle solvent (acetone) in the aquariums was 0.3 ‰. Six mussels were sampled at days of 2, 6, 10, 14 during the uptake and at days of 17, 21 25, and 29 during the depuration periods and selected biomarker methods were applied to the sampled mussels. Mortality of mussels was low during the whole period of the experiment; 2, 1 and 1 individual losses out of 51 mussels in each aquarium were observed in CV, 6 μg L^{-1}, and 9 μg L^{-1} BaA spiked aquariums, respectively.

Details of large scale experiments with PHE

Three different PHE concentrations (250, 500 and 1000 μg L^{-1} nominal values of PHE concentration) below the water solubility were used for the exposure experiment set 2. The exposure experiment lasted 22 days, comprising the first 11 days of the experiment as the uptake period. Mussels were kept in filtered clean seawater-algae mixture without any PHE addition during the depuration period. Carrier solvent (acetone) to seawater ratio in the aquariums was 0.4 ‰. Six mussels were sampled and selected biomarker methods were applied at days of 3, 7, and 11 during the uptake and at days of 14, 18, and 22 during the depuration periods. Mortality of mussels was low during the experiment; 2 and 1 individual losses were observed in CV, and 1000 μg L^{-1} PHE spiked aquariums, respectively.

After the application of the biomarkers, sampled mussels were dissected, wrapped in aluminum foil and stored at -20°C for further PAH analysis.

2.3.2 Small scale experiments with BaA and PHE

The scale of the experiments were reduced 5 times (number of mussels and seawater volume in the aquarium) for ease of use during the daily observations of mussel filtration rate and seawater concentration in the aquariums. Uptake and depuration experiments were performed by applying the same procedure with the large scale experiments and using previously selected two PAHs (BaA and PHE). Other parameters such as algae density in the aquariums and the period of the experiments were remained same as in the large scale experiments.

Details of small scale experiments with BaA

Total period of the experiment was 29 days including 15 days of uptake and 14 days of depuration period. Total number of mussels in the aquarium was 10.

Decrease of algae number in the aquariums was measured at specific time intervals (at 5, 20, 35, 50, 65, 90, 120, 180, 240, 360, 420 and 1440 minutes after start) during the uptake and depuration periods. First five time points (between 5 and 65 minutes) remained same for all sampling days, but rest of the time points have been shifted. Sampling days were 0, 1, 2, 4, 6, 8, 10, 12, and 14 for the uptake period and 16, 17, 19, 21, 23, 25, 27 and 29 for the depuration period. Time points of samplings are shown in Table 2.2.

Table 2.2 : Sampling times for the measurements of algae number decrease and BaA concentration in aquarium seawater during both uptake and depuration periods.

Time points (minutes)	5	20	35	50	65	90	120	180	240	360	420	1440
Uptake (days 0-6)	√	√	√	√	√	√	√	√		√		√
Uptake (days 7-15)	√	√	√	√	√		√		√			√
Depuration (days 16-29)	√	√	√	√	√		√		√		√	√

Every day, previously (24 hours before) prepared 4 different BaA concentrations containing algae were poured into the mussel aquariums. Aquariums were named as CV, BaA1, BaA2 and BaA3 according to the concentrations spiked into the aquariums (only during the uptake period) as seen in Table 2.3.

Table 2.3 : Abbreviated aquarium names according to the spiked BaA concentrations.

Aquarium	CV	BaA1	BaA2	BaA3
BaA concentration	---	3 μg L^{-1}	6 μg L^{-1}	9 μg L^{-1}

Details of small scale experiments with PHE

Total period of the experiment was 22 days including 11 days of uptake and 11 days of depuration period. Total number of mussels in the aquarium was 10.

Decrease of algae number in the aquariums was measured at specific sampling intervals of each day during the uptake and depuration periods (Table 2.4). Sampling days were 1, 3, 5, 7, 9 and 11 for the uptake period and 12, 14, 16, 18, 20 and 22 for the depuration period.

Table 2.4 : Sampling times for the measurements of algae number decrease and PHE concentration in aquarium seawater during both uptake and depuration periods.

Time points (minutes)	5	20	35	50	65	90	120	180	240	360	1440
Uptake (days 1-11)	√	√	√	√	√		√	√		√	√
Depuration (days 12-22)	√	√	√	√	√		√		√	√	√

Every day, previously (24 hours before) prepared 4 different PHE concentrations containing algae were poured into the mussel aquariums. The content of the aquariums and the PHE concentrations are given in Table 2.5.

Table 2.5 : Abbreviated aquariums names according to the spiked PHE concentrations.

Aquarium	CV	PHE1	PHE2	PHE3
PHE concentration	---	250 μg L^{-1}	500 μg L^{-1}	1000 μg L^{-1}

Particle numbers in the seawater between the sizes of 5.32 and 16.07 μm were measured with Beckman Z2 Coulter Counter by taking 10 mL seawater sample at the specified time points of each experiment. PAH concentration in seawater was measured with the Perkin Elmer LS55 Fluorescence Spectrophotometer by taking another 10 mL of sample at the same time points.

2.4 Timelines of the Large Scale Experiments

Timeline charts and the details of the large scale uptake and depuration experiments were explained for BaA and PHE exposures in Figure 2.3 and Figure 2.4, respectively. Six mussels were taken out from the aquarium at each sampling day, shucked and stored at -20°C for further PAH analysis in mussel tissues. The results of the PAH analysis in mussel tissues were determined in terms of ng g^{-1} wet weight.

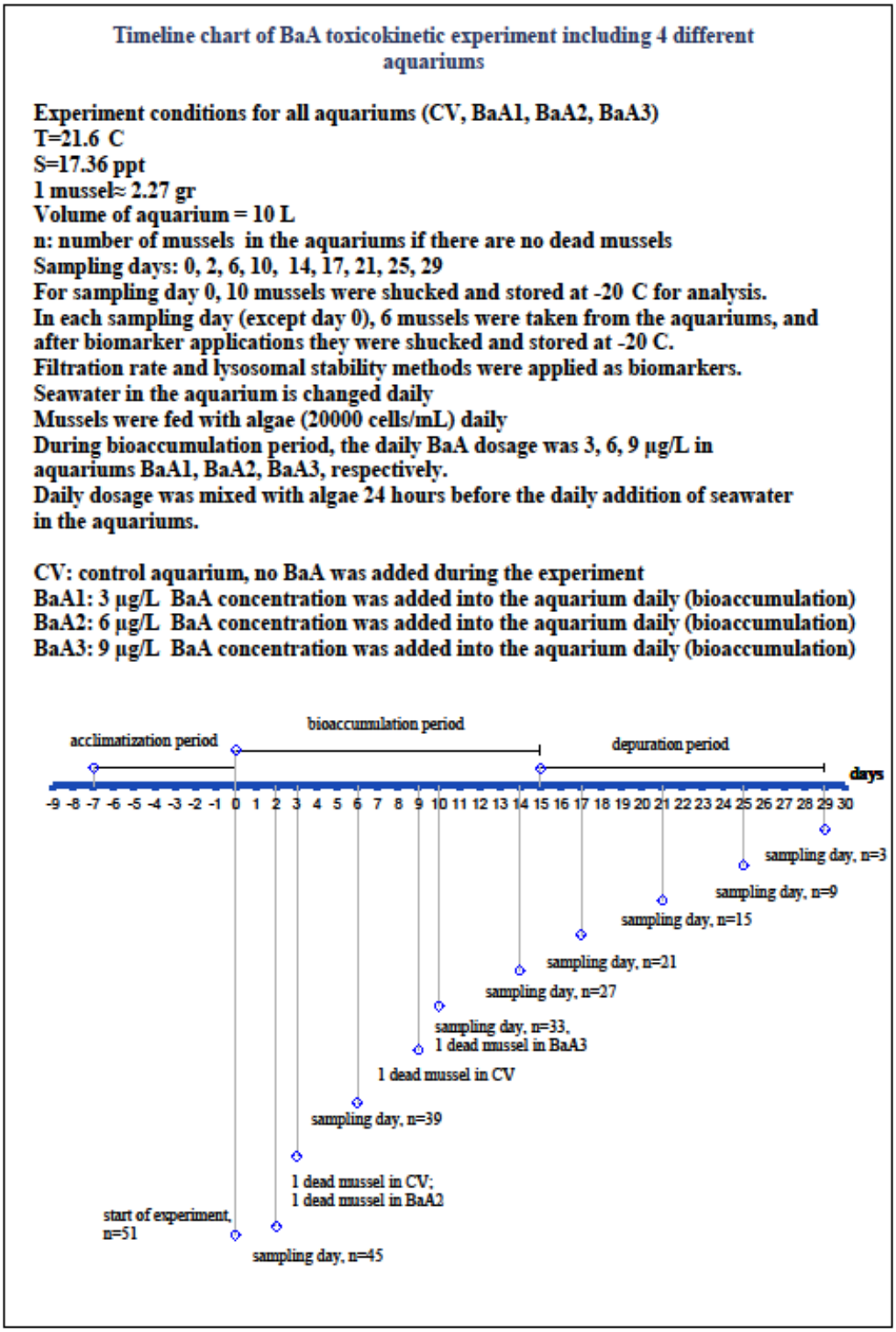

Figure 2.3 : Timeline chart of toxicokinetic experiments performed with BaA.

Timeline chart of PHE toxicokinetic experiment including 4 different aquariums

Experiment conditions for all aquariums (CV, PHE1, PHE2, PHE3)
T=22.6 C
S=17.56 ppt
1 mussel≈ 2.27 gr
Volume of each aquarium = 10 L
n: number of mussels in the aquariums if there are no dead mussels
Sampling days: 0, 3, 7, 11, 14, 18, 22
For sampling day 0, 10 mussels were shucked and stored at -20 C for analysis.
In each sampling day (except day 0), 6 mussels were taken from the aquariums, and after biomarker applications they were shucked and stored at -20 C.
Filtration rate and lysosomal stability methods were applied as biomarkers.
Seawater in each aquarium is changed daily
Mussels were fed with algae (20000 cells/mL) daily
During bioaccumulation period, the daily PHE dosage was 250, 500, 1000 µg/L in aquariums PHE1, PHE2, PHE3, respectively
Daily dosage was mixed with algae 24 hours before the daily addition of seawater in the aquariums.

CV: control aquarium, no PHE was added during the experiment
PHE1: 250 µg/L PHE concentration was added into the aquarium daily (bioaccumulation)
PHE2: 500 µg/L PHE concentration was added into the aquarium daily (bioaccumulation)
PHE3: 1000 µg/L PHE concentration was added into the aquarium daily (bioaccumulation)

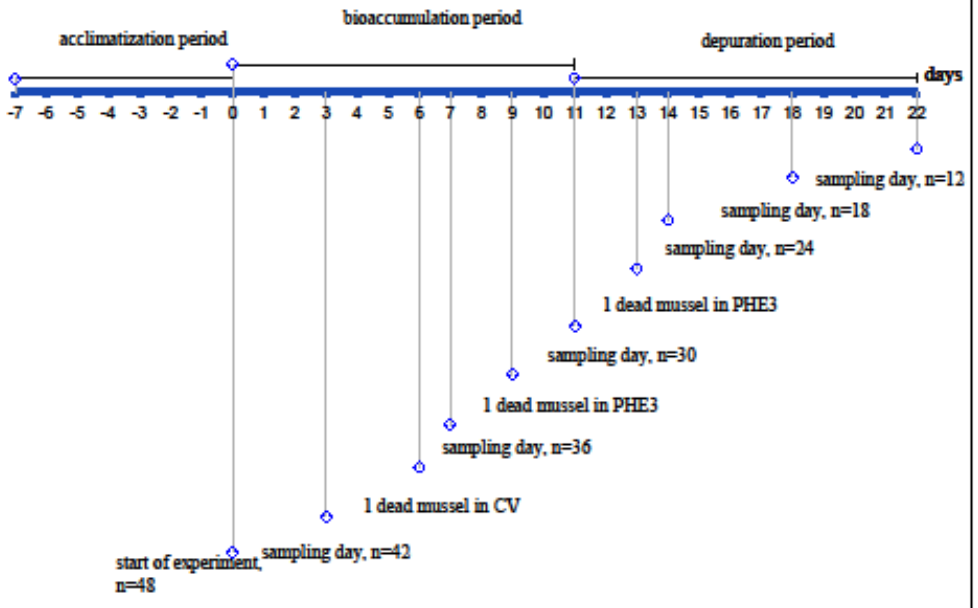

Figure 2.4 : Timeline chart of toxicokinetic experiment performed with PHE.

2.5 Analysis of PAHs

Frozen mussel samples of the large scale experiments were used for the analyses of PAH concentrations in mussel tissues. Seawater samples of both small and large scale experiments were used for the analyses of PAH concentrations in seawater. Analyses of PAH concentrations in mussel tissues and in seawater samples were performed by using high-resolution gas chromatography/high resolution mass spectrophotometer (HRGC/HRMS) and fluorescence spectrophotometer respectively.

2.5.1 Analysis of PAHs in the large scale experiments

The analysis of selected PAHs in mussel tissues was performed with HRGC/HRMS analysis after the application of extraction and clean-up processes. Although the sample preparation procedure for extraction step is same for both BaA and PHE analysis, all steps of the analysis procedure were explained in detail for BaA and PHE analysis separately due to the some differences applied at the clean up and analysis steps.

The analysis of PAH concentrations in mussel tissues was performed in the accredited laboratory of Helmholtz Zentrum München, German Research Center for Environmental Health (GmbH) for the analysis of PAHs according to DIN EN ISO 17025. Permanent quality assurance/quality control (QA/QC) measures are the regularly analyses of an internal control sample, participation in interlaboratory comparison studies and analyses of blank samples.

Analysis of mussels exposed to BaA

In the sample preparation step, about 3.5 g of mussel samples were dissected with IKA Ultra Turrax T18 homogenizer and stored at -20 °C in the freezer until extraction and clean-up processes. In the extraction step, about 1 g of previously prepared samples was extracted with cold extraction procedure. In the cold extraction procedure, firstly the samples were homogenized with anhydrous sodium sulfate and sea sand mixture (2:1 w/w) in the mortar by mixing them until a semi-dry state of mixture and grinding the mixture until they look like uniformly mixed. After homogenization, the mixture were transferred into the column and fitted by knocking to the column. Later, 250 mL solvent (acetone/hexane 1:2 v/v) was added on the top

of the column and the elution was left dropping (approximately 1 drop per second) overnight.

The following day, extracted samples in 250 mL flasks were reduced to approximately 10 mL by using Buchi 011 RE 121 Rotavapor rotary evaporator system at 55°C, 60 rpm and under a pressure between 500 mbar and 250 mbar. These volumetrically reduced samples were transferred into 10 mL volumetric flasks and stored for clean-up process.

In order to remove the interferences, clean-up process of extracted samples were accomplished in two steps; silica gel/alumina B and C18 column. At the first section, a column filled from bottom to top with 10 g silica gel (LGC Standards, Germany), 5 g basic alumina (LGC Standards, Germany, deactivated with 3% water) and 5 g of water-free sodium sulphate was prepared and the column was rinsed with 60 mL n-hexane- (DCM) dichloromethane (1:1) to remove contamination. Later, 30 µL internal standard of deuterated-PAH (D-PAH, a mixture of all 16 EPA PAH as mass-labeled compounds) and 100 µL extracted sample were transferred into the prepared column, 100 mL of n-hexane: DCM (1:1) was slowly dropped into the column and the sample was collected in a 250 mL round flask with a dropping rate of 2 drops per second. After the collection of samples, the volumes were reduced to approximately 1 mL by using Buchi 011 Style Rotovapor rotary evaporator at 55°C, 60 rpm and under a pressure between 400 mbar and 260 mbar (Norm DIN EN ISO/IEC 17025). Afterwards, the samples were carefully reduced to dryness (approximately ½ drop) by light stream of nitrogen and 0.2 mL of acetonitrile (ACN) was added to the volumetrically reduced sample.

At the second step of clean-up process, another column was prepared using PTFE (Polytetrafluoroethylene) frit and 1 g of C18 material (C18 is an octadecyl modified silica gel). In order to remove background contaminations, C18 column was connected to vacuum at 900 mbar and was rinsed with 2 mL of ACN. The samples and 5 mL of ACN were added onto the column and collected in 8 mL of glass vials. After the collection of eluates through C18 column, each eluate volume was reduced almost to dryness in the light stream of nitrogen in the sample concentrator (Trockentemperier- System TCS, Labor Technik Barkey) carefully. At the end of the evaporation process, 3 drops of DCM were added into the eluates three times and

they were immediately transferred into 2 mL micro volume sampling vials to reduce the volume to 50 µL by light nitrogen stream. The samples were stored -20°C until HRGC/HRMS (High resolution gas chromatography/high resolution mass spectrometry) analysis.

At the analysis step of the samples, a high resolution mass spectrophotometer Finnigan MAT 95 (Thermo Electron GmbH, Bremen, Germany) coupled with an Agilent GC 5890 Series II high-resolution gas chromatography (Agilent Technologies, Palo Alto, CA, USA) was used employing isotope dilution methodology. The chromatographic separation was achieved by 1 µL splitless injection (cold injection system CIS3, Gerstel GmbH, Mulheim, Germany) on a Rtx-CLPesticides2 column with a length of 30 m, 0.25 mm ID and 0.2 lm film thickness (Restek GmbH, Sulzbach, Germany). Helium was used as carrier gas with 16 psi head pressure. The gas chromatography oven was programmed as follows: initial temperature 60°C, held for 1.5 min, increased to 225°C at 10°C min^{-1}, then increased to 290°C at 5°C min^{-1}, again increased to 315°C at 15°C min^{-1} and held 315°C for 20 min. The MS (MAT 95; Thermo Scientific, Germany) was operated in ionisation mode and selective ion monitoring (SIM) was applied for detection.

Analysis of mussels exposed to PHE

Dissected and homogenized mussel samples were stored at -20°C after each sampling until extraction and clean-up processes. About 1 g of homogenized sample was mixed with anhydrous sodium sulfate and sea sand mixture (2:1 w/w) and extracted by cold extraction method for tissue analysis of PHE. Homogenized mixture was transferred into a column and 250 mL of solvent mixture (acetone/hexane 1:2 v/v) was added for extraction. The eluent was collected overnight. Subsequently, the volumes of the samples were decreased to approximately 10 mL by using Buchi 011 RE 121 rotary evaporator system at 55°C, 60 rpm and a pressure of 500-250 mbar. Then the samples were transferred into 10 mL volumetric flasks and stored for clean-up process. The extracted sample was purified by passage through mixed columns of silica gel and alumina B. Columns were filled with 5 g of silica gel (LGC Standards, Germany), 2.5 g of basic alumina (LGC Standards, Germany, deactivated with 3% water) and 2.5 g of water-free sodium sulphate from bottom to top and rinsed with 50 mL n-hexane-

dichloromethane (1:1). Internal standard of 50 µL deuterated-PAH (D-PAH, a mixture of all 16 EPA PAH as mass-labeled compounds) and 10 µL extracted sample were transferred into the columns, then 50 mL n-hexane: dichloromethane (1:1) was slowly dropped into the columns, and the sample was collected in 250 mL round flasks with the dropping rate of 2 drops per second. The sample volumes were reduced to approximately 1 mL with Buchi 011 rotary evaporator at 55°C, 60 rpm and a pressure of 400-260 mbar, and then reduced to dryness (approximately ½ drop) by light stream of nitrogen, and 0.2 mL of acetonitrile was added. The volume of the sample in the vials was carefully reduced to almost dryness in a gentle stream of nitrogen at the sample concentrator (Trockentemperier-System TCS, Labor Technik Barkey). Afterwards, three drops of dichloromethane (DCM) were added into the sample three times and sample was immediately transferred into the 2 mL micro volume sampling vial. The volume was reduced to 50 µL by nitrogen stream for analytical determination and the vials were stored at -28°C until the analysis of PHE concentrations in mussel tissues. Analysis were performed using Agilent 5890 Series II high-resolution gas chromatography coupled with Finnigan MAT 95 high resolution mass spectrophotometer (HRGC/HRMS) and Agilent 6890 high-resolution gas chromatography coupled with Finnigan MAT 95S high resolution mass spectrophotometer (HRGC/HRMS) employing isotope dilution method. The chromatographic separation was achieved by 1 µL splitless injection (cold injection system CIS3, Gerstel GmbH, Mulheim, Germany) on a Rtx-CLPesticides2 column with a length of 30 m, 0.25 mm ID and 0.2 µm film thickness (Restek GmbH, Sulzbach, Germany) and 0.1 µL pulsed splitless injection (cold injection system CIS4, Gerstel GmbH, Mulheim, Germany) on a Rtx-Dioxin2 column with a length of 60 m, 0.25 mm ID and 0.2 µm film thickness (Restek GmbH, Sulzbach, Germany), respectively . Helium was used as carrier gas with 16 psi head pressure. The MS (MAT 95 and MAT 95S; Thermo Scientific, Germany) were operated in ionization and electron impact mode, respectively; and selective ion monitoring (SIM) was applied for detection.

Analysis of seawater exposed to BaA and PHE

Ten milliliter of seawater samples were sampled in glass vials from the aquariums two times at each sampling day; one sample of freshly added seawater and one

sample of the same seawater after 24 h. The samples were kept at 4°C until analysis. This procedure was repeated every day for each aquarium of the experiment sets during uptake and depuration periods. Collected samples were centrifuged at 3500 rpm during 10 minutes and then analyzed with Perkin Elmer Model LS 55 Fluorescence Spectrophotometer using the calibration curves of BaA and PHE concentrations. Calibration curves were prepared by diluting the stock solutions with filtered seawater at specified concentration intervals and measuring these calibration standard solutions at excitation and emission wavelengths of 340 and 393 nm for BaA and 209 and 369 nm for PHE analyses, respectively.

2.5.2 Analysis of PAHs in small scale experiments

Ten milliliter of seawater samples were sampled in glass centrifuge tubes from each aquarium at specific time intervals indicated in Table 2.2 and Table 2.4. This sampling procedure was repeated each day of uptake and depuration periods and the samples were measured daily. Collected samples were centrifuged at 5000 rpm for 10 minutes and then analyzed with Perkin Elmer Model LS 55 Fluorescence Spectrophotometer against BaA and PHE standarts. Calibration standards were prepared by diluting the stock solutions with filtered seawater. The excitation and emission wavelengths were 340 and 393 nm for BaA and 209 and 369 nm for PHE.

2.6 Sub-lethal Responses of Organisms by Using Biomarkers

Biomarkers are the responses of organisms to environmental stresses and give essential information for the biomonitoring studies. In order to see the effects of PAH bioaccumulation in the organisms, two biomarker methods which are filtration rate and lysosomal membrane stability were selected. These biomarkers were applied to the mussels at each sampling day of the large scale uptake and depuration experiments.

2.6.1 Filtration rate

The principle of this biomarker method is based on the filtration rate measurements of mussels which refers to the amount of water cleared of particles per unit time, via the consumption of algal cells in a static system (Widdows, 1985). Food quantity, food quality and temperature are the factors affecting the filtration rate (Morton,

1971; Sprung and Rose, 1988; Dorgelo and Smeenk, 1988; Walz, 1978; Reeders and bij de Vaate, 1990; Reeders et al, 1989).

Each mussel shell was gently cleared and rinsed prior to the acclimation period. So, the filtration rate of the mussels would not be affected by the associated particles on the shell. Filtration rates were measured by adding 24000 cell mL^{-1} *Phaeodactylum tricornutum* in the prepared 2 liters of PAH solutions (same concentrations used in the aquariums during uptake and depuration periods). The seawater used to prepare the PAH solutions was filtered with active carbon and then GFC filter. Six beakers, each containing one mussel were used during the filtration rate measurement. Each mussel was observed to be alive and actively filtering before the filtration rate measurements were initiated. Number of algae in the beakers was counted every 15 min during 60 minutes by using Beckman Z2 Coulter Counter. Filtration rate experiment was performed in temperature controlled room at 21±1°C.

Filtration rate of the mussels was determined by using the decline in the number of counted algae over time. The following formula was used for the calculation of filtration rate (FR) as shown in Equation (2.1):

$$FR = \frac{Vol\left[\left(\ln C_0 - \ln C_t\right)\right]}{t} \qquad \textbf{(2.1)}$$

In Equation (2.1), C_0 and C_t indicates the number of algae at specified time intervals. In the experiment, the measurements were repeated 5 times with time intervals of 15 minutes. *Vol* refers the volume of seawater in the beakers in terms of L and t is the time interval in terms of hour. Thus, *FR,* filtration rate of mussels was obtained in terms of Liter per hour ($L\ h^{-1}$).

2.6.2 Lysosomal membrane stability

Neutral red retention (NRR) assay is extensively used for the evaluation of lysosomal membrane stability of marine bivalves. Responses of marine bivalves to contaminants can be assessed with NRR assay (Lowe and Pipe, 1994; Lowe et al, 1995a,b; Zhang and Li, 2006). There are other responses additional to contaminant responses that influences the lysosomal membrane stability of marine bivalves such as seasonal and environmental changes associated with the reproductive cycle, temperature, air exposure and food availability (Harding et al, 2004b), mechanical

disturbances related to post-harvest processing activities such as washing, declumping and storage practices, etc. (Harding et al, 2004a, Zhang and Li, 2006). Stressful period of reduced food quality also affects the lysosomal enzyme activity of mussels (Tremblay et al, 1998, Zhang and Li, 2006). Moreover, salinity and temperature changes affect NRR times (Hauton et al, 1998). The experiments in this study were accomplished in constant temperature and salinity and same environmental and feeding conditions. Although natural variables such as temperature and salinity affect NRR times, they are not as influential as pollutants (Ringwood et al, 1998).

Mussels were acclimatized about a week prior to the experiments. The principle of NRR is based on the retain of neutral red dye in cells after the exposure of lysosomes in healthy cells. The stability of lysosomal membrane decreases with the impact of the natural or artificial stressors combined with the cytotoxic nature of neutral red dye, and this combined effect induces the leaking of lysosomal components (Bresler et al, 1999; Dierickx and van de Vijver, 1991; Haugland, 1996; Dailianisa, 2003).

In the lysosomal membrane stability (NRR assay) technique applied in the experiments, the blood cells (haemocytes) of mussels were withdrawn with a syringe from the adductor muscle of each mussel separately, and injected into physiological saline. Physiological saline is composed of 4.77 g L^{-1} HEPES, 25.48 g L^{-1} NaCl, 13.06 g L^{-1} $MgSO_4$, 0.75 g L^{-1} KCl, 1.47 g L^{-1} $CaCl_2$. The pH of the solution was adjusted as 7.3. Neutral red stock solution was prepared by mixing 1 mL DMSO with 28.8 mg neutral red dye and neutral red working solution was prepared by mixing 10 µL working solution with 5 mL physiological saline. Physiological saline and haemocyte suspensions were spread on glass slides and after waiting 15 minutes in a cooled and dark box, 40 µL of neutral red working solution was added on each slide. An incubation period of 15 minutes was followed and slides were monitored under a light microscope at specific time points during 3 hours (Lowe and Pipe, 1994; Lowe et al, 1995; Dailianisa, 2003). The stability of the haemocytes was determined by examining the blood cells at minutes of 0, 15, 30, 60, 90, 120 and 180. The strength time, which is also taken as the NRR time, was determined with the 50% explosion of haemocytes exposed to the dye.

2.7 Mathematical Model of the Bioaccumulation and Depuration Experiments

2.7.1 Compartment models

In order to understand the interaction between algae, mussels and PAHs in seawater, a modeling study was accomplished using the initial conditions of previously performed uptake and depuration experiments. In this study, the transfer of PAHs was described with a three-compartment model as shown in Figure 2.5. Mussel, algae and surrounding environment (seawater) were expressed as different compartments, and represented as PAH in mussel tissues, PAH in algae and PAH in seawater in terms of ng (for a known volume) as shown in Figure 2.5.

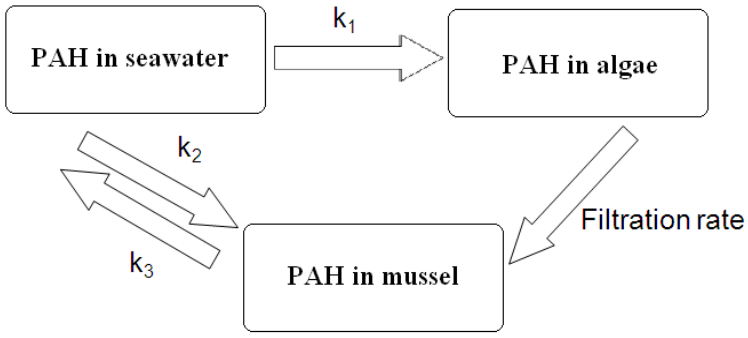

Figure 2.5 : Graphical description of the experiment system as three-compartment model; k_2 and k_3 represents the uptake and depuration rates of mussels through seawater where k_1 indicates PAH uptake rate of algae through seawater.

The relationships between the compartments were defined with different rate constants. The explanations and the units of these rate constants are listed below:

$k_1 \rightarrow (\mu g\ L^{-1}\ day^{-1}\ g^{-1})$ BCF value of *P. tricornutum*

$k_2 \rightarrow (L\ day^{-1}\ kg^{-1})$ PAH uptake rate of mussels from seawater

$k_3 \rightarrow (day^{-1})$ PAH depuration rate of mussels from seawater

In order to find the uptake (k_2) and depuration (k_3) rate constants, Equation (2.2) was used (Barron et al. 1990; Rosen and Lotufo 2007):

$$\frac{dC_m}{dt} = (k_2 C_w) - (k_3 C_m) \qquad \textbf{(2.2)}$$

C_m, C_w, k_2, k_3 and t express PAH concentration in the organism, PAH concentration in the surrounding environment (seawater), PAH uptake rate constant from seawater,

PAH depuration rate constant from seawater and time, respectively. If PAH concentration in water is assumed as constant and PAH concentration in the organism is assumed zero at t=0, Equation (2.2) turns into Equation (2.3) when the system is in the steady state:

$$C_m = \frac{k_2 C_w}{k_3}\left(1 - e^{-k_3 t}\right) \quad \textbf{(2.3)}$$

For the calculation of depuration rate constant (k_3), the linearized form of first order exponential decay equation is used as written in Equation (2.4) where C_{m0} indicates PAH concentration in the organism at the beginning of depuration period.

$$\ln C_m = \ln C_{m0} - k_3 t \quad \textbf{(2.4)}$$

When the system is at steady state, the ratio of uptake and depuration rate constants indicates the accumulation trend of the exposed PAH in the organism compared to the surrounding environment and the food and is expressed with bioconcentration (BCF) and bioaccumulation (BAF) factors respectively according to the PAH exposure method of the organism.

2.7.2 Differential equations

Considering the mass conservation principle in this closed compartment system, total PAH amount entering into the system separates between the three compartments. This fact was described with Equation (2.5).

$$m_{totalPAH} = m_{PAH\,(seawater)} + m_{PAH\,(mussel)} + m_{PAH\,(algae)} \quad \textbf{(2.5)}$$

Transfer of PAHs between the compartments with respect to time was expressed with first order ordinary differential equations for each compartment separately as seen in the Equations (2.6) - (2.8). Sub-equation (2.9) was replaced into the differential equations of (2.6) and (2.8). *M*, *A* and *SW* letters were used as the abbreviations of the PAH in mussel, PAH in algae and PAH in seawater compartments in terms of ng, respectively. Parameters used in the Equations (2.6) - (2.9) were represented with their units in Table 2.6.

Table 2.6 : Parameters in the model equations and their units.

Parameter	Unit (mass units for a known volume)
SW	ng
A	ng
M	ng
k_1	$\mu g\ L^{-1}\ day^{-1}\ g^{-1}$
k_2	$L\ day^{-1}\ kg^{-1}$
k_3	day^{-1}
Volume	L
Filtration rate	$L\ day^{-1}$
Mussel density	$g\ L^{-1}$
Mussel weight	g
Mussel number	number

$$\frac{dSW(t)}{dt} = SW(t)\left[-k_2 * 10^{-3} * MusselDensity - k_1 * 10^{-6} * Volume\right] + M(t) * k_3 \quad \textbf{(2.6)}$$

$$\frac{dA(t)}{dt} = SW(t) * k_1 * 10^{-6} * Volume - A(t) * \frac{FiltrationRate}{Volume} \quad \textbf{(2.7)}$$

$$\frac{dM(t)}{dt} = SW(t) * k_2 * 10^{-3} * MusselDensity + \frac{FiltrationRate}{Volume} * A(t) - k_3 * M(t) \quad \textbf{(2.8)}$$

$$MusselDensity(MusselNumber) = \frac{MusselWeight * MusselNumber}{Volume} \quad \textbf{(2.9)}$$

Model equations were executed using Mathematica programming language. Input parameters used in the model code were rate constants, seawater volume in terms of L, 1 mussel wet weight in terms of g, algae concentration in terms of cell mL^{-1}, wet weight of 1 algae in terms of g, filtration rate of mussels for each day in terms of L day^{-1}, spiked BaA/PHE concentration in terms of $\mu g\ L^{-1}$, initial BaA/PHE concentration of mussel tissues in terms of ng g^{-1}, mussel number and the duration of uptake period.

2.7.3 Parameters used in the model code

Data related with the set-up of the experiment system are shown in Table 2.7.

Table 2.7 : Parameters used in the model equations.

Experiment conditions	Benzo(a)anthracene (BaA)	Phenanthrene (PHE)
Duration	15 days uptake, 14 days depuration	11 days uptake, 11 days depuration
Mussel no	51 mussels	48 mussel
Seawater volume	10 L	10 L
Algae number	20000 cell mL^{-1}	20000 cell mL^{-1}
Exposed concentrations (Aquarium names)	3-6-9 $\mu g\ L^{-1}$ (BaA1-BaA2-BaA3)	250-500-1000 $\mu g\ L^{-1}$ (PHE1-PHE2-PHE3)

Additional to the experiment set-up data in Table 2.7, some data related with algae and mussel have been used in the model code as shown in Table 2.8. They were obtained from the conversions of the experiment measurements for algae and mussel.

Table 2.8 : Variables used in the model code of the experiments with BaA and PHE.

Variable	Unit	For BaA exp.		For PHE exp.	
Total algae	$kg\ m^{-3}$	0.002	wet weight	0.002	wet weight
Total mussel	$kg\ L^{-1}$	0.006528	wet weight	0.010896	wet weight
1 Mussel weight	g	1.28		2.27	

Filtration rate, uptake and depuration rate constants, initial PAH amount in seawater and mussel tissues are other parameters used in the model code and are given in Table 2.9 for each BaA and PHE exposed aquariums. Filtration rates in Table 2.9 were calculated by taking the averages of hourly measurements of small scale experiments at each day of the experiment period.

Table 2.9 : Variables used in the model of BaA and PHE bioaccumulation experiment.

		BaA aquariums			PHE aquariums		
Variable	**Unit**	**3 $\mu g\ L^{-1}$**	**6 $\mu g\ L^{-1}$**	**9 $\mu g\ L^{-1}$**	**250 $\mu g\ L^{-1}$**	**500 $\mu g\ L^{-1}$**	**1000 $\mu g\ L^{-1}$**
Filtration rate	$L\ day^{-1}$	54.5	65.5	65.3	33.8	35.5	25.4
Uptake rate constant (k_2)	$L\ day^{-1}\ kg^{-1}$	66	319	379	179	113	94
Depuration rate constant (k_3)	day^{-1}	0.04	0.14	0.11	0.25	0.22	0.18
Initial PAH in seawater (t=0)	µg	30	60	90	2500	5000	10000
Initial PAH in mussel (t=0)	ng	261	261	261	335758	335758	335758

3. RESULTS AND DISCUSSION

3.1 Results of Large Scale Experiments with BaA

Seawater has been sampled twice a day (when freshly prepared and 24 hours later) during the large scale uptake and depuration experiments. Average seawater salinity, temperature and pH were measured as 17.4±0.01 ppt, 21.6±0.14 °C and 7.5±0.03, respectively for the first seawater samples. Alike, 24 hours later, the parameters in seawater samples were measured as 17.3±0.01 ppt, 21.6±0.12 °C and 7.8±0.04 for the average salinity, temperature and pH values were, respectively.

Control aquarium (CV) was used in order to be aware of unexpected or unwanted experimental conditions during the uptake and depuration periods. Average BaA concentration of mussels in CV aquarium was measured as 18.6 ng g^{-1} wet weight. According to a previous biomonitoring study in Istanbul Strait, BaA concentrations in mussels sampled from an unpolluted site has been measured between 0 (not detected) and 22 ng g^{-1} wet weight in mussels along the coasts of Istanbul Strait (Karacik et al, 2009). This data verifies that the concentration in CV aquarium is at acceptable levels.

3.1.1 Uptake and depuration of BaA

Mussels accumulated BaA in their tissues both through the surrounding environment (seawater) and food (algae) consumption during the uptake period. After the end of uptake period, depuration period began immediately and same mussels start to depure previously accumulated BaA from their tissues. The results of BaA retained by mussels (ng g^{-1} wet weight) for all aquariums together are given in Figure 3.1. The left half of the Figure expresses the bioaccumulation phase whereas the right half of the Figure expresses the depuration phase of the experiment period. BaA was rapidly taken up by mussels from the algae–water exposure system for all concentrations (Figure 3.1). Tissue levels did not reach steady-state concentrations in mussels by the end of the exposure period. Mean BaA concentration in the mussel tissues of CV aquarium was found as 18.6 ng g^{-1} wet weight for the whole

experimental period. The concentrations of BaA in mussel tissues have an increasing trend during the uptake of BaA as clearly seen from Figure 3.1; on the contrary, the concentrations of BaA in mussel tissues are decreasing steadily in the depuration period.

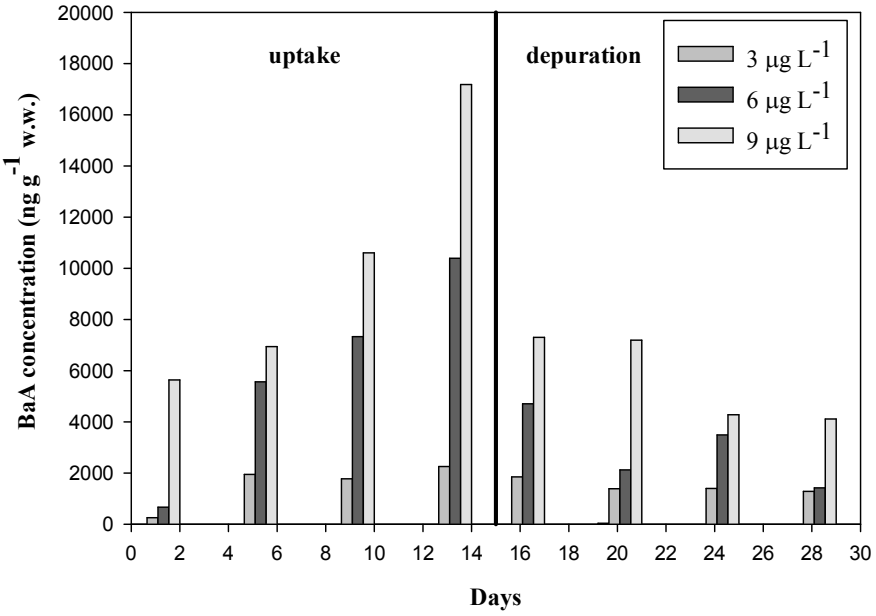

Figure 3.1 : Benzo(a)anthracene (BaA) concentrations in mussel (*M. galloprovincialis*) tissues (ng g^{-1}, wet weight), exposed to 3.0, 6.0, 9.0 µg L^{-1} BaA for a total of 29-day uptake and depuration periods. Control values range from 4 to 38 ng g^{-1} with a mean of 18.6 ng g^{-1}, and are not shown in the figure.

3.1.2 Kinetic rate constants of mussels exposed to BaA

The increase of BaA concentrations in mussels during the uptake period shows a linear trend, whereas the depuration trend can be represented as an exponential function. Therefore, depuration rate constants were calculated by determining the slope of the linear regression between ln-transformed BaA concentrations in mussels and time. The tissue levels for BaA may indicate a two-phase depuration. Upon transferring the mussels to a BaA free system, the chemical exhibited rapid depuration over a 48 hours period, after which the depuration rate reduced. The rate constants for uptake and depuration of BaA concentrations were found between 39 and 450 L day^{-1} kg^{-1} and 0.04 and 0.14 day^{-1}, respectively. BaA concentrations in seawater (C_w) and in mussels (C_m) on the 14^{th} day (last sampling day of the uptake period), uptake and depuration rate constants (k_u, k_d), and bioaccumulation factors (BAFs) are shown in Table 3.1.

Table 3.1 : Measured benzo(a)anthracene (BaA) concentrations in aquariums (μgL^{-1}) and in mussel tissues at the end of uptake period (ng g^{-1}, wet weight), BaA uptake and depuration rate constants (L day^{-1} kg^{-1} and day^{-1}) of mussels (*M. galloprovincialis*) and bioaccumulation factors (BAFs) for the mussels calculated in two different methods as the ratio of rate constants and the ratio of tissue BaA concentration to seawater.

Aquariums	C_w ($\mu g\ L^{-1}$)	C_m (14^{th} day) (ng g^{-1})	k_u (L day^{-1} kg^{-1})	k_d (day^{-1})	BAF_1 $=k_u/k_d$	BAF_2 $=C_m/C_w$
BaA1	3.19	2252	39	0.04	989	706
BaA2	5.34	10394	229	0.08	2916	1947
BaA3	6.26	17180	450	0.14	3184	2745

3.1.3 BCF/BAF of mussels exposed to BaA

Bioaccumulation factors are calculated by either using the uptake and depuration rate constants or by dividing the tissue pollutant concentration by total seawater concentration (dissolved and particulate phases). As was previously reported in several studies (for example Pruell et al, 1986), the uptake route of a chemical depends on its relative abundance in the dissolved and particulate phases. In this study, dissolved and particulate phase BaA concentrations were not measured separately, but by considering the tendency of PAHs mainly to accumulate in the particulate phase (Richardson et al, 2005), the concentration factors were calculated on the basis of total concentration in seawater. As is well known, the tendency for accumulation of organic contaminants in mussels can be correlated with n-octanol/water partition coefficients (K_{ow}) of the compounds. Table 3.2 shows several BCF values of mussels determined by using K_{ow} values of BaA in a linear QSAR equations, Log BCF = a log K_{ow} + b, which relates the BCFs to the K_{ow} values of the chemicals. Generally, QSARs follow a linear path until log K_{ow} is lower than 6. In the equation, *a* and *b* are constants indicating the slope and the intercept of the equation, respectively. This linear relationship breaks down for higher values of log K_{ow} which indicates strongly hydrophobicity (Banerjee and Baughman, 1991; Pavan et al, 2006). Although there is a good correlation between BCF and K_{ow}, there are some limitations of this relationship which may ignore the metabolic degradation of the chemical within the organism. This may cause the over prediction of BCF. However, log K_{ow} have been frequently used for the indication of bioaccumulation potential (for example Axelman et al, 1999; Pavan et al, 2006).

Table 3.2 : Various bioconcentration factors (BCFs) calculated both from different quantitative structure activity relationship (QSAR) equations taken from literature and this study's experiment results (Log K_{ow} (octanol–water coefficient) value of benzo(a)anthracene (BaA) was taken as 5.9 for the calculations).

QSAR formula	Log BCF	BCF	Reference
Log BCF = -0.808+0.858 Log K_{ow}	4.25	17956	Geyer et al. (1982, 1991)
Log BCF = -0.97+0.899 Log K_{ow}	4.33	21582	Geyer et al. (1991)
Log BCF = -1.193+0.790 LogK_{ow}	3.47	2938	Okay and Karacik (2008)
Log BCF = -1.344+0.820 Log K_{ow}	3.49	3119	Okay and Karacik (2008)
Log BCF = -2.220+0.965 LogK_{ow}	3.47	2975	Donkin et al. (1991)
Log BCF = -1.4+0.965 Log K_{ow}	4.29	19656	Pruell et al. (1986)
Log BCF = -1.67+1.02Log K_{ow}	4.35	22284	Arnot and Gobas (2006)
Log BCF = 0.98+0.35Log K_{ow}	3.05	1109	Arnot and Gobas (2006)
BAF_1^* of BaA3 aquarium	3.50	3184	Experimental value (This study)
BAF_2^* of BaA3 aquarium	3.44	2745	Experimental value (This study)

*BAF_1 is the ratio of rate constants whereas BAF_2 is the ratio of tissue concentration over seawater concentration.

High level of BCF values in Table 3.2 indicate that BaA accumulates to a large extent in tissues. Log BCF values vary between 3.05 and 4.35. The results of the experimental study appear to be more consistent with rather low BCF values observed. The underlying reasons can be that the uptake period was not long enough to reach the steady-state condition, along with the presence of algae in the exposure system. For example, two QSAR formulas taken from Arnot and Gobas (2006) have different BCF values due to the usage of different data sets. As they stated, the reason for the lower BCF value is the uncertainty of the sources in the data sets which tend to underestimate BCF. In this study, obtained BCF values are closer to the underestimated BCFs from the Arnot and Gobas (2006) data set. This is probably resulted from not reaching steady-state concentrations during the uptake period. The reduction of bioconcentration of chemicals in *Daphnia* in the presence of organic matter (McCarthy, 1983) is another example for how food reduces BCF values. However, obtained results from this study are between the maximum and minimum values of various QSARs which make them comparable and shows that BCF is a good comparison value for the BaA body burden in mussels.

3.2 Results of Large Scale Experiments with PHE

3.2.1 Uptake and depuration of PHE

The results of PHE concentration accumulated by mussels in terms of μg g^{-1} wet weight are given in Figure 3.2. The left half of the Figure expresses the bioaccumulation phase whereas the right half of the Figure expresses the depuration phase of the experiment period. PHE was rapidly taken up by mussels from the algae-water exposure system for all concentrations. PHE levels in mussel tissues have almost reached steady-state by the end of the exposure period. The trend lines of the uptake period are similar for different PHE concentrations. Mean PHE concentration in the mussel tissues of CV aquarium was found as 3.42 μg g^{-1} wet weight for the whole experimental period. As expected, concentrations of PHE in mussel tissues have an increasing trend during the uptake of PHE as clearly seen from the left half of Figure 3.2; on the contrary, the concentrations of PHE in mussel tissues are decreasing steadily in the depuration period (right half of Figure 3.2). A negligible decrease of PHE levels was observed in CV aquarium during the depuration period of the experiment. That was probably caused due to the depuration of the initial PHE concentration in mussels during the depuration period.

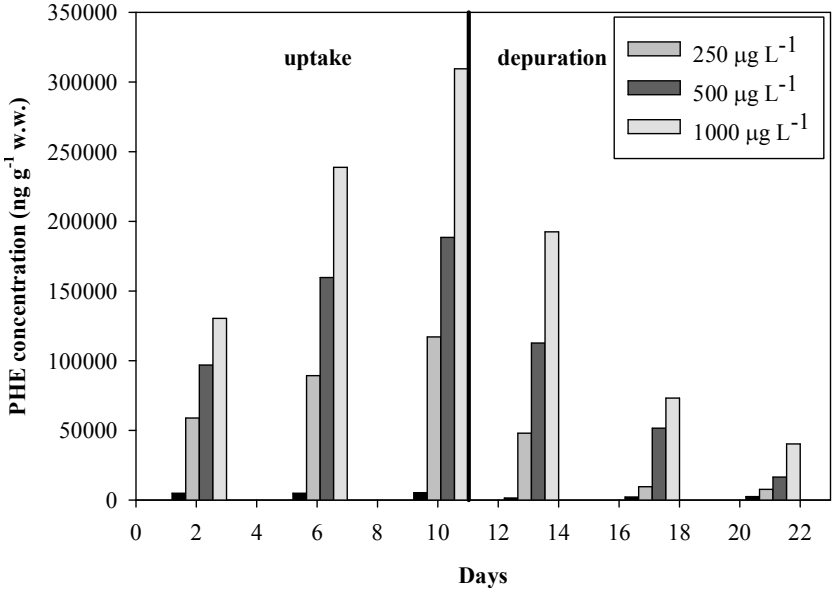

Figure 3.2 : Phenanthrene (PHE) concentrations in mussel (*M. galloprovincialis*) tissues (ng g^{-1}, wet weight), exposed to 250, 500, 1000 μg L^{-1} PHE for a total of 22-day uptake and depuration periods. Control aquarium values are also shown in the figure as the lowest level of each bar with a mean of 3.42 μg g^{-1}.

3.2.2 Kinetic rate constants of mussels exposed to PHE

PHE concentrations in seawater (C_w) and in mussels (C_m) on the last sampling day of the uptake period (11th day), uptake and depuration rate constants (k_u, k_d), and bioaccumulation factors (BAFs) are presented in Table 3.3. Experimental results were used for the calculations of uptake (k_u) and depuration (k_d) rate constants. While PHE concentrations in mussels are inclined to reach the steady-state condition during the uptake period, they show an exponential decay in the depuration period. Depuration rate constants were calculated firstly by using Equation (2.5) to determine the slope of the linear regression between ln-transformed PHE concentrations in mussels and time, and then uptake rate constants were calculated by using Equation (2.4). The level of accumulated PHE exhibited relatively fast elimination over the 72 hours period compared with the following elimination trends upon transferring the mussels into a PHE-free medium. The uptake and depuration rate constants of PHE concentrations were found between 93 and 177 L day^{-1} kg^{-1} and 0.18 and 0.25 day^{-1}, respectively as shown in Table 3.3. Calculations of BAF values in Table 3.3 were performed by either using the ratio of uptake and elimination rate constants (BAF_1) or the ratio of PHE concentration in tissues over total (dissolved and particulate phases) seawater concentration (BAF_2). In the present study, total PHE concentration in seawater (dissolved+particulate) was measured due to the tendency of PAHs to accumulate in particulate phase over 90% according to reported experimental results performed with anthracene, fluoranthene and pyrene (Richardson et al, 2005).

Table 3.3 : Measured phenanthrene (PHE) concentrations in the aquariums (µg L^{-1}) and in mussel tissues at the end of uptake period (µg g^{-1}, wet weight), PHE uptake and depuration rate constants (L day^{-1} kg^{-1} and day^{-1}) of mussels (*Mytilus galloprovincialis*) and two bioaccumulation factors (BAFs) for the mussels calculated as the ratio of rate constants and the ratio of tissue PHE concentration to the surrounding environment.

Aquariums	C_w (µg L^{-1})	C_m (11th day) (µg g^{-1})	k_{uptake} (k_u) (L day^{-1} kg^{-1})	$k_{depuration}$ (k_d) (day^{-1})	BAF_1 (k_u/k_d)	BAF_2 (C_m/C_w)
PHE1	176	117	177	0.25	701	658
PHE2	399	189	112	0.22	513	466
PHE3	695	309	93	0.18	509	441

A positive correlation of PHE concentration in mussel tissues and exposure concentrations in seawater was found for each aquarium (Table 3.3). PHE

concentration in mussel tissues continue increasing as the level of exposure concentrations increase due to the bioaccumulation of PHE in the tissues. The bioaccumulation factor can be deduced from the ratio of uptake and depuration rate constants. Another point seen from Table 3.3 is the inverse correlation of uptake rate constants with the level of exposed PHE concentrations. Despite this, there is not a clear difference between the depuration rate constants of different exposure concentrations. Depuration rates of different exposure levels were found as almost the same. Eventually, bioaccumulation of PHE in mussel tissues can be interpreted as simply dependent on the uptake rate constants.

3.2.3 BCF/BAF of mussels exposed to PHE

As was indicated before, accumulation of organic contaminants in aquatic organisms related with n-octanol/water partition coefficients (K_{ow}) of the compounds. Table 3.4 shows that the calculated BAF values by using several QSARs and also the values obtained from the experimental results of the present study. During the calculations, the values of W_s and K_{ow} for PHE from the experimental data base of EPA's EPI Suite estimation programs (data of Schwarz (1977) in WSKOWWIN v1.41 and data of Hansch et al. (1995) in KOWWIN v1.68) as 4.46 and 1150 µg L^{-1}were used, respectively.

Table 3.4 : Various bioaccumulation factors (BAFs) calculated both from different quantitative structure activity relationship (QSAR) equations taken from literature and from the present study's experiment results (Log K_{OW} (octanol-water coefficient) and W_S (water solubility) values of phenanthrene (PHE) were taken as 4.46 and 1150 µg L^{-1}, respectively for the QSAR calculations).

QSAR Linear regression (standard errors)	Log BAF	BAF	Reference
$LogBAF_w$=-0.682 $LogW_S$ + 4.94	2.85	712	(Geyer et al, 1982)
$LogBAF_w$=0.858 $LogK_{ow}$-0.808	3.02	1044	(Geyer et al, 1982; 1991)
$LogBAF=1.03(0.07)logK_{ow}$-2.22	2.37	236	(Donkin et al, 1991)
$LogBAF=0.82(0.04)logK_{ow}$+0.09(0.24)	3.75	5587	(Arnot and Gobas, 2006)
$LogBAF=0.92(0.05)LogK_{ow}$-1.45(0.27)	2.65	450	(Arnot and Gobas, 2006)
Log BAF_1* of PHE3 aquarium	2.71	509	Experimental value (This study)
Log BAF_2* of PHE3 aquarium	2.64	441	Experimental value (This study)

*BAF_1 is the ratio of rate constants whereas BAF_2 is the ratio of tissue concentration over seawater concentration.

Calculated BAF values range from 236 to 5587 by using QSAR models reported in the literature. Log BAF values of the present study stay within this range as shown in Table 3.4. The large range of BAF values occurs due to the large variety of scanned databases including both experimental and field studies. BAF values found in this study were similar to those in the literature (Table 3.4). BAF_2 values (ratio of concentrations) were found slightly lower than BAF_1 (ratio of rate constants) for all exposure concentrations. This small difference is probably caused due to the different calculation methods.

As a result, experimental values were found in close correlation with each other and also found between the maximum and minimum values of various QSAR values in the literature. These facts make the experimental results comparable and also show that BAF is a good comparison value for the PHE body burden in mussels.

3.3 Results of Small Scale Experiments with BaA

3.3.1 Particle decrease in seawater

The particle numbers between the sizes of 5.32 and 16.07 μm were measured with Beckman Z2 Coulter Counter and the decrease was shown as percentages versus days. Measurements of uptake and depuration periods of each aquarium were drawn separately for the sampling time intervals of each day.

It is apparent that the decrease of algae consumption during depuration period is more apparent compared with the uptake period as seen in Figure 3.3 and Figure 3.4. Besides this rapid consumption, small increases at the particle numbers were measured in the aquariums at an average of 90, 120, 180 and 180 minutes for CV, BaA1, BaA2 and BaA3 aquariums, respectively during the uptake period. Similarly, the same was also observed for CV, BaA1, BaA3 aquariums, at an average of 240, 420 and 420 minutes respectively during the depuration period. Particle increase was not observed during the uptake period of BaA2 aquarium when the average particle numbers were evaluated. The average values of particles in percentages at specific time intervals were shown in Table 3.5 for uptake period and depuration periods.

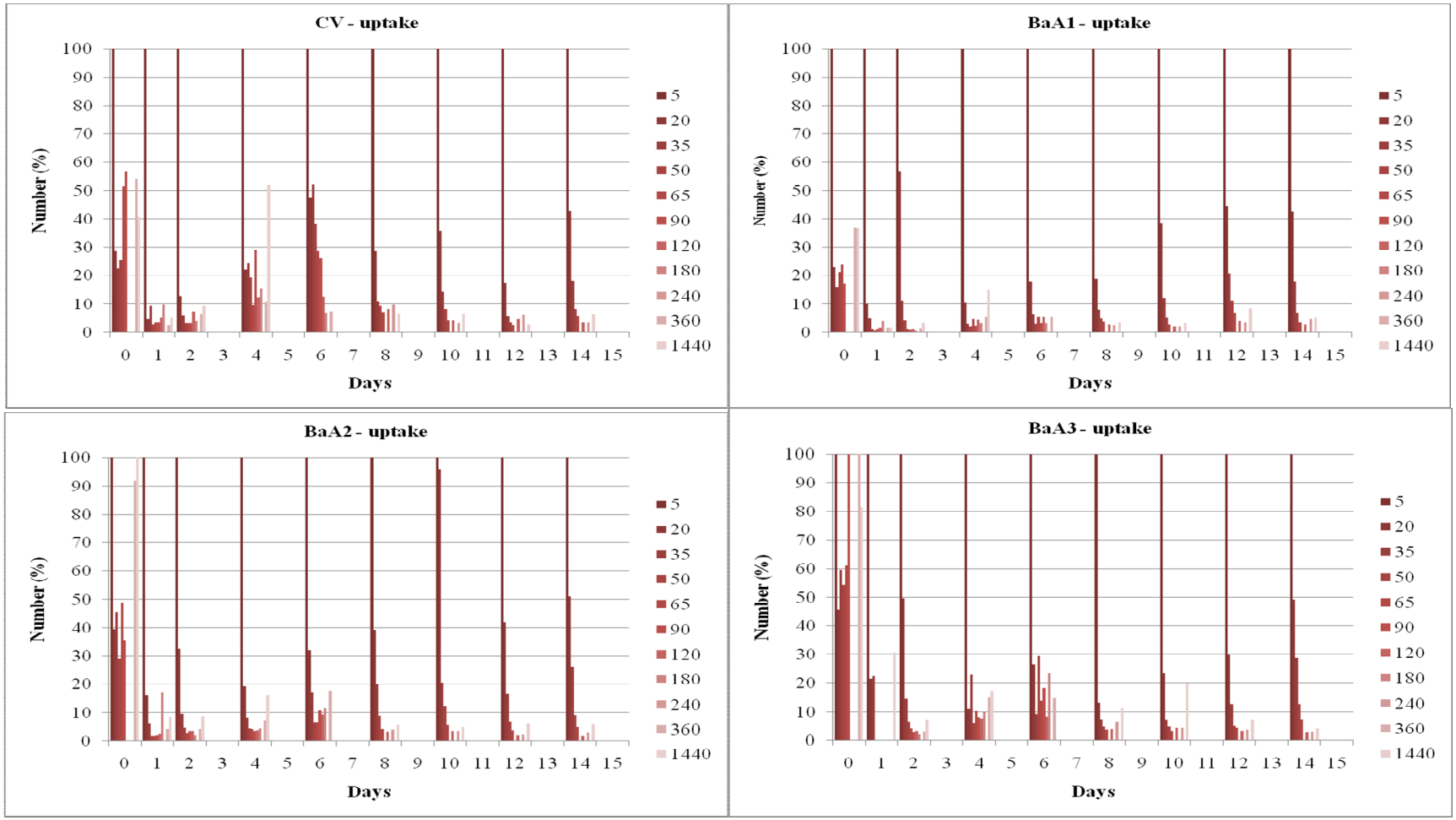

Figure 3.3 : Algae decrease in percentages versus days during BaA uptake at different sampling times.

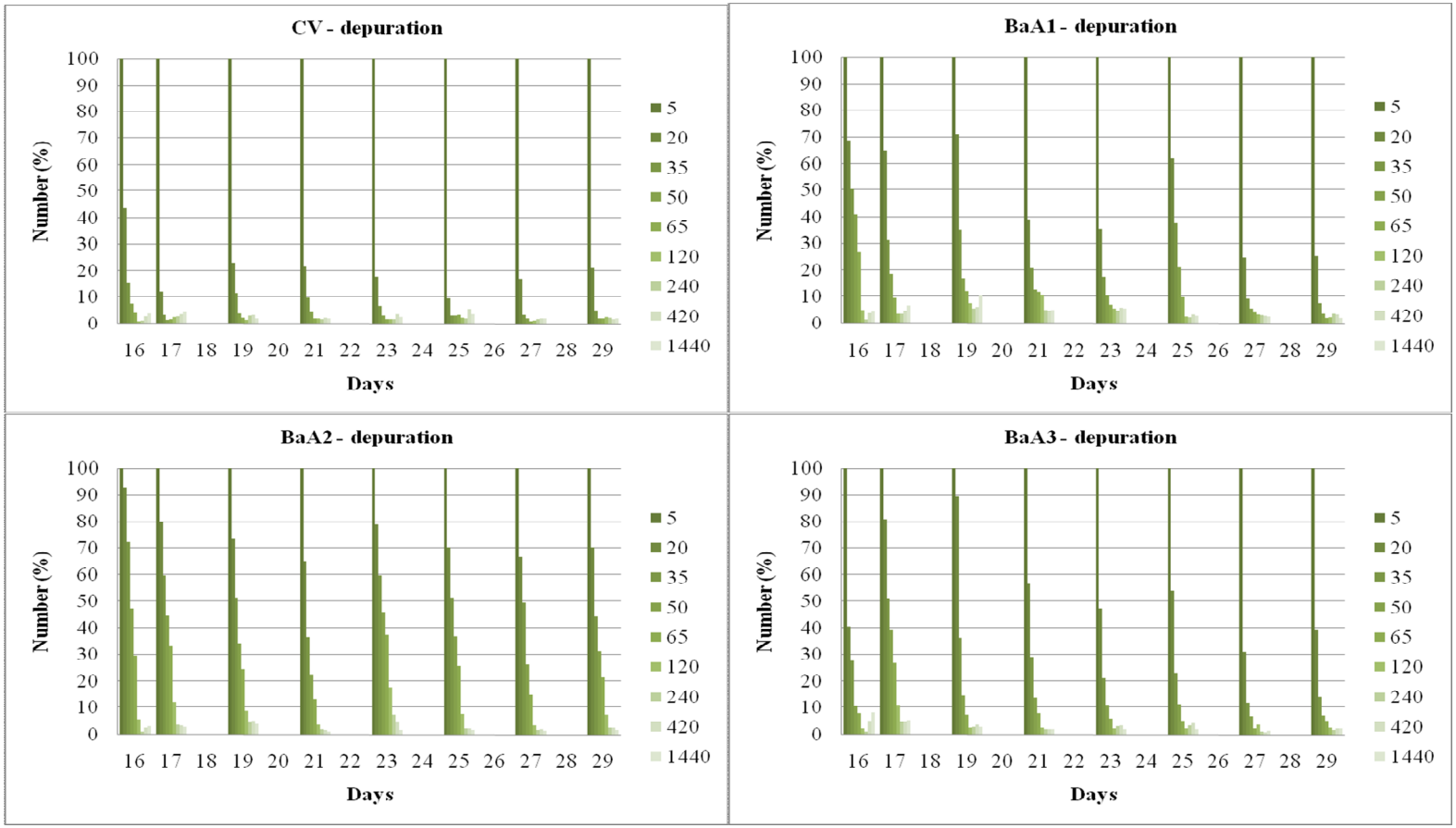

Figure 3.4 : Algae decrease in percentages versus days during BaA depuration at different sampling times.

The data in Table 3.5 also evaluated with two-way ANOVA statistical method. Alpha was taken as 0.05 which expresses %95 confidence interval and *p*-values were found as 0.0027 and 0.0034 for uptake and depuration periods, respectively. This implies that the decreases of particles in all aquariums are not same and significantly different from each other.

Table 3.5 : Particle numbers in percentages for each aquarium during the specific time intervals of uptake and depuration periods.

particle numbers in percentages (%)								
	during the uptake period				during the depuration period			
time (min)	CV	BaA1	BaA2	BaA3	CV	BaA1	BaA2	BaA3
5	100	100	100	100	100	100	100	100
20	30	31	44	34	22	50	75	57
35	18	11	17	17	8	27	53	28
50	12	5	8	9	4	17	36	15
65	9	4	5	6	2	11	25	9
90	11	2	4	6				
120	8	3	4	5	2	6	8	4
180	7	3	7	8				
240	9	4	5	5	2	4	3	3
360	5	3	7	7				
420					3	5	3	3
1440	10	6	8	12	3	5	2	3

In Figure 3.5, average decreases of particles are shown together for the whole experiment period, in order to be able to compare the organisms' responses. Although the decrease rate of particles are not so different for uptake and depuration periods, it was observed that the decrease rate of particles are getting slower in the depuration period in all aquariums except the CV aquarium which theoretically contains no BaA concentration inside. As a result, it can be said that selected PAH has a slowing effect on the depuration mechanism of mussels.

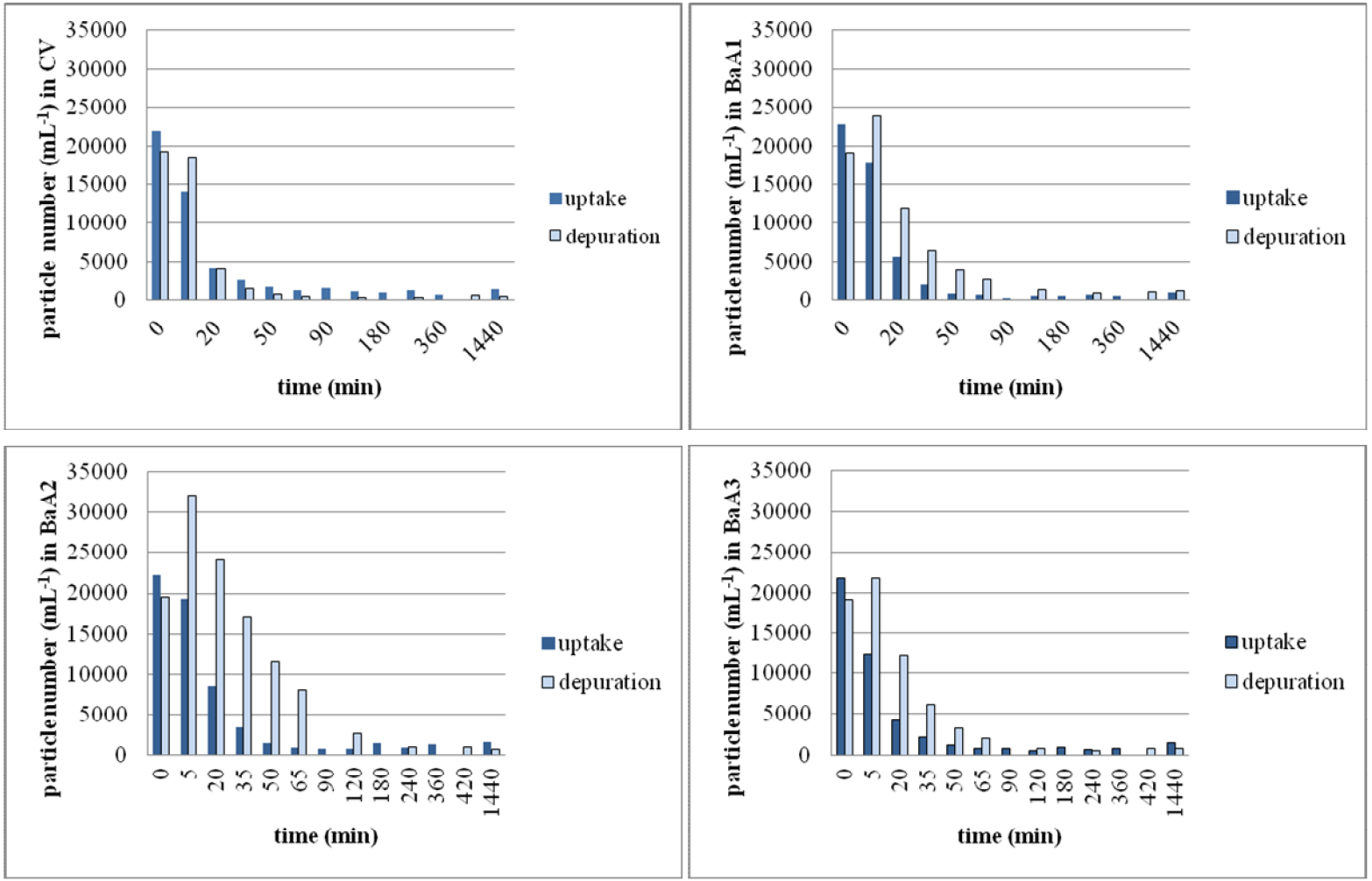

Figure 3.5 : Comparison of average values of particle decrease in all aquariums for the uptake and depuration periods.

3.3.2 BaA concentration in seawater

BaA concentrations in aquariums were measured at the same time intervals with the particle number in seawater. Average concentrations of BaA in aquariums were shown in Figure 3.6. A decrease of BaA concentration expresses the BaA uptake of mussels and this decrease was seen until two hours later of algae and BaA addition into the aquarium, from the time-concentration graphic of uptake period in Figure 3.6. After that time, a slight increase of BaA concentration was also measured which may be caused by the excretion of mussels. Reversely, an increase of BaA concentration in seawater was observed after 5 minutes in the time-concentration graphic of depuration period in Figure 3.6. Probably, this increase in seawater concentration is due to the excretion of BaA by the mussels. The depuration rate of BaA from the tissues is found slower compared to accumulation.

3.3.3 Relation between the consumption of algae and BaA in seawater

When daily BaA concentration graphs were observed, it can be said that BaA uptake rate of mussels was decreased day by day, except the first three days of BaA3 aquarium. The released amount of BaA from mussels into the seawater was also reduced in the depuration period due to the daily addition of clean seawater. Likewise the time-concentration graph of uptake period, the released amount of BaA is less than the uptake amount. The concentration difference in the uptake and depuration periods corresponds to the bioaccumulated BaA in mussel tissues.

The relationship of algae consumption with the remained BaA concentration in seawater is shown in Figure 3.7. Although the particles (algae) in seawater were consumed by the filtration of mussels, there is still some amount of BaA in seawater. This shows that not all of BaA added into the seawater was absorbed or adsorbed by the algal cells. At the depuration period, most of the BaA concentrations are between 0 (not detected) and 1 $\mu g\ L^{-1}$ BaA concentration due to the clean seawater addition. Although the algae were consumed, there is still some amount of BaA related with the particles in the aquarium at the depuration period. That can be caused due to the depuration of mussels by excretion of algae.

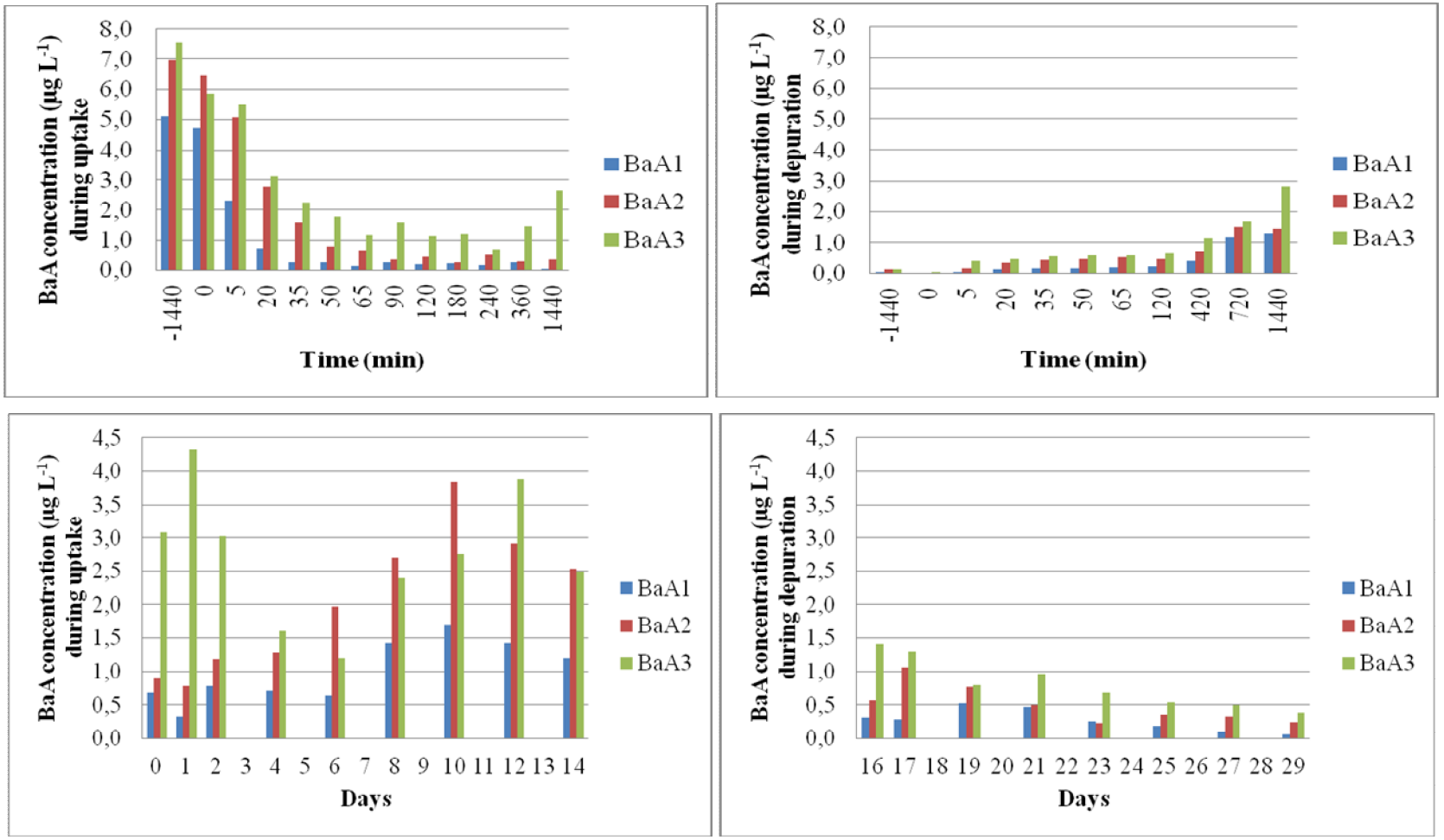

Figure 3.6 : Average BaA concentrations measured in aquarium seawater at specific time intervals during 1 day (1440 minutes) and whole experiment period.

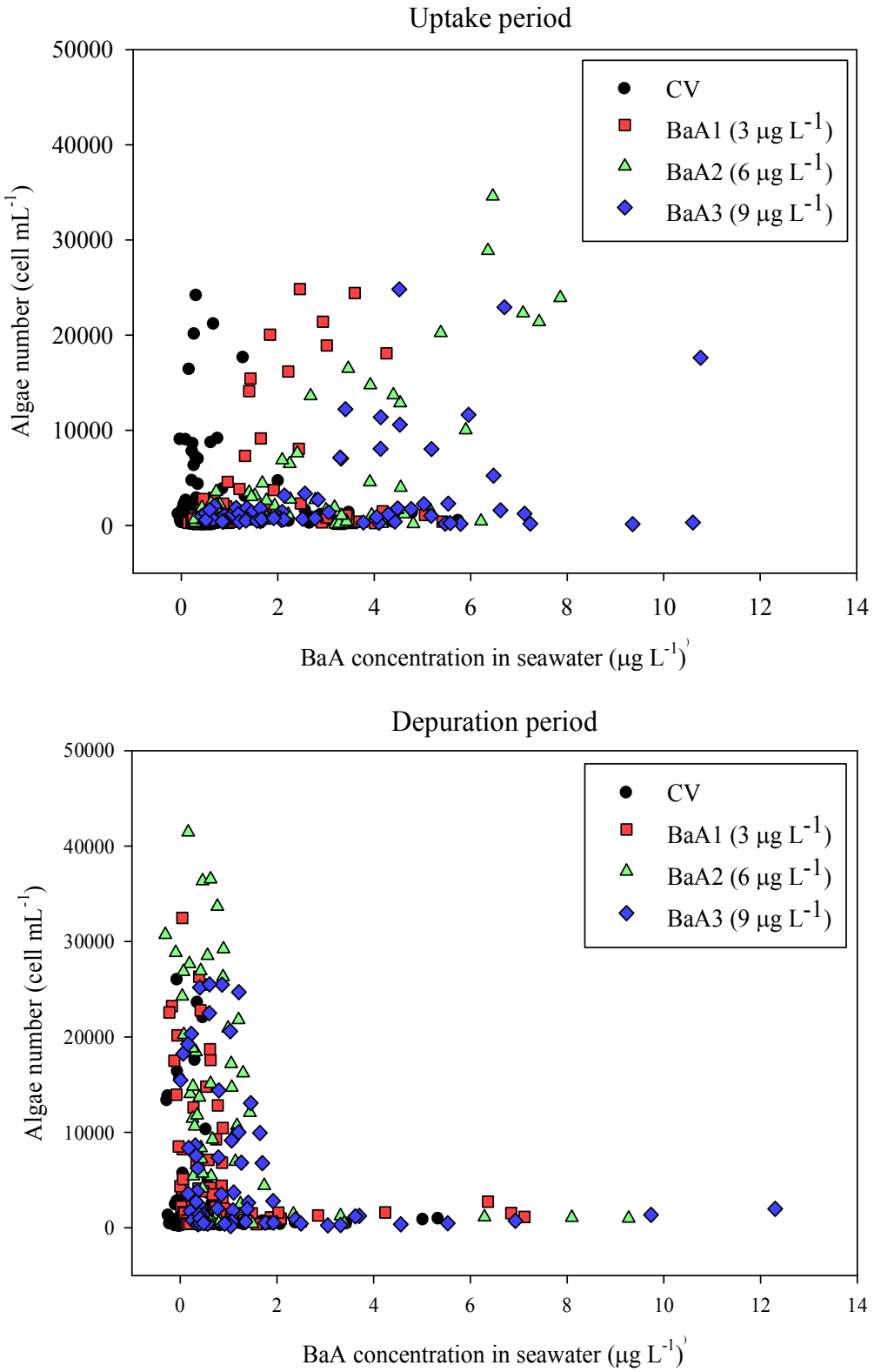

Figure 3.7 : Relationship of particle number and BaA concentration measured in seawater during uptake and depuration periods of all aquariums.

3.4 Results of Small Scale Experiments with PHE

3.4.1 Particle decrease in seawater

Percent particle decreases (percentages) versus sampling days and time intervals in minutes for uptake and depuration periods were shown separately in Figure 3.8 – Figure 3.11. Besides, in order to see the general trend of particle decrease, average values were also calculated and shown in Figure 3.12 and Figure 3.13.

The decrease of particles in the figures indicates the consumption of algae added into the aquariums. It can be said that the algae consumption of mussels increases as the percentage of particle decrease increases.

Figure 3.8 shows particle decrease by percentages versus sampling days at specific time intervals during the uptake period for four different PHE concentration spiked aquariums. Particle decrease is below 20% in the first 20 minutes of CV aquarium whereas for the rest of the aquariums this decrease is slower than CV aquarium. Nevertheless, after the first 65 minutes, it was observed that particle decrease is below 20% for all aquariums during the uptake period.

Figure 3.9 shows the particle decrease by percentages versus sampling days at specific time intervals in all aquariums during the depuration period. Specific difference was not observed for CV aquarium during the depuration period. Slightly rapid consumption of algae was observed for PHE1 aquarium compared with its uptake period. Slowdown of algae consumption at the end of the uptake period of PHE2 aquarium was replaced with a consumption increase at the end of the depuration period of PHE2 aquarium. A different trend was observed in PHE3 aquarium compared with PHE1 and PHE2 aquariums. At the beginning of the depuration period, a slowdown of algae consumption was observed at the beginning of the depuration period, possibly due to the negative effect of PHE uptake and slow adaptation of the organisms. Nevertheless, particle decrease reached below 20% after 120 minutes of water exchange.

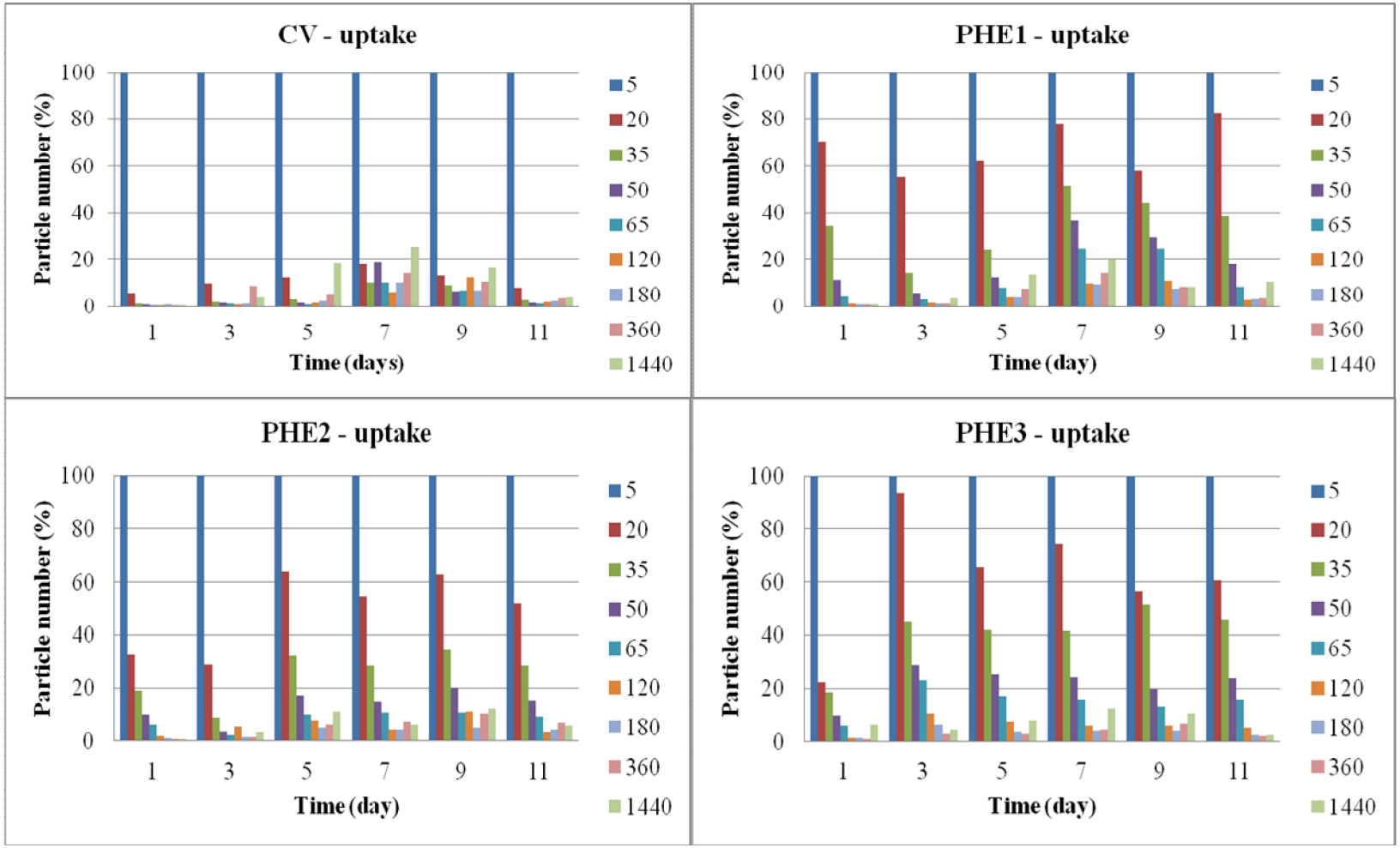

Figure 3.8 : Particle (5.32 - 16.07 µm) decrease in percentages versus days during uptake of PHE at various sampling times.

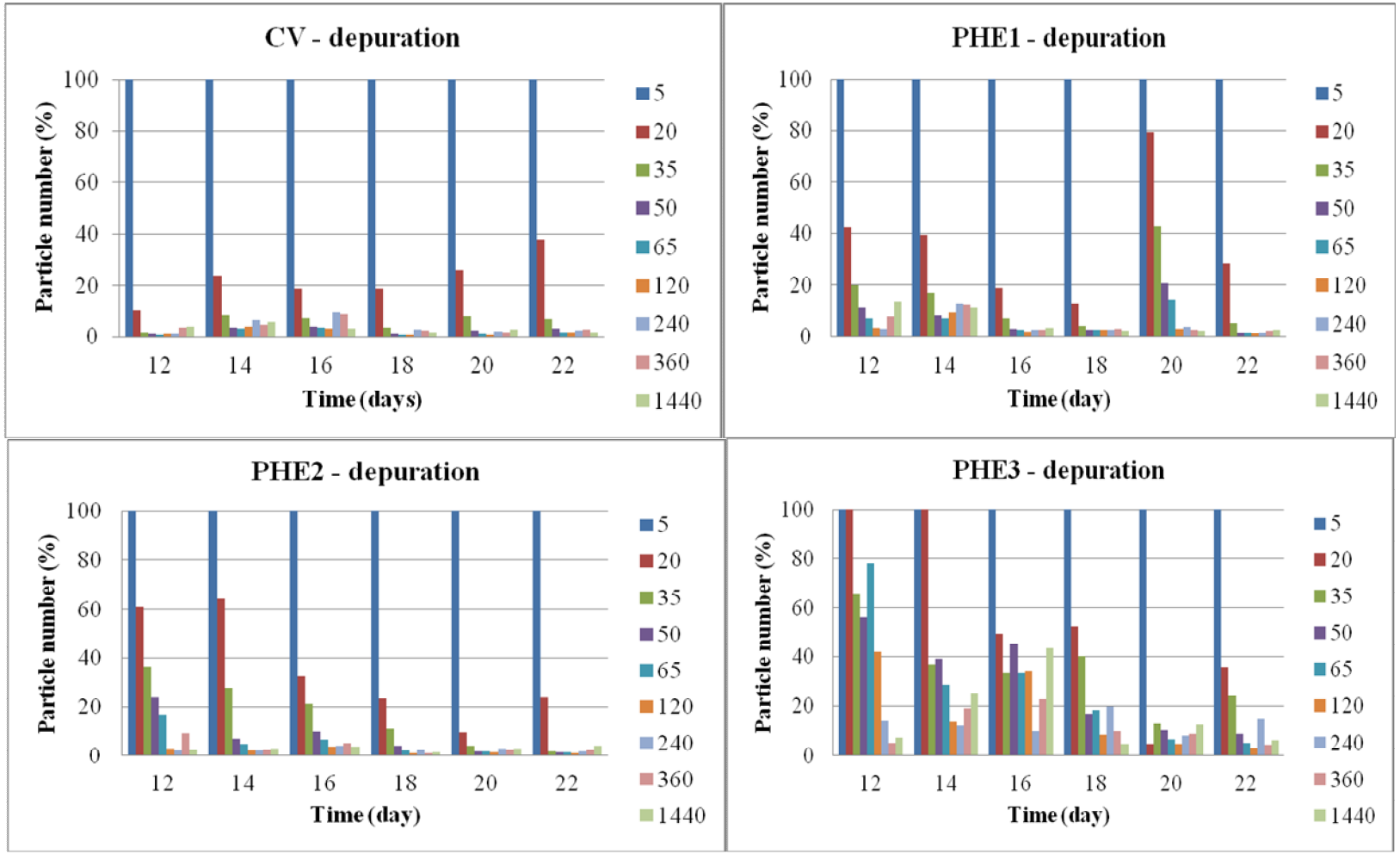

Figure 3.9 : Particle (5.32 - 16.07 µm) decrease in percentages versus days during depuration of PHE at various sampling times.

Figure 3.10 shows particle decrease by percentages versus specific time intervals during the sampling days of uptake period for four different PHE concentration aquariums. Particle decrease is below 20% in the first 20 minutes of CV aquarium likewise the results in Figure 3.8. Particle decrease is below 20% after 90, 50 and 90 minutes for PHE1, PHE2 and PHE3 aquariums, respectively. As a general view, although there is not an apparent difference between the sampling days, there is a slight decrease at the algae consumption at the last days of the uptake period compared with the first days of the uptake period. There is a slight but continuous increase of algae consumption which can be thought as the adaptation of mussels in PHE3 aquarium.

Figure 3.11 shows the percent particle decrease versus specific time intervals in all aquariums during the sampling days of the depuration period. There is a slight increase of algae consumption compared with the uptake period of CV aquarium. This difference can be explained with the spiked acetone into the CV aquarium during the uptake period. That was probably caused due to the depuration of the initial PHE concentration in mussels during the depuration period. Particle decrease is more rapid as expected in the depuration period of PHE1 and PHE2 aquariums. An oscillating trend is observed in PHE3 aquarium and particle decrease is decreased below 20% after 200 minutes of water change. This difference is possibly due to the negative effect of high PHE concentration and the slow adaptation of mussels to that concentration.

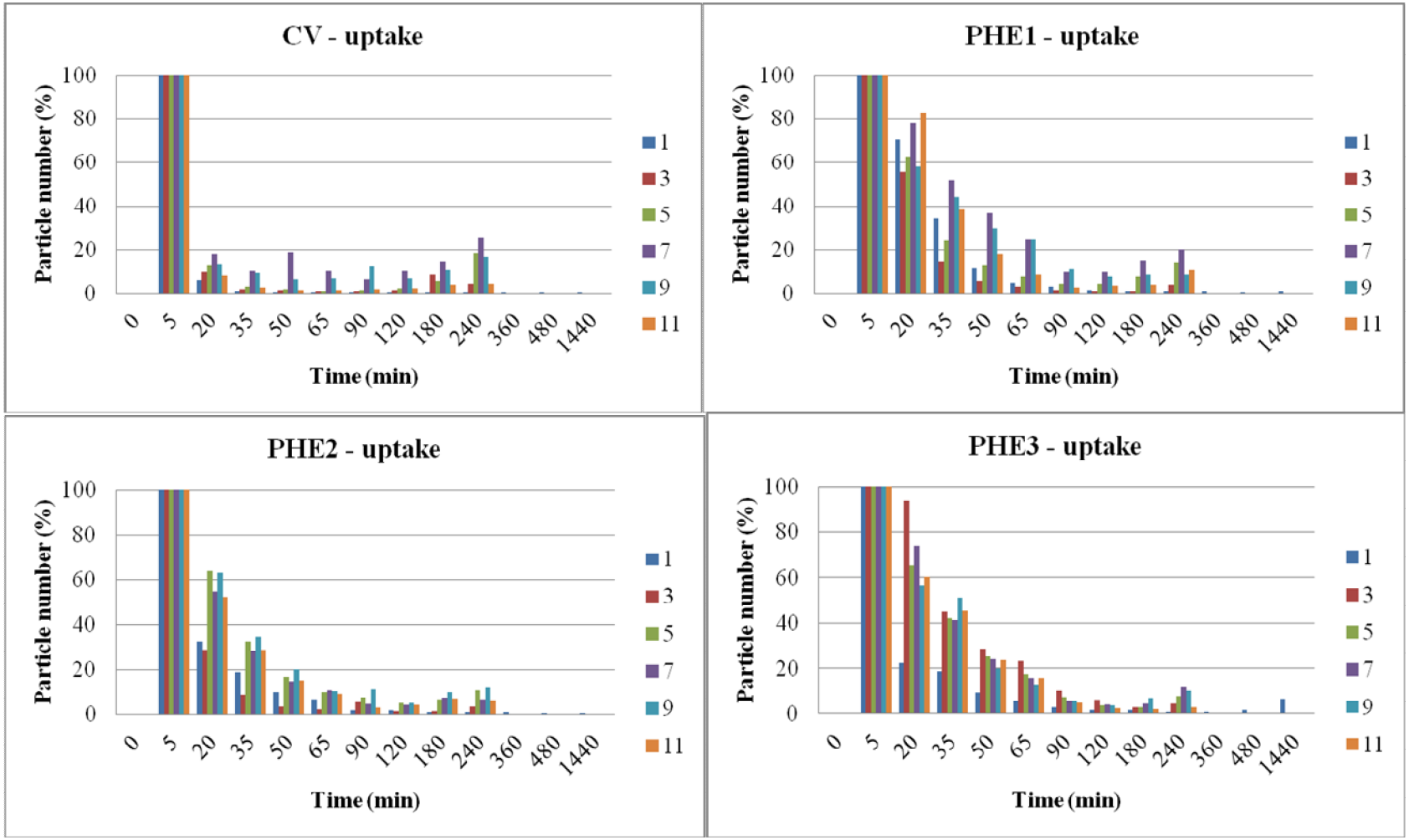

Figure 3.10 : Particle (5.32 - 16.07 µm) decrease in percentages within a day of PHE uptake at various sampling days.

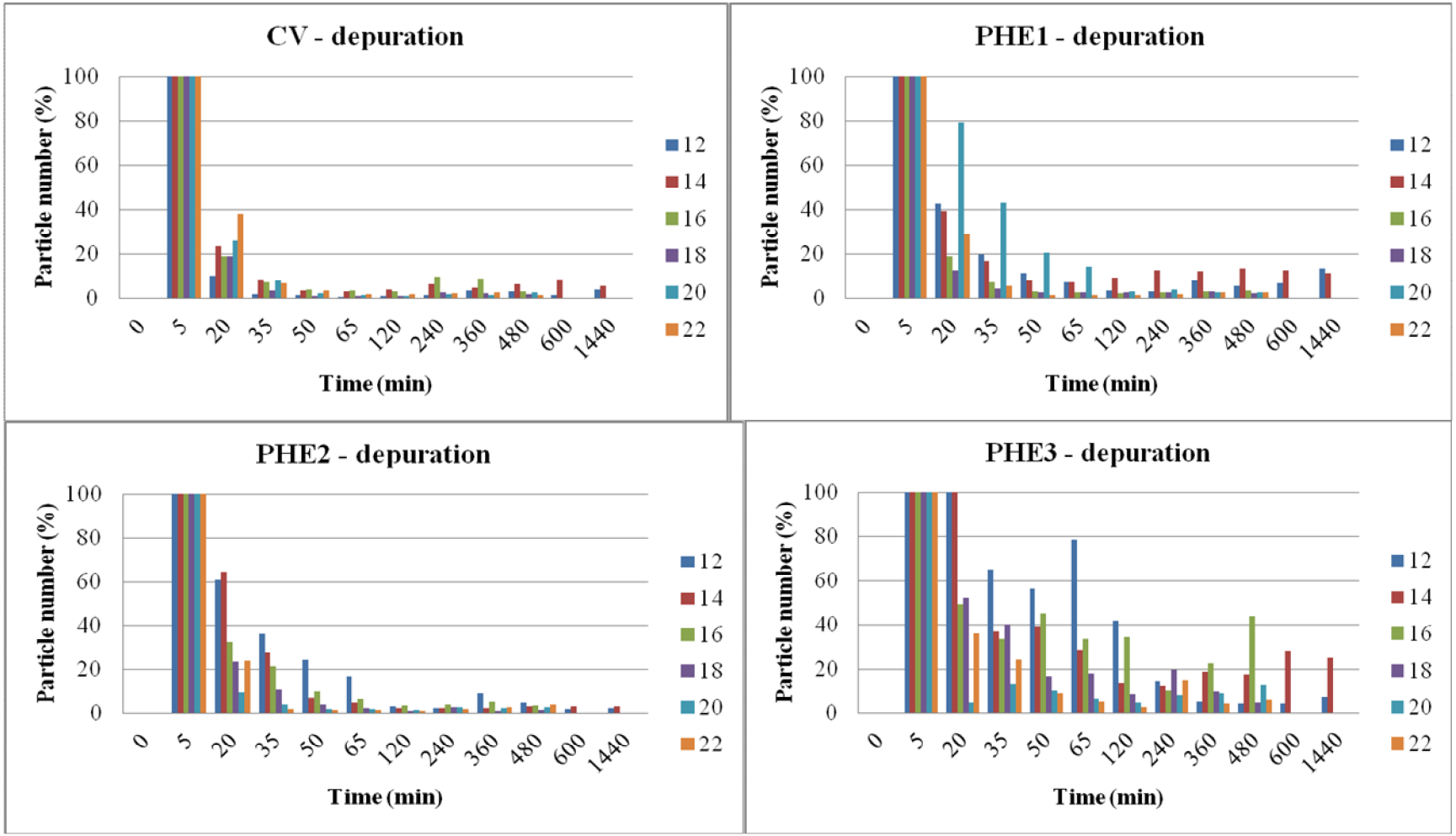

Figure 3.11 : Particle (5.32 - 16.07 µm) decrease in percentages within a day of PHE depuration at various sampling days.

Average decreases of particles by percentages are shown together for the uptake and depuration periods in Figure 3.12 and Figure 3.13 in order to be able to compare the behavior of the organisms for different periods.

Figure 3.12 shows particle decrease by percentages versus specific time intervals of sampling days for average values of uptake and depuration periods for four different PHE concentrations. Average values of percent particle number were observed lower in the depuration period compared with the uptake period for the aquariums of CV, PHE1 and PHE2 in contrast to PHE3 aquarium. Although the difference between the uptake and depuration periods was not apparent, decrease percentage of PHE3 aquarium is slower than other aquariums for both uptake and depuration periods.

Figure 3.13 shows the particle decrease by percentages versus sampling days at specific time intervals for average values of uptake and depuration periods for four different PHE concentration spiked aquariums. All average values were observed below 20% for CV aquarium during both of the periods. Average values in the uptake period were found higher than the values in the depuration period for PHE1 and PHE2 aquariums which is also compatible with Figure 3.12. On the contrary, the trend of PHE3 aquarium results is different. In general, average values of PHE1 and PHE2 aquariums are similar whereas the particle decrease in PHE3 aquarium is the slowest.

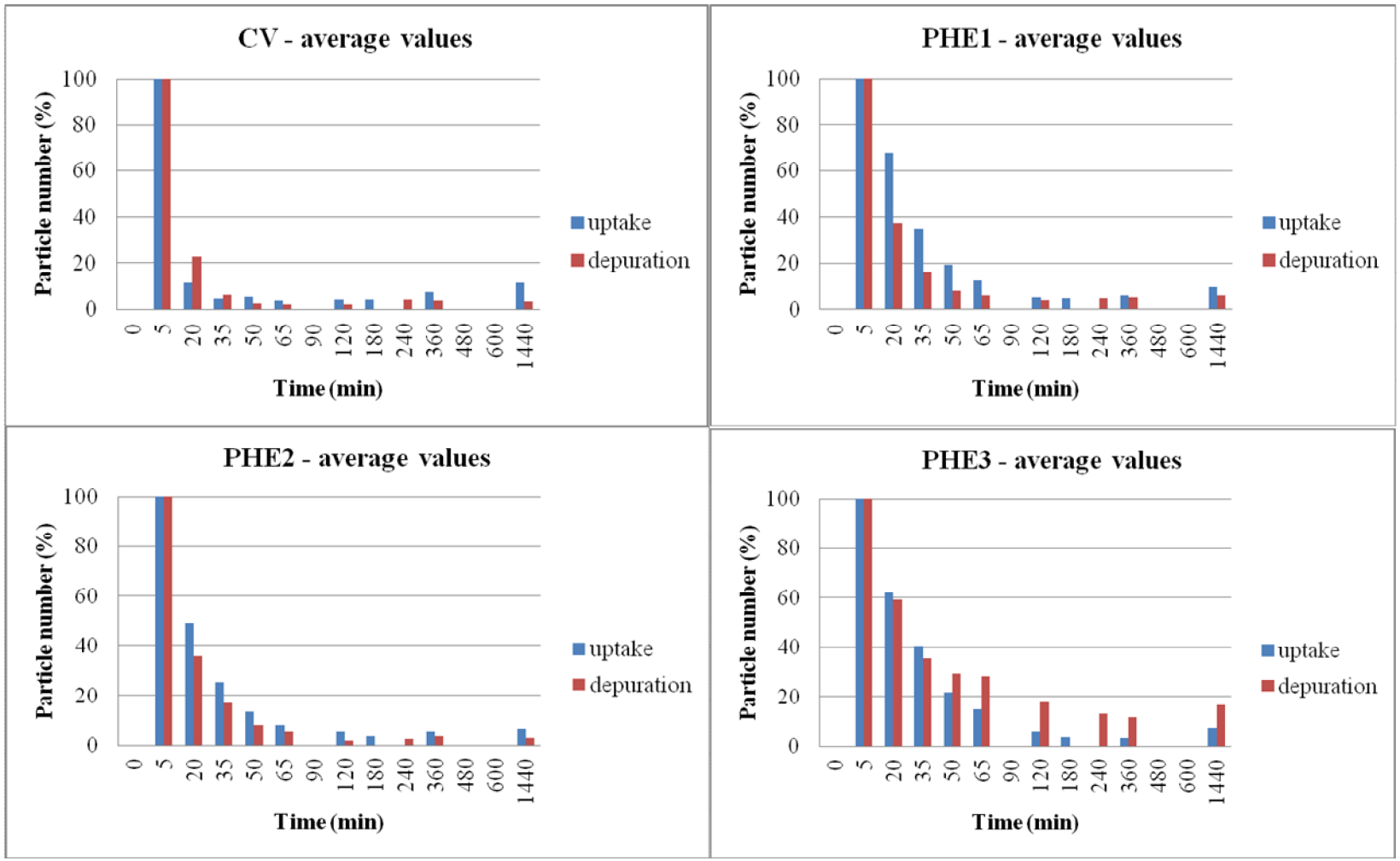

Figure 3.12 : Comparison of average values of particle decrease during uptake and depuration periods.

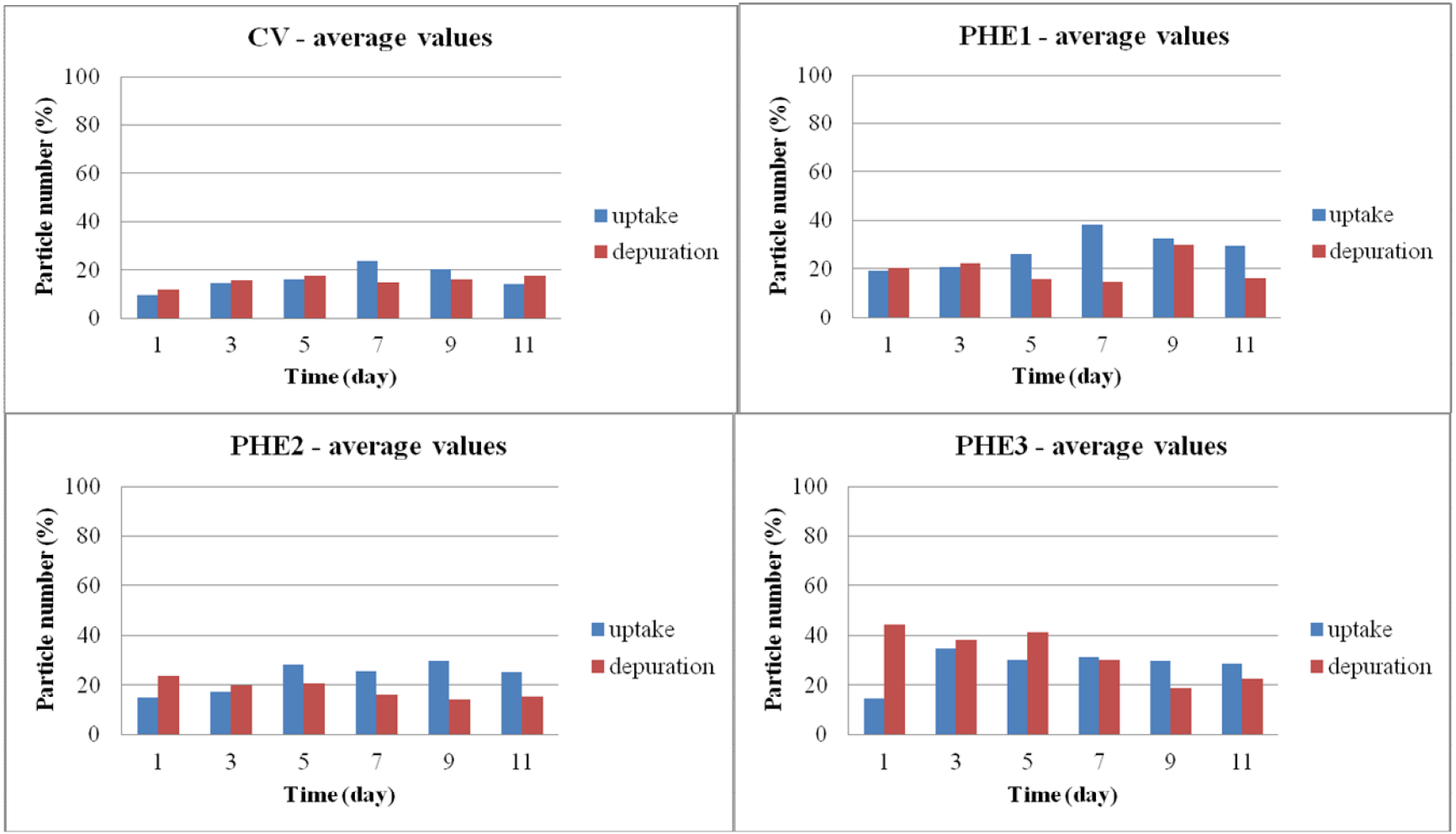

Figure 3.13 : Comparison of average values of particle decrease at sampling days of uptake and depuration periods.

3.4.2 PAH concentration in seawater

Measurements of PHE concentrations in seawater for each aquarium were presented in four different graphs in Appendix A. In these graphs, PHE concentrations in seawater versus time intervals during the sampling days of uptake and depuration periods are represented additional to PHE concentration in seawater versus sampling days at specific time intervals during uptake and depuration periods.

In Figure 3.14, PHE concentration in seawater by percentages versus both specific time intervals and sampling days were shown for the uptake period of PHE1, PHE2 and PHE3 aquariums. This figure can be evaluated similarly with Figure A.1 and Figure A.3 in Appendix A. Although there is not a clear change in PHE concentration, a general trend of PHE concentration decrease is observed for all aquariums which also indicates gradually bioaccumulation of PHE in mussel tissues. Especially at the first 65 minutes, PHE concentration in seawater decreases rapidly whereas PHE concentration in seawater reaches a constant value at the last hours of daily water exchange. This fact shows the bioaccumulation of PHE in the mussels, possibly through the algae consumption due to the positive correlation of algae density and PHE concentration in seawater. It should also be emphasized that the process of PHE transfer is seen more obvious than the figures in Appendix A due to the percentage conversion of represented values.

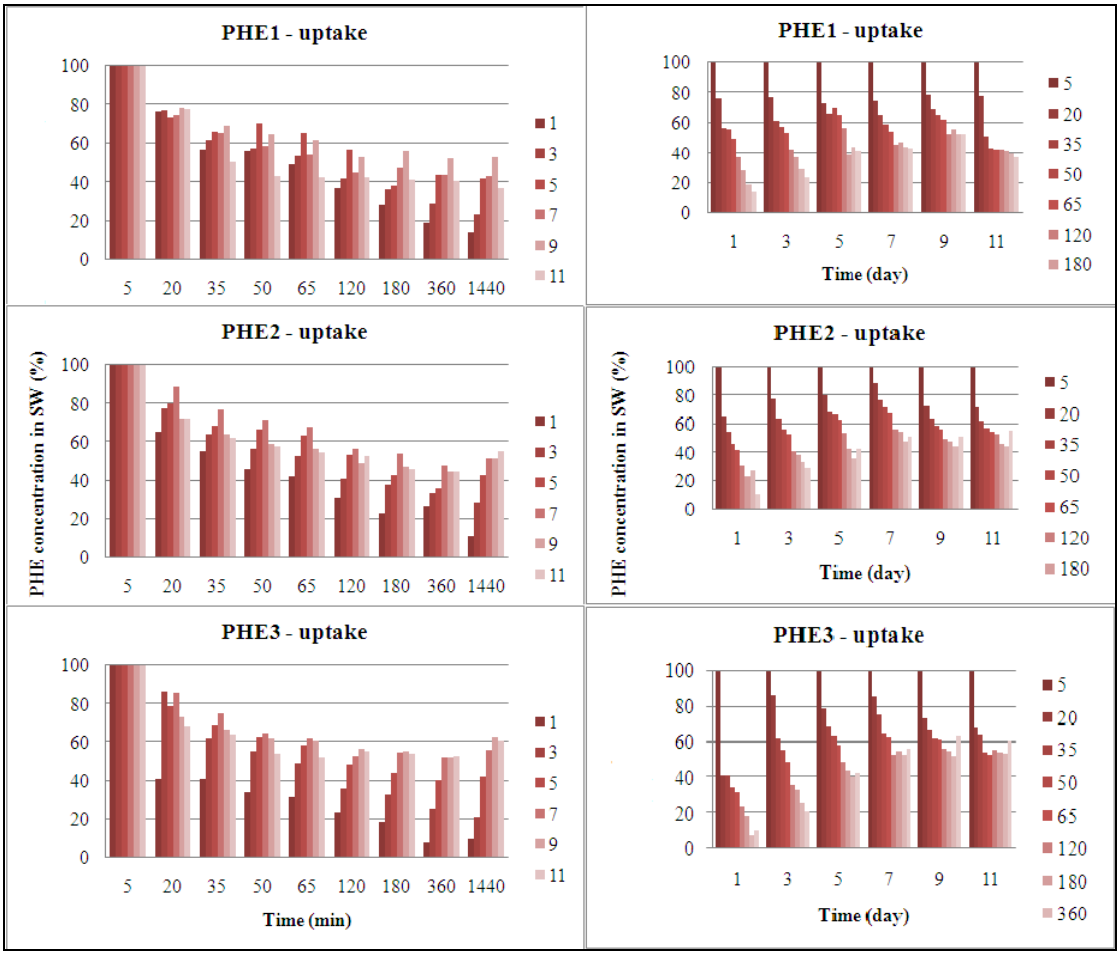

Figure 3.14 : PHE concentration in seawater by percentages during the uptake period of PHE spiked aquariums.

In Figure 3.15, average PHE concentrations in aquarium seawater versus both sampling days and specific time intervals during 24 hours are shown with standard deviations for the uptake period. The decrease of PHE concentration in seawater is seen clearly during the first 120 minutes of daily water exchange in Figure 3.15 (a). After 120 minutes, average values remain constant until the next water exchange. Nevertheless, daily change of average PHE concentration is not clear amongst the sampling days of uptake period as seen in Figure 3.15 (b).

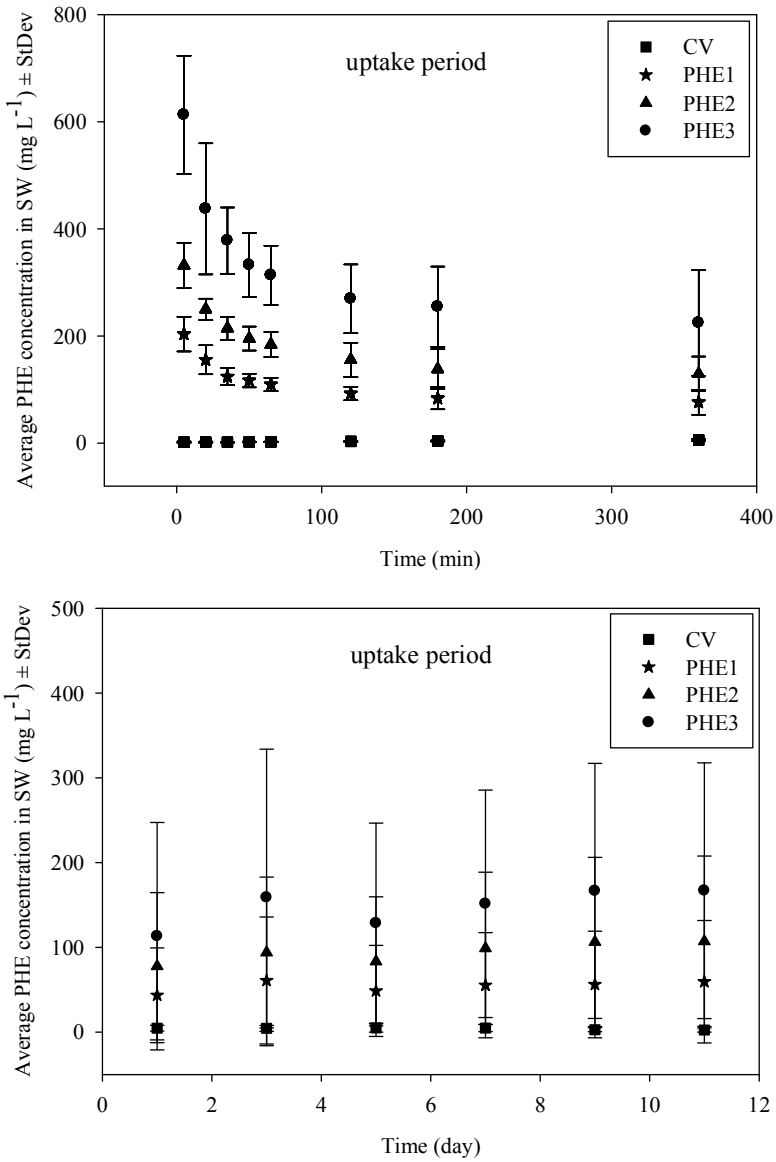

Figure 3.15 : Average PHE concentrations in seawater with standard deviations for all aquariums in 24 hours (above) and in sampling days (below) of the uptake period.

In Figure 3.16, average PHE concentrations in aquarium seawater versus both sampling days and specific time intervals during 24 hours are shown with standard deviations for the depuration period. Slow increase of PHE concentration in seawater is noticeable during the first 120 minutes of daily water exchange in Figure 3.16 (a). After 120 minutes, average values remain constant until the next water exchange. However, daily decrease of average PHE concentration is very clear at the depuration period as seen in Figure 3.16 (b), and after the 18th day average PHE concentration in mussels of PHE aquariums reaches to the same level with the mussels in CV aquarium.

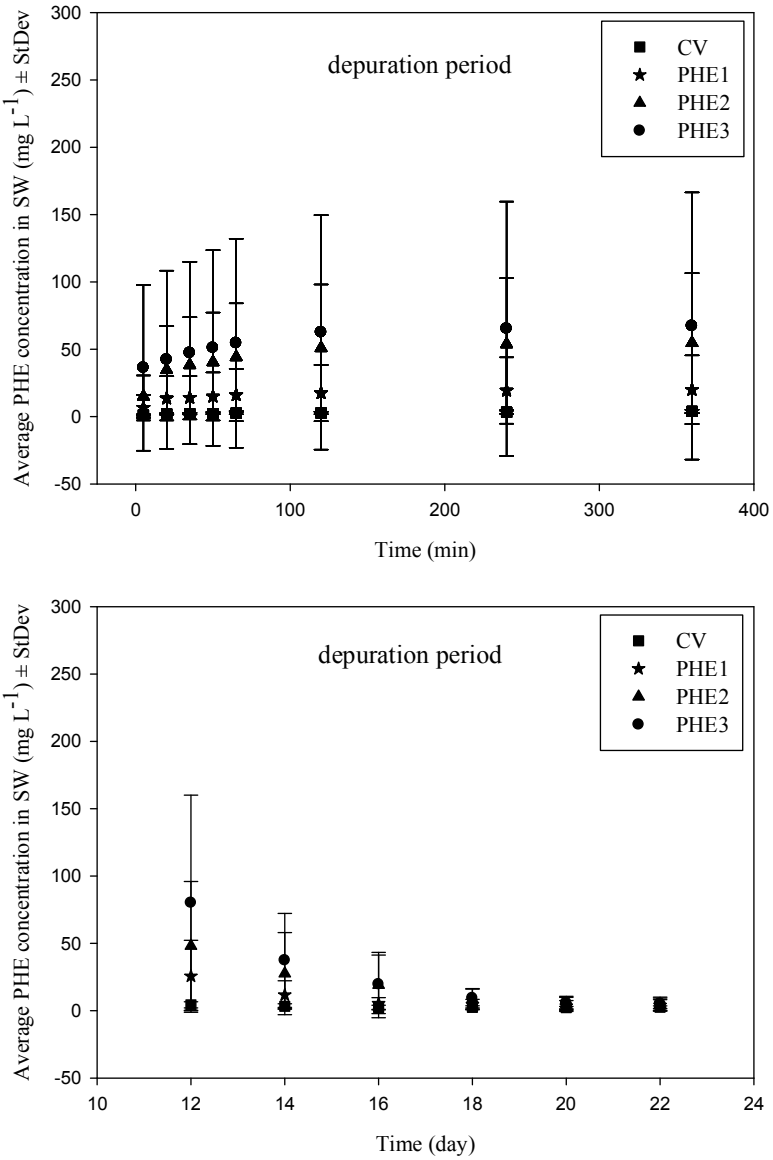

Figure 3.16 : Average PHE concentrations in seawater with standard deviations for all aquariums in 24 hours (above) and in sampling days (below) of the depuration period.

3.4.3 Relation between the consumption of algae and PHE in seawater

Particle number in seawater versus PHE concentration in seawater is shown in Figure 3.17 for all aquariums during both uptake and depuration periods.

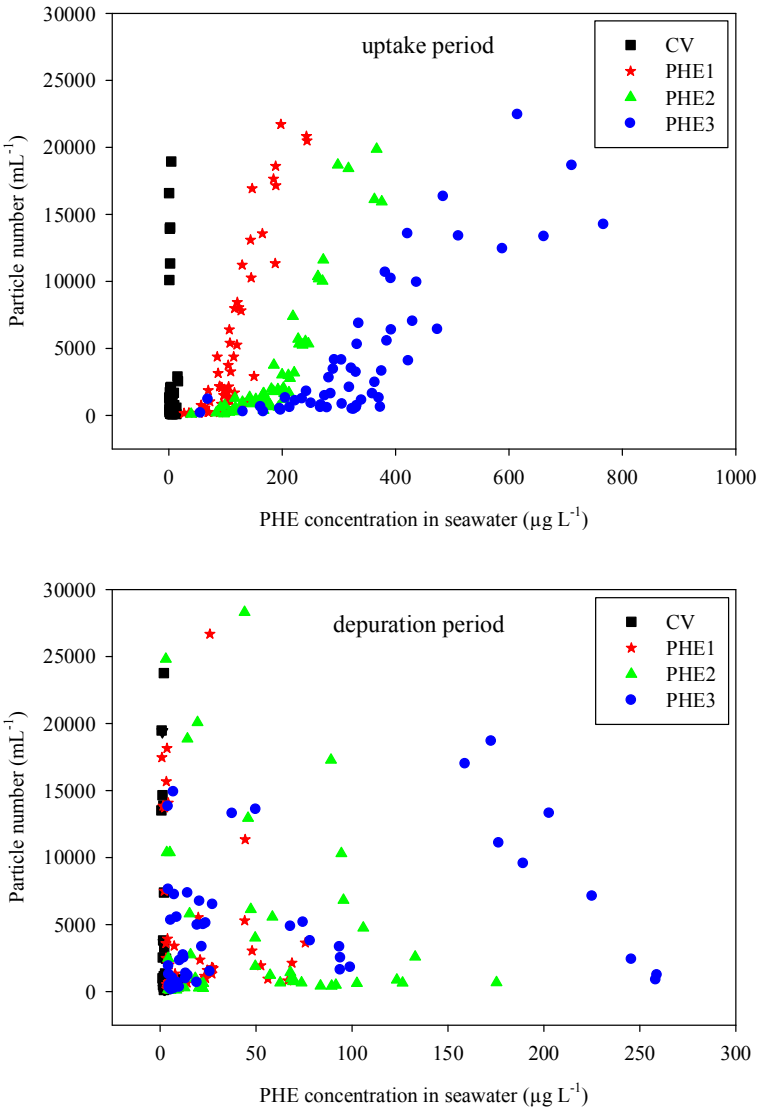

Figure 3.17 : Relationship of particle number and PHE concentration in seawater during uptake (above) and depuration (below) periods.

PHE concentration in seawater also decreases with the decrease of particle numbers due to algae consumption by mussels during the uptake period. Nevertheless, PHE concentration in seawater can still be measured independent from the particle number. This also indicates that all PHE spiked in seawater have not been absorbed by algae but some remained in seawater. In the depuration period, due to the depuration of mussels, a slight increase of PHE concentration was observed with the decrease of particles in seawater.

Figure 3.18 and Figure 3.19 are detailed representations of Figure 3.17 for uptake and depuration periods separately. The daily decrease of PHE concentration in seawater depending on the particle number during the uptake period can be clearly

observed in Figure 3.18 for all aquariums. Even though all particles were consumed, PHE concentration in seawater still can be measured. This fact shows that not all PHE was absorbed by organic particles (algae) in the system but some amount of PHE remained in seawater. In Figure 3.19, relationship between particle number and PHE concentration in seawater is seen (daily measurements). Due to the daily exchange of clean water in the depuration period, PHE concentration in seawater was found under the detection limits at the last days of depuration period. Another point to be paid attention is the negative correlation of particle number with PHE concentration in seawater. Although algae consumed by mussels are not exposed to PHE, mussels release PHE into the seawater during the depuration period due to the previous bioaccumulation of PHE.

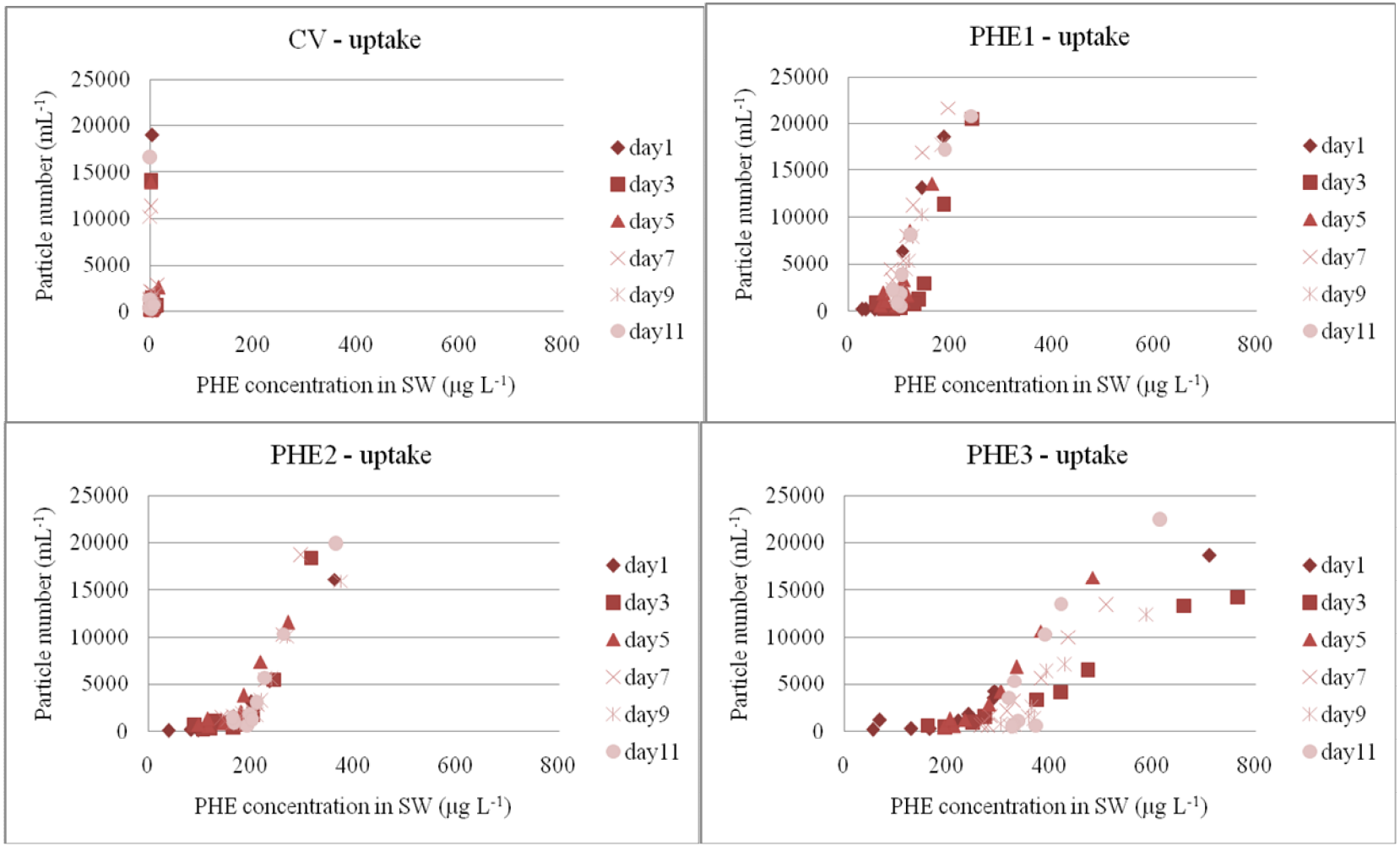

Figure 3.18 : Relationship of particle number with PHE concentration in seawater during the uptake period.

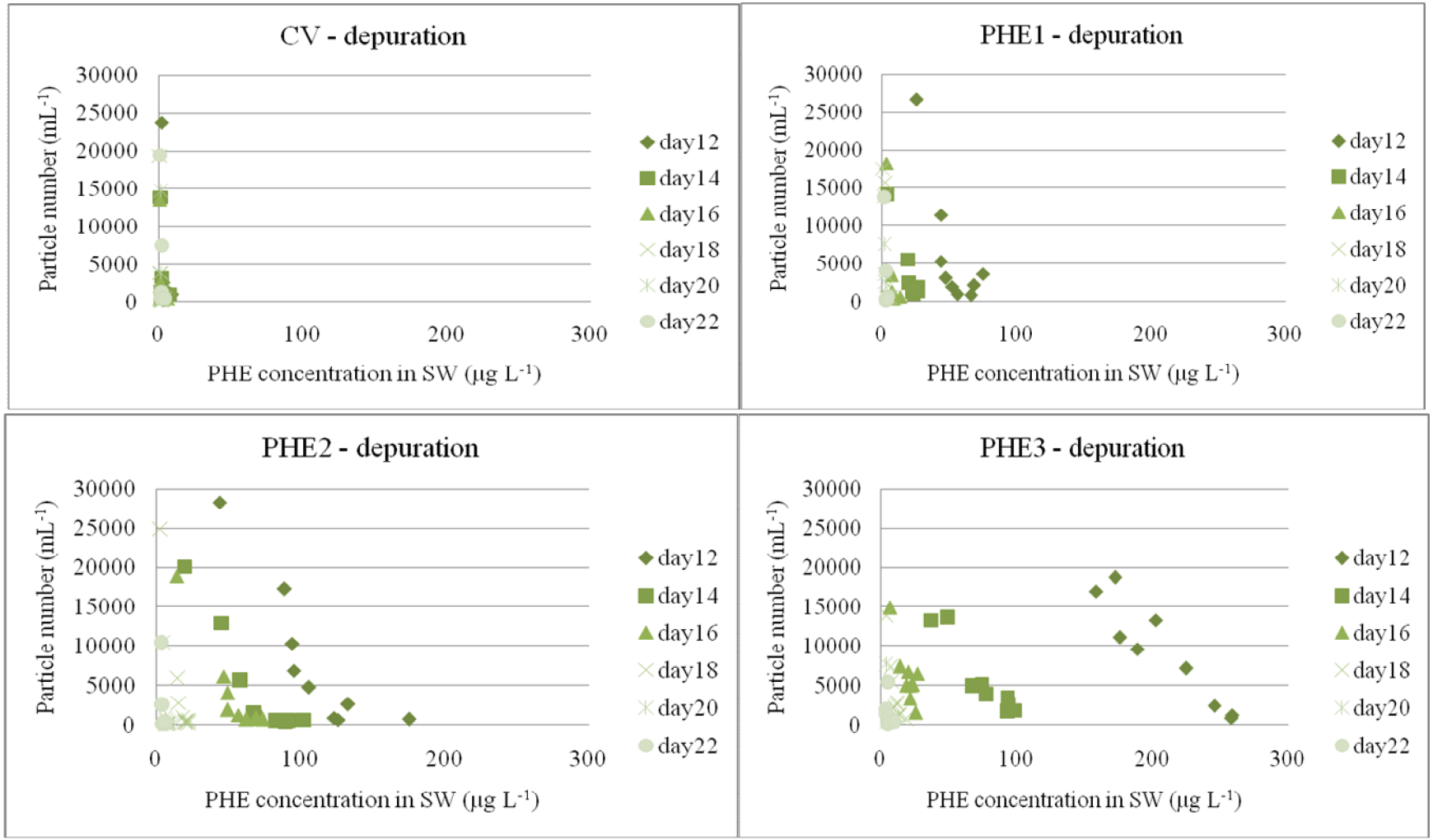

Figure 3.19 : Relationship of particle number with PHE concentration in seawater during the depuration period.

In Figure 3.20, rate constants of particle numbers in seawater versus time are shown for uptake and depuration periods for all aquariums. When all data in the graphs were evaluated, it is seen that there is not a clear difference in rate constants of the aquariums calculated by using the particle numbers.

In Figure 3.21, rate constants of PHE concentration in seawater versus time are shown for uptake and depuration periods for all aquariums. During the uptake period, rate constants of PHE spiked aquariums are similar with each other, except CV aquarium. Daily change of rate constants during uptake period was almost in the same level whereas in depuration period, the rate constants decrease rapidly and reaches to zero almost after 120 minutes.

In the depuration period, a gradual difference is observed between the aquariums until the 9^{th} day, after that day all rate constants becomes zero. Rate constants in the depuration period are observed almost similar to the rate constants in the uptake period in the rate constant versus time (min) graph.

As a summary, rate constants calculated by using the particle numbers and PHE concentrations were found similar for all aquariums.

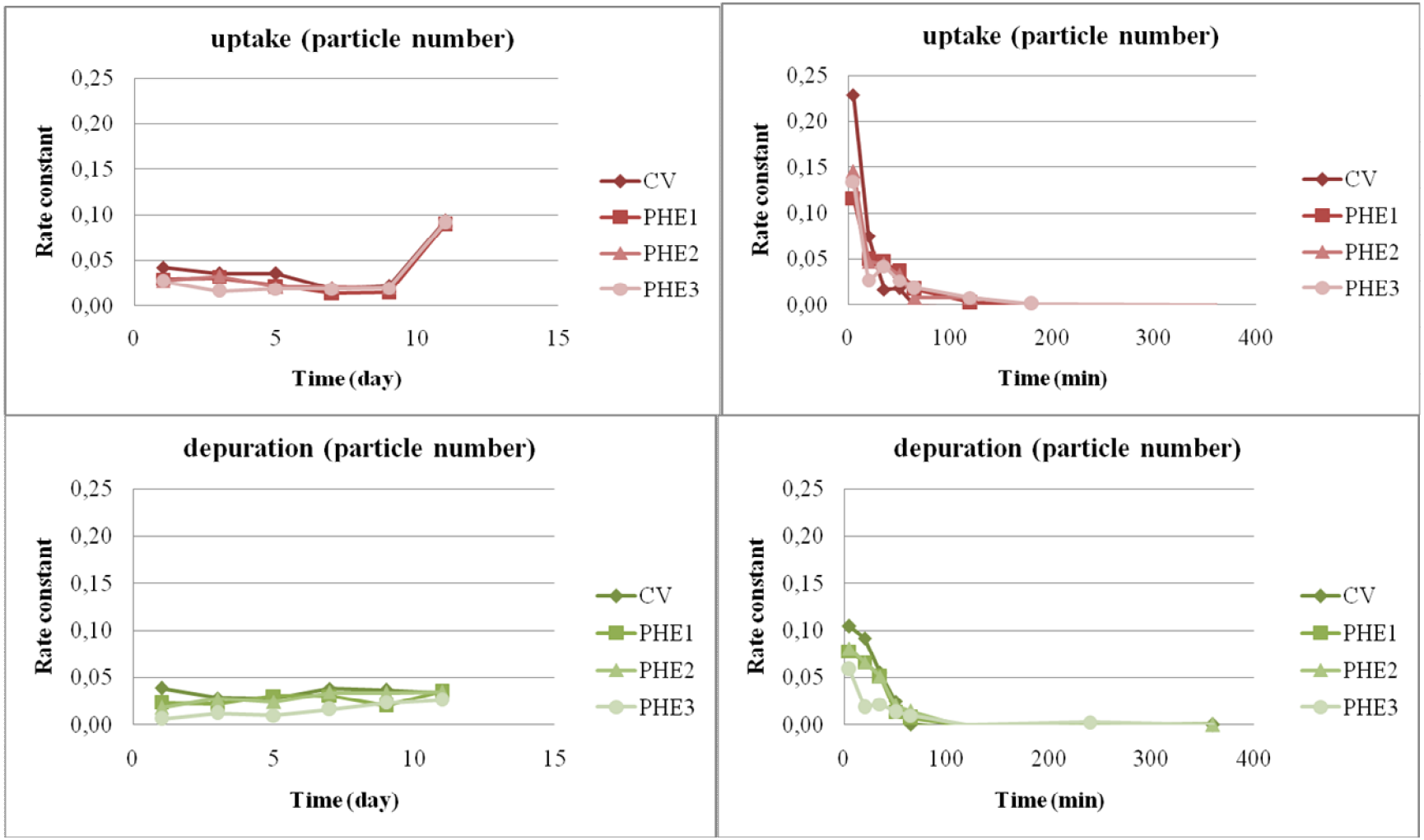

Figure 3.20 : Rate constants of particle number decrease for all aquariums during both uptake and depuration periods.

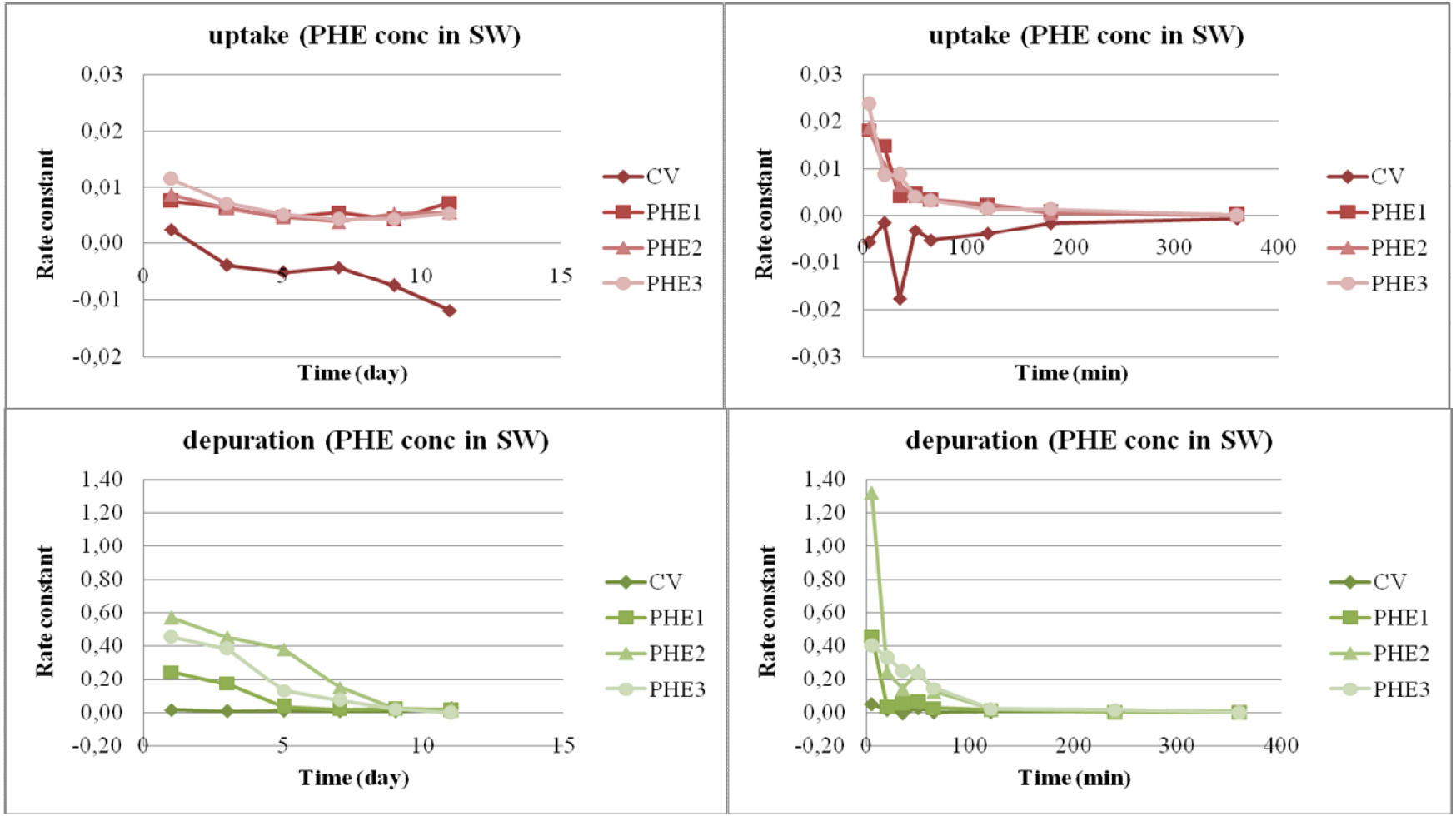

Figure 3.21 : Rate constants of PHE concentration decrease and increment for all aquariums during both uptake and depuration periods, respectively.

3.5 Results of Biomarkers in the Large Scale Experiments

3.5.1 Filtration rates of mussels exposed to BaA

Filtration rates (FRs) of BaA exposed aquariums during the exposure and depuration periods are shown together in Figure 3.22 (mean +1 SE, n=6). The figure is divided into two sections with a line; the left side shows the uptake period while the right side shows the depuration period. Filtration rates in the control aquarium (CV) ranged from 1.39 to 3.46 L hour^{-1}mussel^{-1}. FRs ranged from 0.85 to 3.17 L hour^{-1} mussel^{-1}, from 1.76 to 3.88 L hour^{-1}mussel^{-1}, and from 2.28 to 3.55 L hour^{-1}mussel^{-1} for 3.0 µg L^{-1}, 6.0 µg L^{-1} and 9.0 µg L^{-1} BaA concentrations (BaA1, BaA2 and BaA3 aquariums), respectively.

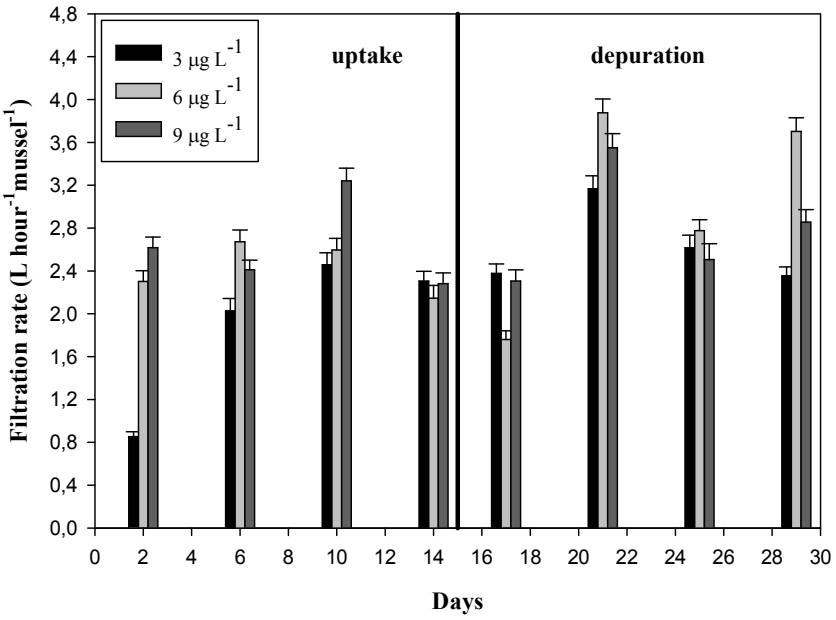

Figure 3.22 : Filtration rate (FR, L hr^{-1} mussel^{-1}) values of mussels (*Mytilus galloprovincialis*) exposed to 3.0, 6.0, 9.0 µg L^{-1} BaA with standard errors during a total of 29-day benzo(a)anthracene (BaA) uptake and depuration periods.

Filtration rates of mussels at different BaA concentrations and sampling days are shown in Table 3.6. Mean, standard deviation and standard error values are also calculated additional to the average filtration rates of each aquarium in Table 3.6. The effect of BaA in filtration rate is not obvious although there are slight differences between the measurements. One apparent result from Figure 3.22 and Table 3.6 is the rates in the depuration period are higher compared with the rates in the uptake period.

Table 3.6 : Average filtration rates (L h^{-1}) of mussels exposed to different concentrations of BaA (3, 6, 9 µg L^{-1} BaA with a control vehicle).

Filtration Rates (Liter $hour^{-1}$)				
day/aquarium	CV	BaA1	BaA2	BaA3
0	2.09	2.09	2.09	2.09
3	1.78	0.91	2.63	2.41
7	2.99	2.07	2.11	2.32
11	1.40	2.15	2.49	3.03
15	3.16	2.03	1.87	2.29
18	2.44	2.42	1.82	2.20
22	3.00	3.13	3.88	3.34
26	3.44	2.37	2.89	2.05
30	3.14	2.30	3.72	2.58
Mean	2.60	2.16	2.61	2.48
std deviation	0.71	0.58	0.76	0.44
std error	0.24	0.19	0.25	0.15

Average filtration rates of mussels in different BaA aquariums during uptake and depuration periods are shown in Table 3.7. Filtration rates of the mussels in CV aquarium were similar for uptake and depuration periods with average values of 2.48 (±0.69) and 3.19 (±0.38) L $hour^{-1}mussel^{-1}$, respectively. The addition of carrier solvent acetone was stopped in the control aquarium, due to the lack of acetone in BaA exposed aquariums during the depuration period. The slight increase in the filtration rates during depuration may have resulted from the lack of acetone in CV aquarium. According to previous field studies performed with the same size and species of mussels, a healthy mussel is known to filter 2-3 L of water per hour (Okay et al, 2003, 2006; Karacik et al, 2009). The values obtained for control mussels are similar to those values reported in the literature for healthy mussels in the same size. Additionally, BaA concentrations did not show any significant effect on the filtration rates of mussels (p=0.09, two-way ANOVA). This observation implies that BaA concentrations used in this study did not show any remarkable effect on the FR of mussels.

Table 3.7 : Average filtration rates (FRs, L hr^{-1} $mussel^{-1}$) of benzo(a)anthracene (BaA)- exposed mussels (*Mytilus galloprovincialis*) by exposure concentrations and time periods of exposure (mean +1 SD). CV is the control-carrier exposure with 0.3 mL L^{-1} acetone.

	Average Filtration Rates ± SD (Liter $hour^{-1}$ $mussel^{-1}$)	
	Uptake	Depuration
CV	2.48 (±0.69)	3.19 (±0.38)
BaA1	1.91 (±0.63)	2.63 (±0.33)
BaA2	2.43 (±0.21)	3.03 (±0.84)
BaA3	2.64 (±0.37)	2.80 (±0.47)

Average filtration rates of all aquariums are shown briefly with numerical values in Table 3.7 and with graphical representation in Figure 3.23.

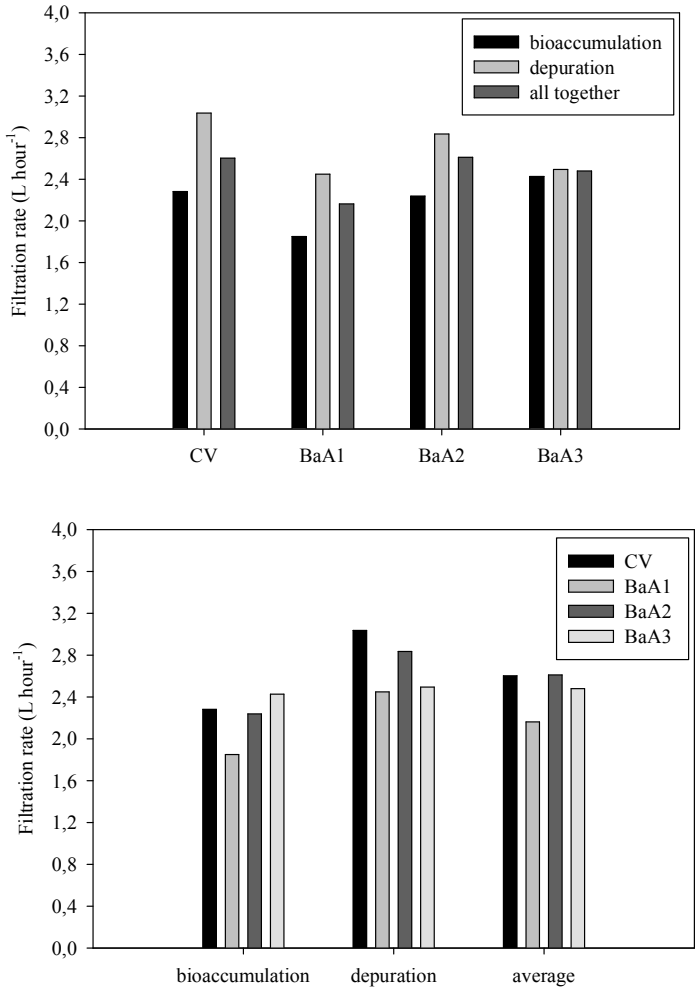

Figure 3.23 : Average filtration rates of BaA exposed mussels with a control aquarium during uptake and depuration periods.

3.5.2 Filtration rates of mussels exposed to PHE

Filtration rates (FR) of mussels during the uptake and depuration periods of PHE are shown in Figure 3.24 (mean ±1.96 SE, n=6). FR of the mussels used in exposure experiments after the acclimation period were found as 1.7 ± 0.60 L hour^{-1} mussel^{-1} (mean ± SD, n=10). Two different periods were separated with a solid line in Figure 3.24. FR of mussels in CV, PHE1, PHE2 and PHE3 aquariums ranged from 1.5 to 2.8 L, from 0.6 to 2.4, from 0.5 to 2.8, and from 0.4 to 2.1 in terms of L hour^{-1} mussel^{-1}, respectively.

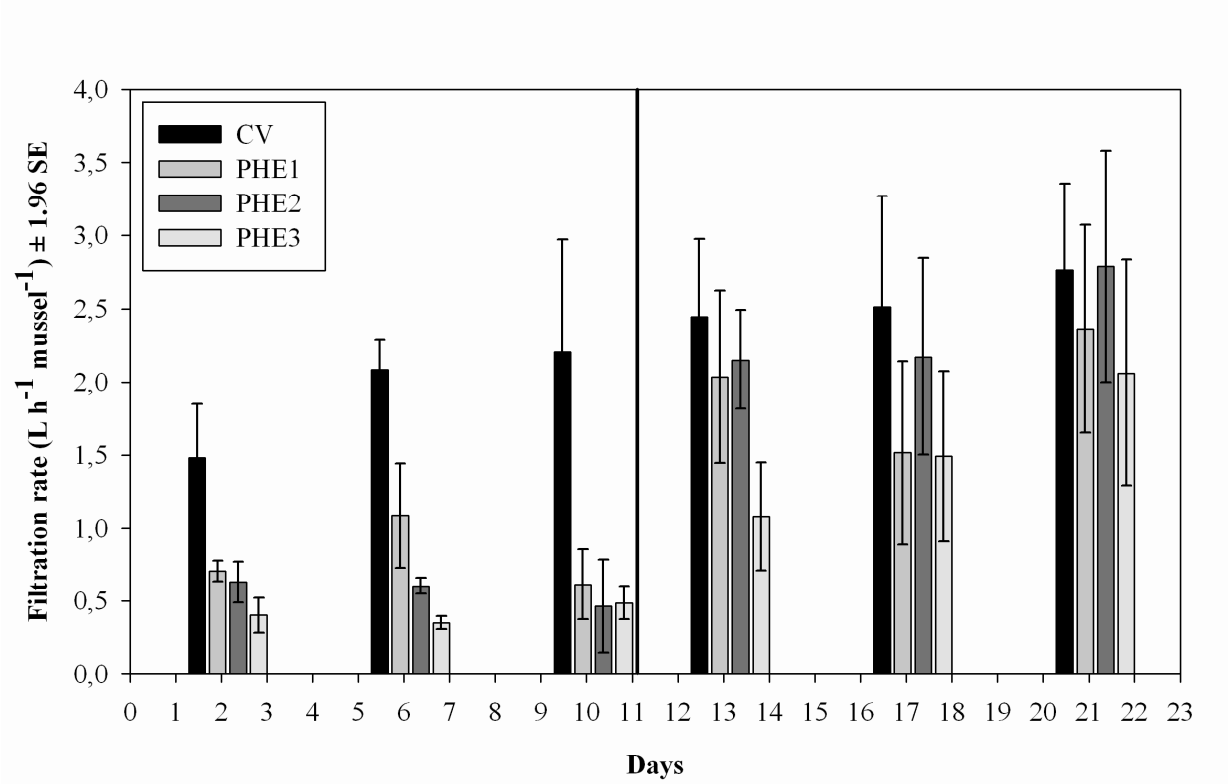

Figure 3.24 : Filtration rates (FR, L hr^{-1} mussel^{-1}) of mussels (*Mytilus galloprovincialis*) exposed to 250, 500, 1000 µg L^{-1} PHE with standard errors during a total of 22-day uptake (left side) and depuration (right side) periods.

Average filtration rates of mussels in different PHE aquariums throughout the uptake and depuration periods are shown in Table 3.8 and Figure 3.25. Comparison of the FR measurements during uptake and depuration periods reveals apparently the negative effect of PHE on FR of the mussels as seen in Figure 3.24 and Figure 3.25.

Table 3.8 : Average filtration rates (FRs, L hr^{-1} $mussel^{-1}$) of mussels (*Mytilus galloprovincialis*) exposed to 250 (PHE1), 500 (PHE2) and 1000 (PHE3) µg L^{-1} nominal values of phenanthrene (PHE) during time periods of uptake and depuration (mean ± 1 SD). CV is the control-carrier exposure with 0.4 ‰ acetone.

	Average filtration rates (L h^{-1} $mussel^{-1}$) ± SD, n=18	
	Uptake	Depuration
CV	1.9±0.68	2.6±0.76
PHE1	0.8±0.36	2.0±0.84
PHE2	0.6±0.25	2.4±0.80
PHE3	0.4±0.13	1.6±0.82

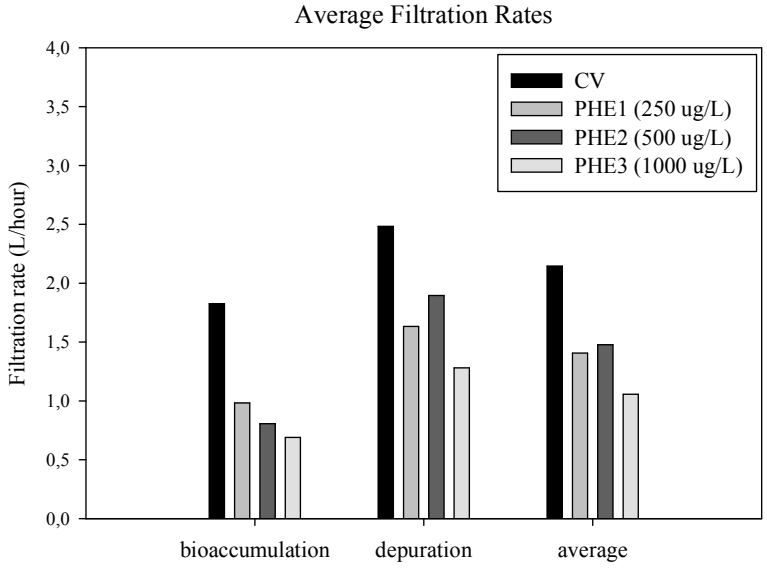

Figure 3.25 : Average filtration rates of PHE exposed mussels during uptake, depuration and whole experiment periods.

FR values during the exposure period were found also lower compared to the values for the healthy mussels reported in the literature (Karacik et al, 2009; Okay et al, 2003, 2006; Sara and Pusceddu, 2008). A slight increase in the FRs of control mussels was observed during the whole experimental period. This is probably because of the gradually adaptation of mussels to carrier solvent acetone during the uptake period. The ratio of carrier solvent acetone was 0.4 ‰ v/v during the experiments. It was found from the literature that 0.1 ‰ and 1‰ v/v of acetone has no negative effect on *Daphnia magna* (Leoni et al, 2008; OECD, 1998, 1999) and *P. tricornutum*, respectively (Okay and Karacik, 2007). Besides, 0.05‰, 0.5‰ and 1‰ v/v of acetone were reported with no toxic effect on *Mytilus* species (Okay et al, 2006; Okay and Karacik, 2008; Okay et al, 2011; Giannapas et al, 2012). Because acetone was not added to PHE aquariums during the depuration period, it was also

not added to the CV aquarium; and eventually FR of CV aquarium mussels continued to increase in the depuration period.

3.5.3 Lysosomal membrane stability of mussels exposed to BaA

The second biomarker method applied in this study was neutral red retention (NRR) assay. The stability of lysosomal membrane of blood cells decreases with the impact of stressors combined with the cytotoxic nature of neutral red dye, and this combined effect induces the leaking of lysosomal components (Bresler et al, 1999; Dailianis, 2003; Dierickx and van de Vijver, 1991; Haugland, 1996). NRR assay is used during the present study to assess the health status of *Mytilus galloprovincialis* exposed to BaA. NRR measurements during the uptake and depuration of BaA is shown in Figure 3.26 (mean +1 SE, n=6).

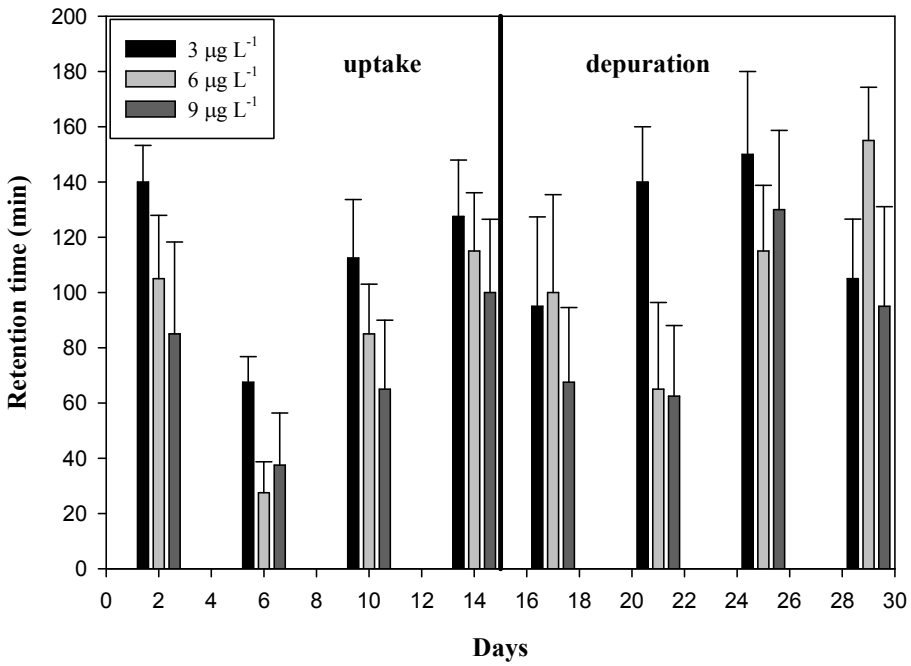

Figure 3.26 : Lysosomal stability retention times (min) of mussels (*Mytilus galloprovincialis*) exposed to 3.0, 6.0, 9.0 µg L^{-1} BaA with standard errors during a total of 29-day benzo(a)anthracene (BaA) uptake and depuration periods.

Retention times decrease as the mussels are exposed to higher BaA concentration which also means a decrease in the lysosomal stability of mussels. During the following days of the exposure period, retention times increase probably because mussels were accommodated to ambient conditions. Average retention times are seen during uptake and depuration periods in Table 3.9.

Table 3.9 : Average neutral red retention time (NRR, min) results of benzo(a)anthracene (BaA) exposed mussels (*Mytilus galloprovincialis*) by exposure concentrations and time periods of exposure (mean +1 SD). CV is the control-carrier exposure with 0.3 mL L^{-1} acetone.

Average NRR (minute) ± SD		
	Uptake	Depuration
CV	145(±36)	147 (±14)
BaA1	112 (±27)	123 (±23)
BaA2	83 (±34)	109 (±32)
BaA3	72 (±23)	89 (±27)

Furthermore, average values of BaA exposed mussels during the uptake period are lower than control values. The increasing trend in NRR time is much clear for the depuration period. Comparing average NRR values in the depuration period with the values in the uptake period, an increment as 1.3%, 9.5%, 30.8% and 23.5% for CV, 3, 6 and 9 μg L^{-1} BaA-exposed mussels (BaA1, BaA2, BaA3 aquariums) are observed, respectively. Increased NRR at the depuration period can be evaluated as the mussels had slightly recovered from BaA exposure and were in better condition at the end of the depuration period. Additional to Figure 3.26 and Table 3.9, figures of concentration dependent dose-response relationship are presented in Appendix 2.

3.5.4 Lysosomal membrane stability of mussels exposed to PHE

NRR measurements in the blood cells of the mussels during the uptake and depuration periods are shown in Figure 3.27 (mean ± 1.96 SE, n=6). Haemocytes of mussels can be thought as representatives of the organism health due to their immune response efficiency (Giannapas et al, 2012; Pipe and Coles, 1995). In neutral red retention (NRR) method, cytotoxic nature of neutral red dye combined with the impact of stressors cause reduction of lysosomal stability, inducing the leakage of lysosomal components (Dierickx and Vandevyver, 1991; Haugland, 1996; Bresler et al, 1999; Dailianis et al, 2003). The decrease in the retention times is interpreted as a decrease in the lysosomal stability of mussel haemocytes exposed to PHE.

In some studies maximum retention times were above 120 min while in other studies NRR times were seen below 60 minutes (Fernley et al, 2000; Lowe, 1995a; Dailianisa et al, 2003). This difference may be explained with the different experimental procedures which are the allowance of mussels for 24-36 hours (shorter than ours) acclimatization prior to the NRR assay (Dailianisa et al, 2003). Initial

NRR measurements of CV aquarium were found as 155 ± 55 min (mean ± SD, n=10) before the start of the experiments.

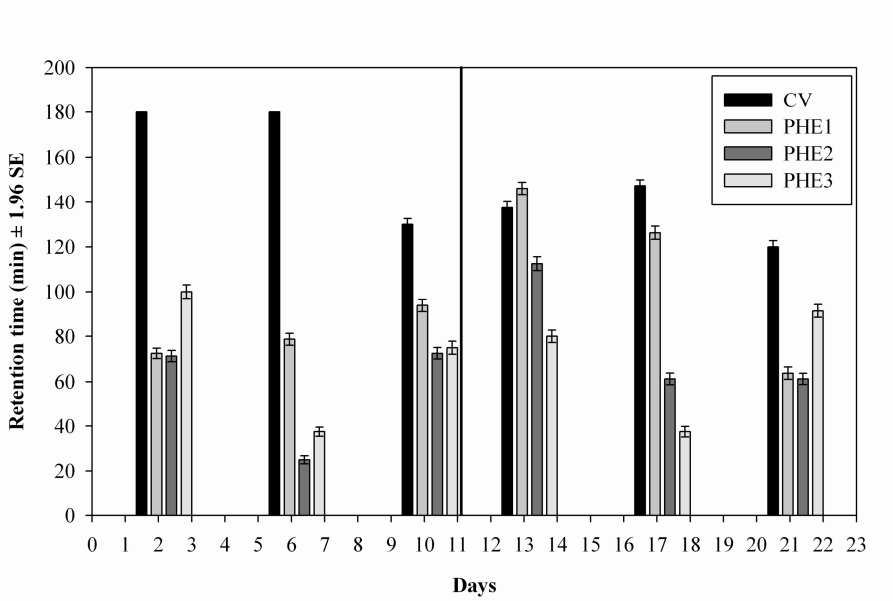

Figure 3.27 : Lysosomal stability retention times (min) of mussels (*Mytilus galloprovincialis*) exposed to 250, 500, 1000 µg L^{-1} PHE with standard errors during a total of 22-day uptake (left side) and depuration (right side) periods.

The decrease of NRR in CV aquarium during the experimental period is possibly due to the negative effect of acetone in the experiment system. Although there is an oscillating trend in NRR results, it is clearly seen from the left half of Figure 3.27 that PHE exposed mussel haemocytes have lower lysosomal stability compared with the mussels in CV aquarium during the exposure period due to the negative effect of PHE exposure.

Table 3.10 indicates the average values of NRR results for different concentrations of PHE. Average values were calculated for uptake and depuration periods separately. It is remarkable that the average retention times of PHE exposed mussels during the uptake period are approximately half of the retention times of mussels in CV aquarium. Retention times of PHE1 and PHE2 showed 37% and 39% increase in depuration period compared to the values measured for uptake period respectively. No increment was observed in PHE3 aquarium. Standard deviations in Table 3.10 indicate that the results are not grouped conveniently together but rather scattered throughout the experiments, especially for PHE2 and PHE3 aquariums. Additional to Figure 3.27 and Table 3.10, figures of concentration dependent dose-response relationship are given in Appendix 2.

Table 3.10 : Average neutral red retention time (NRR, min) results of mussels (*Mytilus galloprovincialis*) exposed to 250 (PHE1), 500 (PHE2) and 1000 (PHE3) µg L^{-1} nominal values of phenanthrene (PHE) during time periods of uptake and depuration (mean ± 1 SD). CV is the control-carrier exposure with 0.4 ‰ acetone.

Average retention time (min) ± SD, n=18		
	Uptake	Depuration
CV	163±41	135±63
PHE1	82±62	112±78
PHE2	56±53	78±72
PHE3	71±72	70±68

3.6 Results of Algae Consumption in the Small Scale Experiments

Measurements of uptake and depuration periods of each aquarium were drawn separately for the sampling time intervals of each day. Additionally, average values of each time interval were calculated in order to see the general trend of particle decrease.

3.6.1 Filtration rates of mussels exposed to BaA

Average filtration rates for 10 mussels together were calculated by using the decrease of particle number and the results were shown in Figure 3.28 and Figure 3.29 for uptake and depuration periods, respectively.

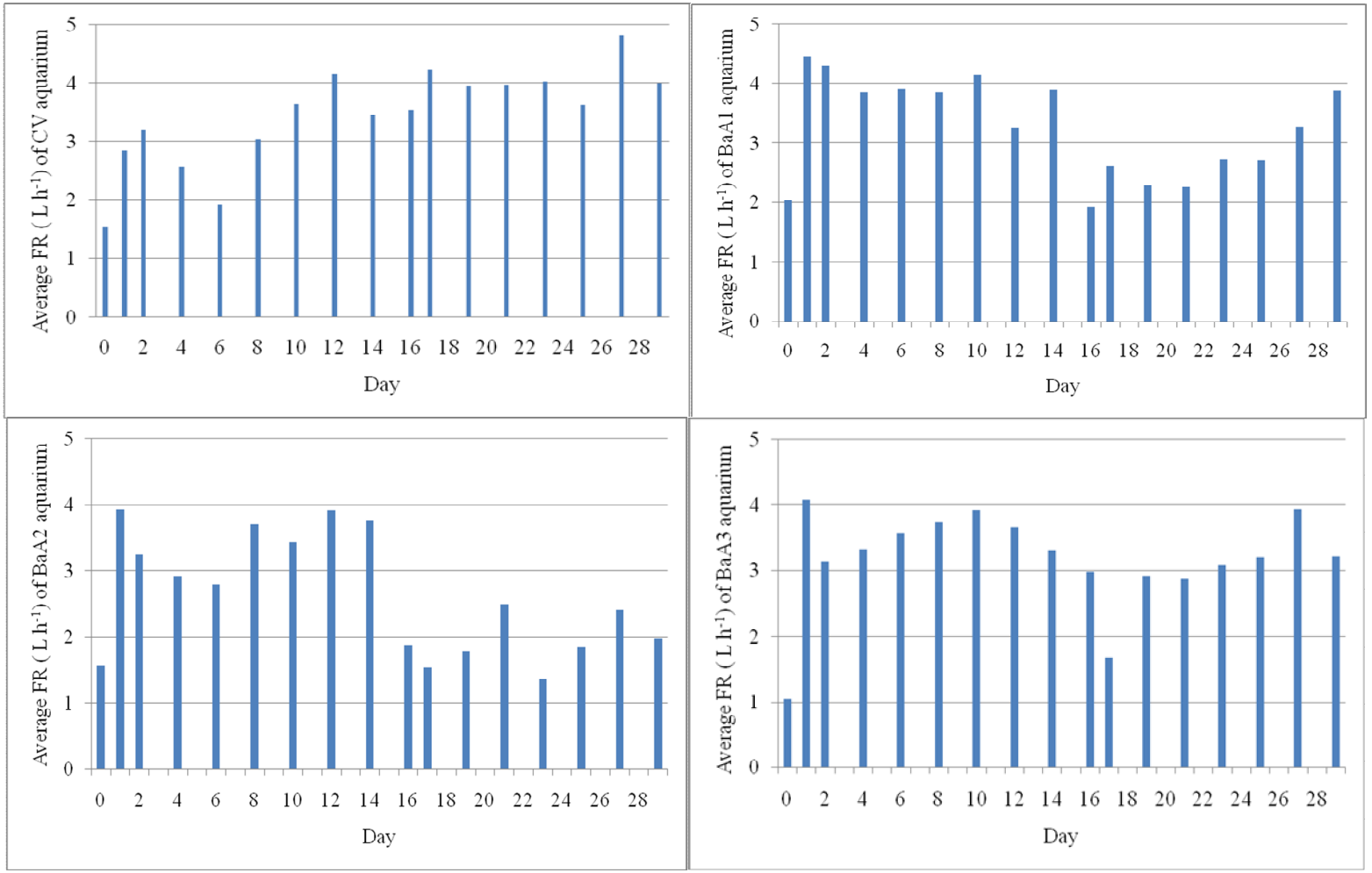

Figure 3.28 : Average filtration rates (L h^{-1}) of 10 mussels for four aquariums during uptake and depuration periods.

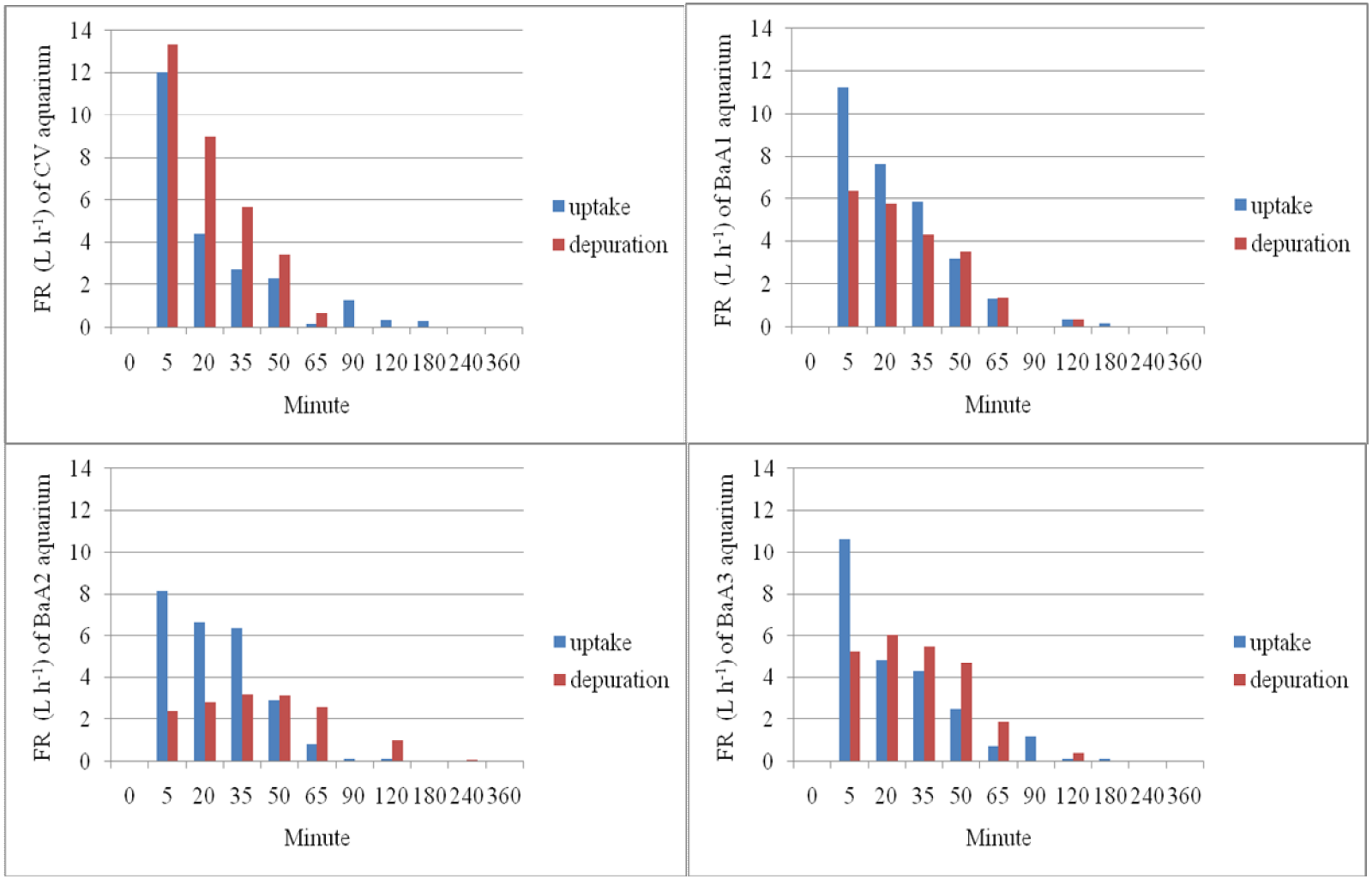

Figure 3.29 : Comparison of average filtration rates of BaA aquariums (each contains 10 mussels) for both uptake and depuration periods.

3.6.2 Filtration rates of mussels exposed to PHE

Average filtration rates of 10 mussels together in terms of L h^{-1} were calculated by using the decrease of particle number over time and the results were shown in Figure 3.30 and Figure 3.31.

Average values of filtration rates versus sampling days for both uptake and depuration periods are shown in Figure 3.30. Even though the values measured in CV aquarium are fluctuating, average filtration rate during 24 hours is approximately 3.5 L h^{-1} for 10 mussels. When the whole period was evaluated, it was observed that the filtration rates are decreasing as the PHE concentration increases. Although the level of filtration rate remains same during the uptake period (approximately 2.5 L h^{-1} for 10 mussels), the values are increasing at the end of the depuration period (approximately 4 L h^{-1} for 10 mussels) for PHE2 aquarium. Filtration rate during uptake period is approximately 2.3 L h^{-1} for 10 mussels for PHE3 aquarium. At the beginning of the depuration period, filtration rate decreases probably due to negative effect of PHE accumulation in the organisms, low depuration and adaptation of organisms; after a while filtration rate begins to increase again and reaches to approximately 3 L h^{-1} for 10 mussels.

Average values of filtration rates versus time during the sampling days for both uptake and depuration periods are shown in Figure 3.31. In general, filtration rates of PHE spiked aquariums were found higher in the depuration period than uptake period. Lower filtration rate of depuration rate in the first 5 minutes compared to the filtration rate of uptake period may be due to the lack of data between 0 and 5 minutes after water exchange. Nevertheless, rest of the filtration rates of CV aquarium was found similar for both uptake and depuration periods. Filtration rates were not so different for PHE1 and PHE3 aquariums for both periods. Because of the negative effect of PHE accumulation in the organisms, lowest filtration rate values were observed for PHE3 aquarium.

Additional figures showing the relationship between filtration rates, sampling days and specific time intervals of sampling days during the sampling days of uptake and depuration periods are in Appendix 3.

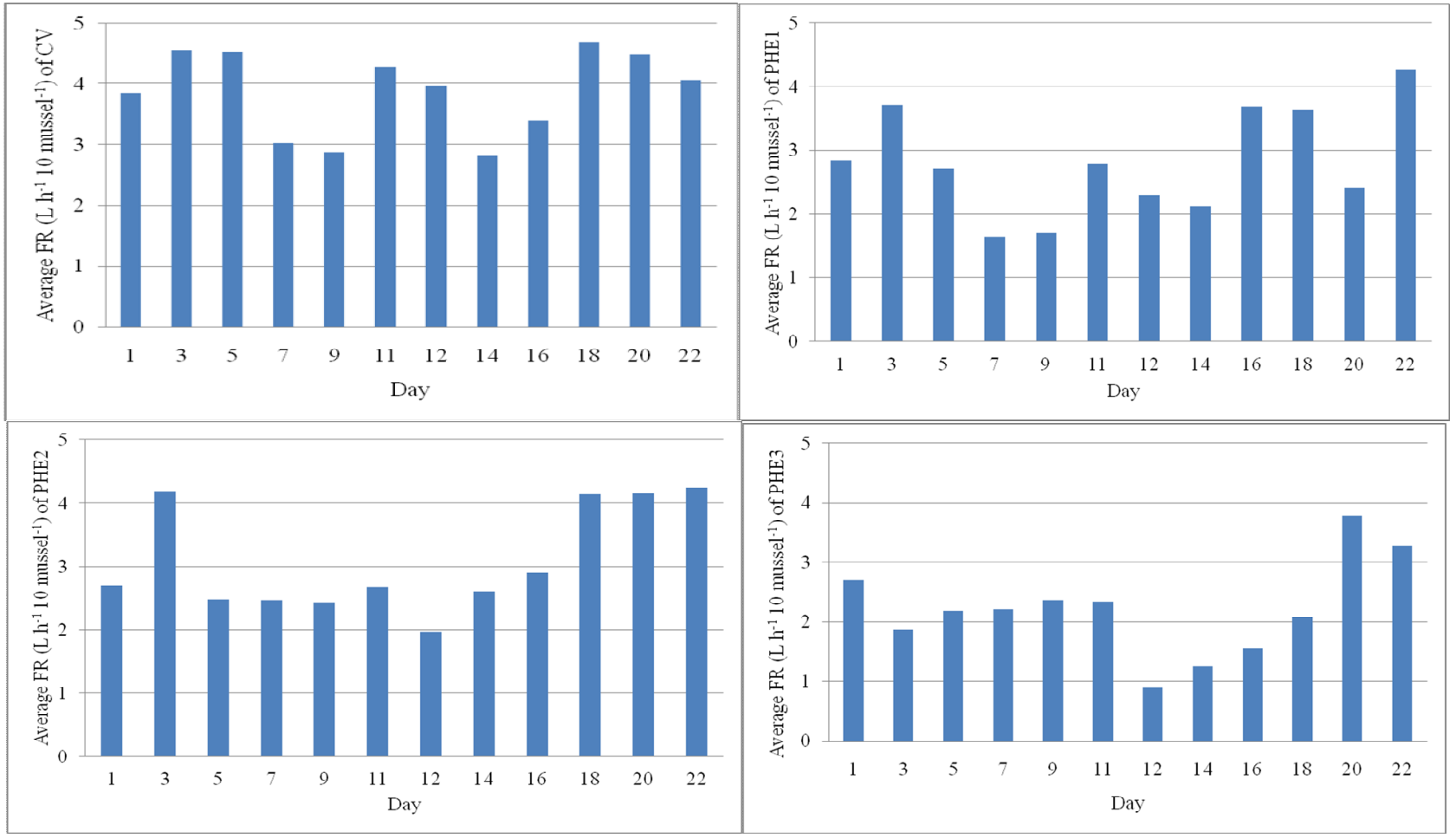

Figure 3.30 : Average filtration rates of aquariums (each contains 10 mussels) for whole experimental period.

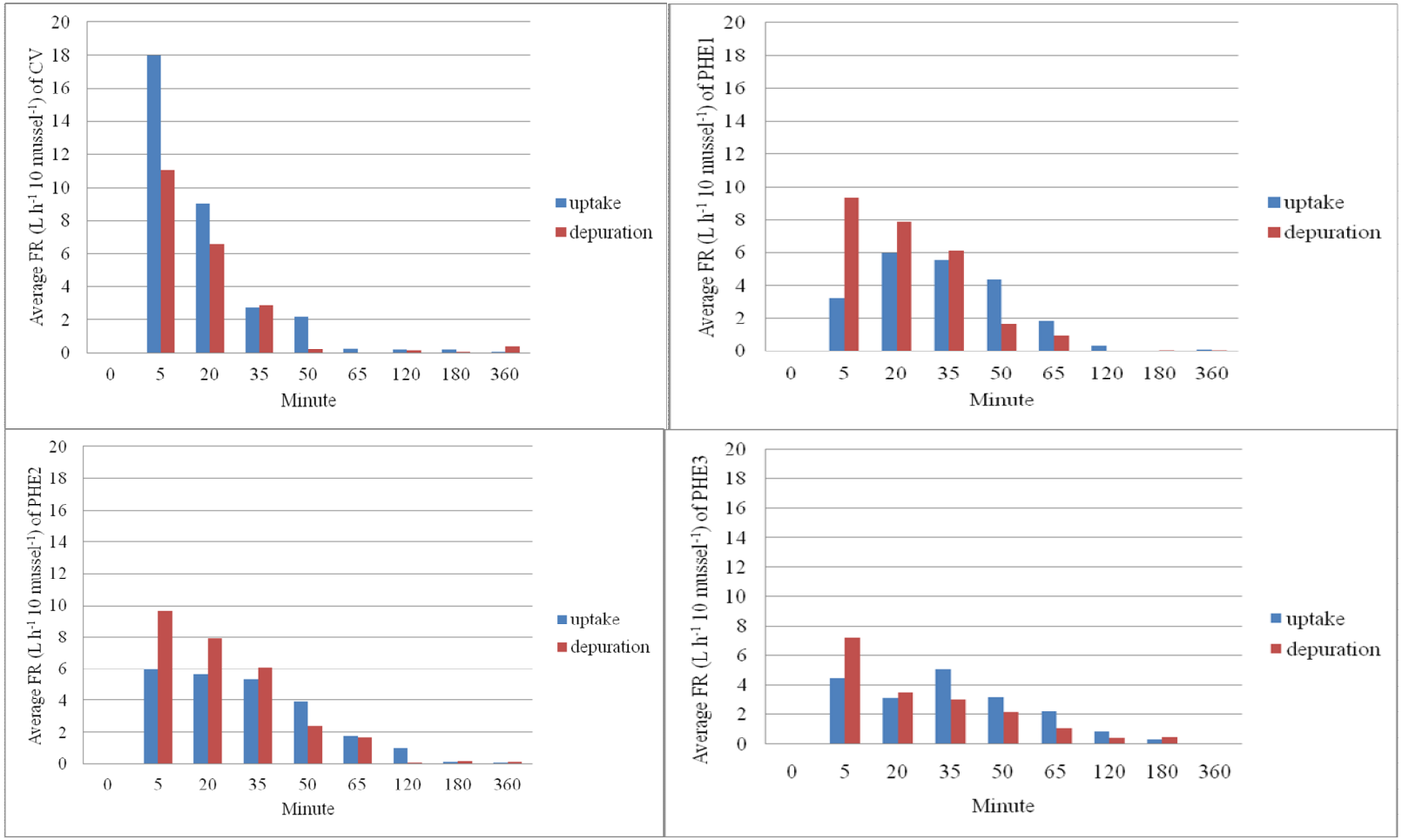

Figure 3.31 : Comparison of average filtration rates of PHE aquariums (each contains 10 mussels) for uptake and depuration periods.

3.7 Comparison of BaA and PHE Exposure Results

Small and large scale experiments were performed under same physical conditions for BaA and PHE exposures. However, some differences were observed in the results of bioaccumulation and biomarkers due to different properties of BaA and PHE such as bioavailability and hydrophobicity.

3.7.1 Bioavailability and hydrophobicity

Aqueous solubility directly affects the bioavailability of PAHs. Additional to aqueous solubility, partition coefficient is also an important factor for bioaccumulation. These properties are different for each chemical. The properties of BaA and PHE have been given in Table 2.1. Although octanol-water partition coefficient (Log K_{ow}) expresses the accumulation potential of lipophilic (hydrophobic) PAHs in tissues, bioavailability of PAHs strongly affects the bioaccumulation levels. Linear correlation of Log K_{ow} with Log BCF/BAF is broken down due to lower bioavailability of chemicals with high Log K_{ow} values (Landrum, 1989; van Hattum et al, 1998; Jensen et al, 2012). Thus, the levels of PHE concentration has been observed higher in mussel tissues compared with the levels of BaA concentration.

3.7.2 Bioaccumulation levels (BCF, BAF, QSAR)

BAF calculations of the large scale experiments have been detailed in Table 3.1 and Table 3.3 for BaA and PHE, respectively. The results of these tables are summarized in Table 3.11.

Table 3.11 : Calculated bioaccumulation factors (BAFs) of BaA and PHE exposed mussels. The results of Table 3.1 and Table 3.3 are collected in this table.

BaA			PHE		
	BAF_1	BAF_2		BAF_1	BAF_2
3 µg L^{-1}	989	706	250 µg L^{-1}	701	658
6 µg L^{-1}	2916	1947	500 µg L^{-1}	513	466
9 µg L^{-1}	3184	2745	1000 µg L^{-1}	509	441

Calculated values in Table 3.11 were given in logarithmic values for easy comparison of results as seen in Table 3.12.

Table 3.12 : Log BAF values of BaA ve PHE bioaccumulation experiments.

	BaA			PHE	
	Log BAF_1	Log BAF_2		Log BAF_1	Log BAF_2
3 μg L^{-1}	3.00	2.85	250 μg L^{-1}	2.85	2.82
6 μg L^{-1}	3.46	3.29	500 μg L^{-1}	2.71	2.67
9 μg L^{-1}	3.50	3.44	1000 μg L^{-1}	2.71	2.64

BAF_1 values was found slightly higher than BAF_2 values as expected since the equation used for the calculation of BAF_1 has some assumptions such as constant chemical concentration in seawater and/or zero initial chemical concentration in the organism. In the experiments, although the chemical concentration in the organism is not zero, it is low enough to ignore. On the other hand, probably the difference may be results from semi-static design of the experiment system instead of flow-through. Although seawater is renewed daily, because of the accumulation trend of the chemical in the organism, chemical concentration in seawater decreases with time until renewing the seawater (next day). However, in the equation it is assumed that the chemical concentration in seawater is constant and as a result, BAF_1 values are calculated higher than BAF_2. Additionally, another reason for lower BAF_2 values may be due to the difference between the measured and nominal chemical concentrations in seawater. The measured values has been found as 106, 89 and 79% of the nominal concentrations for 3 μg L^{-1}, 6 μg L^{-1} and 9 μg L^{-1} BaA and the measured values has been found as 70, 80 and 70% of the nominal concentrations for 250 μg L^{-1}, 500 μg L^{-1} and 1000 μg L^{-1} PHE.

BCF/BAF values can also be compared with the values obtained from QSAR (quantitative structure activity relationship) equations besides experimental study. QSAR equations are important for BCF/BAF predictions of the organisms, because it is almost impossible to perform experiments for all chemicals and all aquatic species. QSAR formulas used for mussel species in literature were collected together.

BCF and BAF values of selected PAHs (BaA and PHE) are calculated using some literature QSAR formula and listed in Table 3.13 and Table 3.14.

Table 3.13 : Calculated BCF/BAF values for BaA and mussel using QSAR equations.

QSAR	$LogK_{ow}$	W_s ($\mu g\ L^{-1}$)	LogBCF	Reference
$Log\ BF_w=5.15-0.843LogW_s$		10	4.31	Ernst (1980)
$Log\ BF_w=4.94-0.682LogW_s$		10	4.26	Geyer et al. (1982)
$Log\ BCF_w=-0.808+0.858LogK_{ow}$	5.9		4.25	Geyer et al. (1982,1991)
$Log\ BCF_w=-0.97+0.899LogK_{ow}$	5.9		4.33	Geyer et al. (1991)
$Log\ BCF=-1.4+0.965LogK_{ow}$	5.9		4.29	Pruell et al. (1986)
$Log\ BCF=-2.220+0.965LogK_{ow}$	5.9		3.47	Donkin et al. (1991)
$Log\ BCF=-1.193+0.790LogK_{ow}$	5.9		3.47	Okay and Karacik (2008)
$Log\ BCF=-1.344+0.820LogK_{ow}$	5.9		3.49	Okay and Karacik (2008)
$Log\ BCF=0.98+0.35LogK_{ow}$	5.9		3.05	Arnot and Gobas (2006)
$Log\ BCF=-1.67+1.02LogK_{ow}$	5.9		4.35	Arnot and Gobas (2006)
$Log\ BCF=-0.333+0.6598LogK_{ow}$	5.9		3.56	BCFBAF v 3.00 (2008)
$Log\ BAF=0.09+0.82LogK_{ow}$	5.9		4.93	Arnot and Gobas (2006)
$Log\ BAF=-1.45+0.92LogK_{ow}$	5.9		3.98	Arnot and Gobas (2006)
BCF_1 of BaA3 aquarium			3.50	Experimental values (This study)
BCF_2 of BaA3 aquarium			3.44	Experimental values (This study)

If the results of QSAR calculations and the experiment are compared, the higher values in literature compared with Table 3.12 can be explained with the duration of the experiment period which is not long enough for BaA to reach steady state condition. On the contrary, experimental results in Table 3.12 are between the ranges of QSAR calculation results for PHE exposure experiment. This can be explained with the closer steady state condition of PHE exposure experiment compared with BaA exposure experiment. This also shows that PHE accumulation occurs in mussel tissues in a shorter period than BaA accumulation. Another important point of the results in Table 3.12 is different BAF values for different exposure concentrations. Although BCF and BAF values are accepted as constant values regardless of the chemical concentration in the surrounding environment, this fact is broken due to the toxic effects of the chemical causing physiological changes in the organism (Arnot and Gobas, 2006).

Table 3.14 : Calculated BCF/BAF values for PHE and mussel using QSAR equations.

QSAR	$LogK_{ow}$	W_s ($\mu g\ L^{-1}$)	LogBCF	Reference
Log BF_w=5.15-0.843LogW_s		1200	2.55	Ernst (1980)
Log BF_w=4.94-0.682LogW_s		1200	2.84	Geyer et al. (1982)
Log BCF_w=-0.808+0.858LogK_{ow}	4.5		3.05	Geyer et al. (1982,1991)
Log BCF_w=-0.97+0.899LogK_{ow}	4.5		3.08	Geyer et al. (1991)
Log BCF=-1.4+0.965LogK_{ow}	4.5		2.94	Pruell et al. (1986)
Log BCF=-2.220+0.965LogK_{ow}	4.5		2.12	Donkin et al. (1991)
Log BCF=-1.193+0.790LogK_{ow}	4.5		2.36	Okay and Karacik (2008)
Log BCF=-1.344+0.820LogK_{ow}	4.5		2.35	Okay and Karacik (2008)
Log BCF=0.98+0.35LogK_{ow}	4.5		2.56	Arnot and Gobas (2006)
Log BCF=-1.67+1.02LogK_{ow}	4.5		2.92	Arnot and Gobas (2006)
Log BCF=-0.333+0.6598LogK_{ow}	4.5		2.64	BCFBAF v 3.00 (2008)
Log BAF=0.09+0.82LogK_{ow}	4.5		3.78	Arnot and Gobas (2006)
Log BAF=-1.45+0.92LogK_{ow}	4.5		2.69	Arnot and Gobas (2006)
BAF_1 of PHE3 aquarium			2.71	Experimental values (This study)
BAF_2 of PHE3 aquarium			2.64	Experimental values (This study)

3.7.3 Biomarkers

Results of mussel filtration rates show that the toxic effect of PHE exposure is much clear than BaA exposure. This is seen obviously in the results for uptake in Table 3.7 and Table 3.8. None of the PHE exposed aquariums was measured above the 1 L h^{-1} $mussel^{-1}$ during the uptake period. The values are increasing during the depuration period. This indicates the recovery of mussels due to PAH depuration in their tissues. Although filtration rates in PHE exposed mussels increased in the depuration period, all values remained lower than the values determined for of CV aquarium. Differences between uptake and depuration periods are more apparent and almost two times higher for PHE exposures compared with BaA exposures. Numerical values of these differences are shown in Table 3.15. According to the results in Table 3.15, differences of uptake and depuration periods are higher for PHE exposed mussels. This is interpreted as the toxic effect of PHE is higher than the toxic effect of BaA on mussel species.

Table 3.15 : Uptake and depuration period differences of average filtration rates (FRs, L hr^{-1} $mussel^{-1}$) of benzo(a)anthracene (BaA) and phenanthrene (PHE) exposed mussels (*Mytilus galloprovincialis*).

Differences between uptake and depuration period FRs (L hr^{-1} $mussel^{-1}$)			
CV	0.7	CV	0.7
BaA1	0.7	PHE1	1.2
BaA2	0.6	PHE2	1.8
BaA3	0.2	PHE3	1.2

When the results in Table 3.9 and Table 3.10 were compared, it is seen that the difference of uptake and depuration periods for lysosomal stability measurements is not as obvious as the filtration rate measurements. This occurs probably due to the difference between physiological and cellular recovery mechanisms. However, higher toxicity of PHE on the lysosomal stability of mussels is apparent compared with BaA.

3.8 Modeling Study of the Experiments

The experiments were modelled to determine the levels of PAH bioaccumulation in mussel tissues during the periods of uptake and depuration and to understand the routes of PAH transfer between algae, mussel and seawater. For that aim, differential equations mainly composed of Equations (2.7), (2.8) and (2.9) are solved iteratively for each day due to the daily renewal process of seawater and algae mixture in the aquariums. Developed model code of bioaccumulation and depuration processes is written in Appendix 4.

Input parameters used in the model code are

- uptake and depuration kinetic rate constants,
- seawater volume in terms of L,
- one mussel wet weight in terms of g,
- spiked algae concentration in terms of cell mL^{-1},
- one algae wet weight in terms of g,
- filtration rate of mussels for each day in terms of L day^{-1},
- spiked PAH concentration in terms of μg L^{-1},

- initial PAH concentration of mussel tissues in terms of µg L^{-1},
- mussel number and
- the duration of uptake period.

Outputs of the model code were generated after the execution of the model code. The graphs of PAH concentration in mussels versus days were calculated for each day and plotted for uptake and depuration periods together. Additional simulations of selected PAH transfer between the compartments (seawater, mussel and algae) at the first day of uptake period are found in Appendix 5.

Comparisons of experimental data with the model outputs of the theoretical data are given in Sections 3.8.1 and 3.8.2.

3.8.1 Comparison of theoretical and experimental data of BaA exposure

Changes of BaA concentration in mussel tissues are seen in Figure 3.32 during the uptake and depuration periods for three different aquariums (3, 6, 9 µg L^{-1} BaA). Blue, red and green dots in Figure 3.32 represent the experiment data of different concentrations of BaA, from higher to the lower BaA concentrations, respectively. It is also seen from Figure 3.32 that BaA transfers more rapidly into mussel tissues as the spiked BaA concentration increases.

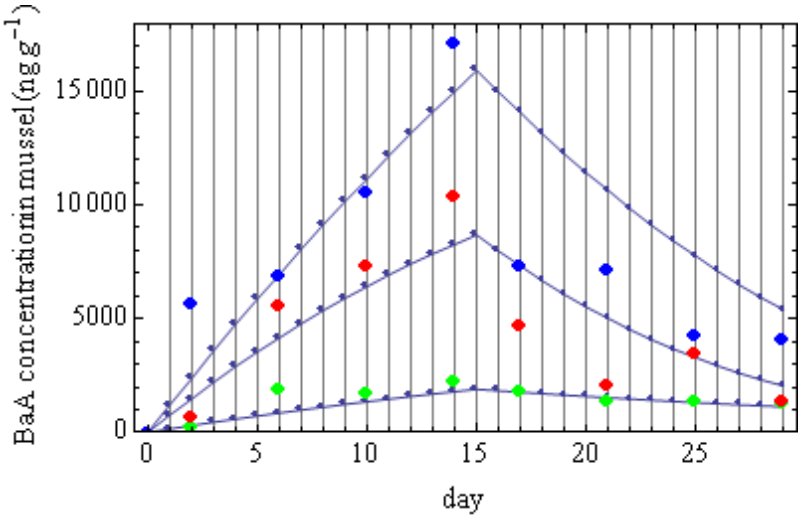

Figure 3.32 : Comparison of experiment data (dots) and 3-compartment mathematical model results of nominal exposure concentrations (line) for BaA spiked aquariums (3, 6, 9 µg L^{-1} BaA) during the uptake and depuration periods.

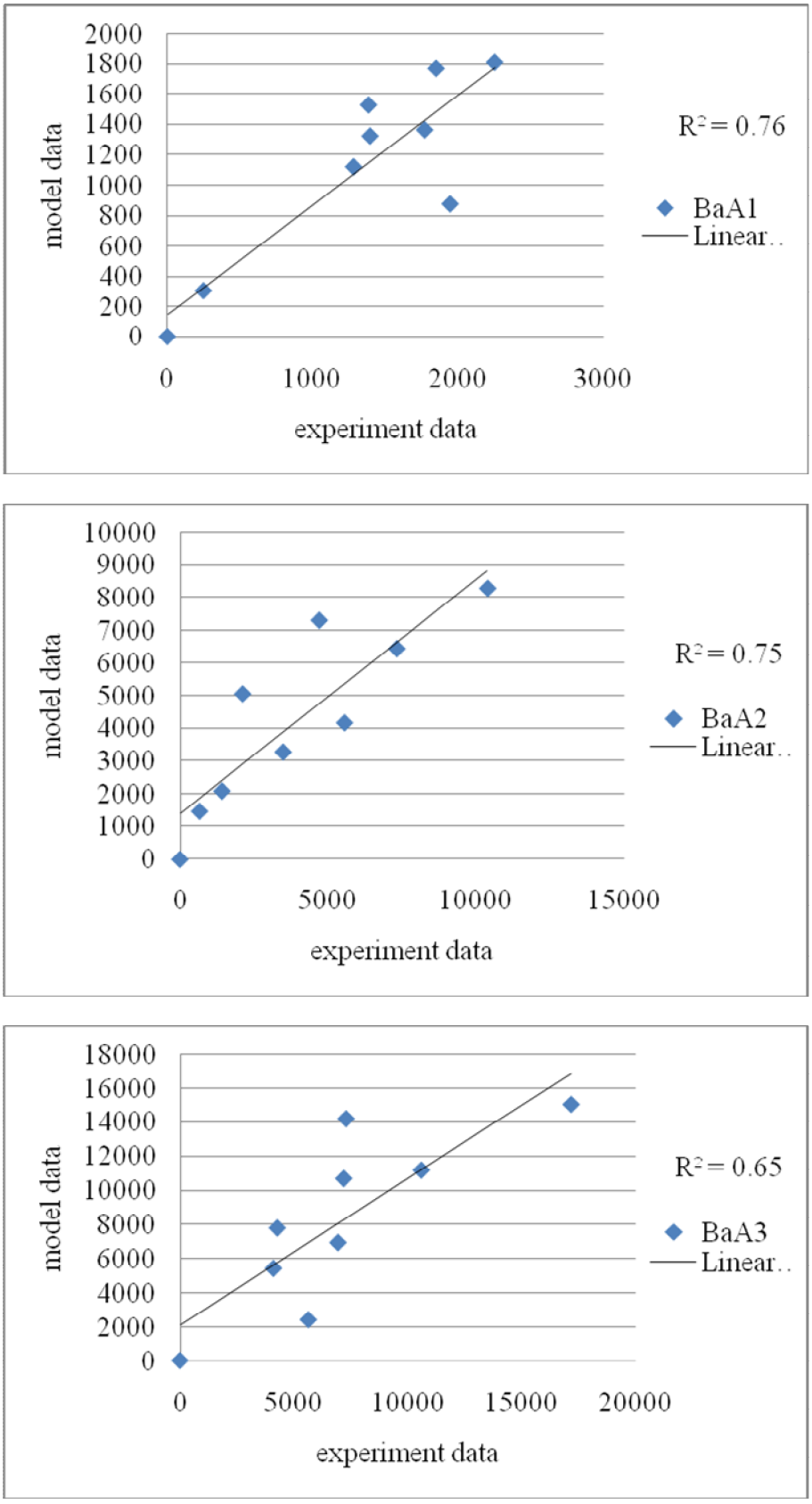

Figure 3.33 : Correlations of experimental and modeling data for BaA spiked aquariums (3, 6, 9 µg L^{-1} BaA) during the uptake and depuration periods.

Correlations of experimental and modeling data are represented with thre graphs in Figure 3.33 for each BaA aquarium separately. It is seen that the correlation decreases with the higher concentrations. The differences of experiment and model data in terms of percentages change between 65% and 93% during uptake period and 97% and 164% during depuration period. This is probably due to hydrophobicity and very low solubility of BaA in seawater besides analytical uncertainty.

3.8.2 Comparison of theoretical and experimental data of PHE exposure

Experimentally measured PHE concentrations in mussel tissues were compared to the results of mathematical model for three different aquariums in Figure 3.34. Blue, red and green dots in Figure 3.34 represent the experiment data of different concentrations of PHE, from higher to the lower PHE concentration, respectively.

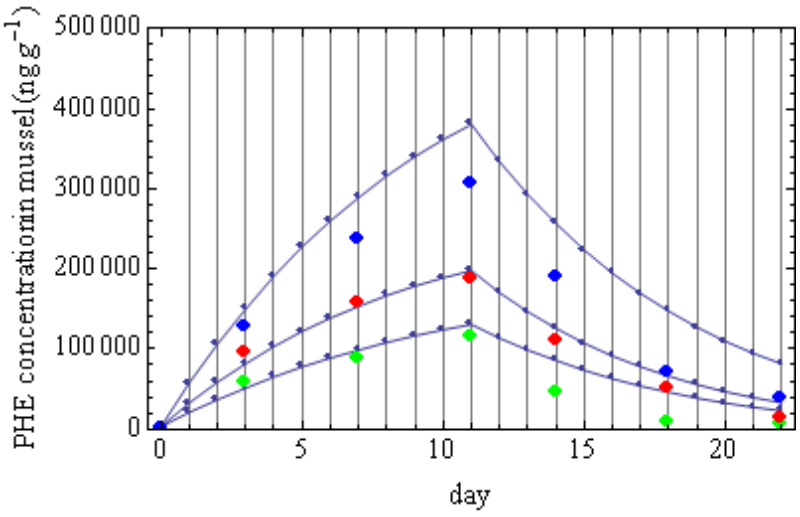

Figure 3.34 : Comparison of experiment data (dots) and three-compartment mathematical model results (line) for PHE spiked aquariums (250, 500, 1000 µg L^{-1} of PHE) during the uptake and depuration periods.

Both uptake and depuration periods are overestimated by the model for the highest PHE concentration, while these periods fit well for the other concentrations. One of the reasons of this overestimation may be the difference between the nominal and measured PHE concentration spiked into the system. On the other hand, the model was developed for a closed system, assuming no evaporation from seawater. The differences of experiment and model data in terms of percentages change between 71% and 90% during uptake period and 149% and 323% during depuration period. High percentages of depuration periods show that additional parameters should be added for the evaluation of depuration periods.

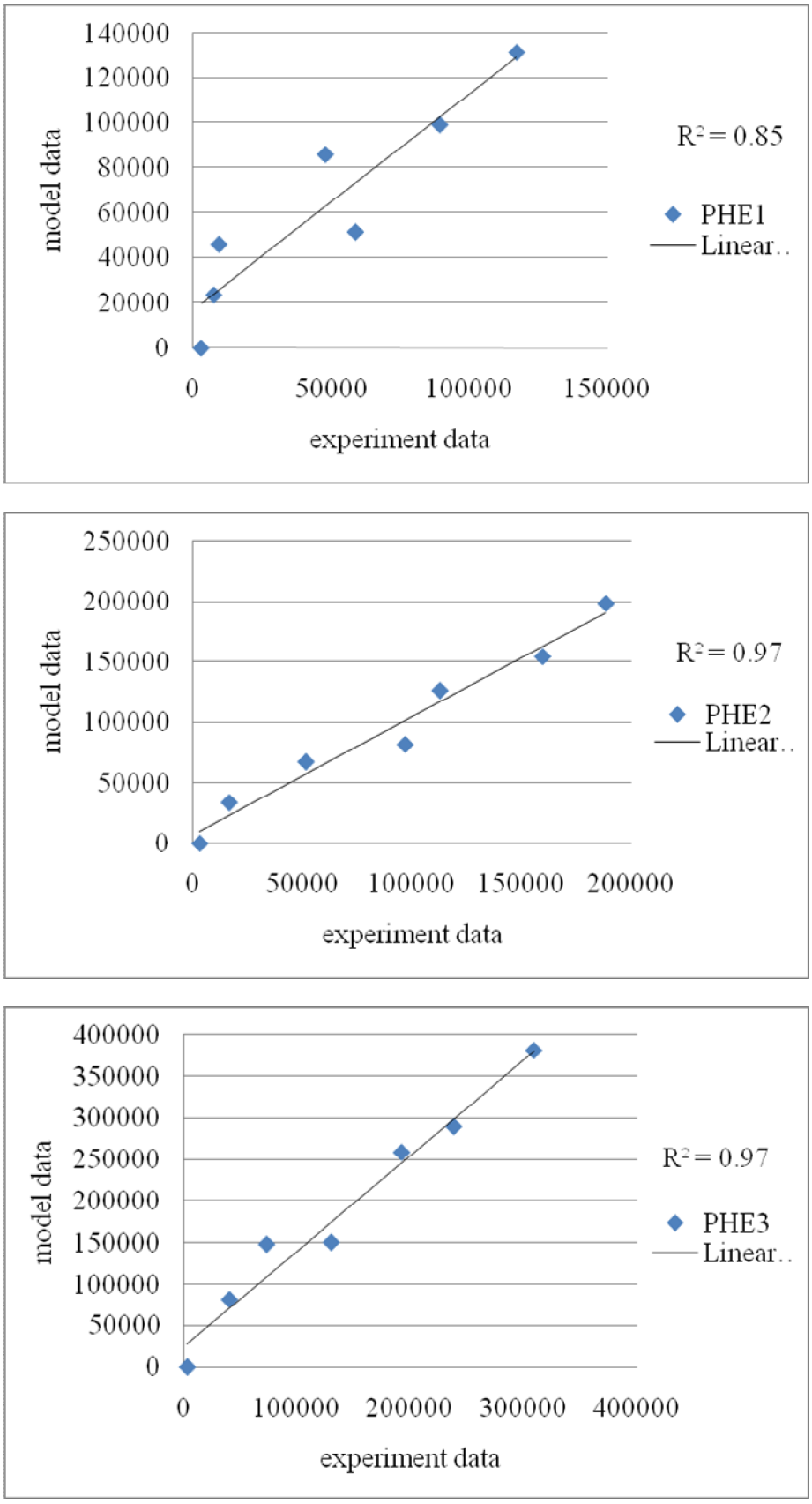

Figure 3.35 : Correlations of experimental and modeling data for BaA spiked aquariums (3, 6, 9 µg L^{-1} BaA) during the uptake and depuration periods.

Correlations of experimental and modeling data are represented with thre graphs in Figure 3.35 for each PHE aquarium separately. It is seen from Figure 3.35 that the correlation coefficient gets better with the higher concentrations. In general, it can be said that generated mathematical model clearly simulates the PHE bioaccumulation and depuration experiments in mussel tissues.

3.9 Different Simulation Scenarios with Different Parameters

Developed model can be used as a predictive tool for the uptake and depuration of three and four ring PAHs in Mediterranean mussel species. The transfer of PAHs occur both via the routes of seawater and food. Input data were derived from the experimental conditions and the developed model was verified with the experiment data. Thus, the model was executed with different variations of input parameters in order to see the uptake and depuration mechanism of mussels under different conditions.

3.9.1 Different concentrations of *P. tricornutum*

The concentration of microalgae in seawater depends on the season as well as the trophic status of the field. Thus, algal concentrations were increased at different levels in the simulations to observe the effect of algal concentration in the accumulation of PAHs. For this purpose, the model was executed for increased numbers of algae. Before the model was executed for increased number of algae, the model was executed for new concentrations of PHE. New concentrations were selected as 3, 6 and 9 µg L^{-1} to be identical with the concentrations of BaA. All other previously described input parameters remained as before. The levels of PHE bioaccumulation in mussels with the concentrations of 3, 6 and 9 µg L^{-1} PHE are seen in Figure 3.36.

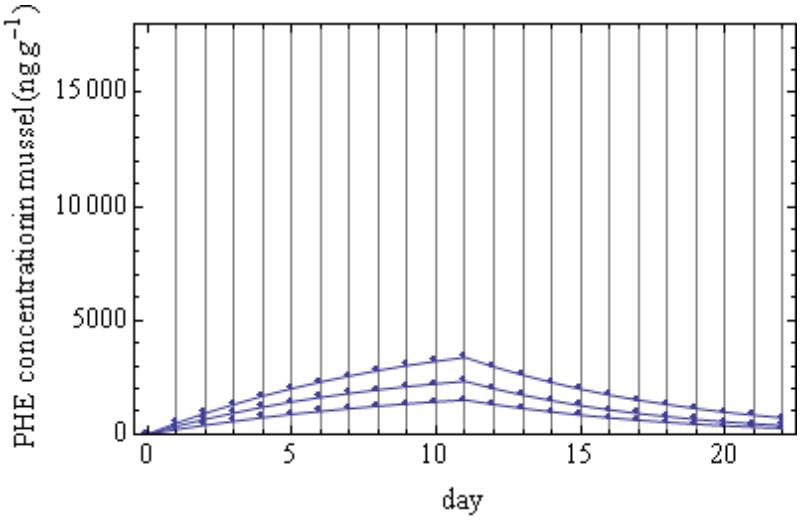

Figure 3.36 : The concentration levels of PHE in mussel tissues exposed to 3, 6, 9 µg L^{-1}. Left half of the graph indicates the uptake phase of PHE whereas the right half indicates the depuration phase of PHE from mussel tissues.

Higher bioaccumulation potential of BaA is clearly seen after the comparisons of Figure 3.32 and Figure 3.36. The level of BaA concentration in mussels reaches to 16000 ng g^{-1} after the exposure of 9 µg L^{-1} BaA while the level of PHE concentration in mussels reaches to 4000 ng g^{-1} after the exposure of 9 µg L^{-1} PHE.

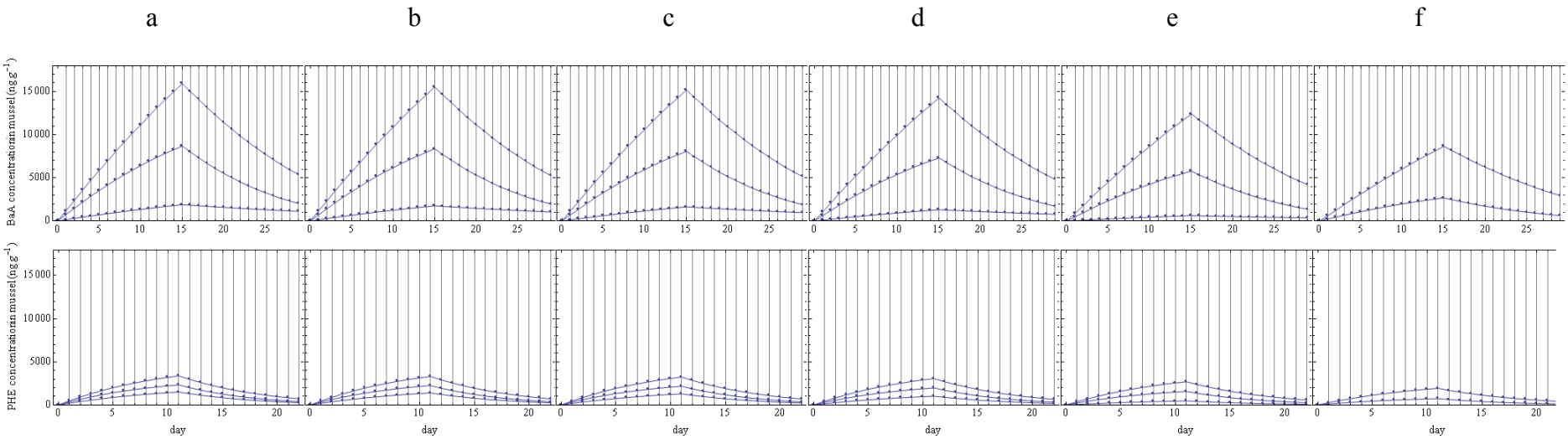

Figure 3.37 : The concentration levels of BaA (upper panel) and PHE (lower panel) in mussels (ng g^{-1}) with increased numbers of algae. The algae numbers are increasing from a toward f as 3, 5, 10, 20 and 40 times of the original number (20000 cell mL^{-1}).

In Figure 3.37, model outputs are seen after the algae numbers were increased at different levels for both BaA and PHE exposures during the uptake and depuration periods. In both PAHs, it is seen that as the numbers of algae increases, the levels of PAH in mussels decrease. This is clearer in BaA exposures compared with PHE exposures due to the high accumulation potential of BaA in mussels. The reverse relationship of algae number and PAH levels can be explained with the constraints of the model which is filtration rate of mussels. As the number of algae increases, PAH accumulation capacity of each cell decreases due to specifically selected exposure level of PAHs. Because the filtration rate of mussel remained same as before, the filtrated cell numbers remain same, but the accumulated PAH levels decrease.

3.9.2 Different types of marine algae

Phaeodactylum tricornutum has been selected as algae species during the laboratory experiments. To observe the effect of different algal species on the levels of PAH bioaccumulation in mussel tissues, six different algal species were used as input data additional to *P. tricotnutum* and the model was executed for these species under the same experiment conditions. The names of used algae specis, their morphology and habitat are listed in Table 3.16. BCF values were calculated with QSAR equations in literature and these QSARs are shown in Table 3.17.

Table 3.16 : Properties of six different algae species used in the simulation scenarios.

Algae species	type	morphology	habitat
Rhodomonos salina	cryptophyte	cone and half sphere	brackish and marine waters
Emiliania huxleyi	coccolithophore	placolith	marine waters
Skeletonema costatum	diatom	long chain	marine waters
Thalassiosira nordenskiöldii	diatom	long chain	marine waters
Phaeodactylum tricornutum	diatom	fusiform, triradiate, oval	marine waters
Isochrysis galbana	flagellate	spherical	marine waters

In Table F.2, QSAR equations of these species were detailed, and calculated BCF values were used as inputs of the model code. Simulations are shown in the following figures for three different BaA and PHE concentrations.

Table 3.17 : QSAR equations of various marine algae species.

Algae species	QSAR equation	Reference
Rhodomonos salina	$LogBCF=1.86LogK_{ow}-3.46$ $LogBCF=1.75LogK_{ow}-2.93$	Berrojalbiz et.al., 2009
Emiliania huxleyi	$LogK_{algw}=0.59LogK_{ow}+2.20$ $LogK_{algw}=0.88LogK_{ow}+0.53$	Gerofke et.al., 2005
Skeletonema costatum	$LogK_{algw}=0.86LogK_{ow}+0.67$ $LogK_{algw}=0.94LogK_{ow}+0.11$	Gerofke et.al., 2005
Thalassiosira nordenskiöldii	$LogK_{algw}=0.91LogK_{ow}+0.20$ $LogK_{algw}=1.02LogK_{ow}-0.41$	Gerofke et.al., 2005
Phaeodactylum tricornutum	$LogK_{algw}=0.90LogK_{ow}-0.99$ $LogK_{algw}=1.07LogK_{ow}-1.71$	Gerofke et.al., 2005
Isochrysis galbana	$LogBCF=1.085LogK_{ow}-3.77$ $LogBCF=0.343LogK_{ow}+0.913$	Vento and Dachs, 2002
1st level of aquatic food web	$LogBAF^{fd}=-0.1301(LogK_{ow})^2+2.5301LogK_{ow}-3.52$ $LogBAF^{t}=-0.2298(LogK_{ow})^2+3.167LogK_{ow}-3.9242$	Voutsas et.al., 2002

Model outputs for *Skeletonema costatum* are seen in Figure 3.38 and Figure 3.39. Outputs of other algae species are shown in Appendix F. It is seen that BaA accumulation level in mussels increase as BCF values decrease when all the outputs were observed. On the contrary, there is a positive correlation of PHE accumulation level in mussels with BCF values. PHE levels in mussels increase with the increasing BCF values. This difference is caused by the different K_{ow} values and the bioavailability of the selected PAHs. Log K_{ow} of BaA is 5.9 whereas Log K_{ow} of PHE is 4.5. It has also be remembered that low molecular weight PAH (PHE) is more bioavailable than the higher molecular weight PAH (BaA). In the light of these informations, it is said that the main factor affecting the bioaccumulation level in mussels is the BCF value of algal species. The levels of PAH concentration in mussels would reach higher levels as the value of BCFs increase. The reason of the inverse correlation of BCF values of algae with the levels of BaA concentration in mussels is due to the low bioavailable fraction of BaA in seawater. Although the adsorption/absorption capacity of algal species increase with the increasing BCF values, final levels of BaA concentration can not increase due to the low BaA concentration in seawater. On the other hand, positive correlations of BCF values of

algae with the levels of PHE concentration in mussels occur due to the high bioavailability of PHE in seawater. As a result, it is observed that the different behavior of different algal species is directly related with their BCF values.

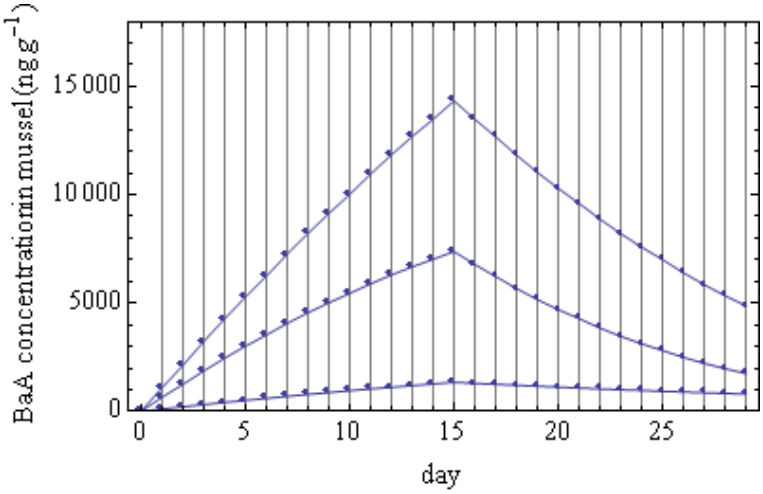

Figure 3.38 : The levels of BaA concentration in mussels exposed to 3, 6, 9 µg L^{-1} BaA and fed with *Skeletonema costatum* (BCF=503762, LogBCF=5.7). Left half of the graph indicates the uptake phase of BaA whereas the right half indicates the depuration phase of BaA from mussel tissues.

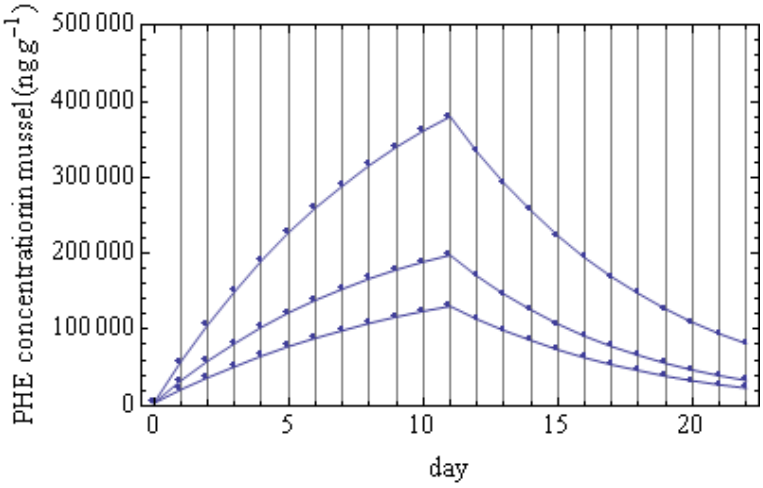

Figure 3.39 : The levels of PHE concentration in mussels exposed to 250, 500, 1000 µg L^{-1} PHE and fed with *Skeletonema costatum* (BCF=28276, LogBCF=4.5). Left half of the graph indicates the uptake phase of PHE whereas the right half indicates the depuration phase of PHE from mussel tissues.

3.9.3 Mussel number

If the number of mussels would remain the same (51 mussels) throughout the experiment as shown in Figure 3.40, BaA accumulation level in mussel tissues would decrease around 40% compared with the condition of decreasing number of mussels at sampling days as shown in Figure 3.32.

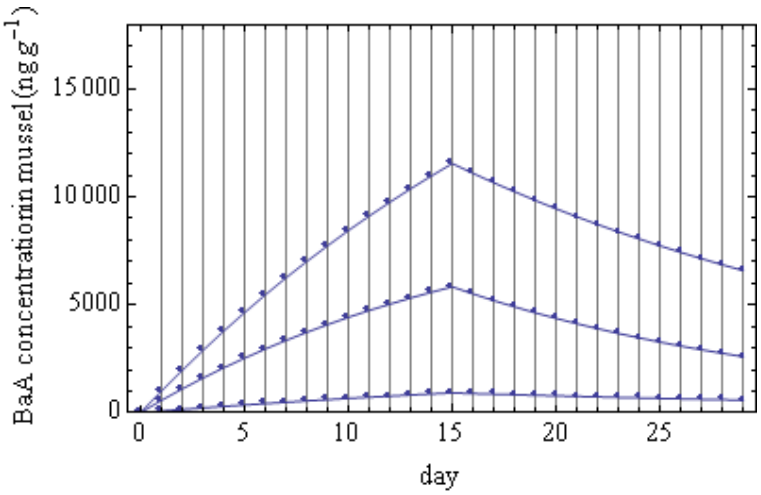

Figure 3.40 : There are 51 mussels in each aquarium exposed to BaA (3, 6, 9 µg L^{-1}) during the uptake (right half) and depuration (left half) periods, without taking out any mussels at sampling days.

Another scenario of mussel number is shown in Figure 3.41. Number of mussels increased twice as before (100 mussels), however the levels of BaA concentration decreased around 35% of the levels in Figure 3.40.

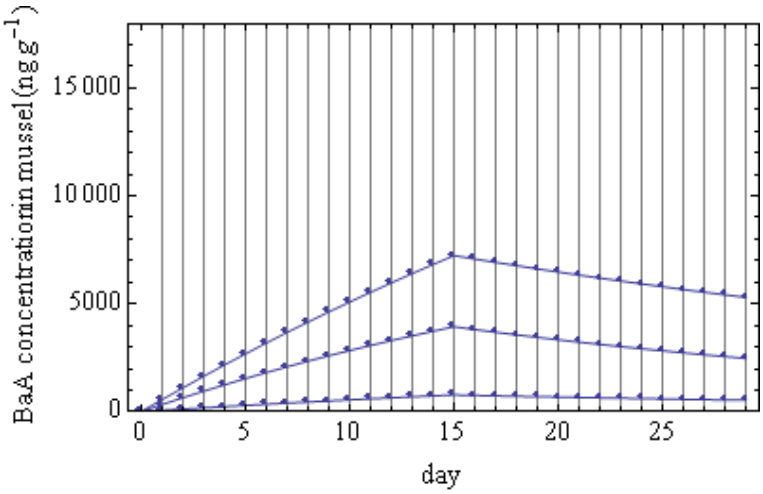

Figure 3.41 : There are 100 mussels in each aquarium exposed to 3, 6, 9 µg L^{-1} BaA during the uptake (right half) and depuration (left half) periods, without taking out any mussels at sampling days.

Similar simulations were also performed for PHE exposure experiments. The number of mussels had not been decreased by taking samples out at sampling days and remained as 48 mussels during both uptake and depuration periods of PHE exposure experiment. Accumulation level of PHE in 48 mussel tissues is shown in Figure 3.42. It is seen in Figure 3.42 that PHE accumulation level in mussel tissues have not been decreased apparently compared with the condition of decreasing number of mussels

at sampling days as shown in Figure 3.34.

This result is different from the result of Figure 3.40 because of the different properties of two PAHs such as hydrophobicity and bioavailability. PHE was absorbed/adsorbed higher than BaA into/onto the algae cells. Additionally, the primary route of PHE bioaccumulation in mussels was consumption of algae cells whereas the primary route of BaA bioaccumulation was seawater uptake. Thus, the level of PHE bioaccumulation in mussels has not been decreased as much as the level of BaA bioaccumulation.

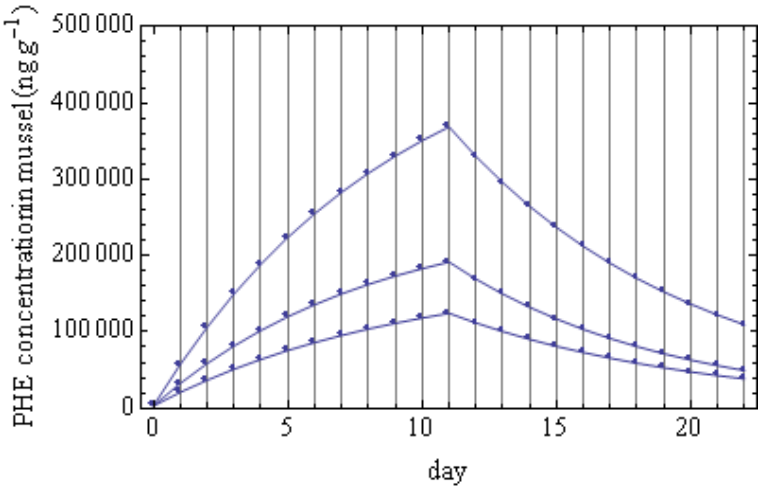

Figure 3.42 : There are 48 mussels in each aquarium exposed to PHE (250, 500, 1000 µg L^{-1}) during the uptake (right half) and depuration (left half) periods, without taking out any mussels at sampling days.

Another mussel number scenario is shown in Figure 3.43. Number of mussels increased twice as before (100 mussels), however the levels of PHE concentration decreased around 30% of the levels in Figure 3.42. This decrease is almost similar with the decrease of mussels exposed of BaA in Figure 3.41. It indicates that the two times of increase in mussel number decreases the bioaccumulation level approximately 30-35%.

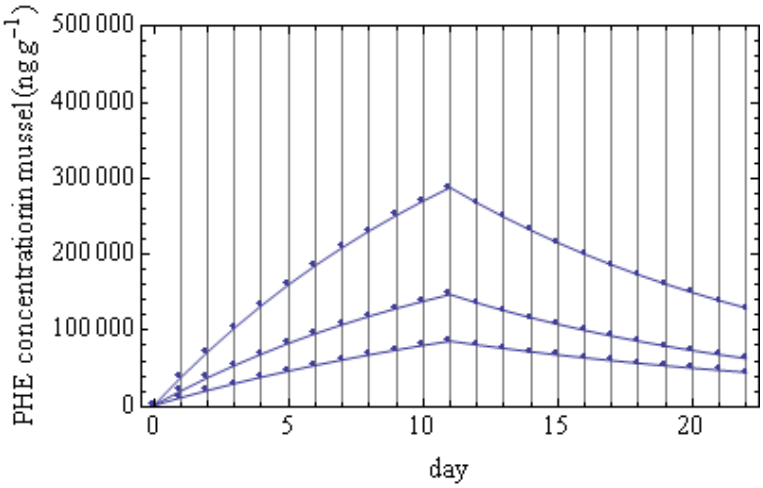

Figure 3.43 : There are 100 mussels in each aquarium exposed to PHE (250, 500, 1000 μg L^{-1}) during the uptake (right half) and depuration (left half) periods, without taking out any mussels at sampling days.

3.9.4 Duration of uptake and depuration periods

Various scenarios of uptake and depuration periods are shown in the figures between Figure 3.44 and Figure 3.49. In each scenario, 50 mussels were remained constant additional to the initial conditions of the performed laboratory experiments with BaA and PHE. It is observed from Figure 3.44, Figure 3.45 and Figure 3.46 that as the duration of uptake period increases, the levels of BaA bioaccumulation in mussels reach slowly to the steady state condition as expected. This is seen more clearly in Figure 3.46 which the uptake period lasts 60 days.

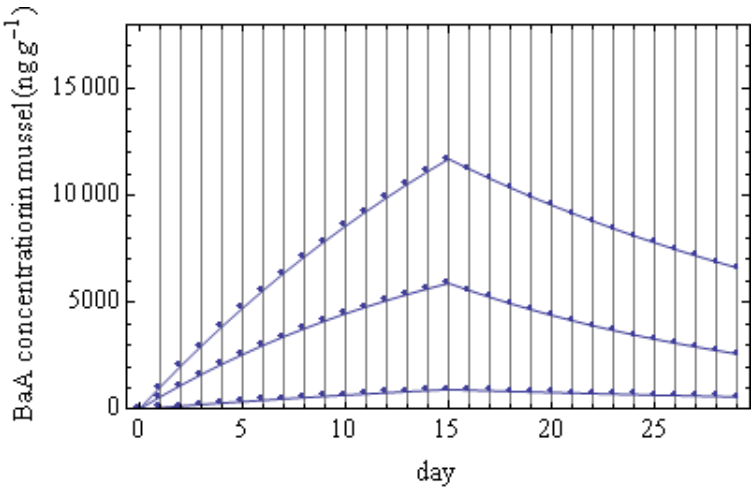

Figure 3.44 : 50 mussels were exposed to three different concentrations of BaA (3, 6, 9 μg L^{-1}) during 15 days of uptake and 15 days of depuration periods. Left side of the graph shows the uptake period whereas the right side of the figure shows the depuration period.

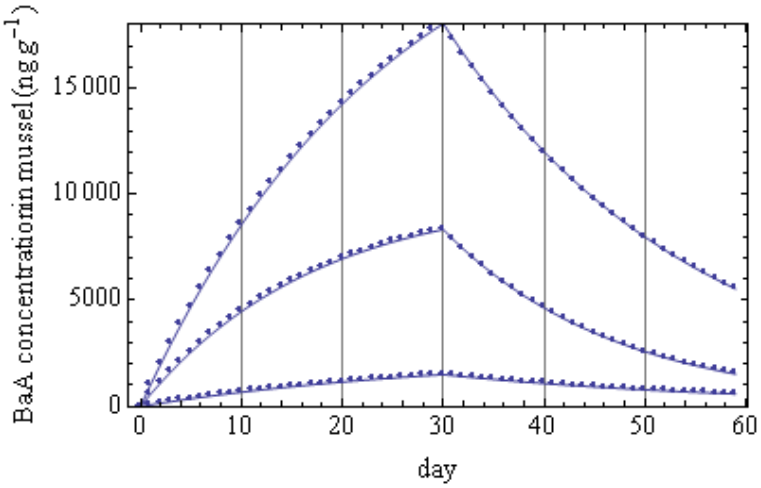

Figure 3.45 : 50 mussels were exposed to three different concentrations of BaA (3, 6, 9 µg L^{-1}) during 30 days of uptake and 30 days of depuration periods. Left side of the graph shows the uptake period whereas the right side of the figure shows the depuration period.

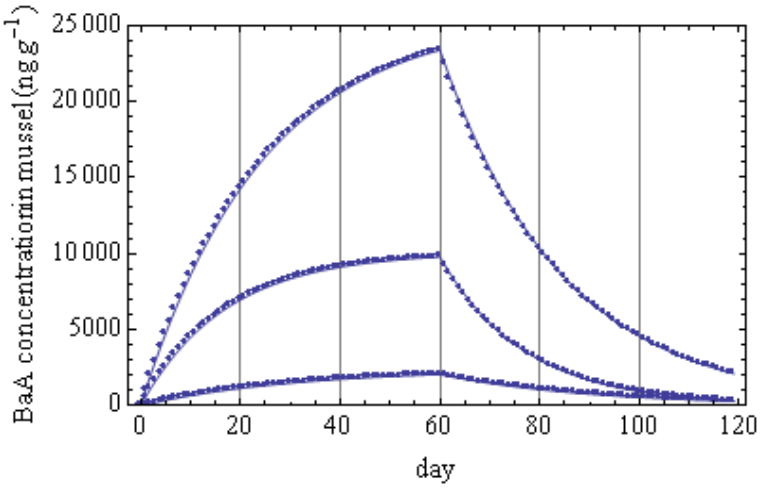

Figure 3.46 : 50 mussels were exposed to three different concentrations of BaA (3, 6, 9 µg L^{-1}) during 60 days of uptake and 60 days of depuration periods. Left side of the graph shows the uptake period whereas the right side of the figure shows the depuration period.

In addition to the scenarios of BaA exposure, similar scenarios were performed for PHE exposure and represented in Figure 3.47, Figure 3.48 and Figure 3.49 for the uptake periods of 22, 44, and 88 days.

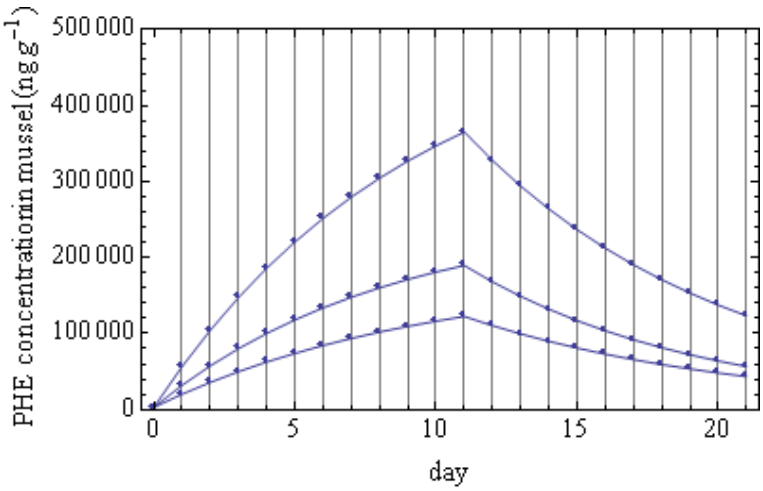

Figure 3.47 : 50 mussels were exposed to three different concentrations of PHE (250, 500, 1000 µg L^{-1}) during 11 days of uptake and 11 days of depuration periods. Left side of the graph shows the uptake period whereas the right side of the figure shows the depuration period.

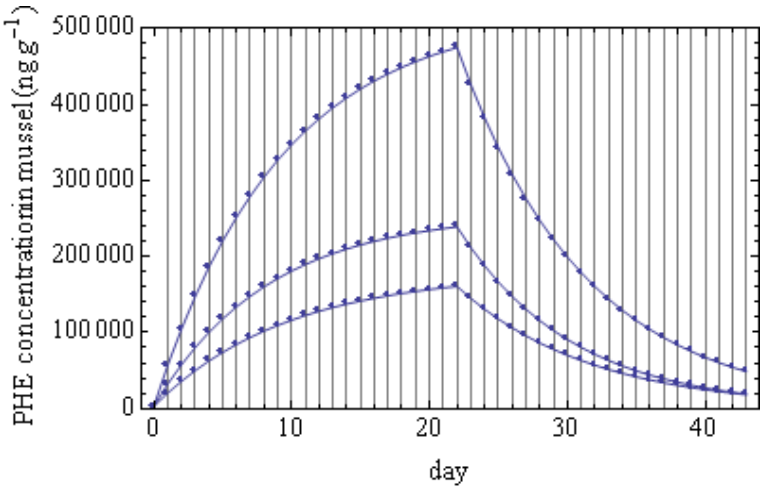

Figure 3.48 : 50 mussels were exposed to three different concentrations of PHE (250, 500, 1000 µg L^{-1}) during 22 days of uptake and 22 days of depuration periods. Left side of the graph shows the uptake period whereas the right side of the figure shows the depuration period.

Scenarios of PHE exposure reach to steady state condition quicker compared with the scenarios of BaA exposure. It is seen from Figure 3.49 that the steady state condition was reached after 44 days of uptake period.

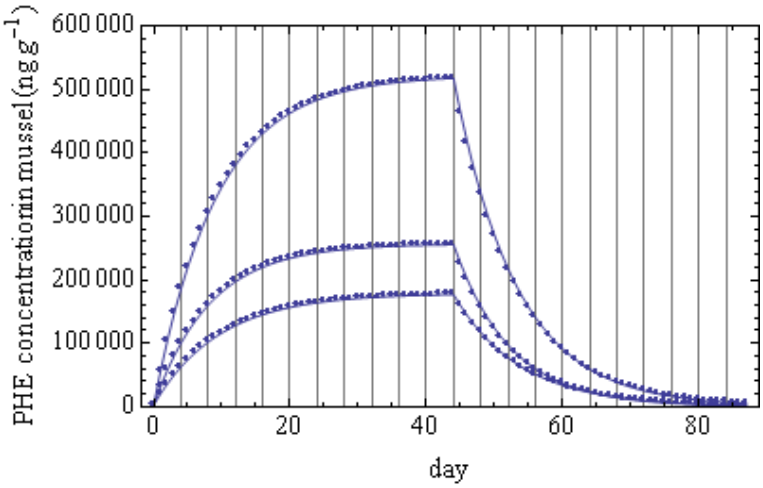

Figure 3.49 : 50 mussels were exposed to three different concentrations of PHE (250, 500, 1000 µg L^{-1}) during 44 days of uptake and 44 days of depuration periods. Left side of the graph shows the uptake period whereas the right side of the figure shows the depuration period.

4. CONCLUSION

Two and three ring PAHs were represented by phenanthrene (PHE) and benzo(a)anthracene (BaA) in this study. PAH concentrations in mussel tissues were determined with the bioaccumulation and depuration experiments. The levels of PAH concentrations in mussels were directly related with Log K_{ow} values of model PAHs. Log K_{ow} of BaA was 5.9 whereas Log K_{ow} of PHE was 4.5. Thus, the bioaccumulation level of BaA was higher than the bioaccumulation level of PHE at the same exposure conditions. This information was also compatible with the QSAR values calculated from this study and literature equations. Exposure concentrations of model PAHs were selected under their solubility limits in water. The selected concentrations were 3, 6 and 9 μg L^{-1} for BaA and 250, 500 and 1000 μg L^{-1} for PHE. The bioavailability of the chemicals is positively related with their solubility limits. Thus, bioaccumulation levels of PHE in mussels are found relativey higher than the levels of BaA in mussels.

Two different biomarker methods were applied to the mussels used in the experiments in order to observe the toxicity of selected PAHs. One of them was filtration rate and the other one was lysosomal membrane stability. Thus, both physiological and cellular responses of mussels were able to be observed during the uptake and depuration periods. It is seen that PHE has more toxic effects on mussels compared with BaA for both biomarkers. Additionally, filtration rate results were more clear compared with lysosomal stability of mussels. It is observed during the filtration rate measurements that the toxic effect of the highest PHE concentration did not reduce during the depuration period.

A mechanistic model was developed to represent the processes of PAH bioaccumulation and depuration in an aquatic food chain. This food chain was formed by Mediterranean species *Mytilus galloprovincialis* and marine diatom *Phaeodactylum tricornutum* that were exposed to selected PAHs. The model was designed as three compartment to represent biota, food and surrounding environment with *Mytilus galloprovincialis*, *Phaeodactylum tricornutum*, and seawater,

respectively. Developed model was based on the bioaccumulation and depuration experiments under laboratory conditions. Each compartment of the model was formulated with a differential equation taking into consideration the compartment interactions such as kinetic rate constants and filtration rate. Thus, the model was turned into a closed loop system and enabled a basic model to predict the highest levels of PAH accumulation, transfer and depuration in mussel tissues. Developing the model as a closed loop system involved omitting loss processes like evaporation and degradation of PAHs. Related parameters of those processes may be added to the equations in the further studies. In spite of the lack of these parameters in the present study, model outputs were verified with experimental data after the successfully run of the model code and the correlation coefficients of the model and experiment data were found as 0.76, 0.75 and 0.65 for BaA aquariums from lower to higher concentrations and 0.85, 0.97 and 0.97 for PHE aquariums from lower to higher concentrations, respectively.

The model was basically formed by the input data, differential equation system and the output graphs. The properties of selected mussel and algae species such as mussel number, mussel weight, algae cell number and concentrations of selected PAHs were used as model input parameters additional to seawater volume, kinetic rate constants and filtration rates of mussels. The model code was written in Mathematica software program which is being used in the fields of science, engineering, and mathematical computations. The system of differential equations was solved with 4^{th} order Runge-Kutta numerical integration method and the model outputs were represented graphically by the curve fitting feature of the software. After the successfully run of the model code, the outputs of the model were represented visually as concentration-day graphs for different PAH exposures. Then, output graphs of the theoretical PAH exposures were compared to the experimental data. Output graphs were compared separately for three different concentrations of two different PAHs. Then, output graphs were collected under one chart for each PAH. All theoretical calculations were compared to experimental data on the same chart and depending on the correlation coefficients between the experiment and modelling data, the model was accepted basically as a qualified model to represent the accumulation, transfer and depuration of PAHs in mussels. Therefore, different scenarios were run using the same model code. These scenarios consist of different algae concentration, different

types of marine algae, increased mussel number and increased duration of uptake and depuration periods.

Although developed model needs some further studies about the mussel growth rate for long durations of uptake and depuration processes, it can also be used as a predictive tool in field studies to observe the accumulation and depuration levels of PAHs in *Mytilus galloprovincialis*. This outcome is supported by the execution of the model with various scenarios. The levels of accumulated PAH concentrations in mussels can be estimated after the releases of PAH in sewater from point and non-point sources. Afterwards, the duration needed for the depuration of mussels can be estimated with the same model. The effect of algal concentrations during exposure and depuration processes can also be observed with this model. Thus, possible algal blooms in the areas of exposed PAHs can be evaluated together with the potential PAH accumulation levels in mussel tissues.

It has been observed that the main route of phenanthrene exposure was through food consumption whereas the main route of benzo(a)anthracene exposure was through seawater. This result can be generalized for three and four ring PAHs assuming that phenanthrene represents three ring and benzo(a)anthracene represents four ring PAHs.

These scenarios are summarized as follows: Firstly, the change in the number of algae cells was observed. Algal concentrations were increased level by level and it is observed in the highest concentration aquariums that 1000 ng g^{-1} BaA concentration difference occurs with 6 times of increased algal concentration and 20000 ng g^{-1} PHE concentration difference occurs with 50 times of increased algal concentration which corresponds to 2.5 times of increased algal concentration for 1000 ng g^{-1} PHE concentration difference.

Different types of marine algae were used in another scenario. Bioconcentration factors of six different species of marine algae for the selected PAHs were calculated and these values were used as the input data of the model. The number of algal cells remained same as the original data during this scenario. After all the output graphs were obtained, it has been observed that different bioconcentration factors affected the output graphs differently. These observations revealed that three-ring benzo(a)anthracene and two-ring phenanthrene accumulate in a different way. As a

result of the model scenarios of different algae species, it is seen that as the bioconcentration factors of algae increases, the level of benzo(a)anthracene accumulation in mussels is decreasing. On the other hand, an increase in the level of phenanthrene accumulation in mussels was observed with the increasing value of bioconcentration factors of different algae species.

Another scenario was run by changing the number of mussels. A decrease in the levels of PAH accumulation around 30-35% was observed when the initial number of mussels were remained unchanged (without any sampling during the experimental period) and doubled under the same experimental conditions.

In addition to all of these scenarios, the durations of accumulation and duration periods are the changeable parameters of the model. The duration of periods was increased as two and four times of the original data for both accumulation and depuration periods. Model outputs revealed that the level of benzo(a)anthracene concentration in mussels reaches to steady state condition at around one third slower rate than the level of phenanthrene concentration in mussels.

Although the developed model was based on experiments and verified with the experimental data, it is not a totally complete model to represent PAH accumulation, transfer and depuration in mussels. To improve the model, the information related to the growth rate of the mussels during the long term exposure experiments should be included. In addition, evaporation and degradation rates of PAHs are the parameters needed to be added in the model. These parameters were left to be completed in further modeling studies. As a result, the developed model reduced the need to perform several laboratory experiments, and also demonstrated that it can be used as a predictive tool of the PAH accumulation and depuration levels in mussels with respect to exposure concentrations and exposure and depuration durations.

REFERENCES

Andersen, M. E. (1981). A physiologically based toxicokinetic description of metabolism of inhaled gases and vapors: analysis at steady state, *Toxicology and Applied Pharmacology, 60*, 509–526.

Andersen, M. E. (2003). Toxicokinetic modeling and its applications in chemical risk assessment, *Toxicology Letters*, *138*, 9–27.

Arfsten, D.P., Schaeffer, D.J. and Mulveny, D.C. (1996). The effects of near ultraviolet radiation on the toxic effects of polycyclic aromatic hydrocarbons in animals and plants: a review, *Ecotoxicology and Environmental Safety, 33*, 1–24.

Arnot, J.A. and Gobas, F.A.P.C. (2003). A generic QSAR for assessing the bioaccumulation potential of organic chemicals in aquatic food webs, *QSAR and Combinatorial Science*, *22(3)*, 337–345.

Arnot, J.A. and Gobas, F. (2004). A food web bioaccumulation model for organic chemicals in aquatic ecosystems, *Environmental Toxicology and Chemistry, 23(10)*, 2343−2355.

Arnot, J.A. and Gobas, F.A. (2006). A review of bioconcentration factor (BCF) and bioaccumulation factor (BAF) assessments for organic chemicals in aquatic organisms, *Environmental Reviews*, *14(4)*, 257–297.

ATSDR. (1990). Toxicological profile for benz(a)anthracene. Publication no. ATSDR/TP-88/04, U.S. Department of Health and Human Services, Public Health Service, Agency for Toxic Substances and Disease Registry, Atlanta, Georgia.

ATSDR. (1995). Toxicological profile for polycyclic aromatic hydrocarbons. U.S. Department of Health and Human Services, Public Health Service, Agency for Toxic Substances and Disease Registry. Date retrieved: 15.02.2013, adress: http://www.atsdr.cdc.gov/toxprofiles/tp69.pdf.

Axelman, J., Næs, K., Naf, C. and Broman, D. (1999). Accumulation of polycyclic aromatic hydrocarbons in semipermeable membrane devices and caged mussels (*Mytilus edulis* L.) in relation to water column phase distribution, *Environmental Toxicology and Chemistry*, *18(11)*, 2454–2461.

Banerjee, S. and Baughman, G.L. (1991). Bioconcentration factors and lipid solubility, *Environmental Science and Technology*, *25*, 536–539.

Bartels, M., Rick, D., Lowe, E., Loizou, G., Price, P., Spendiff, M., Arnold, S., Cocker, J. and Ball, N. (2012). Development of PK- and PBPK-based modeling tools for derivation of biomonitoring guidance values, *Computer Methods and Programs in Biomedicine*, *108(2)*, 773–88.

Baumard, P., Budzinski, H. and Garrigues, P. (1998). PAHs in Arcachon Bay, France: origin and biomonitoring with caged organisms, *Marine Pollution Bulletin, 36(8)*, 577–586.

Baumard, P., Budzinski, H., Garrigues, P., Dizer, H. and Hansen, P.D. (1999). Polycyclic aromatic hydrocarbons in recent sediments and mussels (*Mytilus edulis*) from the Western Baltic Sea: occurrence, bioavailability and seasonal variations, *Marine Environment Research*, *47*, 17–47.

Baumard, P., Budzinski, H., Garrigues, P., Narbonne, J.F., Burgeot, T., Michel, X. and Bellocq, J. (1999). Polycyclic aromatic hydrocarbon (PAH) burden of mussels (*Mytilus sp*.) in different marine environments in relation with sediment PAH contamination, and bioavailability, *Marine Environment Research*, *47*, 415–439.

Beyer, J. (1996). Fish biomarkers in marine pollution monitoring; evaluation and validation in laboratory and field studies, Academic thesis, University of Bergen, Norway.

Bischoff, K.B. (1987). Physiologically based pharmacokinetic modeling, in: P*harmacokinetics in Risk Assessment. Drinking Water and Health*, National Academy Press, Washington, D.C.

Björk, M. and Gilek, M. (1997). Bioaccumulation kinetics of PCB 31, 49, 153 in the blue mussel *Mytilus edulis* L., *Aquatic Toxicology, 38*, 101–123.

Bresler, V., Bissinger, V., Abelson, A., Dizer, H., Sturm, A., Kratke, R., Fishelson, L. and Hansen, P.D. (1999). Marine molluscs and fish as biomarkers of pollution stress in littoral regions of the Red Sea, Mediterranean Sea and North Sea, *Helgoland Marine Research*, *53*, 219–243.

Brooks, K.M. (1997). *Literature Review, Computer Model and Assessment of the Potential Environmental Risks Associated With Creosote Treated Wood Products Used in Aquatic Environments*, prepared for: Western Wood Preservers Institute. Date retrieved: 15.02.2013, adress: http://www.wwpinstitute.org/documents/01creo497.pdf.

Campfens, J. and Mackay, D. (1997). Fugacity-based model of PCB bioaccumulation in complex aquatic food webs, *Environmental Science and Technology, 31*, 577-583.

Ceccherelli, V.U. and Rossi R. (1984). Settlement, growth and production of the mussel *Mytilus galloprovincialis*, *Marine Ecology Progress Series*, *16*, 173-184.

Chiou, C.T., Freed, V.H., Schmedding, D.W. and Kohnert, R.L. (1977). Partition coefficient and bioaccumulation of selected organic chemicals, *Environmental Science and Technology*, *11*, 475–478.

Clason, B., Langston, W.J., and Zauke, G-P. (2004). Bioaccumulation of trace metals in the amphipod *Chaetogammarus marinus* (Leach, 1815) from the Avon and Tamar estuaries (UK): comparison of two-compartment and hyperbolic toxicokinetic models, *Marine Environmental Research*, *57*, 171–195.

Clewell, H.J. and Andersen, M.E. (1985). Risk assessment extrapolations and physiological modeling, *Toxicology and Industrial Health*, *1*, 111–131.

Clewell, H.J. and Andersen, M.E. (1989). Biologically motivated models for chemical risk assessment, *Health Physics, 57(Suppl 1)*, 129–137.

Clewell, H.J., Tan, Y.M., Campbell, J.L. and Andersen, M.E. (2008). Quantitative Interpretation of Human Biomonitoring Data, *Toxicology and Applied Pharmacology*, *231*, 122–133.

Connolly, J.P. (1991). Application of a food chain model to polychlorinated biphenyl contamination of the lobster and winter flounder food chains in New Bedford Harbor, *Environmental Science and Technology, 25*, 760-770.

Coughlan, J. (1969). The estimation of filtering rate from the clearance of suspensions, *Marine Biology, 2*, 356-358.

Dailianisa, S., Domouhtsidoub, G.P., Raftopouloub, E., Kaloyiannia, M. and Dimitriadisb, V.K. (2003). Evaluation of neutral red retention assay, micronucleus test, acetylcholinesterase activity and a signal transduction molecule (cAMP) in tissues of *Mytilus galloprovincialis* (L.), in pollution monitoring, *Marine Environmental Research*, *56*, 443–470.

Davies, R.P. and Dobbs, A. (1984). The prediction of bioconcentration in fish, *Water Research*, *18*, 1253–1262.

Dearden, J.C. (2004). *QSAR Modeling of Bioaccumulation*, chapter 15, CRC Press LLC.

Dearden, J.C., Netzeva, T.I. and Bibby, R. (2002a). Comparison of a number of commercial software programs for the prediction of octanol-water partition coefficients, *Journal of Pharmacy and Pharmacology, 54*, S65–S66.

Dearden, J.C., Netzeva, T.I. and Bibby, R. (2002b). Comparison of a number of commercial software programs for the prediction of aqueous solubility, *Journal of Pharmacy and Pharmacology*, *54*, S66.

Dierickx, P.J. and van de Vijver, I. (1991). Correlation of the neutral red uptake inhibition assay of cultured fathead minnow cells with fish lethality tests, *Bulletin of Environmental Contamination and Toxicology*, *46*, 649–653.

Dimitrov, S., Dimitrova, N., Parkerton, T., Comber, M., Bonnell, M. and Mekenyan, O. (2005). Base-line model for identifying the bioaccumulation potential of chemicals, *SAR and QSAR in Environmental Research*, *16(6)*, 531–554.

Dorgelo, J. and Smeenk, J.W. (1988). Contribution to the ecophysiology of *Dreissena polymorpha* (Pallas) (Mollusca: Bivalvia): growth, filtration rate and respiration, *Verhandlungen des Internationalen Verein Limnologie, 23*, 2202-2208.

D'Souza, R.W. and Andersen, M.E. (1988). Physiologically based pharmacokinetic model for vinylidene chloride, *Toxicology and Applied Pharmacology, 95*, 230–240.

Easterling, M.R., Evans, M.V. and Kenyon, E.M. (2000). Comparative analysis of software for physiologically based pharmacokinetic modeling: simulation, optimization, and sensitivity analysis, *Toxicology Methods*, *10*, 203–229.

Eisler, R. (1987). Polycyclic aromatic hydrocarbon hazards to fish, wildlife, and invertebrates: a synoptic review. U.S. Fish and Wildlife Service Biological Report 85 (1.11). Date retrieved: 15.02.2013, adress: http://www.pwrc.usgs.gov/infobase/eisler/CHR_11_PAHs.pdf.

Fernandes, M.B., Sicre, M-A., Boireau, A. and Tronczynski, J. (1997). Polyaromatic hydrocarbon (PAH) distributions in the Seine River and its estuary, *Marine Pollution Bulletin*, *34(11)*, 857–867.

Geyer, H., Sheehan, D., Kotzias, D., Freitag, D. and Korte, F. (1982). Prediction of ecotoxicological behaviour of chemicals: relationship between physicochemical properties and bioaccumulation of organic chemicals in the mussel, *Chemosphere*, *11*, 1121–1134.

Giannapas, M., Karnis, L. and Dailianis, S. (2012). Generation of free radicals in haemocytes of mussels after exposure to low molecular weight PAH components: immune activation, oxidative and genotoxic effects, *Comparative Biochemistry and Physiology Part C*, *155*, 182-189.

Gibaldi, M. and Perrier, D. (1975). *Pharmacokinetics*, Marcel Dekker Publishing Co, New York, NY.

Gilek, M., Björk, M. and Naf C. (1996). Influence of body size on the uptake, depuration and bioaccumulation of PCB congeners by Baltic Sea blue mussels, *Mytilus edulis* L., *Marine Biology, 125*, 499–510.

Global Invasive Species Database
<http://www.issg.org/database/species/ecology.asp?si=102&fr=1&sts=sss&lang=EN>, date retrieved 10.02.2013.

Gobas, F.A.P.C. (1993). A Model for Predicting the Bioaccumulation of Hydrophobic Organic Chemicals in Aquatic FoodWebs: Application to Lake Ontario, *Ecological Modelling*, *69*, 1–17.

Guillard, R.R.L. and Ryther, J.H. (1962). Studies of marine planktonic diatoms. I. *Cyclotella nana* Hustedt, and *Detonula confervaceae* (Cleve) Gran. *Canadian Journal of Microbiology*, *8*, 229–239.

Hansch, C., Leo, A. and Hoekman, D. (1995). *Exploring QSAR: hydrophobic, electronic, and steric constants*, American Chemical Society, Washington, DC, USA.

Harding, J.M., Couturier, C., Parsons, G.J. and Ross, N.W. (2004a). Evaluation of the neutral red assay as a stress response indicator in cultivated mussels (*Mytilus spp.*) in relation to post-harvest processing activities and storage conditions, *Aquaculture*, *231*, 315–326.

Harding, J.M., Couturier, C., Parsons, G.J. and Ross, N.W. (2004b). Evaluation of the neutral red retention assay as a stress response indicator in cultivated mussels (*Mytilus spp.*) in relation to seasonal and environmental conditions, *Journal of Shellfish Research, 23(3)*, 745–751.

Haugland, R.P. (1996). *Handbook of Fluorescent Probes and Research Chemicals* (6th Ed.) Molecular Probes, Eugene, Oregon.

Hauton, C., Hawkins, L.E. and Hutchinson, S. (1998). The use of the neutral red retention assay to examine the effects of temperature and salinity on haemocytes of the European flat oyster *Ostrea edulis* (L.), *Comparative Biochemistry and Physiology B*, *119*, 619–623.

Hendriks, A.J., van der Linde, A., Cornelissen, G. and Sijm, D. (2001). The power of size. 1. Rate constants and equilibrium ratios for accumulation of organic substances related to octanol-water partition ratio and species weight, *Environmental Toxicology and Chemistry, 20(7)*, 1399−1420.

HSDB. (2001). [On-line database]. National Library of Medicine, Washington, DC. Retrieved February 15, 2013, from http://toxnet.nlm.nih.gov/cgi-bin/sis/htmlgen?HSDB.

Humphries III, L.F. (2006). Effects of polycyclic aromatic hydrocarbon exposure on three life stages of freshwater mussels (bivalvia: unionidae), MSc thesis, North Carolina State University, Raleigh, N.C.

Irwin, R.J., van Mouwerik, M.V., Stevens, L., Seese, M.D. and Basham, W. (1997). Environmental contaminants encyclopedia. National Park Service, Water Resources Division, Fort Collins, Colorado. Distributed within the Federal Government as an Electronic Document (Projected public availability on the internet or NTIS: 1998). Date retrieved: 15.02.2013, address: http://www.nature.nps.gov/water/ecencyclopedia/contents.cfm.

Isnard, P. and Lambert, S. (1988). Estimating bioconcentration factors from *n*-octanol/water partition coefficient and aqueous solubility, *Chemosphere*, *17*, 21–34.

Jensen, L.K., Jæger, I., Honkanen, J.O. and Carroll, J.L. (2012). Bioaccumulation of phenanthrene and benzo[a]pyrene in *Calanus finmarchicus*, *Ecotoxicology and Environmental Safety*, *78*, 225–231.

Jørgensen, S.E., Halling-Sørensen, B. and Mahler, H. (1998). *Handbook of Estimation Methods in Ecotoxicology and Environmental Chemistry*, Lewis Publishers, Boca Raton, FL.

Karacik, B., Okay, O.S., Henkelmann, B., Bernhoeft, S. and Schramm, K-W. (2009). Polycyclic aromatic hydrocarbons and effects on marine organisms in the Istanbul Strait, *Environment International*, *35(3)*, 599−606.

Kenaga, E.E. and Goring, C.A.I. (1980). Relationship between water solubility, soil sorption, octanol-water partitioning and bioconcentration of chemicals in biota, In: Eaten, J.G., Parrish, P.R., Hendricks, A.C. eds. *Aquatic toxicology*. Philadelphia, PA, American Society for Testing and Materials, pp. 78-115 (ASTM Special Technical Publication 707).

Kumar, S., Kumar, M., Thurow, K., Stoll, R. and Kragl, U. (2009). Fuzzy filtering for robust bioconcentration factor modelling, *Environmental Modelling and Software*, *24*, 44–53.

Landrum, P.F. (1989). Bioavailability and toxicokinetics of polycyclic aromatic hydrocarbons sorbed to sediments for the amphipod *Pontoporeia hoyi, Environmental Science and Technology, 23*, 588−595.

Landrum, P.F., Lee II, H. and Lydy, M.J. (1992). Toxicokinetics in aquatic systems: Model comparisons and use in hazard assessment, *Environmental Toxicology and Chemistry, 11*, 1709−1725.

Leoni, B., Bettinetti, R. and Galassi, S. (2008). Sub-lethal effects of acetone on *Daphnia magna*, *Ecotoxicol*ogy, **17**, 199−205.

Leung, H-W. (1991). Development and utilization of physiologically based pharmacokinetic models for toxicological applications, *Journal of Toxicology and Environmental Health, 32*, 247–267.

Linkov, I., Burmistrov, D., Cura, J. and Bridges, T. (2002). Risk-based management of contaminated sediments: consideration of spatial and temporal patterns in exposure modeling, *Environmental Science and Technology, 36*, 238−246.

Lowe, D.M., Fossato, V.U. and Depledge M.H. (1995a). Contaminant-induced lysosomal membrane damage in blood cells of mussels *Mytilus galloprovincialis* from the Venice Lagoon: an in vitro study, *Marine Ecology Progress Series, 129*, 189–196.

Lowe, D.M., Soverchia, C. and Moore, M.N. (1995b). Lysosomal membrane responses in the blood and digestive cells of mussels experimentally exposed to fluoranthene, *Aquatic Toxicology*. *33*, 105–112.

Lowe, D.M. and Pipe, R.K. (1994). Contaminant induced lysosomal membrane damage in marine mussel digestive cells: an in vitro study, *Aquatic Toxicology*, *30*, 357–365.

Luoma, S.N. and Rainbow, P.S. (2005). Why is metal bioaccumulation so variable? Biodynamics as a unifying concept, *Environmental Science and Technology*, *39*, 1921–1931.

Mackay, D, and Fraser, A. (2000). Bioaccumulation of persistent organic chemicals: mechanisms and models, *Environmental Pollution*, *110*, 375−391.

Marino, D.J. (2005). Physiologically Based Pharmacokinetic Modeling Using Microsoft Excel and Visual Basic for Applications, *Toxicology Mechanisms and Methods, 15*, 137–154.

McCarthy, J.F. (1983). Role of particulate organic matter in decreasing accumulation of polynuclear aromatic hydrocarbons by *Daphnia magna*, *Archives of Environmental Contamination and Toxicology*, *12*, 559–568.

Mekenyan, O.G, Ankley, G.T., Veith, G.D. and Call, D.J. (1994). QSAR estimates of excited states and photoinduced acute toxicity of polycyclic aromatic hydrocarbons, *SAR and QSAR in Environmental Research*, *2*, 237−247.

Monteduro, R.A., Pellizzato, F., Sperni, L. and Pavoni, B. (2007). Contamination in *Mytilus galloprovincialis* by chlorinated hydrocarbons (PCBs and pesticides), PAHs and heavy metals in the lagoon of Venice, *Polycyclic Aromatic Compounds, 27(5)*, 437–459.

Morrison, H.A., Gobas, F.A.P.C., Lazar, R. and Haffner, G. D. (1996). Development and verification of a bioaccumulation model for organic contaminants in benthic invertebrates, *Environmental Science and Technology*, *30*, 3377−3384.

Morrison, H.A., Gobas, F.A.P.C., Lazar, R., Whittle, D.M. and Haffner G.D. (1997). Development and verification of a benthic/pelagic food web model for PCB congeners in Western Lake Erie, *Environmental Science and Technology, 31*, 3267−3273.

Morrison, H.A., Whittle, D.M., Metcalfe, C.D. and Niimi, A.J. (1999). Application of a food web bioaccumulation model for the prediction of polychlorinated biphenyl, dioxin and furan congener concentrations in Lake Ontario aquatic biota, *Canadian Journal of Fisheries and Aquatic Science*, *56*, 1389−1400.

Morton B.S. (1971). Studies of *Dreissena polymorpha* (Pall.). V. Some aspects of filter-feeding and the effect of micro-organisms upon the rate of filtration. *Proceedings of the Malacological Society of London, 39*, 239−301.

Neff, J.M. (1979). Polycyclic aromatic hydrocarbons in the aquatic environment: sources, fates, and biological effects, Applied Science, Barking, Essex.

Nendza, M. (1998). *Structure-Activity Relationships in Environmental Sciences*, Chapman and Hall, London.

Newstead, J.L. and Giesy, J.P. (1987). Predictive models for photoinduced acute toxicity of polycyclic aromatic hydrocarbons to *Daphnia magna*. *Environmental Toxicology and Chemistry, 6*, 445−461.

Nichols, J.W., McKim, J.M., Andersen, M.E., Gargas, M.L., Ckewell, H.J. and Erickson, R.J. (1990). A physiologically based toxicokinetic model for the uptake and disposition of waterborne organic chemicals in fish, *Toxicology and Applied Pharmacology*, *106*, 433−447.

Nichols, J.W., McKim, J.M., Lien, G.J., Hoffman, A.D. and Bertelsen, S.L. (1991). Physiologically based toxicokinetic modeling of three waterborne chloroethanes in rainbow trout (*Oncorhynchus*). *Toxicology and Applied Pharmacology*, *110*, 374−389.

Nichols, J.W., McKim, J.M., Lien, G.J., Hoffman, A.D., Bertelsen, S.L. and Gallinat, C.A. (1993). Physiologically-based toxicokinetic modeling of three waterborne chloroethanes in channel catfish *Ictalurus punctatus, Aquatic Toxicology*, *27*, 83−112.

Okay, O.S., Tolun, L., Telli-Karakoc, F., Tufekci, V., Tufekci, H., Olgun, A. and Morkoc, E. (2003). The changes of T-PAH levels and health status of mussels in Izmit bay (Turkey) after Marmara earthquake and subsequent refinery fire, *Environment International*, *28*, 671−675.

Okay, O.S., Tolun, L., Tufekci, V., Telli-Karakoc, F. and Donkin, P. (2006). Effects of pyrene on mussels in different experimental conditions, *Environment International*, *32*, 538−544.

OECD. (1998). *Daphnia magna Reproduction Test*. OECD guidelines for testing of chemicals, Paris.

OECD. (1999). *Acetone Cas No: 67-64-1*, SIDS Initial Assessment Report (SIAR) for the 9th SIAM, Paris.

Okay, O.S. and Karacik, B. (2007). Photoinduced toxicity of selected PAHs to the marine microalga *Phaeodactylum tricornutum*. *Journal of Environmental Science and Health Part A- Toxic/hazardous Substances and Environmental Engineering*, *42*, 707−714.

Okay, O.S. and Karacik, B. (2008). Bioconcentration and phototoxicity of selected PAHs to marine mussel *Mytilus galloprovincialis*. *Journal of Environmental Science and Health Part A- Toxic/hazardous Substances and Environmental Engineering*, *43*, 1234−1242.

Okay, O.S., Ozdemir, P., and Yakan, S.D. (2011). Efficiency of butyl rubber sorbent to remove the PAH toxicity, *Journal of Environmental Science and Health Part A*, *46*, 909−913.

Pavan, M., Worth, A.P. and Netzeva, T.I. (2006). Review of QSAR models for bioconcentration. European Commission EUR 22327 EN – DG Joint Research Centre, Institute for Health and Consumer Protection, Scientific and Technical Research Series, Italy.

Piccardo, M.T., Coradeghini, R. and Valerio, F. (2001). Polycyclic aromatic hydrocarbon pollution in native and caged mussels, *Marine Pollution Bulletin*, *42(10)*, 951 – 956.

Pipe, R.K. and Coles, J.A. (1995). Environmental contaminants influencing immune function in marine bivalve mollusks, *Fish and Shellfish Immunology*, *5*, 581−595.

Poston, T. (2001). Treated wood issues associated with overwater structures in marine and freshwater environments, white paper submitted to Washington Department of Fish and Wildlife.

Pruell, R.J., Lake, J.L., Davis, W.R. and Quinn, J.G. (1986). Uptake and depuration of organic contaminants by blue mussels (*Mytilus edulis*) exposed to environmentally contaminated sediment, *Marine Biology*, *91*, 497–507.

Ramsey, J.C. and Andersen, M.E. (1984). A physiologically based description of the inhalation pharmacokinetics of styrene in rats and humans, *Toxicology and Applied Pharmacology*, *73*, 159–175.

Raoux, C.Y. and Garrigues, P. (1993). Modelisation of the mechanisms of PAH contamination of marine coastal sediments from the Mediterranean Sea. In: Garrigues, P. and Lamotte, M. (Eds.), Pol. Arom. Comp. (vol. 3): Synthesis, Properties, Analytical Measurements, Occurrence and Biological Effects. G. B. Science Publishers, Paris, pp. 443–450.

Reeders H.H. and bij de Vaate A. (1990). Zebra mussels *(Dreissena polymorpha)*: a new perspective for water quality management, *Hydrobiologia, 200/201*, 437 −450.

Reeders H.H., bij de Vaate A. and Slim F.J. (1989). The filtration rate of *Dreissena polymorpha* (Bivalvia) in three Dutch lakes with reference to biological water quality management, *Freshwater Biology*, *22*, 33−141.

Richardson, B.J., Tse, E.S-C., De Luca-Abbott, S.B., Martin, M. and Lam, P.K.S. (2005). Uptake and depuration of PAHs and chlorinated pesticides by semi-permeable membrane devices (SPMDs) and green-lipped mussels (*Perna viridis*), *Marine Pollution Bulletin*, 51, 975–993.

Ringwood, A.H., Deanna, E.C. and Hoguet, J. (1998). Effects of natural and anthropogenic stressors on lysosomal destabilization in oysters *Crassostrea virginica, Marine Ecology Progress Series*, 166, 163–171.

Roesijadi, G., Anderson, J. W. and Blaylock, J. W. (1978). Uptake of hydrocarbons from marine sediments contaminated with Prudhoe Bay crude oil: influence of feeding type of test species and availability of polycyclic aromatic hydrocarbons, *Journal of the Fisheries Research Board of Canada*, 35, 608− 614.

Rossmann, R. (Ed.). (2005). MICHTOX: A mass balance and bioaccumulation model for toxic chemicals in Lake Michigan. USEPA, Office of Research and Development, National Health and Environmental Effects Research Laboratory, Mid-Continent Ecology Division, Large Lakes Research Station, Grosse Ile, Michigan. EPA/600/R-05/158, 140 pp.

Ryan, W.S. (2003). *Development and application of a model describing the bioaccumulation and metabolism of PAHs in marine benthic food web*, Simon Fraser University.

Sara, G. and Pusceddu, A. (2008). Scope for growth of *Mytilus galloprovincialis* (Lmk., 1819) in oligotrophic coastal waters (Southern Tyrrhenian Sea, Italy), *Marine Biology*, *156*, 117−126.

Scala, S., Carels, N., Falciatore, A., Chiusano, M.L. and Bowler, C. (2002). Genome properties of the diatom *Phaeodactylum tricornutum. Plant Physiology*, *129(3)*, 993−1002.

Schwarz, F.P. (1977). Determination of temperature dependence of solubilities of polycyclic aromatic hydrocarbons in aqueous solution by a fluorescence method, *Journal of Chemical and Engineering Data*, *22*, 273−277.

Sprung, M. and Rose, U. (1988). Influence of food size and food quantity in the feeding of the mussel *Dreissena polymorpha, Oecologia, 771,* 526−532.

Stadnicka, J., Schirmer, K. and Ashauer, R. (2012). Predicting concentrations of organic chemicals in fish by using toxicokinetic models, *Environmental Science and Technology*, *46*, 3273−3280.

Thomann, R. V. (1989). Bioaccumulation model of organic chemical distribution in aquatic food chains, *Environmental Science and Technology*, *23(6)*, 699−707.

Tremblay, R., Myrand, B. and Guderley, H. (1998). Temporal variation of lysosomal capacities in relation to susceptibility of mussels, *Mytilus edulis*, to summer mortality, *Marine Biology, 132*, 641–649.

Url-1 <*http://it.wikipedia.org/wiki/Mytilus_galloprovincialis*>, date retrieved 01.03.2013

U.S. EPA. Quantitative Structure Activity Relationship
<http://www.epa.gov/nrmrl/std/qsar/qsar.html>, date retrieved 16.02.2013.

U.S. EPA. (1996). EPA Integrated Risk Information System (IRIS) electronic database, public domain information available from the government, EPA Criteria and Assessment Office, Cincinnati, OH. Date retrieved: 16.02.2013, address: http://www.epa.gov/iris/.

U.S. EPA Priority Pollutants
<http://epa.gov/waterscience/methods/pollutants.htm>, date retrieved 16.02.2013.

U.S. EPA Phenanthrene fact sheet
http://www.epa.gov/osw/hazard/wastemin/minimize/factshts/phenanth .pdf, date retrieved 16.02.2013.

Walz N. (1978). The energy balance of the freshwater mussel *Dreissena polymorpha* Pallas in laboratory experiments and in Lake Constance. I. Pattern of activity, feeding and assimilation efficiency, *Archiv für Hydrobiologie Supplement,* **55**, 83−105.

Wang, W.X. (2002). Interactions of trace metals and different marine food chains, *Marine Ecology Progress Series*, *243*, 295–309.

Widdows, J. (1985). Physiological procedures. In: The effects of stress and pollution on marine animals, B. Bayne et al. (Ed.) Praegeer, New York, pp. 161−178.

van Brummelen, T.C., van Hattum, B., Crommentuijn, T. and Kalf, D.F. (1998). Bioavailability and Ecotoxicty of PAH. In: Neilson, A.H. (Ed.). PAH and Related Compounds – Biology. (Vol. 3-J, The Handbook of Environmental Chemistry). Springer-Verlag, Berlin Heidenberg, pp.

203−263.

van der Oost, R., Beyer, J. and Vermeulen, N.P.E. (2003). Fish bioaccumulation and biomarkers in environmental risk assessment: a review, *Environmental Toxicology and Pharmacology*, *13*, 57−149.

van Hattum, B., Pons, M.J.C. and Montanes, J.F.C. (1998). Polycyclic aromatic hydrocarbons in freshwater isopods and field-partitioning between abiotic phases, *Archives of Environmental Contamination and Toxicology*, *35*, 257−267.

Voutsas, E., Magoulas, K. and Tassios, D. (2002). Prediction of the bioaccumulation of persistent organic pollutants in aquatic food webs, *Chemosphere*, *48*, 645–651.

Zauke, G-P. (2008). Toxicokinetic models as predictive tools in biomonitoring metals in zooplankton: a synthesis of ideas, *Hydrobiologia*, *614*, 3–18.

Zhang, Z. and Li, X. (2006). Evaluation of the effects of grading and starvation on the lysosomal membrane stability in pacific oysters, *Crassostrea gigas* (Thunberg) by using neutral red retention assay, *Aquaculture*, *256*, 537–541.

Zhou, Q., Zhang, J., Fu, J., Shi, J. and Jiang, G. (2008). Biomonitoring: an appealing tool for assessment of metal pollution in the aquatic ecosystem, *Analytica Chimica Acta*, *606*, 135–150.

APPENDICES

APPENDIX A: PHE concentration in seawater

APPENDIX B: Lysosomal membrane stability of mussels exposed to BaA

APPENDIX C: Filtration rates of mussels exposed to PHE in the small scale experiments

APPENDIX D: Model code written in Mathematica software

APPENDIX E: Transfer of BaA and PHE between the three compartments at the 1st day of uptake period

APPENDIX F: Scenarios with different marine algae species

APPENDICES

APPENDIX A: PHE concentration in seawater

Observations of PHE concentration in seawater were presented in the figures between Figure A.1 and Figure A.4. Data of the figures were obtained from the small scale experiments performed with PHE.

Figure A.1 shows PHE concentration in the aquarium seawater versus time during the sampling days of uptake period. Although there is not a distinctive change of PHE concentration in the aquariums, a general trend of PHE concentration decrease is observed for all aquariums which also indicates PHE bioaccumulation in mussel tissues, gradually.

In Figure A.2, PHE concentration in seawater versus time during the sampling days of depuration period is shown. Due to the clean water exchange during the depuration period, it can be said that PHE concentration results from the organisms in aquariums. In the first days of depuration period, increase of PHE concentration in seawater is clear whereas in the following days, a distinctive decrease is observed especially after 14^{th}, 18^{th} and 16^{th} days for the PHE1, PHE2 and PHE3 aquariums, respectively.

In Figure A.3, PHE concentration in seawater versus time during uptake period is shown. In general, it is observed that at the last hours of daily water exchange, PHE concentration in seawater reaches a constant value. PHE concentration in seawater decreases rapidly, especially at the first 65 minutes. This fact shows the bioaccumulation of PHE in the mussels, possibly through the algae consumption due to the positive correlation of algae density and PHE concentration in seawater.

In Figure A.4, PHE concentration in seawater versus time during depuration period is shown. At the first days of depuration period, PHE in mussels was released into the seawater with the depuration process whereas the rate of depuration decreases at the following days (approximately after the 16^{th} day) of depuration period. This fact is also seen in Figure A.1. When the PHE release is evaluated within each day, the

concentration in seawater increases gradually until the end of 24 hours of water exchange, and then it becomes constant after the 18^{th} day. As a general view, although the depuration rates are slow, depuration process of PHE concentration in mussel tissues is continuous along the depuration period.

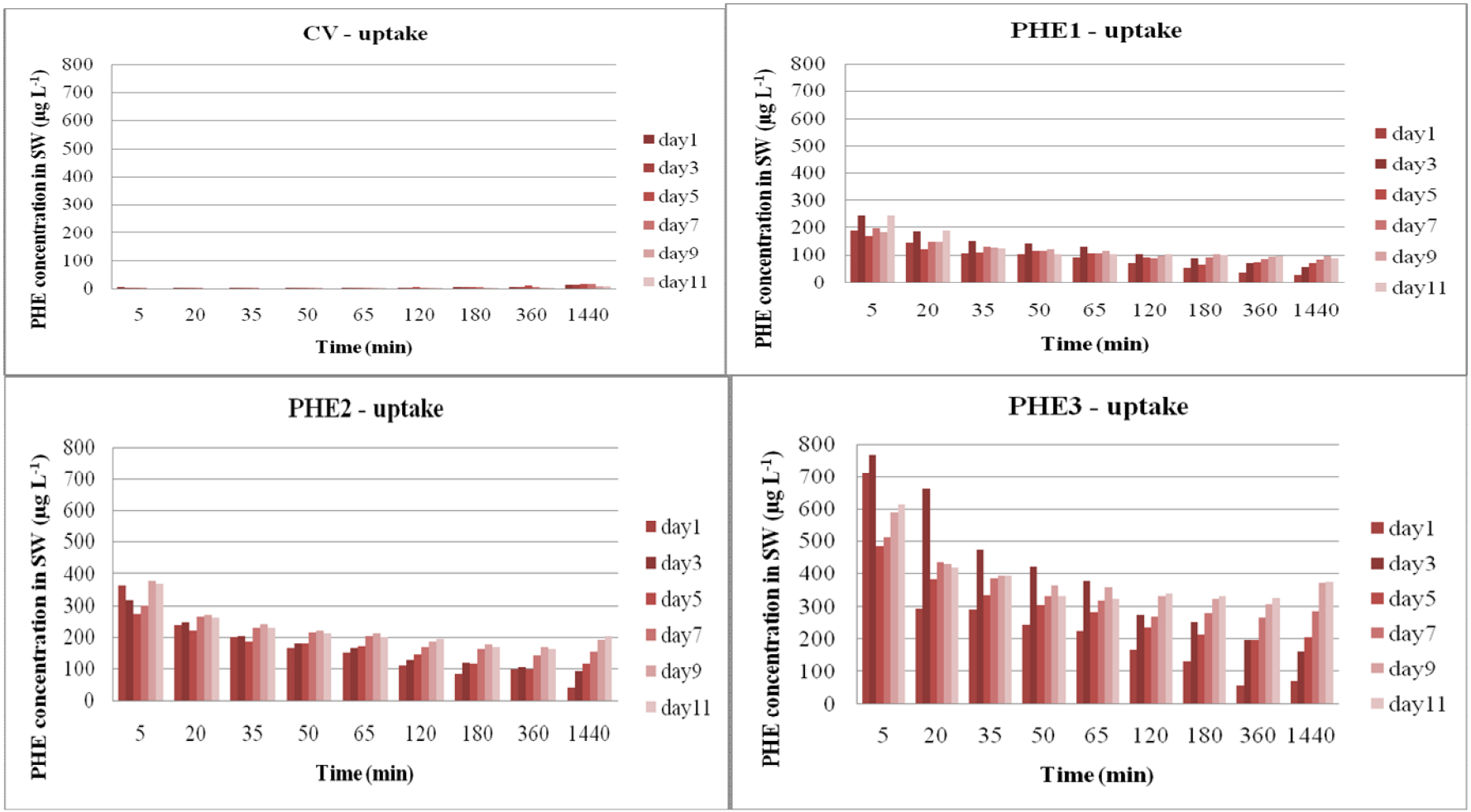

Figure A.1 : PHE concentration in seawater during 24 hours of uptake period.

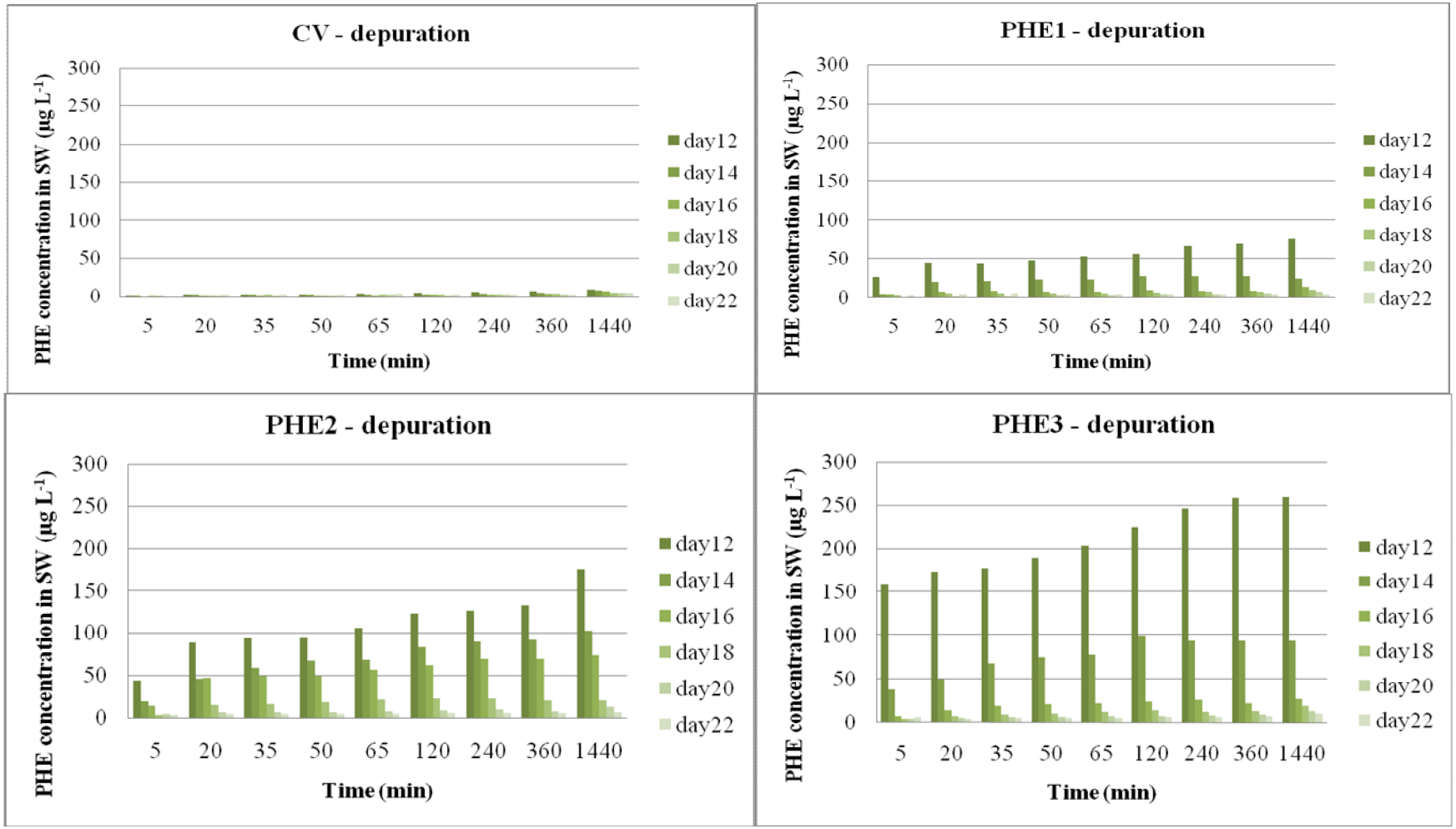

Figure A.2 : PHE concentration in seawater during 24 hours of depuration period.

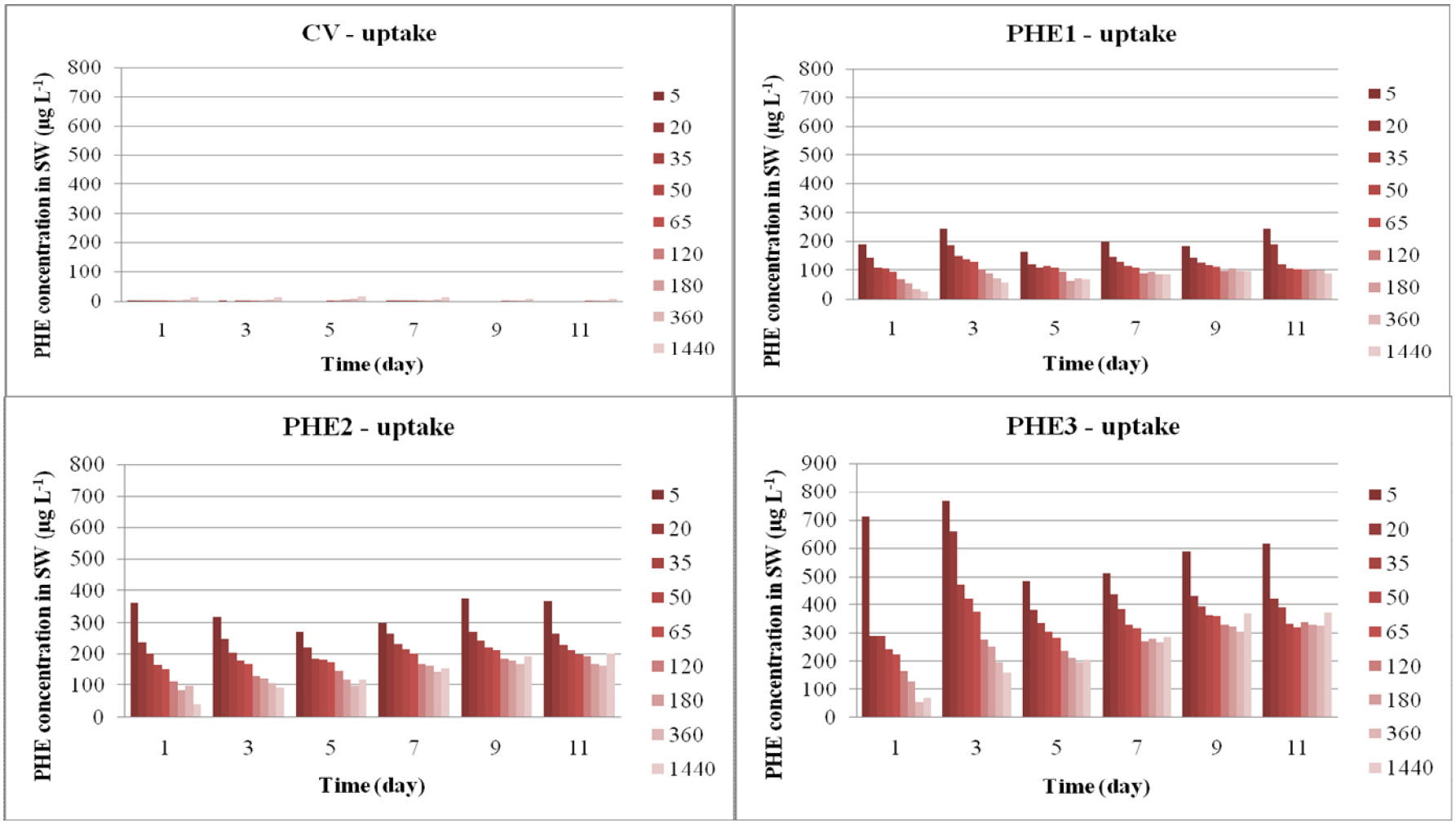

Figure A.3 : PHE concentration in seawater versus time for uptake period.

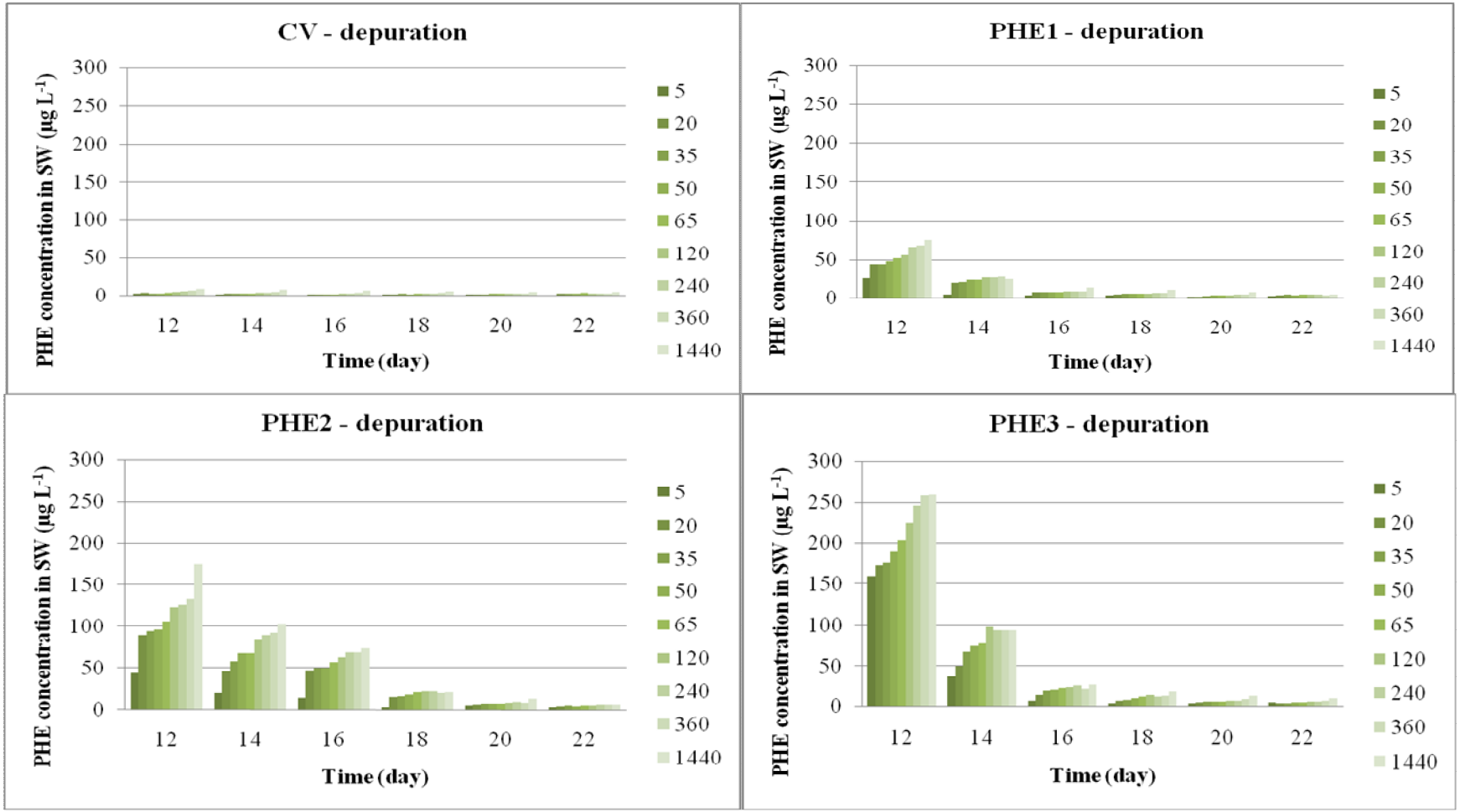

Figure A.4 : PHE concentration in seawater versus time for depuration period.

APPENDIX B: Lysosomal membrane stability of mussels exposed to BaA

Results of selected biomarker NRR assay in the large scale experiment performed with BaA are represented in the following figures.

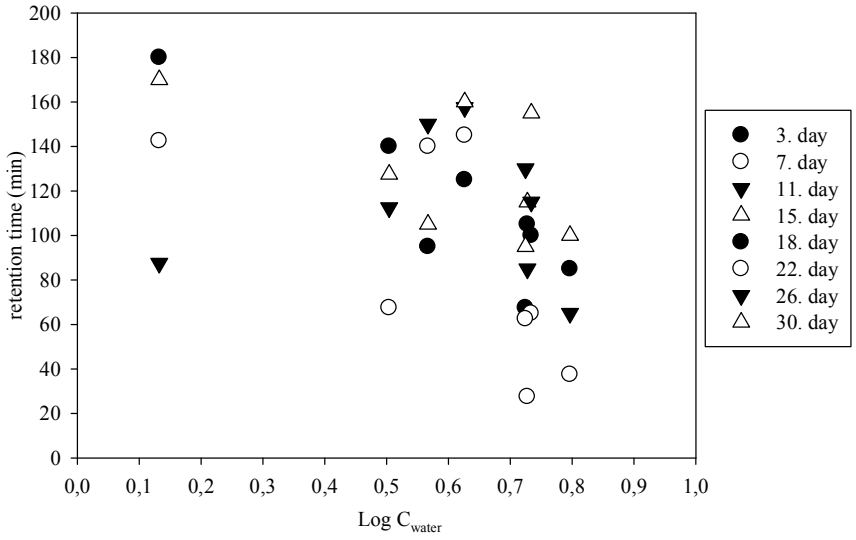

Figure B.1 : Retention time and Log C_w relationship of BaA exposed mussels during uptake and depuration periods.

Dark colored shapes indicate the data in the uptake period whereas light colored shapes indicate the data in the depuration period in Figure B.1. In all BaA exposed aquariums, the lowest time belongs to the 7^{th} day measurement. In general, retention times in the depuration period are higher than the retention times in the uptake period.

It is seen From Figure B.2 that as the concentration in the organisms increases, the retention time of neutral red dye decreases. While only one measurement of BaA1 (3 µg L^{-1}) aquarium is under %50 of retention time, more than half of the measurements of BaA3 (9 µg L^{-1}) aquarium is under %50 of retention time.

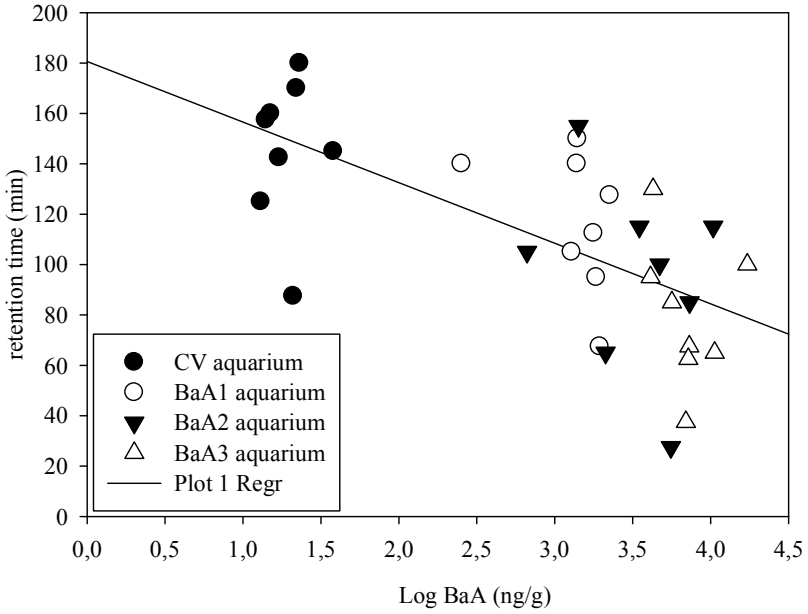

Figure B.2 : The relationship of retention time with logarithmic values of BaA concentrations in mussel tissues during the whole experiment period.

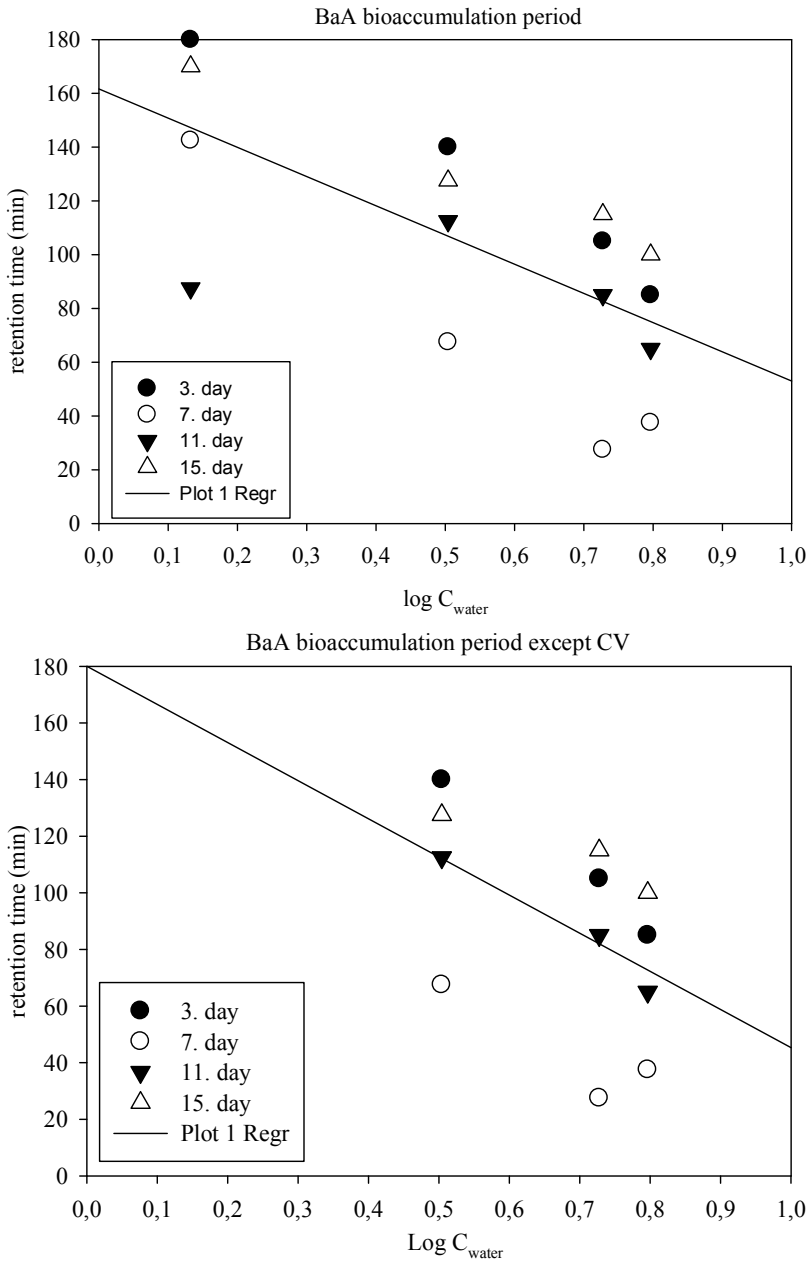

Figure B.3 : Retention time and Log C_w relationship of BaA exposed mussels during uptake and depuration periods (a) with and (b) without CV aquarium.

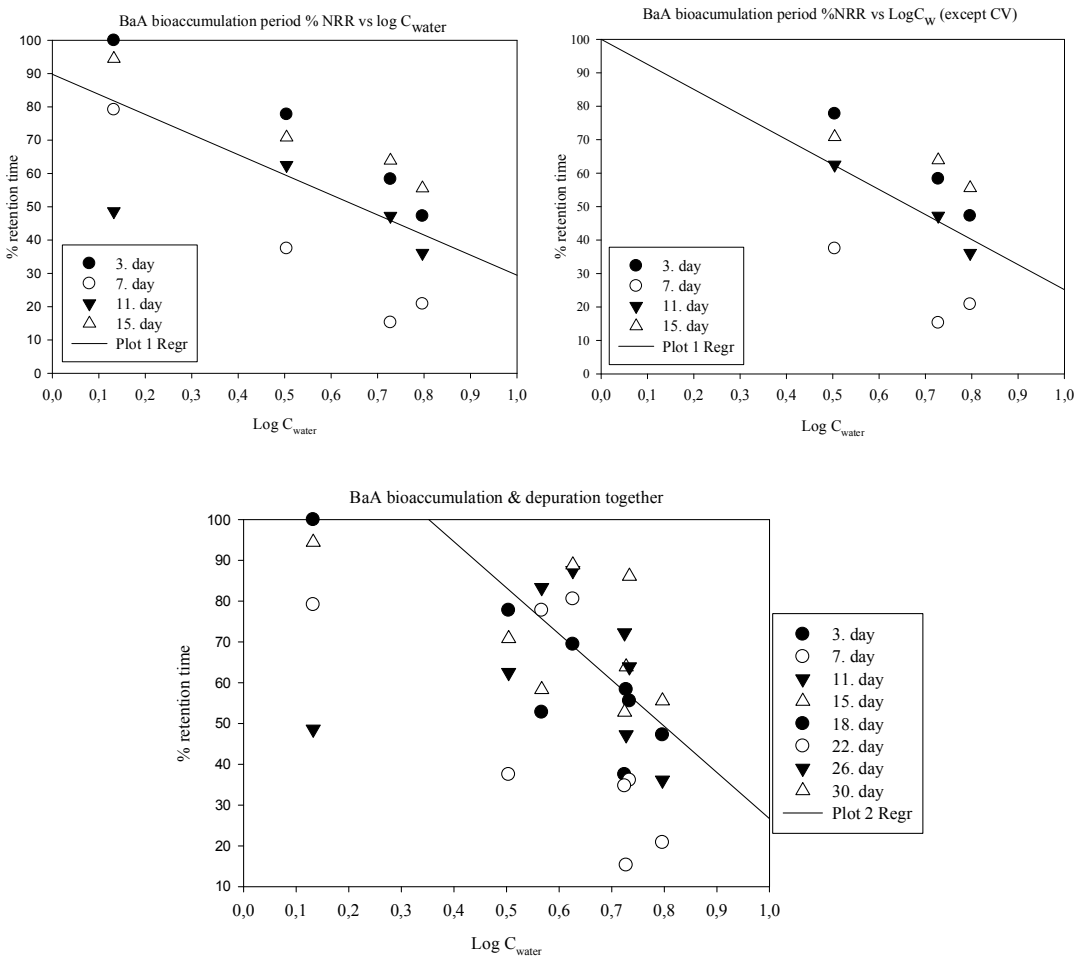

Figure B.4 : Retention time (%) and Log C_w relationship of BaA exposed mussels during uptake period (a) with and (b) without CV aquarium and (c) whole experiment period.

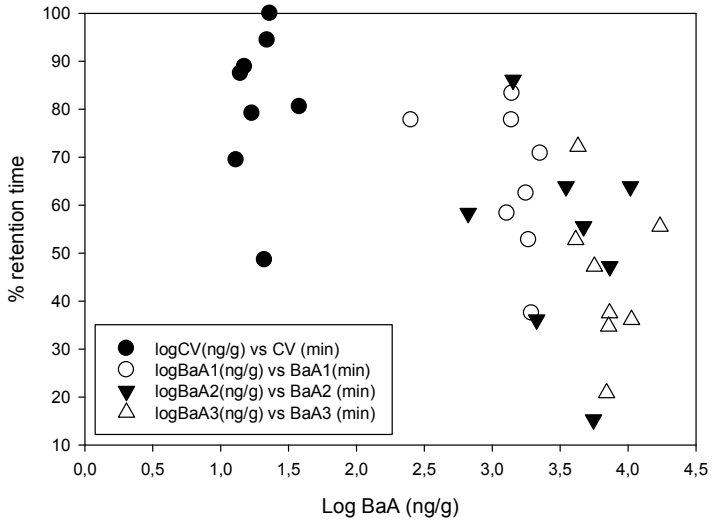

Figure B.5 : The relationship of retention time and BaA concentrations in mussel tissues for BaA exposed mussels.

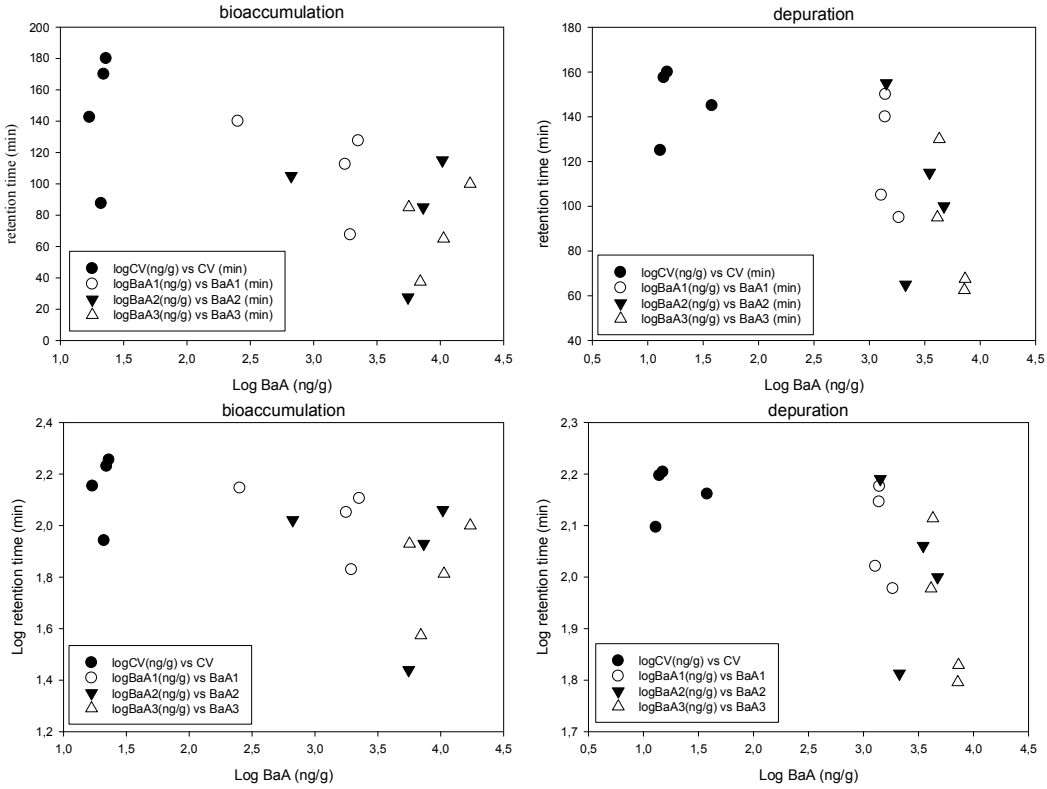

Figure B.6 : The relationship of BaA concentrations of mussels with retention time for uptake and depuration period.

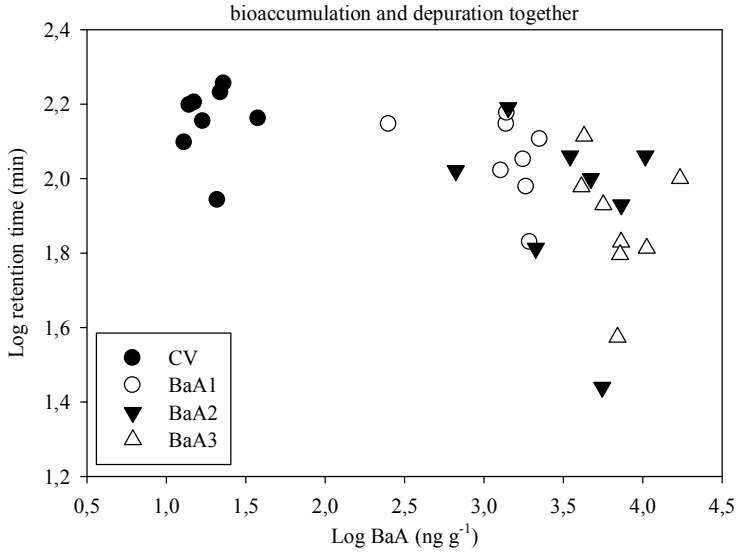

Figure B.7 : The relationship of BaA concentrations of mussels with retention time for uptake and depuration period.

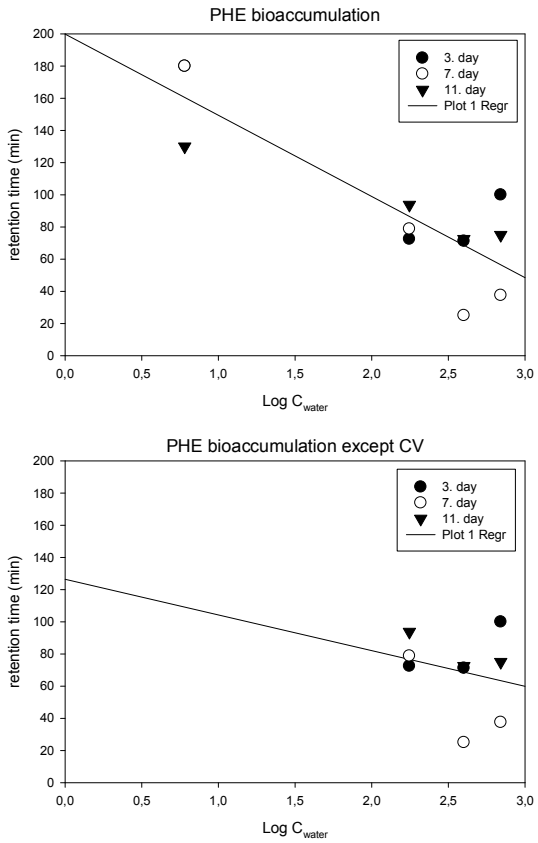

Figure B.8 : The relationship of retention time and seawater concentration (C_w) in all aquariums with (above) and without (below) CV aquarium.

APPENDIX C: Filtration rates of mussels exposed to PHE in the small scale experiments

In Figure C.1, filtration rates are shown versus time during uptake period. The results show that mussels in CV aquarium have a different filtration rate trend compared with the PHE spiked aquariums. Filtration rates of PHE aquariums do not exceed 5 L h^{-1} for 10 mussels and reach zero level after 90 minutes of water exchange.

In Figure C.2, filtration rates are shown versus time during the sampling days of depuration period. There is no an apparent difference in CV aquarium during the depuration period compared with the results of uptake period. In PHE1 and PHE2 aquariums, an increase of filtration rate was observed at the last days of depuration period whereas in PHE3 aquarium, there was not any apparent increase of filtration rate, possibly due to the negative effect of high PHE concentration accumulated in the organisms.

In Figure C.3, filtration rates are shown versus sampling days of uptake period at specific time intervals. Due to the decrease of algae density in seawater, filtration rate in CV aquarium also decrease at the first 35 minutes of water exchange. Filtration rate of mussels in CV aquarium was found approximately 15 L h^{-1} for 10 mussels which is also compatible with the results of previous experiments performed with the reference mussels (used in the experiments) collected from Rumeli Kavağı. In general, it was observed that filtration rate has a lower value as the PHE concentration increases during the uptake period.

In Figure C.4, filtration rates are shown versus time for depuration period. There is not an apparent difference of filtration rate in CV aquarium compared with the uptake period. Filtration rates increased more in PHE1 aquarium and less in PHE2 aquarium during the depuration period. Nevertheless, increase of filtration rate was not observed in PHE3 aquarium during the depuration period.

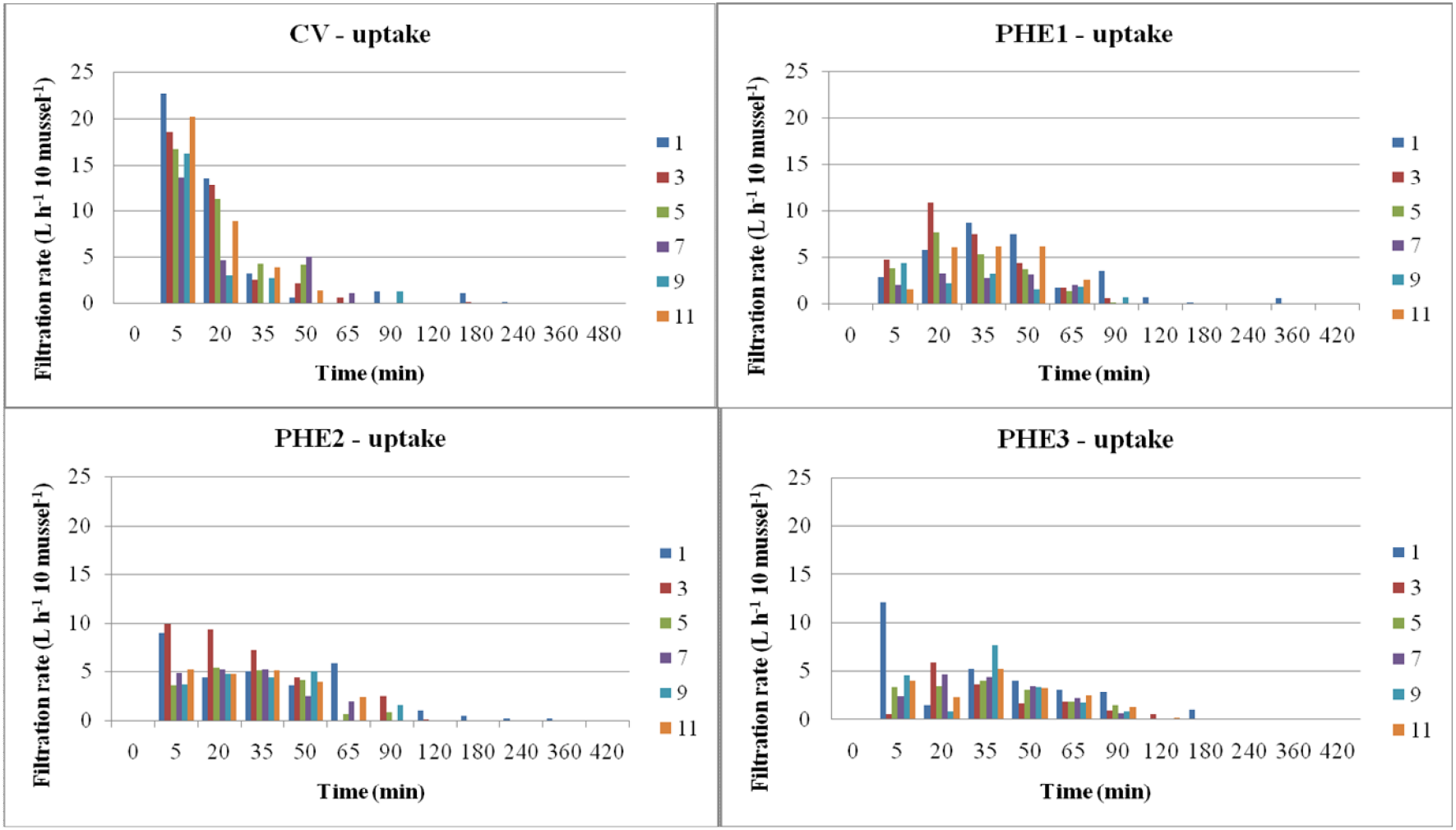

Figure C.1 : Filtration rates of aquariums (each contains 10 mussels) within a day for sampling days during PHE uptake period.

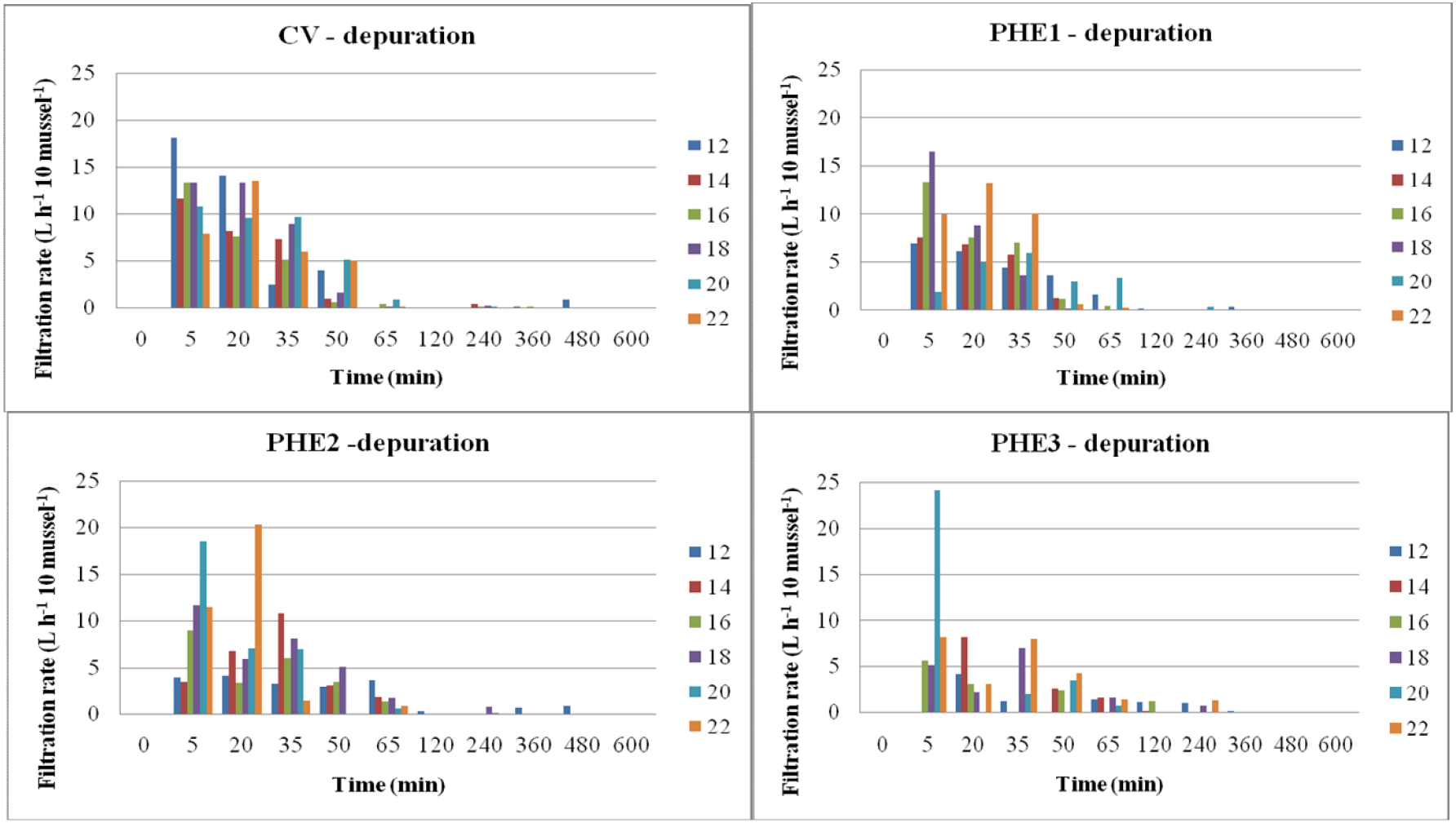

Figure C.2 : Filtration rates of aquariums (each contains 10 mussels) within a day for sampling days during the depuration period.

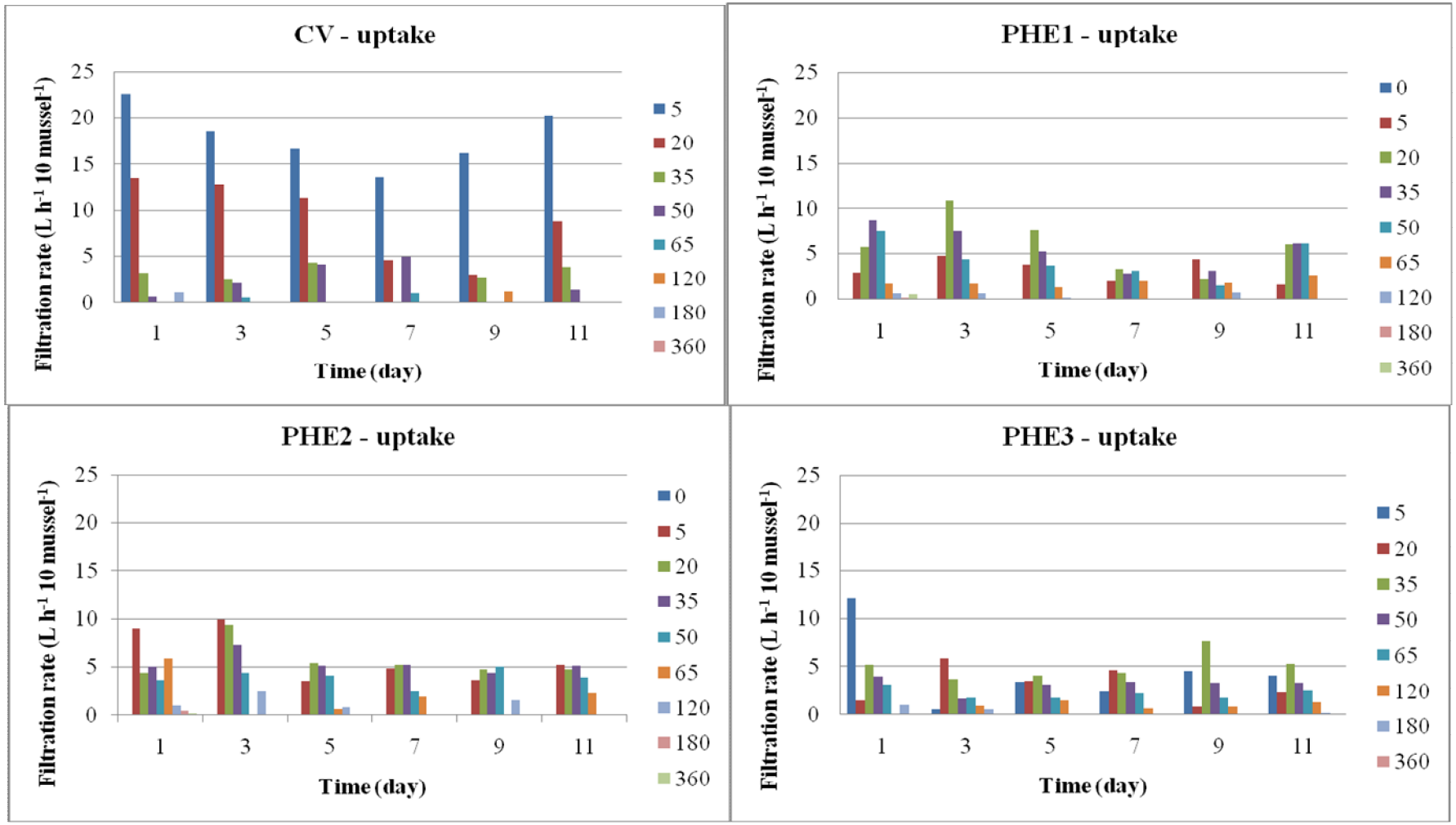

Figure C.3 : Filtration rates of aquariums (each contains 10 mussels) during the sampling days of PHE uptake period.

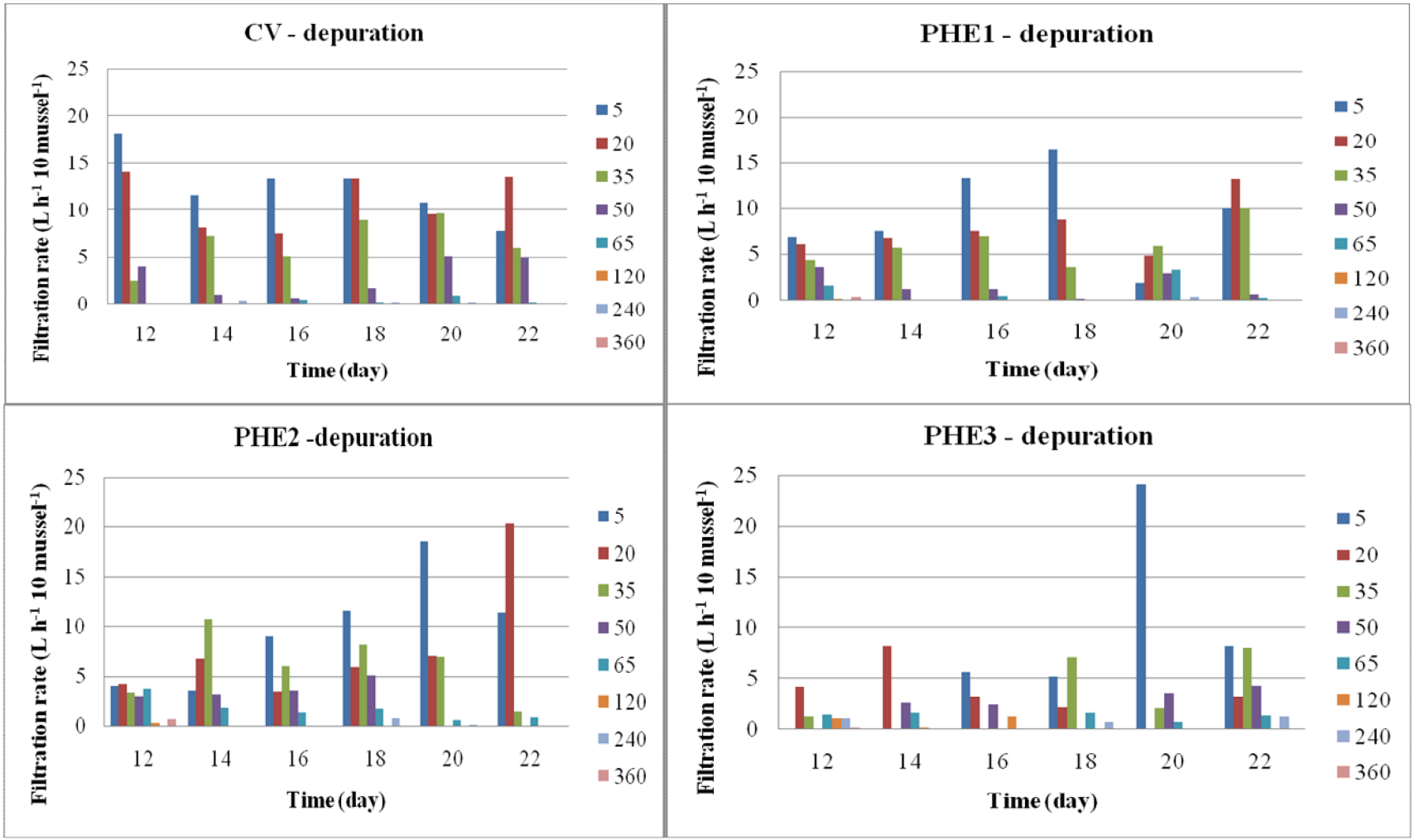

Figure C.4 : Filtration rates of aquariums (each contains 10 mussels) during the sampling days of depuration period.

APPENDIX D: Model code written in Mathematica software

The model code written below was given only for one PAH exposure in order to avoid repetitions and to be more deductive.

```
Clear["Global`*"]
<<PlotLegends`
(* timepoints represents sampling days *)
timepoints={0.,2.,6.,10.,14,17,21,25,29};
(* BaA1values represent BaA concentrations in mussels exposured to the lowest BaA concentration*)
BaA1values={4,252,1946,1772,2252,1850,1386,1396,1283};
BaA1data=Transpose[{timepoints,BaA1values}];
(*rate constants for BaA1 aquarium were defined below*)
Clear[rule1];
rule1={
k11v → 52547 (*BCF_algae*),
k12v→ 0 (*319 (m^3/kg*d) PAH uptake rate of algae from seawater*),
k13v→ 0 (*0.87 (1/day) PAH depuration rate of algae from seawater*),
k14v→ 54.48 (* (L/day) filtration rate of mussel*),
k15v→ 65.50 (* (L/ (day kg)) PAH uptake rate of mussel from seawater*),
k16v→ 0.04   (* 1/day PAH depuration rate of mussel from seawater*)};
(*some basic definitions related with the food chain*)
Volume=10; (*volume of seawater in the aquarium in terms of L *)
MusselWeight=1.28; (* wet weight of 1 mussel in terms of g *)
AlgaeNumber=20000; (*algae concentration in the aquarium at time 0 in terms of cell mL^-1*)
AlgaeWeight=100*10^-12; (*wet weight of 1 algae cell in terms of g*)
(*1 algae cell is assumed as 100 pg wet weight*)
filtrationRateBaA1={{0,33.30},{1,193.47},{2,97.98},{3,97.98},{4,67.95},{5,67.95}
,{6,73.91},{7,73.91},{8,92.37},{9,92.37},{10,99.65},{11,99.65},{12,77.91},{13,77.
91},{14,91.73},{15,91.73},{16,44.32},{17,62.28},{18,62.28},{19,54.43},{20,54.43
},{21,54.29},{22,54.29},{23,64.94},{24,64.94},{25,64.07},{26,64.07},{27,78.46},{
28,78.46},{29,91.33}};
Clear[AlgaeBaA1,AlgaeBaA2,AlgaeBaA3];
(*decrease of algae in terms of cell mL^-1 algae conc in the system,Algae[0]==20000*)
AlgaeBaA1[t_,filtrationRateBaA1_]:=AlgaeNumber*Exp[-
```

(filtrationRateBaA1/Volume)*t];

A1=AlgaeBaA1[t,filtrationRateBaA1]/AlgaeNumber;

Initial values for Seawater, Algea and Mussels and the List with the Mussel numbers

(*Algae was exposed to PAH 24 hours earlier in a 5L seawater bottle*)

AlgaeDensity0=AlgaeNumber*AlgaeWeight*10^(-3); (*total algae density in 1 L seawater in terms of g/L*)

(* (20000 cell/mL*100 pg/cell)/(1000*10^(12)) *)

Seawater0hBaA1=3000*Volume;(*total BaA spiked into the lowest BaA aquarium filled with 10 L seawater at time 0 in terms of ng*)

BCFalgae=52547;

Ainit=AlgaeDensity0*Volume*10^(-3)*BCFalgae;

SinitBaA1=Seawater0hBaA1-10^(9)*Ainit;

Minit=261.12 (* 1.28*51*4 *);

MusselNumberListBaA1={{0,51},{1,51},{2,45},{3,45},{4,45},{5,45},{6,39},{7,39},{8,39},{9,39},{10,33},{11,33},{12,33},{13,33},{14,27},{15,27},{16,27},{17,21},{18,21},{19,21},{20,21},{21,15},{22,15},{23,15},{24,15},{25,9},{26,9},{27,9},{28,9},{29,3}};

daysUptake=15;

Here, the system of differential equations is defined

AlgaeDensityBaA1[t_,filtrationRateBaA1_]:=AlgaeWeight*AlgaeBaA1[t,filtrationRateBaA1]/Volume

MusselDensityBaA1[MusselNumberBaA1_]:=MusselWeight*MusselNumberBaA1/Volume

Clear[solution1];

solution1[k11_?NumberQ,k12_?NumberQ,k13_?NumberQ,k14_?NumberQ,k15_?NumberQ,k16_?NumberQ,filtrationRateBaA1_,MusselNumberBaA1_,S10_,M10_,A10_]:=NDSolve[{

simS1'[t]==simS1[t]*(-k15*10^(-3)*MusselDensityBaA1[MusselNumberBaA1]-k11*AlgaeDensityBaA1[t,filtrationRateBaA1])+simM1[t]*k16,

simA1'[t]==simS1[t]*k11*AlgaeDensityBaA1[t,filtrationRateBaA1]-simA1[t]*(filtrationRateBaA1/Volume),

simM1'[t]==simS1[t]*k15*10^(-3)*MusselDensityBaA1[MusselNumberBaA1]+filtrationRateBaA1/Volume*simA1[t]-simM1[t]*k16,

simS1[0]==S10,simA1[0]==A10,simM1[0]==M10},

{simS1[t],simA1[t],simM1[t]},{t,0,2}][[1]];

PlotBaA1=Plot[{(simS1[t]/.(solution1[k11v,k12v,k13v,k14v,k15v,k16v,filtrationRateBaA1[[1,2]],MusselNumberListBaA1[[1,2]],SinitBaA1,Minit,Ainit]/.rule1))/.t-> z,

(simM1[t]/.(solution1[k11v,k12v,k13v,k14v,k15v,k16v,filtrationRateBaA1[[1,2]],M

usselNumberListBaA1[[1,2]],SinitBaA1,Minit,Ainit]/.rule1))/.t-> z,

(simA1[t]/.(solution1[k11v,k12v,k13v,k14v,k15v,k16v,filtrationRateBaA1[[1,2]],MusselNumberListBaA1[[1,2]],SinitBaA1,Minit,Ainit]/.rule1))/.t-> z},{z,0,1},

PlotStyle->{RGBColor[0.1,0,0],RGBColor[0,0,0.1],RGBColor[0,0.1,0]},LabelStyle->{"Helvetica",15},GridLines->{{0},{0}},Frame->True,FrameLabel->{"day","mass (ng)"},ImageSize->400,PlotRange-> {0,90000},AxesOrigin->{0,0},PlotLabel->Style["",FontSize-> 15,FontFamily-> "Helvetica"],LabelStyle->{"Helvetica",15},PlotLegend->{"Seawater","Mussel","Algae"},LegendPosition-> {0.45,0.2},LegendSize-> 0.3,ShadowOffset->{0,0}];

Show[PlotBaA1, PlotRange-> All]

Definition of the errorFunction

Clear[errorFunction1];

errorFunction1[k11_?NumberQ,k12_?NumberQ,k13_?NumberQ,k14_?NumberQ,k15_?NumberQ,k16_?NumberQ,data_,Sinitp_,Ainitp_,Minitp1_]:=Block[

{Sloc,Aloc,Minit0loc1},

Sloc=Sinitp;

Aloc=Ainitp;

Minit0loc1=Minitp1;

maxDays=Length[MusselNumberListBaA1];

err1=0;dataIndex=2;

For[day$index=1,day$index<=daysUptake,day$index=day$index+1,

(*If measured values are available today*)

If[(MusselNumberListBaA1[[day$index,1]]==2
)||(MusselNumberListBaA1[[day$index,1]]==6) ||
(MusselNumberListBaA1[[day$index,1]]==10)
||(MusselNumberListBaA1[[day$index,1]]==14),

(* calculate the distance/error resp.*)

err1=err1+Abs[((simM1[t]/.solution1[k11,k12,k13,k14,k15,k16,filtrationRateBaA1[[day$index,2]],MusselNumberListBaA1[[day$index,2]],Sloc,Minit0loc1,Aloc] /.{t->0})/(MusselWeight*MusselNumberListBaA1[[day$index,2]])-
data[[dataIndex,2]])];

dataIndex++;];

(*Define the next Starting value for the Mussels*)
Minit0loc1=(simM1[t]/.solution1[k11,k12,k13,k14,k15,k16,filtrationRateBaA1[[day$index,2]],MusselNumberListBaA1[[day$index,2]],Sloc,Minit0loc1,Aloc] /.{t->1});

If[day$index>1 &&
day$index<daysUptake,Minit0loc1=Minit0loc1*(MusselNumberListBaA1[[day$index+1,2]]/MusselNumberListBaA1[[day$index,2]])];];

(*Now depuration phase begins (day$index>daysUptake), so initialise Water and Algae with 0 *)

Sloc=0;

```
Aloc=0;

For[day$index=daysUptake+1,day$index<=Length[MusselNumberListBaA1],day$i
ndex=day$index+1,

If[(MusselNumberListBaA1[[day$index,1]]==17
)||(MusselNumberListBaA1[[day$index,1]]==21)                    ||
(MusselNumberListBaA1[[day$index,1]]==25                        )||
(MusselNumberListBaA1[[day$index,1]]==29 ),

(* calculate distance *)

err1=err1+Abs[((simM1[t]/.solution1[k11,k12,k13,k14,k15,k16,filtrationRateBaA1[[
day$index,2]],MusselNumberListBaA1[[day$index,2]],Sloc,Minit0loc1,Aloc]    /.{t-
>0})/(MusselWeight*MusselNumberListBaA1[[day$index,2]])-
data[[dataIndex,2]])];

dataIndex++; ];

Minit0loc1=(simM1[t]/.solution1[k11,k12,k13,k14,k15,k16,filtrationRateBaA1[[day
$index,2]],MusselNumberListBaA1[[day$index,2]],Sloc,Minit0loc1,Aloc] /.{t->1});

If[day$index>1                                                  &&
day$index<Length[MusselNumberListBaA1],Minit0loc1=Minit0loc1*(MusselNumb
erListBaA1[[day$index+1,2]]/MusselNumberListBaA1[[day$index,2]])]; ];

err1 ];
```

Test the error function with your experimental rate constants

```
errorFunction1[k11v,k12v,k13v,k14v,k15v,k16v,BaA1data,SinitBaA1,Ainit,Minit]/.
rule1
```

The following code defines a function for Plotting Simulation and Data

```
Clear[ShowResults1];

ShowResults1[data_,ruleLoc1_,Sinitp_,Ainitp_,Minitp1_]:=Block[{Sinit,Ainit,Minit
loc1},

Sinit=Sinitp;

Ainit=Ainitp;

Minitloc1=Minitp1;

massInMussels$ListBaA1={}; massInAlgae$ListBaA1={};

dataFig1=ListPlot[data,GridLines->Automatic,PlotStyle->{Red},PlotMarkers-
>{Automatic,10}];

For[day$index=1,day$index<=daysUptake,day$index=day$index+1,

AppendTo[massInMussels$ListBaA1,

Table[(simM1[t]/.(solution1[k11v,k12v,k13v,k14v,k15v,k16v,filtrationRateBaA1[[d
ay$index,2]],MusselNumberListBaA1[[day$index,2]],Sinit,Minitloc1,Ainit]/.ruleLoc
1 )/.{t->tv}),{tv,0,1,1/24.}] ];

AppendTo[massInAlgae$ListBaA1,

Table[(simA1[t]/.(solution1[k11v,k12v,k13v,k14v,k15v,k16v,filtrationRateBaA1[[da
y$index,2]],MusselNumberListBaA1[[day$index,2]],Sinit,Minitloc1,Ainit]/.ruleLoc
```

```
1 )/.{t->tv}),{tv,0,1,1/24.}] ];

Minitloc1=(simM1[t]/.(solution1[k11v,k12v,k13v,k14v,k15v,k16v,filtrationRateBaA
1[[day$index,2]],MusselNumberListBaA1[[day$index,2]],Sinit,Minitloc1,Ainit]/.rul
eLoc1)/.{t->1});

If[day$index>1 &&
day$index<Length[MusselNumberListBaA1],Minitloc1=Minitloc1*(MusselNumber
ListBaA1[[day$index+1,2]]/MusselNumberListBaA1[[day$index,2]])] ];

Sinit=0;

Ainit=0;

For[day$index=daysUptake+1,day$index<=Length[MusselNumberListBaA1],day$i
ndex=day$index+1,

AppendTo[massInMussels$ListBaA1,

Table[(simM1[t]/.(solution1[k11v,k12v,k13v,k14v,k15v,k16v,filtrationRateBaA1[[d
ay$index,2]],MusselNumberListBaA1[[day$index,2]],Sinit,Minitloc1,Ainit]/.ruleLoc
1)/.{t->tv}),{tv,0,1,1/24.}] ];

AppendTo[massInAlgae$ListBaA1,

Table[(simA1[t]/.(solution1[k11v,k12v,k13v,k14v,k15v,k16v,filtrationRateBaA1[[da
y$index,2]],MusselNumberListBaA1[[day$index,2]],Sinit,Minitloc1,Ainit]/.ruleLoc
1 )/.{t->tv}),{tv,0,1,1/24.}] ];

Minitloc1=(simM1[t]/.(solution1[k11v,k12v,k13v,k14v,k15v,k16v,filtrationRateBaA
1[[day$index,2]],MusselNumberListBaA1[[day$index,2]],Sinit,Minitloc1,Ainit]/.rul
eLoc1 )/.{t->1});

If[day$index>1 &&
day$index<Length[MusselNumberListBaA1],Minitloc1=Minitloc1*(MusselNumber
ListBaA1[[day$index+1,2]]/MusselNumberListBaA1[[day$index,2]])] ];

graphsListBaA1={};

MassInMusselTimeCourseTableDaysBaA1={};

ConcentrationInMusselTimeCourseTableDaysBaA1={};

hours=0;

days=0;

For[i=1,i<=Length[MusselNumberListBaA1],i++,

For[j=1,j<Length[massInMussels$ListBaA1[[i]]],j++,

If[j==1 (* value in the morning of that day *),

AppendTo[MassInMusselTimeCourseTableDaysBaA1,{days,massInMussels$ListBa
A1[[i,j]]}];

AppendTo[ConcentrationInMusselTimeCourseTableDaysBaA1,{days,massInMussel
s$ListBaA1[[i,j]]/(MusselWeight*MusselNumberListBaA1[[i,2]])}]

days++; ]; ] ]

Print[TableForm[{ListPlot[MassInMusselTimeCourseTableDaysBaA1,Joined-
>True,PlotMarkers->{Automatic,5},PlotRange->{0,600000},LabelStyle-
```

```
>{"Helvetica",15},ImageSize->400,GridLines->Automatic,Frame-
>True,FrameLabel->{"day","BaA mass in mussel (ng)","Daily values of Mass in
Mussels"}],simFig1=ListPlot[ConcentrationInMusselTimeCourseTableDaysBaA1,Jo
ined->True,PlotMarkers->{Automatic,5},PlotRange->{0,18000},LabelStyle-
>{"Helvetica",15},Frame->True,FrameLabel->{"day","BaA concentration in mussel
(ng g^-1)"},ImageSize->400,GridLines->{Range[30],None},PlotRange-
>{{0,30},All}]},TableDirections->Row]];

Show[simFig1,dataFig1] ];

ShowResults1[BaA1data,rule1,SinitBaA1,Ainit,Minit]
```

APPENDIX E: Transfer of BaA and PHE between the three compartments at the 1st day of uptake period.

Transfer of BaA between the three compartments (seawater, mussel and algae) at the first day of uptake period is simulated. Gradient of BaA in seawater, mussel and algae compartments were represented with red, blue and green lines, respectively. Due to the low concentration of algae in the aquariums, green line in the figures is not seen as clearly as the blue and green lines. Except the lowest concentration, dynamic interaction of BaA between mussel tissues and seawater is similar which may also point out a breaking point for the equilibrium between mussel tissues and seawater concentration. Due to the low amount of algae added in the system, it is evaluated that BaA transfer mainly occurs between the mussel and seawater compartments.

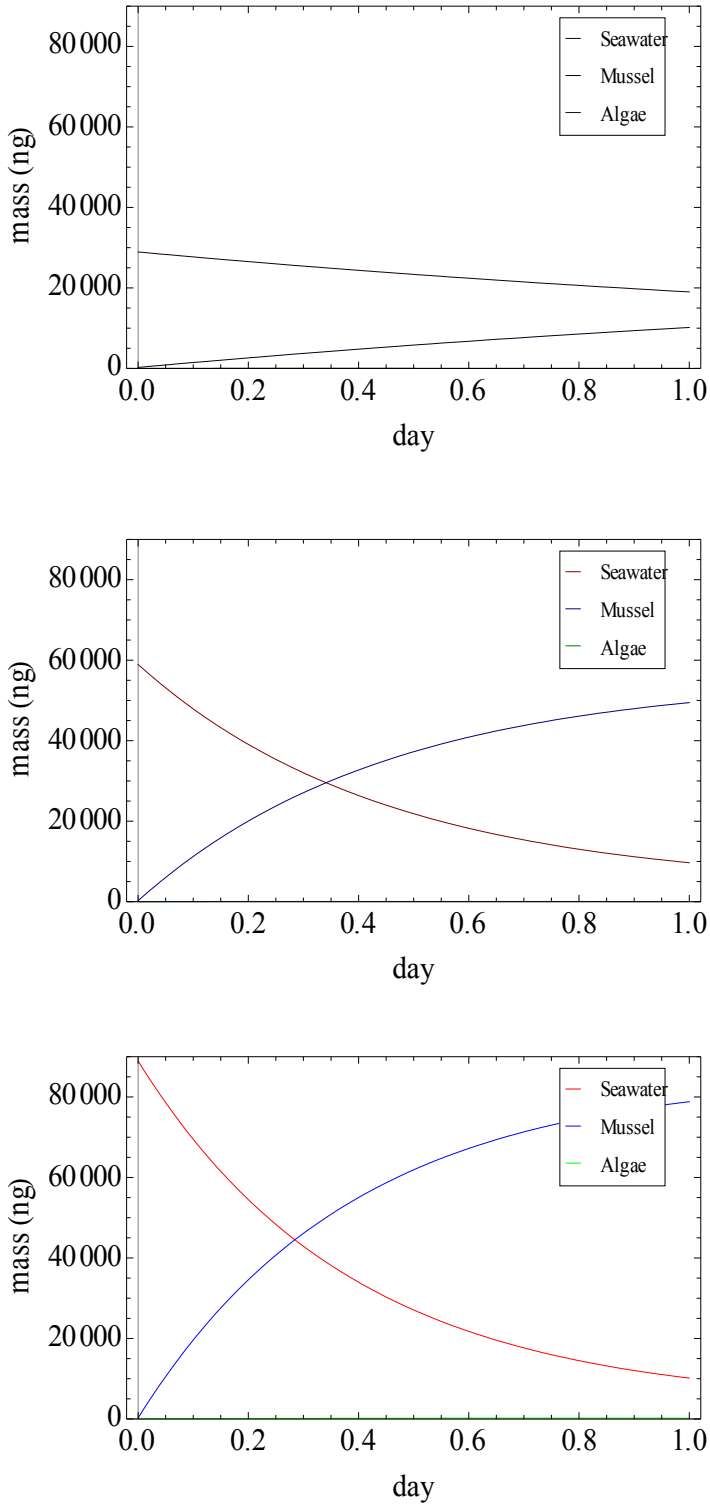

Figure E.1 : Transfer of BaA between algae (green), mussel (blue) and seawater (red) during the first 24 hours of the uptake period. In the below graph, three different exposure concentrations were combined together.

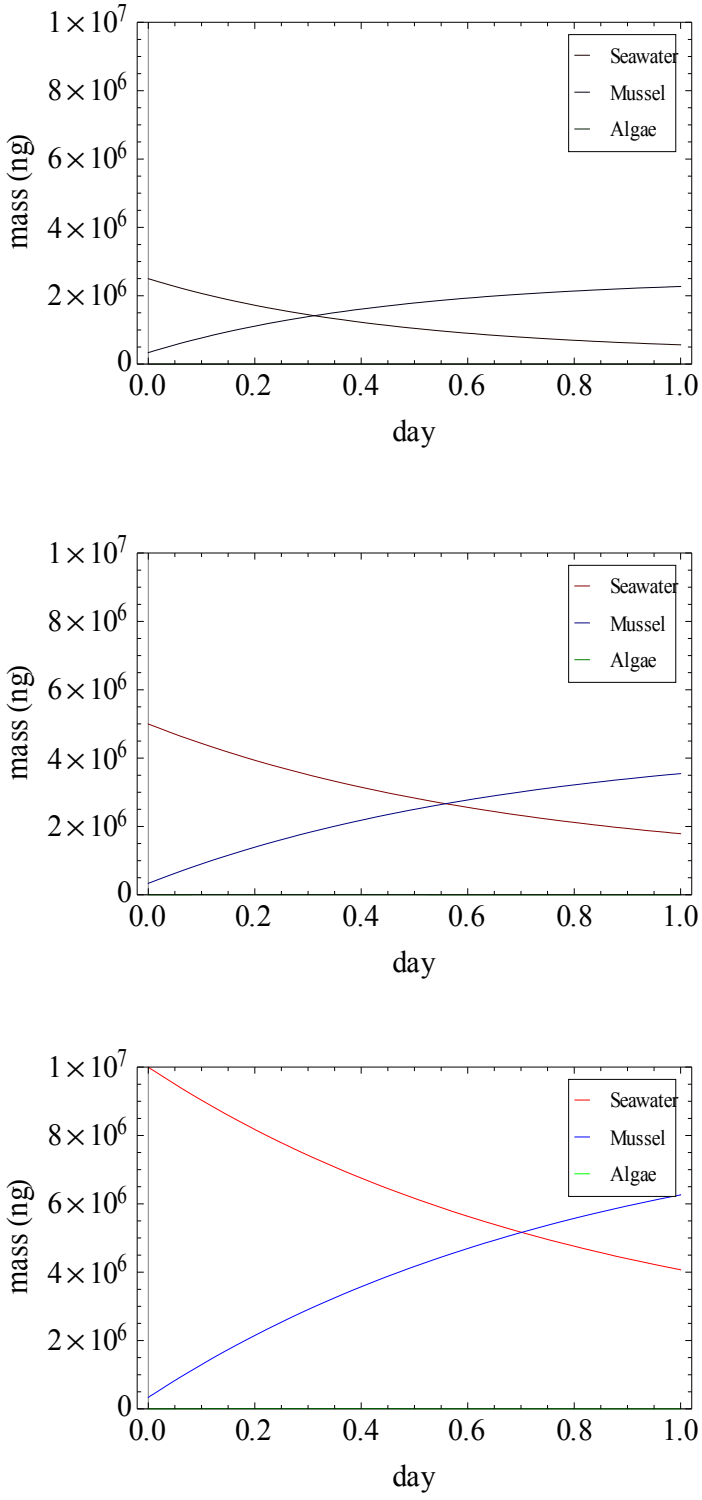

Figure E.2 : Transfer of PHE between algae (green), mussel (blue) and seawater (red) during the first 24 hours of uptake period.

When the graphical outputs of different PHE aquariums in Figure E.2 were compared, it is observed that as the PHE concentration increases, the intersection of seawater and mussel compartments was moved towards to the end of 24 hours. It can

be deduced that PHE equilibrium between the mussel tissues and seawater takes longer time as the PHE concentration increases. Due to the low amount of algae added in the system, it is also evaluated that PHE transfer mainly occurs between the mussel and seawater compartments.

APPENDIX F: Scenarios with different marine algae species

Different kinds of algae were used in the simulation scenarios.

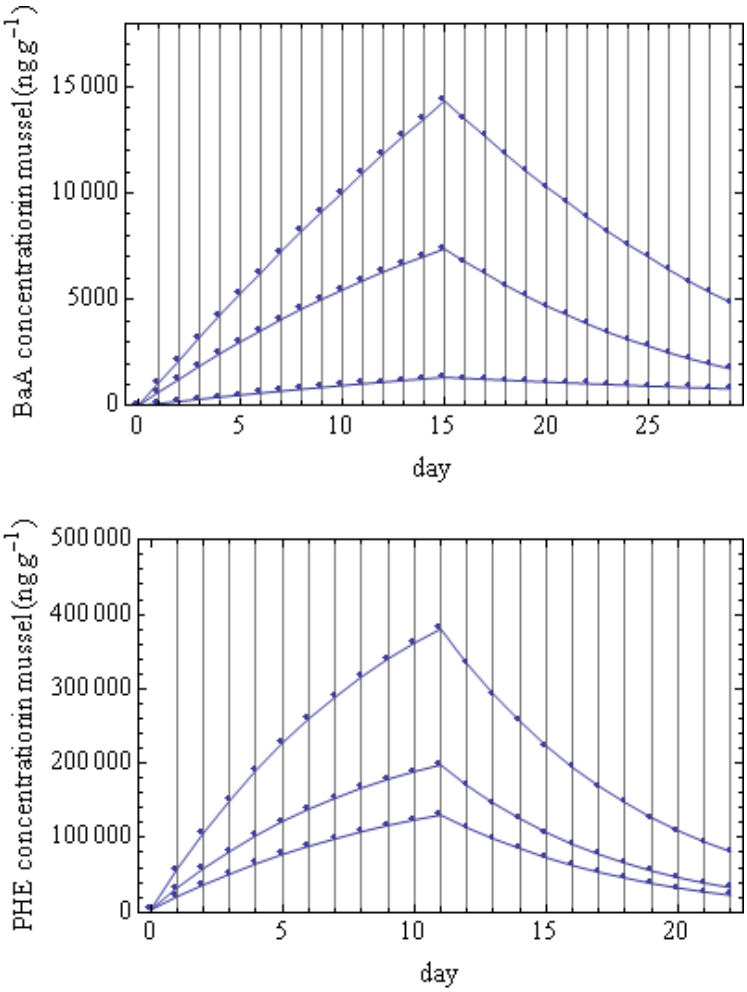

Figure F.1 : The concentration levels of BaA (above) and PHE (below) exposed mussels fed with *Emiliana huxleyi*. Log BCF of *Emiliana huxleyi* was calculated as 5.7 for BaA, and 4.7 for PHE using QSAR equation.

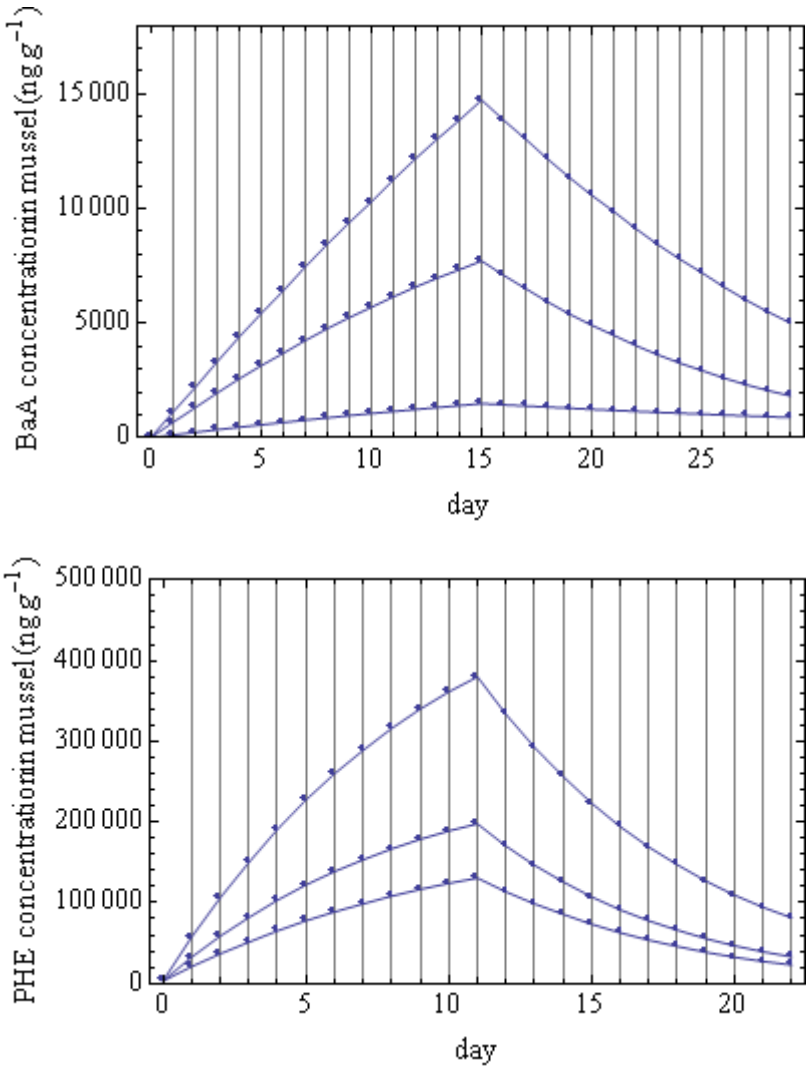

Figure F.2 : The concentration levels of BaA (above) and PHE (below) exposed mussels fed with *Thalassiosira nordenskiöldii*. Log BCF of *Thalassiosira nordenskiöldii* was calculated as 5.6 for BaA, and 4.2 for PHE using QSAR equation.

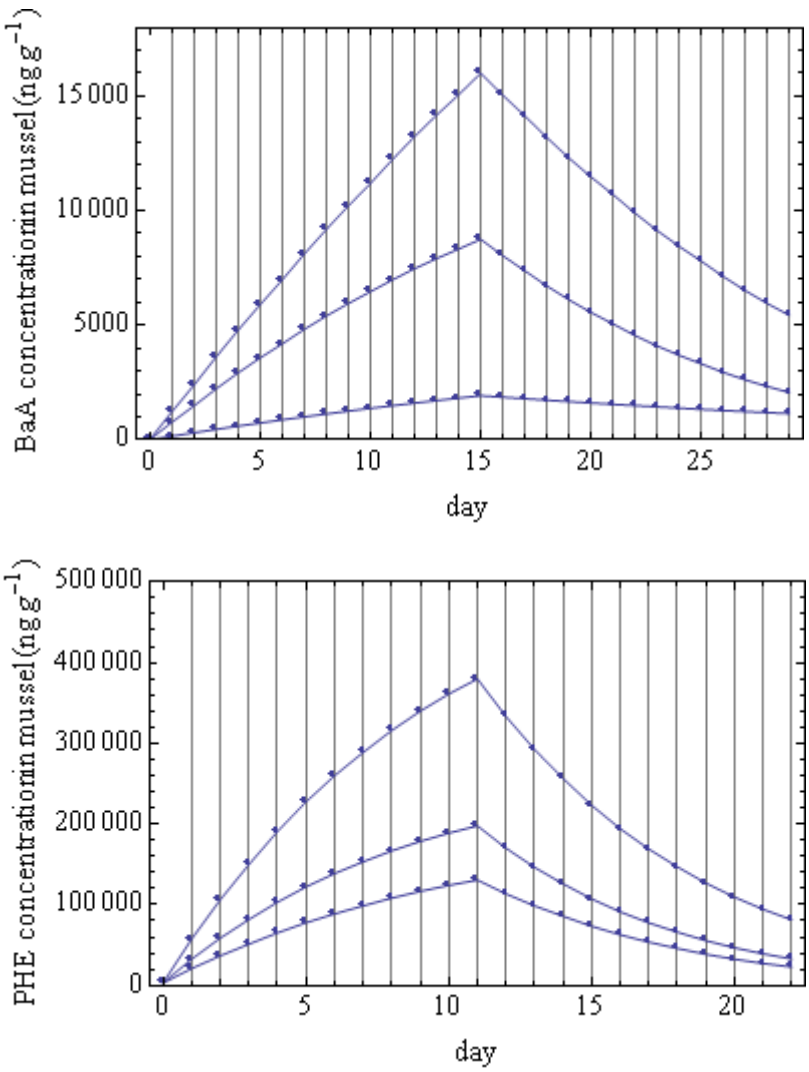

Figure F.3 : The concentration levels of BaA (above) and PHE (below) exposed mussels fed with *Pheaodactylum tricornutum*. Log BCF of *Pheaodactylum tricornutum* was calculated as 4.5 for BaA, and 3.1 for PHE using QSAR equation.

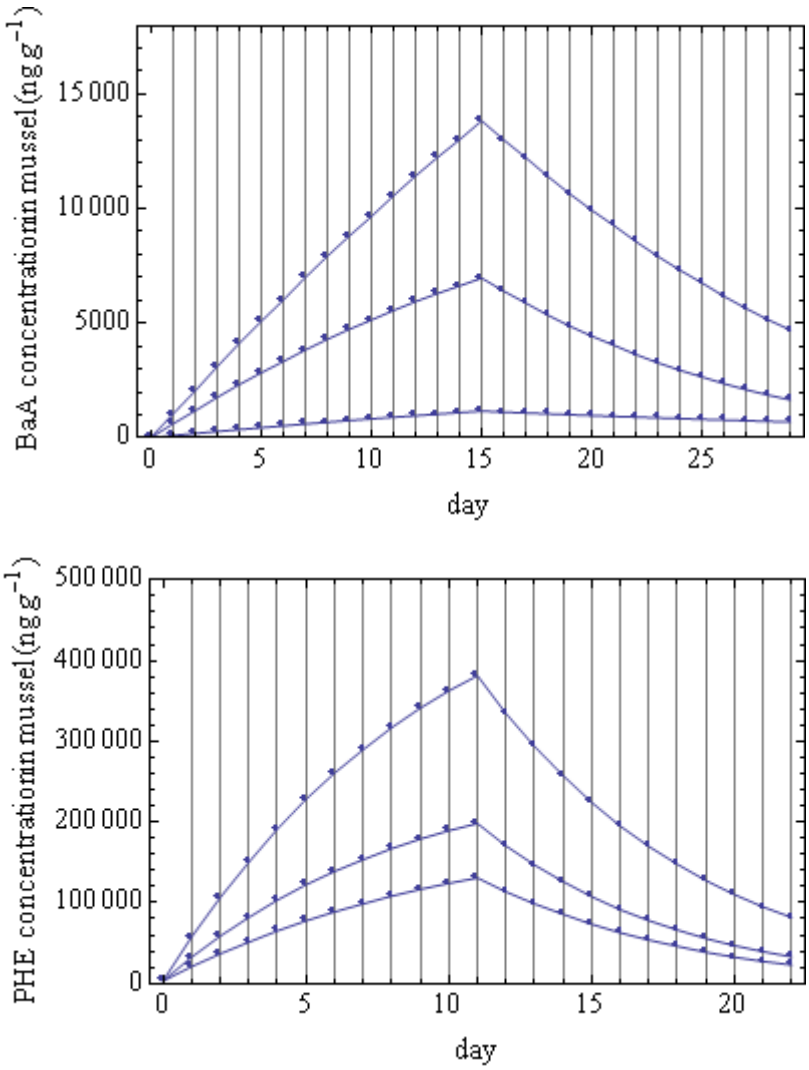

Figure F.4 : The concentration levels of BaA (above) and PHE (below) exposed mussels fed with *Isochrysis galbana*. Log BCF of *Isochrysis galbana* was calculated as 5.8 for BaA, and 5.2 for PHE using QSAR equation.

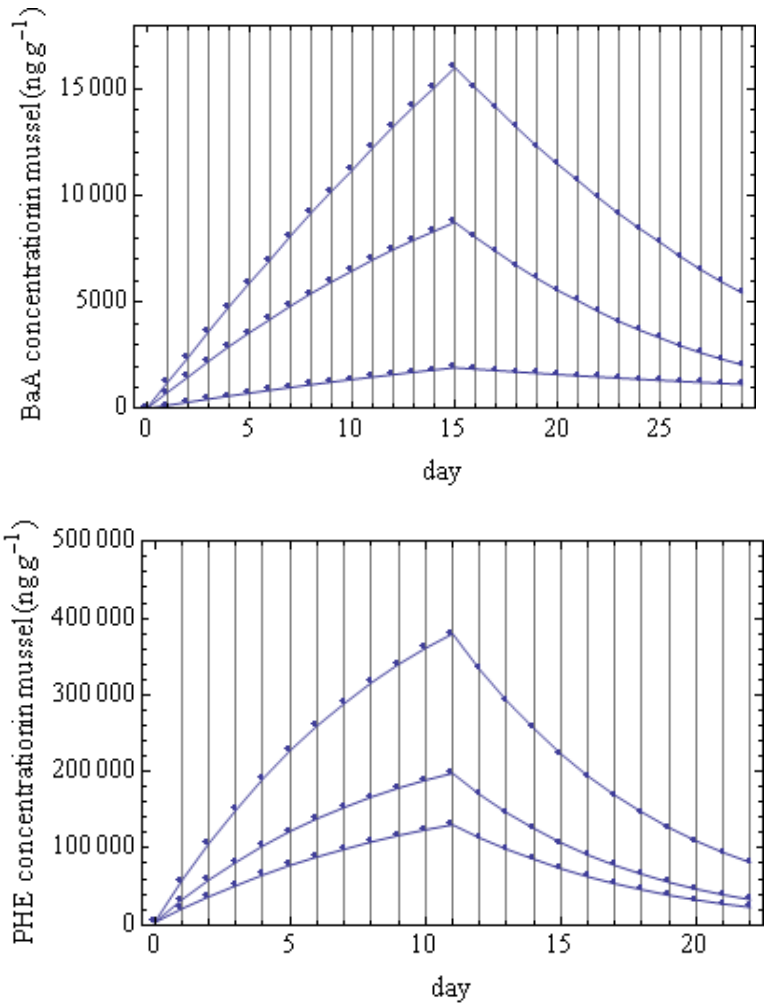

Figure F.5 : The concentration levels of BaA (above) and PHE (below) exposed mussels fed with *Rhodomonas salina*. Log BCF of *Rhodomonas salina* was calculated as 4.5 for BaA, and 1.9 for PHE using QSAR equation.

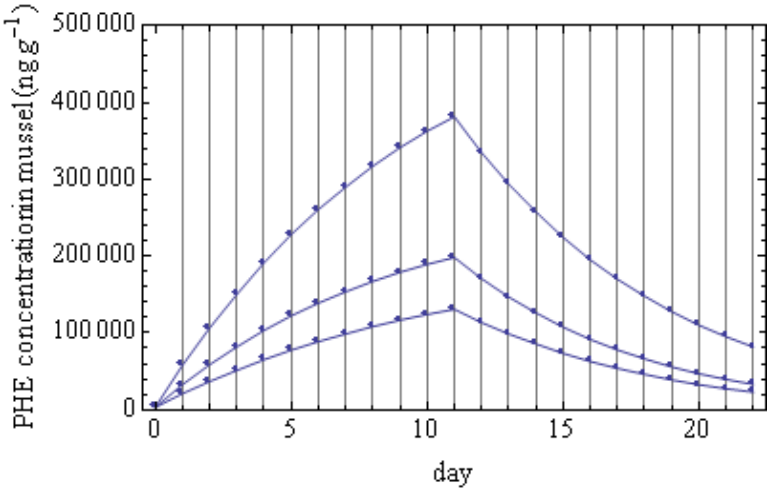

Figure F.6 : The level of PHE concentration in mussels assuming that they were fed with the first level of aquatic food web (free dissolved particles), with a LogBCF of 5.23.

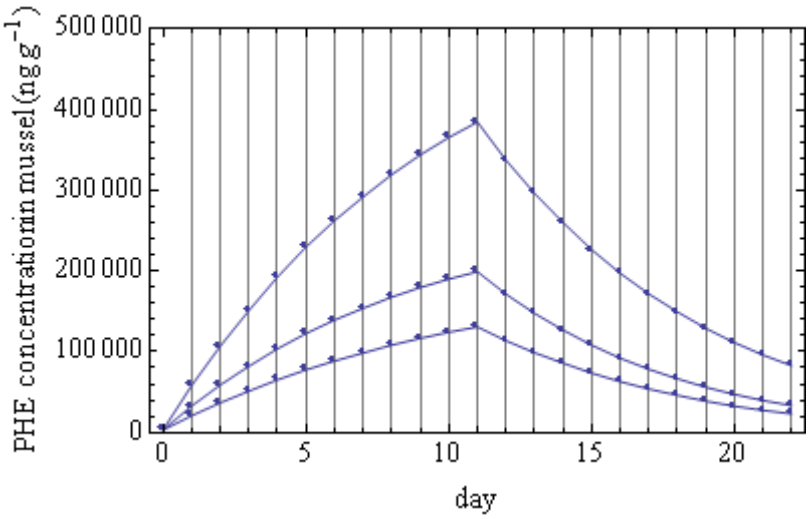

Figure F.7 : The level of PHE concentration in mussels assuming that they were fed with the first level of aquatic food web (total particles), with a LogBCF of 5.67.

CURRICULUM VITAE

Name Surname: Sevil Deniz YAKAN DÜNDAR

Place and Date of Birth: Ordu, 26.06.1982

Address: Istanbul Technical University, Faculty of Naval Architecture and Ocean Engineering, Maslak, Istanbul

E-Mail: yakans@itu.edu.tr

B.Sc.: Istanbul Technical University, Faculty of Naval Architecture and Ocean Engineering, Department of Shipbuilding and Ocean Engineering (2005)

M.Sc.: Istanbul Technical University, Faculty of Naval Architecture and Ocean Engineering, Department of Shipbuilding and Ocean Engineering (2007)

Professional Experience and Rewards:

- PhD research scholarship of Higher Education Council of Turkey (6 months)
- "Determination of level and effects of pollution caused by ship-building and marina activities in the natural waters" Researcher in BMBF (Germany) – TUBITAK (Turkey) Collaboration Research Project – (01.07.2011 – 01.07.2014)
- "Pollution monitoring of the Northern Aegean coast by use of transplanted mussels: determination of priority pollutants and their levels and development of suitable biomarkers" Researcher in GSRT (Greece) - TUBITAK (Turkey) Collaboration Research Project – (15.02.2011 – 15.02.2013)

List of Publications and Patents:

- Okay O.S., Ozdemir P., **Yakan S.D.**, 2011: Efficiency of butyl rubber sorbent to remove the PAH toxicity. *Journal of Environmental Science and Health Part A-Toxic/Hazardous Substances and Environmental Engineering*, Vol.46, Iss.8, p.909-913.
- Ceylan D., Dogu S., Karacik B., **Yakan S.D.**, Okay O.S., Okay O., 2009: Evaluation of Butyl Rubber as Sorbent Material for the Removal of Oil and Polycyclic Aromatic Hydrocarbons from Seawater. *Environmental Science and Technology*. Vol.43, Iss.10, p.3846–3852.

PUBLICATIONS/PRESENTATIONS ON THE THESIS

- **Yakan S.D.**, Henkelmann B., Schramm K.-W., Okay O.S., 2011: Bioaccumulation Depuration Kinetics and Effects of Benzo(a)anthracene on *Mytilus galloprovincialis*. *Marine Pollution Bulletin*, Vol.63, Iss.5-12, p.471-476.

▪ **Yakan S.D.**, Henkelmann B., Schramm K.-W., Okay O.S., 2013: Bioaccumulation - Depuration Kinetics and Effects of Phenanthrene on Mediterranean Mussel (*Mytilus galloprovincialis*). *Journal of Environmental Science and Health*, Part A Vol.48, Iss.9, p.1037-1046.

▪**Yakan S.D.**, Okay O.S., 2013: Filtration Rates of *Mytilus galloprovincialis* Exposed to Phenanthrene in a Semi-continuous Experimental System Portekiz. *17th Pollutant Responses in Marine Organisms (PRIMO) Congress*, 5 – 8 May 2013, Faro, Portugal.

▪ **Yakan S.D.**, Klasmeier J., Focks, A., Okay O.S., 2012: Modelling PAH Bioaccumulation in *Mytilus galloprovincialis* with a Three-compartment Model. *6th SETAC World Congress and SETAC Europe 22nd Annual Meeting*, 20 – 24 May 2012, Berlin, Germany.

▪ **Yakan S.D.**, Henkelmann B., Schramm K.-W., Okay O.S., 2011: Bioaccumulation and Depuration Kinetics and the Effects of Phenanthrene on *Mytilus galloprovincialis*. *15th International Symposium on Toxicity Assessment*, 3 – 8 July 2011, Hong Kong SAR, China.

▪ **Yakan S.D.**, Focks A., Klasmeier J., Okay O.S., 2011: A Mathematical Model for PAH Bioaccumulation in *Mytilus galloprovincialis*. *15th International Symposium on Toxicity Assessment*, 3 – 8 July 2011, Hong Kong SAR, China.

▪ **Yakan S.D.**, Henkelmann B., Schramm K.-W., Okay O.S., 2010: Bioaccumulation and Depuration Kinetics and Effects of BaA in Mediterranean mussel. *6th International Conference on Marine Pollution and Ecotoxicology*, 31 May – 3 June 2010, Hong Kong SAR, China.